

HARD ANODIZING

by

PAUL JOHN CUNNINGHAM, B.Sc., M.Sc.

A Thesis submitted for
the degree of Doctor of
Philosophy of the University
of Aston in Birmingham.

FEBRUARY 1982.

SUMMARY.

The University of Aston in Birmingham.

HARD ANODIZING.

Paul John Cunningham.

Submitted for the degree of Doctor of Philosophy.

1982.

Thick anodic oxide films were produced on aluminium using the sulphuric acid hard anodizing process. Low acid concentrations, low temperatures, high current densities and short processing times minimised oxide dissolution and gave the least porosity.

Scanning electron microscopy and potential-time measurements were used to study the anodizing process. Flaws in the oxide initially present on the aluminium surface were randomly distributed and provided low resistance paths for the anodizing current. Nucleation at flaws produced localised growths of anodic oxide which in cross-section were lens shaped nodules. Internal growth stresses cracked the outer layer of the nodules and caused characteristic rosette patterns. Anodizing became less and less localised as the nodules, or hillocks, grew and merged to cover the whole surface.

The results established that the hard anodizing process was essentially the same as conventional sulphuric acid anodizing with an inner barrier layer and an outer porous layer of oxide. The nucleation and growth of oxide in the initial stages of hard anodizing remained localised for a longer period and the pore volume was smaller than for conventional anodizing. The results enabled re-interpretation and a new explanation of the results of Csokán and others whose fibre theory, now shown to be incorrect, differed from the Keller-Hunter-Robinson model which was further developed quantitatively by Wood and O'Sullivan.

Pretreatment affected the initiation of anodizing and during its study icing defects (electropolishing defects) were observed when electropolishing under specific conditions. These were investigated, found to occur when the electrolyte and operating conditions were on the borderline between electropolishing and anodizing, and a mechanism for their formation proposed.

Key words: Aluminium, Anodizing, Hard Anodizing, Electropolishing Defects.

DECLARATION.

I declare that no part of the work described in this thesis was done in collaboration, and that the work has not been submitted for any other academic award.

Paul John Cunningham.

Paul John Cunningham.

ACKNOWLEDGEMENTS.

The author acknowledges the financial support given by the Science Engineering Research Council for the work reported in this thesis.

I also extend grateful thanks to the following, without whose invaluable assistance and understanding this thesis would never have been possible.

The technical staff of the Department of Metallurgy and Materials Engineering for their valued help - with a special mention of thanks to Mr Paul Cox.

Mrs Paula Sliwinski whose efficiency and helpfulness resulted in the typed thesis.

A special thank you to Dr D.J. Arrowsmith, and I add my recognition, gratitude and appreciation for his excellent suggestions, encouragement, advice and belief in my ability throughout the course of this work.

Finally, words cannot totally acknowledge the appreciation I feel towards my parents for their patience and moral support, without which this thesis would certainly never have been completed.

Research is to see what everybody else has seen, and to think what nobody else has thought.

Anon.

CONTENTS.

	Page No.
TITLE PAGE.	i
SUMMARY.	ii
DECLARATION.	iii
ACKNOWLEDGEMENTS.	iv
CONTENTS.	v
LIST OF TABLES.	ix
LIST OF FIGURES.	xii
CHAPTER ONE. INTRODUCTION & LITERATURE SURVEY.	1
1.1 FILM MORPHOLOGY.	6
1.1.1 FORMATION CHARACTERISTICS OF BARRIER-TYPE ANODIC OXIDE FILM.	10
1.1.2 POROUS-TYPE ANODIC OXIDE FILMS.	
1.1.3 STRUCTURE.	11
1.1.4 PORE FORMATION THEORIES.	19
1.2 PRODUCTION OF THICK, HARD POROUS ALUMINIUM OXIDE FILMS.	19
1.3 THE HARDNESS OF ANODIC OXIDE FILMS.	25
1.4 THE MEASUREMENT OF HARDNESS.	27
1.5 ABRASION RESISTANCE OF THE ANODIC OXIDE FILM.	34
1.6 THICKNESS TESTING OF ANODIC OXIDE FILMS.	34
1.6.1 DESTRUCTIVE THICKNESS TESTS.	36
1.6.1.1 GRAVIMETRIC (STRIP AND WEIGH) METHOD.	36
1.6.1.2 THICKNESS BY MICRO-SECTIONING.	37
1.6.2 NON-DESTRUCTIVE THICKNESS TESTS.	38
1.6.2.1 THICKNESS MEASUREMENT WITH AN OPTICAL SPLIT-BEAM MICROSCOPE.	38
1.6.2.2 EDDY CURRENT THICKNESS TESTING.	39
1.6.2.3 THICKNESS BY ELECTRICAL BREAKDOWN VOLTAGE OR RESISTANCE.	40
1.7 COATING RATIO.	41

	Page No.	
1.8	PRETREATMENT AND STRUCTURE.	43
1.9	THE EFFECT OF ALLOY COMPOSITION ON HARD ANODIZING.	44
1.10	HARD ANODIZING - COMMERCIAL PROCESSES.	48
1.10.1	USE OF DILUTE SULPHURIC ACID ELECTROLYTES.	52
1.10.2	CURRENT SUPPLY.	54
1.10.3	THE USE OF MIXED ACID ELECTROLYTES.	59
CHAPTER TWO: EXPERIMENTAL PROCEDURE AND TECHNIQUES.		62
2.1	INTRODUCTION.	62
2.2	MATERIALS USED.	62
2.3	SPECIMEN SIZE.	63
2.4	CHEMICAL SOLUTIONS.	63
2.4.1	ANODIZING SOLUTIONS.	63
2.5	SPECIMEN PREPARATION.	63
2.6	PRETREATMENTS.	63
2.6.1	"AS RECEIVED"	64
2.6.2	SAND BLASTED.	65
2.6.3	MECHANICALLY ABRADED AND POLISHED.	65
2.6.4	CHEMICAL ETCHING.	65
2.6.5	CHEMICAL POLISHING.	66
2.6.6	ELECTROPOLISHING.	66
2.6.7	HEAT TREATMENT.	66
2.7	ANODIZING - EXPERIMENTAL SET-UP.	67
2.8	SCANNING ELECTRON MICROSCOPY.	69
2.9	OPTICAL MICROSCOPY.	72
2.10	POTENTIAL - TIME INVESTIGATIONS.	72
2.11	MICROHARDNESS TESTING.	73
2.12	DETERMINATION OF THICKNESS BY CHEMICAL STRIPPING.	74

	Page No.
2.13 COATING RATIO.	76
2.14 ELECTROLYTIC DETACHMENT OF ANODIC OXIDE FILM.	76
CHAPTER THREE: RESULTS.	77
3.1 ANODIZING OF THE ALUMINIUM ALLOYS.	77
3.1.1 PRETREATMENTS.	78
3.1.2 ETCHING.	83
3.1.3 CHEMICAL POLISHING.	85
3.1.4 ELECTROPOLISHING.	86
3.1.5 HEAT TREATMENT.	87
3.2 POTENTIAL - TIME.	90
3.3 MICROHARDNESS.	94
3.4 THICKNESS.	96
3.5 COATING RATIO.	101
3.6 ELECTROLYTIC DETACHMENT OF ANODIC OXIDE FILM.	104
3.7 MISCELLANEOUS EXPERIMENTS.	105
3.8 FIGURES FROM EXPERIMENTAL WORK.	107
CHAPTER FOUR: DISCUSSION.	186
4.1 INTRODUCTION.	186
4.2 NUCLEATION AND GROWTH OF HARD ANODIZED FILMS.	187
4.3 ICING DEFECTS.	203
4.4 POTENTIAL - TIME.	206
4.5 MICROHARDNESS.	211
4.6 THICKNESS.	211
4.7 COATING RATIO.	213
4.8 EXAMINATION OF DETACHED OXIDE FILM AND ANODIZED SPECIMEN AFTER ANODIC FILM REMOVAL.	214
4.8.1 EXAMINATION OF DETACHED OXIDE FILM.	214

	Page No.
4.8.2 EXAMINATION OF ANODIZED SPECIMEN AFTER ANODIC FILM REMOVAL.	215
CHAPTER FIVE: CONCLUSIONS.	225
CHAPTER SIX: FURTHER WORK.	227
7. APPENDICIES.	229
APPENDIX I. CHEMICAL COMPOSITION OF ALUMINIUM ALLOYS USED.	229
APPENDIX II. CALCULATION OF CURRENT DENSITY.	230
APPENDIX III. UNITS.	231
APPENDIX IV. "BURNING" OF ANODIC OXIDE FILM.	232
8. BIBLIOGRAPHY.	236
8.1 EXTENDED BIBLIOGRAPHY.	237
9. REFERENCES.	275

LIST OF TABLES.

Table No.		Page No.
1.1	Classification of the two types of Anodic Oxide Film that are formed on aluminium when anodized.	7
1.2	Anodizing ratio, for the Barrier layer lying adjacent to the metal surface for porous films formed on aluminium in four commonly used electrolytes.	10
1.3	Influence of Various Factors on the Properties of Anodic Films and the Progress of the Anodic Process.	22
1.4	Hardness of various materials obtained by Bierbaum method.	29
1.5	Thickness of Oxide vs Function of anodic coating.	35
1.6	Commercial processes for hard anodizing.	50
1.7	Comparison of sulphuric acid and organic acid electrolytes for anodizing aluminium.	61
2.1	Composition of Super & Commercial purity aluminium.	62
3.1	Experiment 3.1.	78
3.2	Experiment 3.2. S.P.Al "As rolled", c.d. 23.8 A/dm ² , electrolyte temperature -8°C.	78
3.3	Experiment 3.3. S.P.Al "As rolled", c.d. 39.7 A/dm ² , electrolyte temperature -8°C.	79
3.4	Experiment 3.4. S.P.Al "As rolled", c.d. 6.6 A/dm ² , electrolyte temperature -8°C.	79
3.5	Experiment 3.5. S.P.Al "Sand Blasted", c.d. 5.4 A/dm ² , electrolyte temperature -8°C.	80
3.6	Experiment 3.6. S.P.Al "As rolled", c.d. 33.0 A/dm ² , electrolyte temperature -8°C.	80
3.7	Experiment 3.7. 5% H ₂ SO ₄ at -6°C and c.d 22.1 A/dm ² .	81
3.8	Experiment 3.8. c.d. 33.0 A/dm ² , electrolyte temperature -8°C.	81
3.9	Experiment 3.9. Scored surface, electrolyte temperature -8°C.	82

Table No.		Page No.
3.10	Experiment 3.10. S.P.Al etched in 10% NaOH at 60°C for 2 mins. Anodized at 35.7 A/dm ² in 10% H ₂ SO ₄ at -8°C.	83
3.11	Experiment 3.11. S.P.Al etched in 10% NaOH at 60°C for 2 mins and anodized at 11.0 A/dm ² in 10% H ₂ SO ₄ at -8°C (-6°C on removal).	83
3.12	Experiment 3.12. All of the alloys shown in Appendix I were etched in 10% NaOH at 60°C for 2 mins and anodized at various current densities in 10% H ₂ SO ₄ solution at -8°C. Six of these alloys experimental details are given.	84
3.13	Experiment 3.13. S.P.Al, chemically polished in 78% H ₃ PO ₄ - 6% H ₂ SO ₄ - 6% HNO ₃ - 0.5% CuSO ₄ at 98°C for 90 secs and anodized at various current densities in 10% H ₂ SO ₄ at -8°C.	85
3.14	Experiment 3.14.	86
3.15	Experiment 3.15. S.P.Al heat treated and air-cooled, c.d. 5.5 A/dm ² , electrolyte temperature -8°C.	87
3.16	Experiment 3.16. S.P.Al heat treated and water quenched, c.d. 5.3 A/dm ² , electrolyte temperature -8°C.	88
3.17	Experiment 3.17. C.P.Al heat treated and air-cooled, c.d. 7.1 A/dm ² , electrolyte temperature -8°C.	88
3.18	Experiment 3.18. C.P.Al heat treated and water quenched, c.d. 6.9 A/dm ² , electrolyte temperature -8°C.	88
3.19	Experiment 3.19. Alloy I, heat treated and air-cooled and mechanically polished to 1 μm, c.d. 22.0 A/dm ² , electrolyte temperature -8°C.	89
3.20	Experiment 3.20. Alloy I, heat treated and water quenched and mechanically polished to 1 μm, c.d. 22.0 A/dm ² , electrolyte temperature -8°C.	89
3.21	Experiment 3.21. Alloy II, heat treated and air-cooled and mechanically polished to 1 μm, c.d. 22.0 A/dm ² , electrolyte temperature -8°C.	89
3.22	Experiment 3.22. Alloy II, heat treated and water quenched and mechanically polished to 1 μm, c.d. 22.0 A/dm ² , electrolyte temperature -8°C.	90
3.23	Experiment 3.23. Temperature of electrolyte -8°C.	90
3.24	Experiment 3.24. Temperature of electrolyte -8°C.	91

Table No.		Page No.
3.25	Experiment 3.25. Temperature of electrolyte -8°C .	91
3.26	Experiment 3.26.	92
3.27	Experiment 3.27.	92
3.28	Experiment 3.28. Temperature of electrolyte -5°C . Etched specimens etched in 10% NaOH solution at $60 \pm 2^{\circ}\text{C}$ for 1 minute.	93
3.29	Vickers hardness values of coatings on various alloys, hard anodized in 10% H_2SO_4 at -8°C for various current densities.	94
3.30	Experiment 3.29. C.P.Al. "As rolled", anodized at three current densities in 10% v/v H_2SO_4 at -8°C .	97
3.31	Experiment 3.30. C.P.Al. "As rolled", anodized at three current densities in 15% v/v H_2SO_4 at -8°C .	97
3.32	Experiment 3.31. C.P.Al. "As rolled", anodized at three current densities in 20% v/v H_2SO_4 at -8°C .	98
3.33	Experiment 3.32. C.P.Al. "As rolled", anodized at three current densities in 5.4% v/v H_2SO_4 at -0°C .	98
3.34	Experiment 3.33. C.P.Al. "As rolled", anodized at three current densities in 16.6% v/v H_2SO_4 at -0°C .	99
3.35	Experiment 3.34. C.P.Al. "As rolled", anodized at three current densities in 27.6% v/v H_2SO_4 at -0°C .	99
3.36	Experiment 3.35. C.P.Al. "As rolled", anodized at three current densities in 27.6% v/v H_2SO_4 at 21°C .	100
3.37	Experiment 3.36. C.P.Al "As rolled" 10% H_2SO_4 electrolyte.	101
3.38	Experiment 3.37. Anodizing carried out in 10% H_2SO_4 at -5°C .	103
3.39	Experiment 3.38. Temperature of electrolyte 0°C .	105
7.1	Chemical composition of alloys used.	229
7.2	Conversion examples for A/dm^2 to $\text{A}\cdot\text{m}^{-2}$.	231

LIST OF FIGURES.

Fig. No.		Page No.
1.1.	Structure of a typical cell of an anodic oxide coating, showing basic units which determine its size.	13
1.2	Curves based on results of anodizing in 20 per cent H_2SO_4 bath at 25-30°C with c.d. 2 A/dm ² .	20
2.1	Laboratory set-up of apparatus used for anodizing of aluminium alloys.	70
3.1	Typical surface topography of S.P.Al in the "As rolled" condition after hard anodizing for 110 minutes at 5.1. A/dm ² . T.a. 70°	107
3.2	S.P.Al "As rolled", after 15 secs anodizing at 23.8 A/dm ² . Showing hillock shaped features. T.a. 70°	107
3.3(i)	S.P.Al "As rolled", after 30 secs anodizing at 23.8 A/dm ² . T.a. 70°	108
3.3(ii)	As Fig. 3.3(i), showing greater detail. T.a. 70°	108
3.4	S.P.Al "As rolled", after 60 secs anodizing at 23.8 A/dm ² . T.a. 45°	109
3.5(i)	S.P.Al. "As rolled", after 300 secs anodizing at 23.8 A/dm ² T.a. 70°	109
3.5(ii)	As Fig. 3.5(i), showing greater detail of the concentric ring cracks formed due to growth of the alumina. T.a. 70°	110
3.6(i)	S.P.Al "As rolled", after 1 sec anodizing at 39.7 A/dm ² . T.a.70°	110
3.6(ii)	As Fig. 3.6(i), showing greater detail of hillock shaped features. T.a. 70°	111
3.7	S.P.Al "As rolled" after 5 secs anodizing at 39.7 A/dm ² . T.a. 70°	111
3.8	S.P.Al "As rolled", after 15 secs anodizing at 39.7 A/dm ² T.a. 70°	112
3.9(i)	C.P.Al "As rolled", after 5 secs anodizing at 6.6 A/dm ² . T.a. 70°	112
3.9(ii)	As Fig. 3.9(i), showing greater detail. T.a. 70°	113
3.10(i)	C.P.Al "As rolled", after 15 secs anodizing at 6.6 A/dm ² . T.a. 70°	113

Fig No.		Page No.
3.10(ii)	As Fig. 3.10(i), showing greater detail. T.a. 70°	114
3.11(i)	C.P.Al "As rolled", 52 secs anodizing at 60 A/dm ² . Shows circular defect. T.a. 70°	114
3.11(ii)	As Fig. 3.11(i), showing greater detail of the defect surface. T.a. 70°	115
3.12	S.P.Al surface after being sand blasted. T.a. 70°	115
3.13	As Fig. 3.12. after 41 minutes anodizing at 5.4 A/dm ² . T.a. 70°	116
3.14(i)	C.P.Al "As rolled", after 8 minutes anodizing at 33 A/dm ² . Shows how at high glancing angle the hillock shaped features resemble "rosettes". T.a. 10°	116
3.14(ii)	As Fig.3.14(i) at a low glancing angle of T.a. 70°	117
3.15	Alloy I, P180 abraded, after 15 minutes anodizing in 5% H ₂ SO ₄ at 22.1 A/dm ² . T.a. 45°	117
3.16(i)	Alloy I, 1 μm polish, after 12 minutes anodizing in 5% H ₂ SO ₄ at 22.1 A/dm ² . T.a. 70°	118
3.16(ii)	As Fig. 3.16(i), showing more detail. T.a. 70°	118
3.17	Alloy II, P180 abraded, after 18 minutes anodizing in 5% H ₂ SO ₄ at 22.1 A/dm ² . T.a. 70°	119
3.18	Alloy II, P180 abraded, after 23 minutes anodizing in 5% H ₂ SO ₄ at 22.1 A/dm ² . No agitation, shows "burning". T.a. 45°	119
3.19(i)	Alloy II, 1 μm polish, after 14 minutes anodizing in 5% H ₂ SO ₄ at 22.1 A/dm ² . T.a. 45°	120
3.19(ii)	As Fig. 3.19(i), showing oxide growth at grain boundaries. T.a. 45°	120
3.20	H30 alloy, P180 abraded, after 2½ minutes anodizing at 33.0 A/dm ² . T.a. 45°	121
3.21(i)	H30 alloy, 1 μm polish, after 2 minutes anodizing at 33.0 A/dm ² . T.a. 70°	121
3.21(ii)	As Fig. 3.21(i), giving greater detail of surface produced. T.a. 70°	122
3.22	Alloy I, 1 μm polish, scored, after 6 minutes anodizing at 11.0 A/dm ² . T.a. 70°	122

Fig No.		Page No.
3.23	Alloy II, 1 μm polish, scored, after $7\frac{1}{2}$ minutes anodizing at 11.0 A/dm^2 . T.a. 70°	123
3.24	C.P.Al "As rolled", scored, after $16\frac{1}{2}$ minutes anodizing at 16.6 A/dm^2 . T.a. 70°	123
3.25	S.P.Al etched in 10% NaOH at 60°C for 2 minutes, showing scratch lines and etch pits. T.a. 45°	124
3.26(i)	As Fig. 3.25, after 30 secs anodizing at 35.7 A/dm^2 . T.a. 45°	124
3.26(ii)	As Fig. 3.26(i), but unscratched region. T.a. 45° *	125
3.27(i)	As Fig. 3.25, after 30 secs anodizing at 35.7 A/dm^2 . Showing defect rings. T.a. 70°	125
3.27(ii)	As Fig. 3.27(i) at a different position on the surface at a high glancing view. T.a. 70°	126
3.28(i)	As Fig. 3.25, after 120 secs anodizing at 35.7 A/dm^2 . Shows spalling and curling of outer layer of oxide. T.a. 10°	126
3.28(ii)	As Fig. 3.28(i) at lower glancing angle. T.a. 45°	127
3.28(iii)	As Fig. 3.28(ii), showing greater detail of spalling and curling of outer layer of oxide. T.a. 45°	127
3.29	As Fig. 3.25, after 480 secs anodizing at 35.7 A/dm^2 . T.a. 45°	128
3.30(i)	As Fig. 3.25, after 57 mins anodizing at 11.0 A/dm^2 . T.a. 45°	128
3.30(ii)	As Fig. 3.30(i), showing greater detail. T.a. 45°	129
3.30(iii)	As Fig. 3.30(ii), showing greater detail. T.a. 45°	129
3.31	Alloy BB3 etched in 10% NaOH at 60°C for 2 minutes after 17 minutes anodizing at 10.4 A/dm^2 . T.a. 45°	130
3.32	Alloy 5182 (etched), after $15\frac{1}{2}$ minutes anodizing at 9.0 A/dm^2 . T.a. 45°	130
3.33	Alloy 2117CP (etched), after 15 minutes anodizing at 10.4 A/dm^2 . T.a. 45°	131
3.34	Alloy 2117HP (etched), after $18\frac{1}{2}$ minutes anodizing at 9.0 A/dm^2 . T.a. 45°	131
3.35	Alloy 2002 (etched), after 17 minutes anodizing at 10.9 A/dm^2 . T.a. 45°	132

Fig No.		Page No.
3.36	Alloy 609 (etched), after 14½ minutes anodizing at 10.4 A/dm ² . T.a 45°	132
3.37	S.P.Al chemically polished in 78% H ₃ PO ₄ - 16% H ₂ SO ₄ - 6% HNO ₃ - 0.5% CuSO ₄ at 98°C for 90 secs. T.a 45°	133
3.38	As Fig. 3.37, after 4½ minutes anodizing at 41.6 A/dm ² . T.a. 45°	133
3.39(i)	Optical photomicrograph of pyramid shaped icing defects, gassing defects also visible.	134
3.39(ii)	Typical icing defects, showing striations and central blip. T.a. 70°	134
3.40	S.P.Al etched surface, showing scratch lines and etch pits. T.a. 45°	135
3.41(i)	S.P.Al electropolished for 60 secs, showing gassing defects and radial spread dissolving the air-formed oxide film. T.a. 45°	135
3.41(ii)	As Fig. 3.41(i), showing icing defects formed at high current density regions. T.a. 70°	136
3.41(iii)	As Fig. 3.41(i), showing the association of icing defects with gassing defects. T.a. 70°	136
3.42	Icing defect around a gassing defect after 120 seconds electropolishing. T.a. 80°	137
3.43(i)	Surface topography after electropolishing and then hard anodized. Shows depressions at sites of prior icing defects. T.a 45°	137
3.43(ii)	As Fig. 3.43(i), showing greater detail of the depressions at the sites of prior icing defects. T.a. 70°	138
3.44	S.P.Al electropolished for 90 secs at 10.0 A/dm ² , showing a few gassing defects. T.a 70°	138
3.45	As Fig. 3.44, after anodizing for 37 minutes at 10.0 A/dm ² Showing the replication of the gassing defects and the characteristic nodular oxide growth. T.a. 70°	139
3.46	S.P.Al heat treated and air-cooled, after 27 minutes anodizing at 5.5 A/dm ² . T.a 45°	139
3.47	S.P.AL, heat treated and water quenched, after 34 minutes anodizing at 5.3 A/dm ² . T.a 45°	140
3.48	C.P.AL, heat treated and air-cooled, after 22 minutes anodizing at 7.1 A/dm ² . T.a 70°	140
3.49	C.P.AL, heat treated and water quenched, after 17 minutes anodizing at 6.9 A/dm ² . T.a 45°	141

Fig. No.		Page No.
3.50	Alloy I, heat treated and air-cooled and mechanically polished to $1\ \mu\text{m}$, after 11 minutes anodizing at $22.0\ \text{A}/\text{dm}^2$. T.a. 70°	141
3.51	Alloy I, heat treated and water quenched and mechanically polished to $1\ \mu\text{m}$, after 12 minutes anodizing at $22.0\ \text{A}/\text{dm}^2$. T.a. 70°	142
3.52	Alloy II, heat treated and air-cooled and mechanically polished to $1\ \mu\text{m}$, after 12 minutes anodizing at $22.0\ \text{A}/\text{dm}^2$. T.a. 10°	142
3.53	Alloy II, heat treated and water quenched and mechanically polished to $1\ \mu\text{m}$, after 10 minutes anodizing at $22.0\ \text{A}/\text{dm}^2$. T.a. 70°	143
3.54	C.P.Al "As rolled", after 70 minutes anodizing at $13.3\ \text{A}/\text{dm}^2$ in $10\% \text{H}_2\text{SO}_4$ at 17°C . Shows a powdery coating. T.a. 70°	143
3.55	Pot - time curves for anodized specimens from Experiment 3.23.	144
3.56	Pot - time curves for anodized specimens from Experiment 3.24,	145
3.57	Pot - time curves for anodized specimens from Experiment 3.25,	146
3.58	Pot - time curves for anodized specimens from Experiment 3.26.	147
3.59	Pot - time curves for anodized specimens from Experiment 3.27.	148
3.60 to 3.65	Pot - time curves for anodized specimens from Experiment 3.28,	149
3.66	Microhardness indentation ladder across oxide.	155
3.67	Plot of thickness against time for data from Experiment 3.29.	156
3.68	Plot of thickness against time for data from Experiment 3.30.	157
3.69	Plot of thickness against time for data from Experiment 3.31.	158
3.70	Plot of thickness against time for data from Experiment 3.32.	159
3.71	Plot of thickness against time for data from Experiment 3.33.	160
3.72	Plot of thickness against time for data from Experiment 3.34.	161
3.73	Plot of thickness against time for data from Experiment 3.35.	162
3.74(i)	Effect of temperature and immersion time on surface appearance when anodizing carried out at $24.0\ \text{A}/\text{dm}^2$.	163
3.74(ii)	Effect of temperature and immersion time on surface appearance when anodizing carried out at $8.5\ \text{A}/\text{dm}^2$.	164
3.75	Effect of temperature and time of anodizing on coating ratio at a constant current density of $24.0\ \text{A}/\text{dm}^2$.	165

Fig. No.		Page No.
3.76	Effect of temperature and time of anodizing on coating ratio at a constant current density of 8.5 A/dm^2	166
3.77(i)	Underside of oxide electrolytically detached from alloy BB3. T.a 45°	167
3.77(ii)	As Fig. 3.77(i). T.a. 10°	167
3.77(iii)	As Fig. 3.77(i). T.a. 60°	168
3.78(i)	Underside of oxide electrolytically detached from alloy 2117CP. T.a 45°	168
3.78(ii)	As Fig. 3.78(i), showing greater detail.	169
3.78(iii)	Optical photomicrograph of cross-section, showing "conical asperities" of unanodized aluminium.	169
3.79	Cross-sectional view of Specimen No.1 from Exp. 3.38, showing structure after chemical dissolution of oxide. T.a. 10°	170
3.80(i)	Cross-sectional view of Specimen No.2 from Exp. 3.38, showing structure after chemical dissolution of oxide T.a. 10°	170
3.80(ii)	As Fig. 3.80(i). T.a. 10°	171
3.81(i)	Cross-sectional view of C.P.Al, chemically polished and anodized for $4\frac{1}{2}$ minutes at 41.6 A/dm^2 , after chemical dissolution of oxide. T.a 10°	171
3.81(ii)	As Fig. 3.81(i), showing greater detail. T.a. 10°	172
3.82(i)	Cross-sectional view of C.P.Al, chemically polished and anodized for 13 minutes at 18.9 A/dm^2 , after chemical dissolution of oxide. T.a 10°	172
3.82(ii)	As Fig. 3.82(i). T.a. 10°	173
3.83(i)	As Fig. 3.82(i). Showing "island" growth at basis metal-oxide interface. T.a 55°	173
3.83(ii)	As Fig. 3.83(i), showing more detail. T.a. 55°	174
3.84	Same pretreatment as 3.81(i), but anodized for 36 minutes at 10.5 A/dm^2 , after chemical dissolution of oxide. T.a. 60°	174
3.85(i), (ii) and (iii)	are a sequence of electronphotomicrographs, showing "sheets" of oxide. T.a 60°	175
3.86(i)	Interface of chemically polished C.P.Al with unanodized surface to the left and the oxide chemically removed surface to the right. T.a. 45°	176

Fig. No.		Page No.
3.86(ii)	As Fig. 3.86(i), but on basis metal with oxide removed showing another feature - a cylinder of material. T.a. 70°	177
3.86(iii)	As Fig. 3.86(ii) showing greater detail. T.a 70°	177
3.87(i) to (xi)	C.P.Al "As rolled", anodized in 10% H ₂ SO ₄ at -8°C and oxide chemically stripped in boiling H ₃ PO ₄ - CrO ₃ solution. T.a. 45°	178
3.87(i)	15 minutes anodizing at 5.8 A/dm ² .	178
3.87(ii)	30 minutes anodizing at 5.8 A/dm ² .	178
3.87(iii)	60 minutes anodizing at 5.8 A/dm ² .	178
3.87(iv)	3 minutes anodizing at 10.7 A/dm ² .	178
3.87(v)	7½ minutes anodizing at 10.7 A/dm ² .	178
3.87(vi)	30 minutes anodizing at 10.7 A/dm ² .	178
3.87(vii)	47 minutes anodizing at 10.7 A/dm ² .	179
3.87(viii)	3 minutes anodizing at 19.2 A/dm ² .	179
3.87(ix)	7½ minutes anodizing at 19.2 A/dm ² .	179
3.87(x)	10 minutes anodizing at 19.2 A/dm ² .	179
3.87(xi)	15 minutes anodizing at 19.2 A/dm ² .	179
3.88(i) to (iii)	C.P.Al "As rolled", anodized in 15% H ₂ SO ₄ at -8°C and chemically stripped in boiling H ₃ PO ₄ - CrO ₃ solution. T.a 45°	180
3.88(i)	15 minutes anodizing at 6.3 A/dm ² .	180
3.88(ii)	30 minutes anodizing at 11.5 A/dm ² .	180
3.88(iii)	10½ minutes anodizing at 22.2 A/dm ² .	180
3.89(i) to (ix)	C.P.Al "As rolled", anodized in 20% H ₂ SO ₄ at -8°C and chemically stripped in boiling H ₃ PO ₄ - CrO ₃ solution. T.a. 45°	181
3.89(i)	15 minutes anodizing at 5.8 A/dm ² .	181
3.89(ii)	30 minutes anodizing at 5.8 A/dm ² .	181
3.89(iii)	60 minutes anodizing at 5.8 A/dm ² .	181
3.89(iv)	3 minutes anodizing at 10.4 A/dm ² .	181
3.89(v)	7½ minutes anodizing at 10.4 A/dm ² .	181

Fig No.		Page No.
3.89(vi)	29 minutes anodizing at 10.4 A/dm ² .	181
3.89(vii)	3 minutes anodizing at 19.2 A/dm ² .	182
3.89(viii)	7½ minutes anodizing at 19.2 A/dm ² .	182
3.89(ix)	11 minutes anodizing at 19.2 A/dm ² .	182
3.90	C.P.Al "As rolled", anodized in 10% H ₂ SO ₄ at -8°C for 3 minutes at 52.0 A/dm ² and oxide chemically stripped off. T.a. 45.	182
3.91	C.P.Al "As rolled", anodized in 10% H ₂ SO ₄ at -8°C for 3 minutes at 11.0 A/dm ² and oxide chemically stripped off. T.a. 45.	182
3.92(i)	C.P.Al etched in 10% NaOH, anodized for 2 minutes at 29.6 A/dm ² in 27.6 % H ₂ SO ₄ at 0°C. T.a. 45°	183
3.92(ii)	As Fig. 3.92(i), with anodic oxide chemically stripped off. T.a. 45°	183
3.93(i)	C.P.Al etched in 10% NaOH, anodized for 2 minutes at 15.4 A/dm ² in 27.6% H ₂ SO ₄ at 0°C. T.a. 45°	184
3.93(ii)	As Fig. 3.93(i), with anodic oxide chemically stripped off. T.a. 45°	184
3.94(i)	C.P.Al etched in 10% NaOH, anodized for 2 minutes at 8.2 A/dm ² in 27.6% H ₂ SO ₄ at 0°C. T.a. 45°	185
3.94(ii)	As Fig. 3.94(i), with anodic oxide chemically stripped off. T.a. 45°	185
4.1	Diagrammatic representation of nucleation and growth of hard anodic oxide film.	201
4.2	Diagrammatic representation of chemical dissolution of the anodic oxide film.	218

HARD ANODIZING.

CHAPTER ONE.

1. INTRODUCTION AND LITERATURE SURVEY.

The electrochemical process of HARD ANODIZING aluminium has been derived from, and is closely related to, conventional anodizing of aluminium. The aluminium surface to be treated is made the anode in a colder electrolyte and with higher current densities and higher voltages than the conventional anodizing process. The flow of electricity through the anode converts the surface of the metal into aluminium oxide of such thickness and hardness that its resistance to wear and abrasion, and its electrical and thermal insulating properties are significantly increased so that the article being anodized acquires distinctive characteristics, making it suitable for a wide variety of engineering and other purposes.

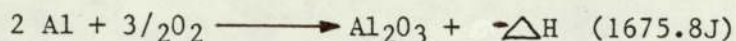
Aluminium is the most abundant metal, and the third most abundant element in the earth's crust, but is never found free in nature. It is a relatively cheap metal in terms of cost per unit volume; it is in fact the cheapest non-ferrous metal and the second cheapest of all commercially important metals.

Since its introduction as an industrial metal, there has been considerable economic incentive to give it consideration for an increasing number of design applications. Pure aluminium, a silvery-white metal, possesses many desirable characteristics, for example its light weight, high strength to weight ratio, machinability, thermal and electrical conductivity, availability, ductility and low cost. Its desirability, however, is often limited by its softness, its

easily abraded surface, its susceptibility to corrosion and its tendency to galling when in contact with another surface.

These generally unfavourable characteristics, though, have been offset a great deal by alloying with elements such as copper, magnesium, silicon, manganese and other elements to impart a variety of useful properties. Aluminium and its alloys respond to a wide variety of such basic treatments as anodic oxidation, electro-brightening, electroplating, chemical oxidation, chemical immersion and etching to produce many types of films, coatings or surface effects for various commercial processes.

Because of the high affinity of aluminium surfaces for oxygen:



the metal is always covered with a highly resistant oxide film. This naturally occurring oxide film (alumina) which spontaneously forms on the surface of the aluminium when exposed to the atmosphere is extremely thin (0.01 - 0.02 μm thick), hard and unreactive, but does afford some protection to the underlying metal, giving resistance to corrosion. Essentially the same phenomenon occurs on aluminium alloys. It is to this film that aluminium owes its high resistance to corrosion despite its unfavourable position in the electrochemical series.

The oxide, alumina, occurs in various impure forms. It occurs naturally as ruby, sapphire, emery and corundum (being second only to diamond on the Moh's scale of hardness) and is used in glass making and refractories.

Heating the metal in air will further increase the oxide film thickness, but may be accompanied by discolouration and a change in mechanical properties.

This ability of aluminium and its alloys to form adherent

oxide films led to the development of electrochemical processes used to enhance this natural oxide film to produce an oxide film which is of controllable thickness and quality which is attractively finished, has excellent corrosion resistance and possesses other commercially desirable qualities.

These electrochemical processes are known commercially as anodic oxidation , anodic treatment or ANODIZING.

It is probably true to say that commercially the anodized finish is unique to aluminium. Other metals can be anodized, particularly titanium and zinc, but these are somewhat esoteric applications of the anodizing process, and aluminium is the only metal which is treated on a large industrial scale.

It is generally recognised that H. Buff⁽¹⁾ in 1857 discovered the behaviour of aluminium when made the anode in sulphuric acid solutions. After these initial observations, many other workers concerned themselves with the interesting rectifying effect and other electrical properties of coatings formed under various conditions using sulphuric acid solutions. The result of these workers' efforts was of important scientific interest and laid down the foundations for later practical applications. It was found that by varying the electrolyte strength, composition, temperature and power supply, the properties of the oxide film were further enhanced. In 1904 W. R. Mott⁽²⁾ described several anodic processes utilizing a variety of electrolytes. Mott not only proposed a theory for the formation of anodic coatings but also discovered the high absorptive characteristics of these coatings. He also proposed the use of these anodic films for protection against corrosion and for electrical insulation. This date would seem to mark the recognition of the tremendous industrial potential of anodic

coatings on aluminium alloys. In the early 1900's (3,4) patents began to appear describing the anodic treatment of aluminium in various electrolytes for the formation of films for capacitors and rectifiers.

The first commercial process was not developed until 1923, when Bengough and Stuart(5) patented their chromic acid anodizing process. This was closely followed in 1924(6) by the oxalic acid anodizing process and this technique was the first to afford thick, hard, anodic coatings on a wide range of aluminium alloys. A sulphuric acid process was patented in the U.K. in 1927 by Gower and O'Brien.(7)

Since these early patents there have been literally hundreds of patents and publications dealing with the process of anodizing aluminium. The literature concerned with anodic oxidation of aluminium is vast, so only literature pertinent to the present study as been reviewed. The industrial importance of the hardness and abrasion resistance of anodic films is obvious from the many reports cited in the literature, together with the fact that the majority of hard anodizing processes have been patented.

However, most of the published studies consist of either acceptability programmes which test the effectiveness of the various anodizing conditions, or employ a fixed anodizing schedule which compares the properties of films formed on a range of aluminium alloys. Hence, the "Art" (Commercial development) of the hard anodizing process seems to be fairly well established although the commercial development has not been accompanied with published research on the mechanism of hard anodizing or the structure of the hard anodic oxide coatings formed.

This was because of

- (i) the difficulties of resolving a very fine structure which occurs when hard anodic coatings are formed on aluminium and

(ii) the complexity that arises from the intermetallics present in the aluminium alloys.

Present day understanding of anodizing is based upon the study of high purity aluminium anodized in phosphoric acid, which gives comparatively large pores which can be studied electron optically more easily than the very fine pore characteristics formed by sulphuric acid anodizing.

Anodizing, as used in the context of this thesis can be defined as:

An electrochemical process used for producing decorative and protective films on articles made from aluminium and its alloys, whereby a direct current at sufficient voltage is passed through a suitable electrolyte in which aluminium is the anode and a suitable inert material e.g. lead or carbon, the cathode. This is contrary to the electroplating processes.

In general anodizing is carried out with a maximum of 10V to 15V a.c. or d.c. in concentrated or medium strength acid, or less frequently alkaline electrolytes. The temperature of the electrolyte varies between 15°C and 30°C depending upon the process. The anodic oxide films produced consist of a compact layer close to the basis metal (called the barrier layer), and a much thicker 30-35 μm outer layer having a porous columnar structure with a hardness of VPN 40 to 80 Kgmm^{-2} . The mechanical properties of the aluminium surface are materially improved by the presence of the oxide film. As a consequence of its porosity and chemical properties it can be coloured with organic or inorganic dyes and thus used for decorative purposes. Sealing of the pores imparts excellent corrosion resistance and is

carried out by impregnation with oil, lacquer or by hydration of the aluminium oxide, brought about by boiling in water or a suitable aqueous solution. Where the sealing action is produced by the closing of the pores in consequence of the increase in volume.

1.1 FILM MORPHOLOGY.

Essentially two distinct types of oxide films may be found on aluminium depending upon the solvent action of the electrolyte used during oxidation.⁽⁸⁾ Electrolytes in which the oxide film formed is completely insoluble produce barrier-layer type films. Examples of such electrolytes are neutral boric acid solutions, ammonium borate or tartate aqueous solutions, citric, malic and glycollic acids. Electrolytes in which the oxide film is slightly soluble produce porous-type films. Examples of such electrolytes are numerous, but the more important commercial electrolytes are sulphuric, chromic, oxalic and phosphoric acids at almost any concentration.

These two types of films differ in the thickness that can be produced and in the thickness controlling parameters. Apart from the temperature of the electrolyte, barrier films thickness is controlled by the voltage applied,⁽⁹⁾ whereas porous films thickness depends upon the current density and time of anodizing.

The maximum film thickness of film that can be produced for barrier-type films is restricted to a voltage below the oxide breakdown voltage value⁽¹⁰⁾ i.e., 500-700 V, or 0.7 - 1 μm . Porous film thickness being time dependent can grow to many times the thickness limit placed on barrier films. For porous films, apart from the current density and anodizing time, electrolyte temperature is an important factor in determining the film thickness. At low temperatures

(< 5°C) the porous film formed is thick, compact and hard - HARD ANODIZING. At high temperatures (60-75°C) the porous film is thin, soft, an non-protective.

Table 1.1.(11) below shows a summary of the two types of anodic oxide films that can be formed on aluminium when anodized.

Table 1.1.(11)

Classification of the two types of Anodic Oxide Film that are formed on Aluminium when anodized.

	BARRIER TYPE	POROUS TYPE
STRUCTURE	Thin, Compact non-porous.	Inner layer - thin, compact, barrier type. Outer layer - thick and porous.
THICKNESS	Voltage dependent to extent of $14 \text{ \AA} \cdot \text{V}^{-1}$	Inner layer - voltage dependent, eg., sulphuric acid ($10 \text{ \AA} \cdot \text{V}^{-1}$). Outer layer - voltage independent, current density, time and temperature dependent.
TYPICAL ELECTROLYTES	Solution of boric acid - borax. Barrier-type electrolytes.	Sulphuric, phosphoric, oxalic and chromic acid aqueous solution. Pore - forming electrolytes.
USES	Electrolytic capacitors.	In the sealed condition can be used in any situation where excellent corrosion resistance is required. Prior to sealing, the adsorption of coloured dye stuffs has wide application in decorative structure. Also provides an excellent base for paints and metal electro-deposits.

Diggle, Downie and Goulding⁽¹¹⁾ gave a fairly comprehensive review of anodic oxide films on aluminium and the following is taken from that review paper.

1.1.1 FORMATION CHARACTERISTICS OF BARRIER-TYPE ANODIC OXIDE FILMS.

Ideally, barrier films are non-porous thin oxide layers which conduct both electrons (electronic current) and ions (ionic current) at high electric field strength. The field strength is the voltage drop across the oxide film divided by its thickness, this drop is not always equal to the applied voltage.

Below a minimum electric field strength the ionic conduction is negligible, and electronic current becomes the predominant mode of charge transport; the magnitude of this electronic current, whether at a high or low electric field strength is governed by the electronic conductivity of the oxide film. Aluminium oxide films have a low electronic conductivity and a high ionic conductivity, and hence, at a high electric field strength, ionic conduction is the predominant mode of charge transport. If barrier films can be assumed to be completely non-porous, the films will continue to grow as long as ionic currents continue to flow, the ionic current being dependent on the electric field strength present across the oxide film, i.e., the voltage drop across the film (V) divided by its thickness (d), the metal, and the metal oxide parameters, e.g., the activation energy for ion motion. Therefore, the extent of the ionic current at any one electric field strength will vary from metal to metal. The detectable movement of ions, i.e., detectable in that an experimentally observable thickness change occurs across an oxide film, requires the presence of some certain electric field strength E' ; since the

magnitude of the ionic current at any value of E' depends upon the metal, this certain electric field would also be expected to vary from metal to metal.

The thickness of a barrier film is dependent upon V and is usually quoted in terms of the anodizing ratio (the number of angstroms of oxide formed per volt applied, $\text{\AA} \text{V}^{-1}$); therefore, with knowledge of the anodizing ratio and the volts applied, the oxide film thickness is simply but approximately calculated by $(\text{\AA} \text{V}^{-1}) \times (\text{volts})$. By inspection the anodizing ratio is seen to be equivalent to the reciprocal of the certain field strength (as defined above) required for ion motion, and hence the anodizing ratio also varies from metal to metal e.g. For aluminium the $\text{\AA} \text{V}^{-1}$ is 13.0⁽⁹⁾ and for silicon $\text{\AA} \text{V}^{-1}$ is 13.8.⁽¹²⁾

In systems where porous type films occur, i.e., where the barrier type oxide film is very sparingly soluble and where pore formation is favourable, the electric field strength does not decrease to the point at which ionic current is low, since at this point experimentally detectable growth would effectively cease, and the film would not be of the porous type. V/d is greater than that value for a totally non-porous film, and therefore the anodizing ratio is lower than the value given above.

Table 1.2 below shows the $\text{\AA} \text{V}^{-1}$ ratios which have been established^(13,14,15) for some typical pore forming electrolytes used in the anodizing of aluminium.

Table 1.2. Anodizing ratio, for the barrier layer lying adjacent to the metal surface for porous films formed on aluminium in four commonly used electrolytes.

Electrolyte concentration (Temp. °C)	Anodizing ratio (Å V ⁻¹)
15% Sulphuric acid(10)	10.0
2% Oxalic acid(24)	11.0
4% Phosphoric acid(24)	11.9
3% Chromic acid(38)	12.5

Since the formation of a porous anodic oxide film arises from some form of conversion of an initially formed barrier film, the mechanism of barrier film formation is important i.e., ionic charge transport. A number of theories on ion charge transport have been postulated by a number of workers.

Mott⁽¹⁶⁾ and Cabrera and Mott⁽¹⁷⁾: Cabrera-Mott Theory (Metal-Oxide interface control); Verwey⁽¹⁸⁾: Verwey Theory (Bulk oxide control) and Dewald^(19,20): Dewald Theory (Dual-barrier control with space charge). Further reference to these theories is beyond the scope of this thesis and the review by Diggle et al⁽¹¹⁾ should be consulted for further explanation.

1.1.2 POROUS - TYPE ANODIC OXIDE FILMS.

It is generally considered⁽¹¹⁾ that the phenomena of the formation of porous layers and the concurrent dissolution process can be

summarized as follows:

- (a) Ionic migration, initially to form a barrier layer which, in the complete absence of electrolyte solvent power, will remain as a barrier layer.
- (b) In electrolytes with solvent power, a conversion process operative when the barrier layer reaches a certain thickness. This barrier layer to porous layer conversion is believed to be a field assisted electrochemical process.(21)
- (c) The porous layer thickness due to the conversion process in (b) becomes a function of current density, time, electrolyte temperature, and to a limited extent, electrolyte concentration.
- (d) Outer surface dissolution by the bulk electrolyte, which is seen as purely a chemical process, results in porous films which are experimentally thinner than those expected from the amount of charge passed calculations. This process is strongly temperature dependent in the range 5-70°C and weakly dependent upon the electrolyte concentration.

1.1.3 STRUCTURE.

As early as 1932⁽²²⁾ it was known that the oxide film on aluminium consisted of two regions: an outer region of thick porous type oxide and a thin, compact inner region lying adjacent to the metal.

From the many electronoptical investigations (15,23,24,25,26,27,28) both by replicating techniques and direct transmission technique, and from some gas adsorption studies^(29,30) the structure of the porous anodic film would appear to be that reported by Keller, Hunter and Robinson.⁽¹⁵⁾ The technique they used for obtaining their micrographs

was as follows. The aluminium, after a suitable surface pretreatment, was immersed in the anodizing electrolyte and a constant voltage was applied. The time of formation was not specified in the original paper, but has been reported⁽³¹⁾ to have been five minutes. Following formation of the film, the specimen film was then either examined by transmission electron microscopy, from which pore densities were determined, or the oxide film was stripped off in chromic-phosphoric acid, to reveal the metal-oxide interface structure. The surface revealed was seen to be covered with a large number of hemispherical depressions, whose number per square centimetre corresponded to the pore density found by direct transmission. On the basis of the information gained a model was proposed for the porous oxide film.

Essentially the micrographs were interpreted as showing a thick outer layer, containing fine, regular, almost cylindrical, parallel-sided pores perpendicular to the macroscopic surface of the specimen, penetrating a close-packed hexagonal, cellular structure and extending from the outer surface as far as a thin, compact, scalloped, barrier layer which separated the porous layer from the metal. The diameter of the oxide cells was approximately twice the barrier layer thickness and proportional to the forming voltage, each cell containing a single star shaped pore (not proven) whose dimensions were independent of voltage but dependent upon electrolyte type and conditions. It was postulated that the structure maintained itself during growth by the development of regions of hot, concentrated acid at the pore bases, which permitted the local rate of dissolution to keep up with the overall growth rate.

Wood, O'Sullivan, and Vaszko⁽³²⁾ have shown that the geometrical pore model of Keller et al is essentially correct. This work was furthered by O'Sullivan and Wood.⁽²⁷⁾

The structure of a typical cell of an anodic oxide coating is shown in Fig 1.1.

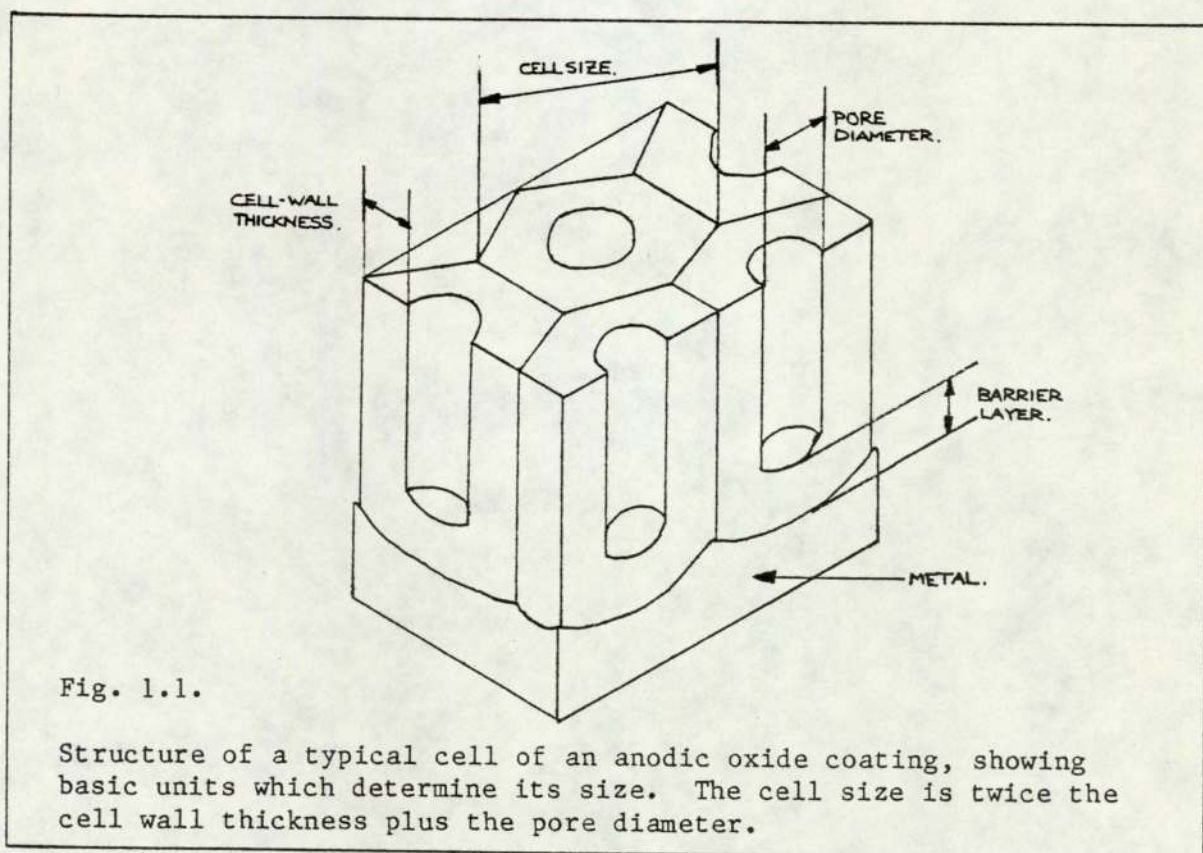


Fig. 1.1.

Structure of a typical cell of an anodic oxide coating, showing basic units which determine its size. The cell size is twice the cell wall thickness plus the pore diameter.

The regularity of the pores was first demonstrated in section by Booker, Wood and Walsh^(23,24) and various minor changes in morphology have been observed by other workers; Renshaw,⁽³³⁾ Zalivalov et al,⁽³⁴⁾ Franklin and Stirland⁽³¹⁾ and Paolini et al.⁽²⁹⁾

Certain inconsistencies and criticisms of the model postulated by Keller et al have been mentioned by a number of workers. Hoar and Mott⁽²¹⁾ indicated that it was not necessary to postulate the hot, concentrated acid at the bases of the pores, the high dissolution rates could be explained in terms of field-assisted dissolution.

Csokán (35,36,37) in an investigation of hard anodic oxide films, has reported that the pore structure is not regular as was previously believed. The structure observed experimentally was one in which the pore distribution was irregular and where the pores themselves were twisted and bent or otherwise distorted. The occurrence of a high density of pore openings at the surface appeared to produce a fibrous structure (fibre bundles), whose size, shape and orientation varied considerably. This produced what appears to be, under polarized light, a laminated structure lying parallel to the aluminium surface. The aluminium subgrain structure was suggested to influence, at least partially, the orientation of the groups of pore channels. That pore colonies can occur at some preferred sites has also been suggested by Renshaw.(33)

The porous structure, instead of being represented as an array of regularly distributed, densely packed oxide cells, has been suggested(38,39) to be a fibrous structure, the hollow fibres of alumina containing water and the acid anion standing vertical to the aluminium surface.

The models proposed by Csokán(35) and by Ginsberg and Wefers(38) are similar in that a fibrous structure is proposed, which can be either regular(38) or irregular.(35)

However, it is not entirely clear what these authors ment by this fibrous structure and a great deal of controversy has arisen over the appearance of such fibres and the interpretation given to such work. Workers that have looked at these structures since have not been able to distinguish any of these fibres and state that there is no difference between hard anodic coatings and conventional porous films. A possible explanation of what was being observed by these

authors will be given in the discussion chapter of the thesis.

Since it is the case that the electrolyte used in the anodizing process governs, to some extent, not only the type of film but also the dimensions of the film structure, it is not surprising that the structure proposed by Keller et al⁽¹⁵⁾ for a film formed at room temperature is different, in structural detail, from the that reported by Csokán at 0-5°C. For these low-temperature films it might be predicted that the pore mouth diameter and the oxide cell size will be smaller. The maximum film thickness will be greater, and the film will be mechanically harder and more abrasion-resistant owing to the general tightening up of the porous structure.

Murphy and Michelson⁽⁴⁰⁾ considered the pores of the oxide to be of secondary importance and emphasized the significance of more randomly arranged, hydrogen-bonded regions containing the acid anion, which separated fine sub-micro crystallites of largely anhydrous oxide, in determining the film structure and conduction through it. They suggested, without direct visual evidence, that the growth occurred in a transition region between the barrier layer and the porous layer. The structure which they have proposed as been described as a triple layer or a colloidal gel model. The suggested composition of the three layers is as follows:

- (i) An inner, relatively compact, anhydrous form of alumina.
Most probably of non-uniform composition with small submicrocrystallites joined by regions in which the oxide structure is not so uniform and where hydration can occur.
- (ii) An intermediate transition region, where the conversion of the inner anhydrous region to an outer region of high hydration is seen. The hydration, present in this region, is intermediate

between that of the inner and outer regions. The structure can be regarded again as submicrocrystallites surrounded by regions of moderately hydrated material; it is through these regions of hydrated oxide that electrolytic conduction is assumed to occur.

- (iii) An outer region consisting mainly of hydrated oxide, where the extent of hydration and oxide density varies. It was suggested that it is this region, of high hydration extent and where the minimum number of submicrocrystallites, exists, that possesses the precursors of the pores which are observed upon electronoptical examination.

The electric field strength present during anodizing was assumed^(21,40) to be sufficient to draw OH^- ions and water molecules in the direction of the barrier layer; the OH^- ions and the water molecules in the barrier layer - porous layer interface were suggested to cause a modification of the preformed barrier layer into a more hydrous oxide in localized regions, thereby tending to decrease the effective barrier layer thickness. At the same time, the field in this interface is such as to cause migration of protons away from the barrier layer. This results in a tendency to de-protonate or de-hydrate the oxide in that region. The opposing actions of these two processes were suggested⁽⁴⁰⁾ to explain the observed dependence of the barrier film thickness on the applied formation voltage.

The structure is of the laminar type suggested by Csokan⁽³⁵⁾ for hard anodic oxide film, but, unlike the Csokán model, pores were not thought to penetrate the outer sections completely to the inner layer. The pores were suggested to only penetrate a short distance through the outer layer, in which case the pores form a much less significant

between that of the inner and outer regions. The structure can be regarded again as submicrocrystallites surrounded by regions of moderately hydrated material; it is through these regions of hydrated oxide that electrolytic conduction is assumed to occur.

- (iii) An outer region consisting mainly of hydrated oxide, where the extent of hydration and oxide density varies. It was suggested that it is this region, of high hydration extent and where the minimum number of submicrocrystallites, exists, that possesses the precursors of the pores which are observed upon electronoptical examination.

The electric field strength present during anodizing was assumed^(21,40) to be sufficient to draw OH^- ions and water molecules in the direction of the barrier layer; the OH^- ions and the water molecules in the barrier layer - porous layer interface were suggested to cause a modification of the preformed barrier layer into a more hydrous oxide in localized regions, thereby tending to decrease the effective barrier layer thickness. At the same time, the field in this interface is such as to cause migration of protons away from the barrier layer. This results in a tendency to de-protonate or de-hydrate the oxide in that region. The opposing actions of these two processes were suggested⁽⁴⁰⁾ to explain the observed dependence of the barrier film thickness on the applied formation voltage.

The structure is of the laminar type suggested by Csokan⁽³⁵⁾ for hard anodic oxide film, but, unlike the Csokán model, pores were not thought to penetrate the outer sections completely to the inner layer. The pores were suggested to only penetrate a short distance through the outer layer, in which case the pores form a much less significant

part in this theory than they do in the Keller et al⁽¹⁵⁾ model.

Apart from structural differences, the Keller et al model and Murphy and Michelson model also differ with regard to the mechanism by which anions reach the barrier layer (or inner layer (i)). In the Keller et al model, the anions are considered to diffuse by mass transport down the pore length to the barrier layer surface; in the Murphy and Michelson model, the anions move through the oxide phase on a hydrogen bonded network in which the anion progresses by moving from one lattice unit to the next, making and breaking hydrogen bonds as it proceeds.

A similar model has been suggested by Bogoyavlenskii⁽⁴¹⁾ in which the film was seen as micelles of $\text{Al}(\text{OH})_3$ gel-like material oriented vertically to the aluminium surface by action of the electric field. The micelles, or nonons as the author terms them, are supposedly separated by pores through which further material required for continued growth is transported. These micellular interspaces reach from the outer surface of the nonons to the metal surface, the continuity of the barrier layer, which is observed experimentally, was considered to be due to the filling of the pore ends by nonons when the current was removed. This proposal is unacceptable, since current-voltage^(13,14) and capacitance behaviour⁽⁴²⁾ both indicate the presence of a compact oxide layer adjacent to the aluminium throughout the porous film formation process.

Shreider,⁽⁴³⁾ accepting the presence of pores at the centres of oxide cells, as proposed by Keller et al also suggested that the film is composed of a gel-like $\text{Al}(\text{OH})_3$, apart from the difference in composition of the film, the model proposed is essentially that outlined earlier.⁽¹⁵⁾

Although the Murphy and Michelson and Bogoyavlenskii models offered some new concepts in the structure of porous films, they both lacked experimental varification.

The microcrystallite model.⁽⁴⁴⁾ Some evidence for the concept of small crystallites, separated by hydrated regions containing hydroxyl groups, molecular water and the acid anion was provided by the infra-red spectroscopy studies of Dorsey⁽⁴⁵⁾ and O'Sullivan, Hockey and Wood⁽⁴⁶⁾ who used a combination of infra-red spectroscopic, isotopic exchange and electron microscopic techniques to propose the following morphological and structural model for unsealed films. A freshly prepared anodic film is a relatively open array of amorphous, largely anhydrous, alumina microcrystallites, the surface of which carry hydroxyl groups or ions. Regions between microcrystallites contain molecular water and probably the acid anion. Electron microscopy shows the long cylindrical pores to extend from the barrier layer to the exterior surface. Certain aspects of this model are similar to that proposed by Murphy and Michelson^(40,47) although in the latter model, regular porosity was excluded in favour of a model possessing porosity in the form of intercrystallite voids, with such porosity increasing with distance from the metal substrate.

Alvey⁽⁴⁴⁾ proposed that the anodic oxide film consisted of anhydrous alumina microcrystallites surrounded by a hydrous phase or matrix containing H_2O , OH^- , H^+ , Al^{3+} and the acid anion. There is probably no distinct interface between the microcrystallite and the intercrystalline material, but the ordered Al_2O_3 structure becomes disordered by the inclusion of H_2O , OH^- , H^+ and the acid anion. Furthermore, the intercrystallite matrix is considered to be extensively hydrogen bonded and any molecular water that is present is not "loose"

but forms part of the hydrogen-bonded network.

1.1.4 PORE FORMATION THEORIES.

Since the first observations of the porous nature of alumina films produced in certain electrolytes, a number of theories have been proposed to account for the pore formation using what evidence was available at the time. These early theories include those due to Setoh and Miyata⁽²²⁾ involving nascent oxygen, Wernick⁽⁴⁸⁾ involving peptization of an $\text{Al}(\text{OH})_3$ gel, Baumann's⁽⁴⁹⁾ oxide kernel theory, and Akahori⁽⁵⁰⁾ involving both vapourization of the electrolyte and melting of the aluminium. These theories have been reviewed by Wernick and Pinner⁽⁵¹⁾ and will not be considered further as they have been superseded by more recent evidence, notably the work of Wood, Thompson and their co-researchers.

1.2 PRODUCTION OF THICK, HARD POROUS ALUMINIUM OXIDE FILMS.

As previously stated, aluminium is always covered by a naturally occurring oxide film of between 0.01-0.02 μm in thickness. Very much thicker oxide films may be obtained artificially either by chemical (MBV, Alrok, Alodine, etc., processes) or anodic (Normal and Hard anodizing) treatment.

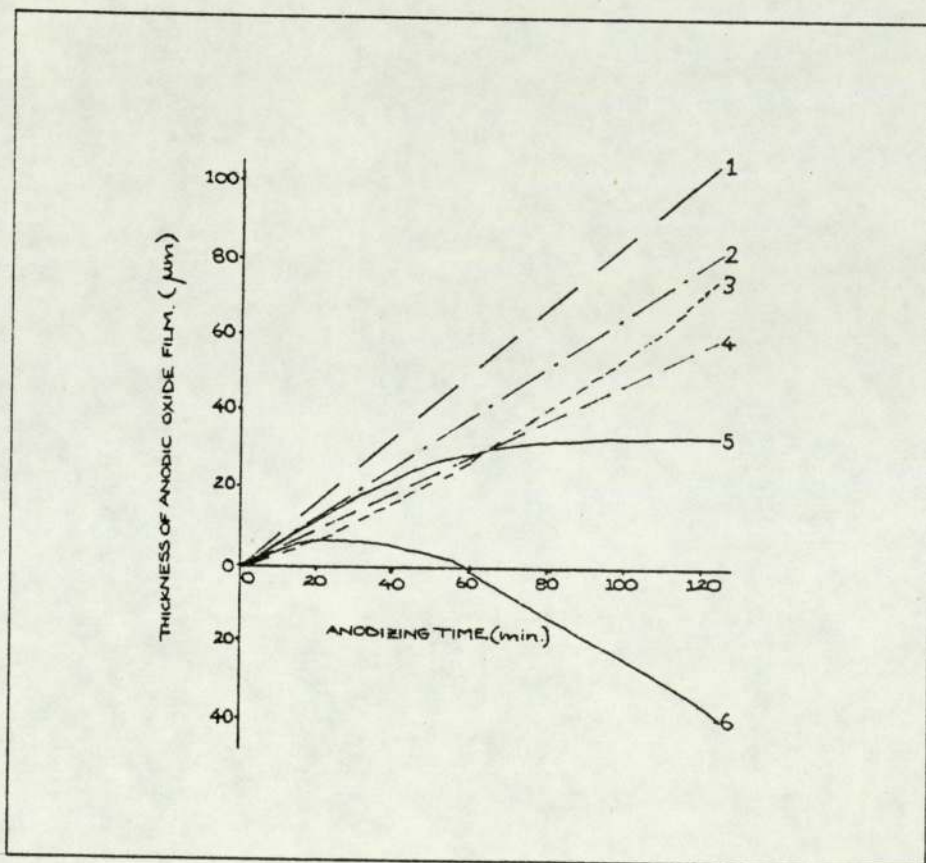
It is found that in anodic oxidation there does not occur an unlimited increase in thickness of the film, the growth of the film has a limiting thickness which is influenced by the electrolyte concentration and aggressiveness, the bath temperature, increase in current density, time of treatment and the composition of the alloy.

This limit to growth in thickness is due to the fact that the formation of the oxide slows down as the anodizing is continued.

This is possibly due to the reduction in anodic current density or to electrochemical side reactions at the anode, also the rate of chemical dissolution of the oxide tends to increase with time and with a rise in temperature of the anode. i.e., this leads to greater porosity of the oxide film and consequently a greater true surface area.

The above was confirmed by Tomashov⁽⁵²⁾ when he obtained the curves shown in Fig. 1.2. below based on the anodizing of aluminium in 20 per cent H_2SO_4 at 25-30°C with a current density of 2 A/dm². (He stated that for other conditions of anodizing the numerical relations would be different, but the general features would remain the same.)

Fig. 1.2. Curves based on results of anodizing in 20 per cent H_2SO_4 bath at 25-30°C with c.d. 2 A/dm².



The different curves relate to the following variables:

4. Reduction in thickness of the metal with time of anodizing.
2. Theoretical increase in thickness of a compact film and of other side reactions.
1. The same as curve 2 but assuming a porosity of 25 per cent in the film formed.
3. Solution of the film.
5. Actual growth in thickness of the film - difference between curves 1 and 3.
6. Change in overall dimensions of the part - difference between curves 5 and 4.

The various factors which influence the properties of the anodic films as well as the progress of the anodic process are summarized in Table 1.3⁽⁵²⁾ on page 22.

Table 1.3(52) Influence of Various Factors on the Properties of Anodic Films and the Progress of the Anodic Process.**

FACTORS	LIMITING FILM THICKNESS.	POROSITY OF FILM.	ADHESION & ADSORPTION PROPERTIES OF THE FILM.	HARDNESS OF FILM.	PROTECTIVE & ANTICORROSION PROPERTIES OF FILM.	VOLTAGE ACROSS BATH IN ANODIZING.	SOLUBILITY OF ALUMINIUM IN BATH IN COURSE OF ANODIZING.
Lower temp. of anode.	+	-	-	+	±	+	-
Lower conc ⁿ of electrolyte. (H ₂ SO ₄)	+	-	-	+	±	+	-
Use of less aggressive [†] electrolyte.	+	-	-	+	±	+	-
Increasing homogeneity of structure of aluminium alloy.	+	-	-	+	+	+	-
Increasing current density* while leaving amount of electricity passed unchanged.	+	-	-	+	±	+	-
Use of A.C. instead of D.C.	-	+	+	-	-	-	+
Reduction in time of anodizing.	±	-	-	+	-	+	-
Temperature increase.	-	+	+	-	±	-	+

** The + sign indicates an increase and the - sign a decrease in the particular property, while the \pm sign indicates that the property passed through a maximum as a result of the particular change of the given factor.

±(44) The aggressiveness of an electrolyte is controlled by the nature of the acid anion rather than the acidity of the solution.

* With the proviso that an increase in the current density is not accompanied by a rise in temperature of the anode. High current densities are used to produce films of a given thickness and hardness in shorter processing times in order to reduce the effects of the attack due to the electrolyte exposure of the surface, giving rise to a softening effect on the film which is being formed. Although the coating increases in thickness as the current density continues to flow, the thickness is not in direct proportion to the amount of current passed because of the above mentioned solvent action of the electrolyte.

Increase of the limiting thickness, therefore, might be attained by lowering the temperature, acid concentration or by increasing the current density. Of these alternatives both decrease in acid concentration and increase in current density require an increase in voltage (in the former case, by increasing the resistance of the bath solution) and thus lead to a local temperature rise at the anode. Cooling of the electrolyte is therefore the principle factor in the production of thick coatings, and due to the local heating effect of the current, resulting from the high electrical resistance of the film, it has in certain cases been found best to cool the actual anode.(52)

Thick, porous anodic films can be formed on aluminium in phosphoric acid,⁽²⁷⁾ oxalic acid,⁽⁵³⁾ and chromic acid.⁽²⁸⁾ However, the majority of thick, porous anodic films are formed in sulphuric acid electrolytes. For the production of films having high surface hardness, cold sulphuric acid and oxalic acid electrolytes are normally used.⁽⁵⁴⁾ However, sulphuric acid is considered to be superior to any other electrolyte, mainly because it can be cooled to below 0°C without crystallization, and the production of hard surface are favoured at this temperature.⁽⁵⁵⁾ [Sulphuric acid is, perhaps, the most versatile anodizing electrolyte known. It produces consistent films under a wide range of extreme conditions. It is cheap, can be cooled below 0°C in solution with water without crystallizing and conducts an electric current readily.]

Because a thickness of 25 μm or more is one of the primary requirements of a hard anodic coating, in fact if an anodic film less than 25 μm thick is required on aluminium there is no reason for the user to specify any particular type of anodizing. However, if thicker oxide coatings are specified then they are known as "HARD" anodic films.

By itself, however, the production of thick films does not necessarily ensure that they will be hard. It has been shown by Keller, Hunter and Robinson⁽¹⁵⁾ and others that increasing the forming voltage may significantly increase not only the thickness of the anodic coating but also its hardness by increasing the size of the individual cells of which the coating is built, and consequently decreases the porosity. At the same time the lesser porosity increases the corrosion resistance, as does the thicker barrier layer, formed at the higher voltages used.

Hard anodizing can be likened to conventional anodizing as hard chromium plating is likened to decorative chromium plating. Essentially,

in practice most hard anodizing processes employ sulphuric acid as the electrolyte, using concentrations between 5 to 20 per cent (vol) at high current densities 2 to 40 A/dm² and high forming voltages of 20 to 120 volts and temperatures below 10°C, with vigorous air or mechanical agitation or both. The oxide films produced are between 12.5 to 200 μm thick, giving a minimum hardness of 400 VHN. To achieve these properties the film is usually unsealed. Sealing involves hydration of the anodic oxide with some loss in hardness and wear resistance, but an improvement in the anodic oxides corrosion resistance and fatigue resistance.

A number of other electrolytes, many of them containing mixtures of acids, are also used and often enable the use of higher operating temperatures and increased current densities. Many of these mixtures were primarily developed as integral colour anodizing electrolytes. The thickest anodic coatings formed on aluminium are produced by hard anodizing processes.

Hard anodic films give increased wear and abrasion resistance and are also used where electrical insulation, corrosion prevention and salvage of over machined or worn parts is required.

1.3 THE HARDNESS OF ANODIC OXIDE FILMS.

Anodically formed films are usually extremely hard and adhere tenaciously to the base metal on which they are formed. The films produced are usually too thin to increase the effective hardness of the relatively soft base metal itself, and will not protect it from heavy impact or high load scratching, although they will resist low load scratching and thus protect the appearance and reflectivity of a polished surface. Conventional anodic films have a hardness value

approaching that of razor steel, whereas films formed by hard anodizing processes exhibit hardnesses comparable with that of chromium.(56)

A primary requirement of a hard anodic film is its hardness. However, the term "Hard anodizing" is somewhat ambiguous because the aluminium oxide formed is actually no harder than that formed by a conventional anodic coating. For example, aluminium oxide powder is intrinsically hard, but a layer of this powder has no hardness whatever, so that hardness testing of an anodically produced layer may be no more than a measure of the cohesive forces of a layer of hard particles in a comparatively porous matrix influenced to some extent by the soft base metal and bearing little relation to the hardness of the particles comprising the structure.

The hardness of the film varies throughout its depth and is inversely proportional to the porosity; thus it is softer at the surface layers due to the solubility of the film in the electrolyte and to hydration of the outer layers of the coatings.

The conditions employed in hard anodizing processes (i.e., low temperatures, dilute electrolytes, high current densities and formation voltages) result in a reduced electrolyte solvent action on the film, reduced time to form the film of given thickness. Thicker cell walls are formed and consequently a denser coating structure. i.e., harder films than those formed conventionally. It is these thick, dense (hard) aluminium oxide coatings that resist abrasion, wear and corrosion significantly better than a conventionally produced anodic oxide film.

Alvey⁽⁴⁴⁾ stated that the criteria for hard anodizing was that the majority of the processes used the conditions as stated above.

The inherent hardness of the anodic film is primarily dependent

upon the extent to which pore wall material is affected during the process of anodizing. The conditions which reduce pore-wall dissolution and promote film hardness are as follows:

1. Total surface area of the oxide exposed to the solvent action of the electrolyte is inversely proportional to film formation voltage. Hence, for a given electrolyte; high voltage conditions limit the effect of pore-wall dissolution and consequently increase the hardness of the film.
2. Rate of pore-wall dissolution is reduced by conditions of low electrolyte aggressiveness. Films formed in dilute acids at low temperatures therefore exhibit lower total porosities and increased hardness.
3. Both macro and micro porosities of a given film are decreased by shorter formation times, which reduce the extent of pore-wall dissolution. Shorter formation times for films of a given thickness are achieved by conditions of increased voltage and current density, which produce harder films. Apart from reducing macroporosity, a decreased electrolyte contact time severely retards formation of micropores, with the result that microporosity towards the outer surface is reduced and the film exhibits a less marked hardness differential across the oxide thickness.

1.4 THE MEASUREMENT OF HARDNESS.

Hardness is a measurement of the resistance of a material to local permanent deformation (either by abrasion, scratching or indentation) but is not dependent on a single physical property, care must therefore be taken when deducing other types of behaviour from hardness values. (See 1.5) Hardness is directly related to strength,

whereas ductility is inversely related to strength - brittle materials usually having a high hardness.

Hardness is usually assessed by the resistance to indentation, whereby a standard shaped indenter is pressed into the material under test by the application of a known load for a specific time interval. Measurements are made of the indentation produced and a value of hardness is obtained by dividing the load by the area of the indentation, thus hardness has the dimensions of pressure.

The usual methods of determining hardness, i.e., Brinell, Rockwell and Vickers contributes little to any assessment of the hardness of the anodic film. These tests point - load the hard anodic film, forcing it into the much softer aluminium substrate. Thus, the value of hardness obtained is influenced by the mechanical properties of the particular alloy and temper, from which the coating was formed.

The use of the Marten's Scratch Hardness Test also gives doubtful values, in which the width of the scratch produced by a diamond point under a certain load is measured.⁽⁵⁷⁾ The results obtained are only approximate and do not take into account variations of the basis metal or variations occurring throughout the coating itself. A modification of the Marten's scratch technique was adopted by Fischer⁽⁵⁸⁾ who determined the hardness of various standard coatings on aluminium alloys in terms of weight (Kg), required to make a scratch penetrate the film. This technique compared the relative hardness of the films.

Spencer⁽⁵⁹⁾ stated that the Marten's Scratch Test is frequently used to evaluate hardness on smooth surfaces where the hard anodic coating is at 50 μm . When using the Marten's Scratch Test, the coating should not be scratched through to bare metal by a hardened

stylus (R_c 66) using a 2000 gramme load with a $25 \mu\text{m}$ radius point on the stylus as it moves over the work surface at a 45 degree angle. This test is performed on unsealed coatings.

Tomashov⁽⁵²⁾ stated that the hardest anodic films produced on aluminium have a hardness on the Moh's scale of between seven and nine. i.e., between that of quartz and corundum. The more porous films are of course softer, the hardest films being obtained on pure aluminium or on aluminium alloys with a homogeneous structure. The hardness of the films is not uniform over their thickness, the hardest, and also the densest, are the layers adjoining the metal, the outer layer of the film has the lowest hardness and density. The results of scratch hardness values are given and also the results of hardness tests on cross-sections of anodic films obtained by using the microhardness tester.

Kliemann⁽⁶⁰⁾ produced the table below comparing the hardness of various materials using the Bierbaum method. (This is carried out microscopically by means of a loaded diamond point scratching the surface. The resulting scratch width is measured microscopically.)

Table 1.4 Hardness of various materials obtained by Bierbaum method.

MATERIAL	ABRASIVE CYCLES PER UNIT PENETRATION
Razor Steel	1550
Glass	2000
Chromium	3100
Aluminium	80
Aluminium hardcoat	
Face of film	140
Centre of film	3000
Base of film	5000

A similar table with similar values was obtained by Tomashov.(52)

Owens(61) states that indentation is the most practical test method, after its proper use is determined. Indentations are made with a portable microhardness tester and a Knoop braille. The less amorphous and more crystalline the structure, the smaller the indentations obtained. Wear is inversely proportional to the size of the indentation. Samples with a 25 μm coating must withstand Knoop indentation using a 500g load, as follows: The length of the major diagonal must not exceed 150 μm for copper - bearing alloys and 130 μm for all other alloys.

Machlin and Whitney(62) used a Knoop indenter under a 500g load to measure the hardness of thick films. Their results were so variable that they considered this technique to be a tool for control and inspection of coatings rather than a measure of true coating hardness.

Campbell(63) obtained by ordinary testing methods the following:

Vickers hardness at 1g load	500
Vickers hardness at 10g load	300
Brinell hardness on alloy of 90 Brinell	90
The Moh's hardness value of between 7 and 9.	

Practically the coating was found to be file hard and very brittle. The apparent hardness by the file test is about 700 VPN but this value was largely a matter of personal judgement.

In practice a useful qualitative hardness test is carried out by rubbing a fine emery paper or cloth, of grade 00, two or three times over the anodic oxide film surface. If the coating is satisfactory the paper should skid over the surface and should not abrade the coating more than is shown by a faint trace of whitening of the emery.(64)

Even though conventional hardness testing is not satisfactory on anodized surfaces for indicating the properties of the coating because of the relative thinness of the coating, it is possible to use micro-indentation testing on cross-sections of the oxide that have been mounted and polished by metallographic techniques. The load applied to the diamond indenter in such a test is very low (15g to 100g) the indentation being measured at relatively high magnification (x 400). Thus making it possible to test hardness at various positions through the depth of the coating⁽⁵²⁾ also known as The Hardness Ladder Search.⁽⁶⁵⁾

As hard anodizing is most frequently applied to aluminium alloys containing substantial amounts of other elements, Campbell⁽⁶⁶⁾ found unanodized particles in the coating and care must therefore be taken to select a representative location for indentation.

Brace⁽⁶⁷⁾ has shown that the VPN values obtained for anodic oxide coatings are not independent of the load nor of the hardness of the base metal and so care should be taken when comparing results from different sources. For example, for an anodic coating formed on a commercially pure aluminium an increase in load from 7.5g to 30g produced an increase in hardness from 353 to 496 VPN.

Pullen⁽⁶⁸⁾ had shown how the microhardness of normally anodized anodic coatings varies across the thickness of the anodic coating, the layers adjacent to the metal being the hardest with a progressive decrease proceeding from the metal to the oxide surface. As the anodizing temperature is reduced this effect becomes less until at 0°C the hardness of a 25 μm film is practically uniform ranging from 430 to 390 Kg/mm^2 across the whole thickness of the anodic oxide profile. This decrease in hardness differential at lower temperatures

is supported by Laszewska⁽⁶⁹⁾ who found similar hardnesses for sulphuric acid films formed between -8°C and 0°C . Campbell⁽⁶⁶⁾ using a two-stage process, was able to produce a film which exhibited a reversed hardness trend across its thickness. This was achieved by operating at 8 A/dm^2 initially and then reducing to 4 A/dm^2 to form a softer coating, the resultant film had a hardness of 230 Kg/mm^2 adjacent to the metal compared with 450 Kg/mm^2 on the outer position.

Tajima⁽⁷⁰⁾ was able to form a relatively hard oxide film (400 Kg/mm^2) in 2 per cent oxalic acid solution at a temperature of 12°C using a current density of only 1 A/dm^2 .

A mixed electrolyte of $\text{Al}_2(\text{SO}_4)_3 \cdot 18\text{ H}_2\text{O}$ and oxalic acid dihydrate containing small additions of glycerol⁽⁷¹⁾ is claimed to produce continuous films of up to $70\text{ }\mu\text{m}$ at ambient temperatures, with a hardness ranging from 396 to 520 Kg/mm^2 .

Oechslin⁽⁷²⁾ has reported in considerable detail the Vickers hardness values of a wide range of alloys hard anodized to various film thicknesses using the Oxal process (developed in Switzerland). The hardest films (in excess of 500 Kg/mm^2) are produced on pure aluminium or alloys with the lower levels of alloy additions. It is usually necessary, however, to couple the hard surface with a high mechanical strength and hardness in the basis metal than is possible with pure aluminium. The preferred alloys being the Al-Mg-Si alloys which gave films ranging in hardness from 425 - 480 Kg/mm^2 .

Film thickness has a marked effect on the hardness profiles of films formed on all the alloys. For film thickness of $150\text{ }\mu\text{m}$ there is a difference of about 100 Kg/mm^2 between the film surface and the layers near the metal/oxide interface, while this is only 10-50 Kg/mm^2 for films of $50\text{ }\mu\text{m}$ thickness.

Lysaght⁽⁷³⁾ reviews Vickers microhardness testing and states that the weaker the chosen measuring force - or the smaller the indentation - the more will the test be confined to the surface layers of the substrate. Mechanical polishing may change the surface hardness, electrolytic micro-polishing is therefore recommended. The measuring accuracy is $0.2 \mu\text{m}$ i.e., for an indentation of $10 \mu\text{m}$ diagonal and an error of 2 per cent in the diagonal, then as the value is squared in the calculation the error will be 4 per cent of the hardness value. With larger indentations the effect of reading error will correspondingly decrease.

Alvey, Thompson and Wood⁽⁷⁴⁾ stated that with reference to microhardness tests on porous films, the intrinsic hardness of the anodic alumina, is indeterminate. The measurements being severely affected by the inherent porosity of the oxide film. In fact the resulting indentation is not a measure of the plastic compressability of the film material but the result of the collapse of pore wall material into the voidage of adjacent pores.

Therefore, the hardness value obtained was interpreted as the inherent hardness for the film and not the intrinsic hardness of the anodic alumina itself. The hardness was found to depend on the relative direction of the pores with respect to the direction of the indentation. Surface measurements being parallel to the pore direction and profile measurements being perpendicular to the pore direction. This restricted examination of hardness measurements to profile only.

The relevant British Standard⁽⁶⁵⁾ gives detailed instructions on the preparation and carrying out of the Vickers microhardness test and requires that the readings so obtained shall not be less than 350 Kg/mm^2 .

1.5 ABRASION RESISTANCE OF THE ANODIC OXIDE FILM.

The abrasion resistance of anodic films has been used extensively as a measure of "hardness", but it is doubtful whether there is any exact mathematical correlation between a series of such measurements and hardness as expressed by the VPN. At best, if the abrasion resistance is high or low, then the surface hardness of the anodic film may be high or low, but no absolute correlation can be made between the degree of change of abrasion resistance or microhardness from one type of film to another. Thus, Campbell⁽⁶⁶⁾ states that a hard coating registering 450 VPN will have the wear resistance of a tool steel of 950 VPN. Also, even though there is often a significant increase in hardness between the base metal and anodic film, there is often no such increase in the abrasion resistance. This is due to the fact that the hardness measurements deal with one given small section of the anodic film, whereas the abrasion resistance is an average figure for the whole film.

Measurement of the abrasion resistance is carried out using various techniques such as

- (i) Scratch method⁽⁶⁶⁾
- (ii) Resistance to rubbing wear⁽⁷⁵⁾
- and (iii) Erosion by impinging abrasive material (B.S. 1615. 1972).

Generally, the tests measuring directly the wear resistance of the coating are a more reliable guide to its subsequent performances than hardness measurements alone.

1.6 THICKNESS TESTING OF ANODIC OXIDE FILMS.

Thickness is the most frequently specified property of anodic oxide coatings and its importance lies not only in its effect on

service life, but also in that it is a major factor in determining the price at which anodized work is sold to the anodizer's customer. Failure to produce the minimum required thickness or recording of values significantly in excess of the required level provide an indication that the anodizing process is not under control. If the coatings are too thin then this will give rise to an unfulfilled contract to a customer, whilst too thick a coating represents a lost profit to the anodizer.

Anodic coating thickness falls into broad categories associated with its function, as described in Table 1.5 (76) below.

Table 1.5.(76) Thickness of oxide vs Function of anodic coating.

THICKNESS RANGE ($\mu\text{m}'\text{s}$)	FUNCTION
1 - 2	Paint base.
5 - 15	Decorative, bright anodized. Corrosion resistance (Chromic acid).
15 - 30	Dyed coatings. General decorative applications.
Usually 25	Outdoor, architectural uses.
30 - 100	Hard anodizing, engineering applications.

Thickness may be measured destructively or non-destructively. Early test methods were essentially destructive and depend upon either the use of separate test-pieces, the removal of coating from the sample being tested, or sectioning through the component. More recently

non-destructive techniques have been developed which have made possible the routine checking of film thickness on individual pieces at low cost.

Chemical destructive tests do not take into account variations in density of anodic coatings resulting from different pore structures. Metallographical destructive tests are limited in scope by virtue of the accuracy of the operator and the resolving power of the microscope used. Non-destructive tests, whilst being considered not very accurate, probably provide the anodizer with the most effective means of thickness control.

1.6.1 DESTRUCTIVE THICKNESS TESTS.

1.6.1.1 GRAVIMETRIC (STRIP AND WEIGH) METHOD.

This was one of the first methods used and is still the most commonly used chemical destructive test and is based upon the fact that a solution consisting of phosphoric acid (sp.gr. 1.75) 3.5 per cent (w/v), chromic anhydride (CrO₃) AnalaR 2.0 per cent (w/v) used at 85 - 100°C will strip an anodic coating from the metal without attacking the base metal. The anodized specimen (anodized surface area known) is first weighed and then stripped in the above solution, washed, dried and re-weighed and immersed until a constant weight is obtained. The loss of mass is taken as the mass of anodic coating. Coating thickness is calculated from the expression.

$$T = \frac{1000M}{a\rho}$$

Where T is the thickness of coating (in μm)

M is the mass of the coating (in mg)

a is the surface area of anodic coating (in mm^2)

ρ is the density of the coating (in g/cm^3), taken as 2.5.

This method is applicable to all hard anodic coatings except

those coated or impregnated with organic material. Test pieces should be cut so that their area is easily measured. (Small errors in area producing large errors in film thickness.) Alloys containing large amounts of elements (>2 per cent of copper and/or silicon) give a blackened surface when stripping is complete, which alters the weight loss figure if the test piece is left in the solution for too long. The above method is specified in B.S. 5599: 1978 Appendix B.

Other chemical solutions have been proposed for checking the thickness of anodic coatings, particularly strong sodium hydroxide solutions (100 g/l at 25°C), where the time taken to penetrate the coating has been used to measure the coating thickness. However, according to Kape⁽⁶³⁾ such a test is extremely unreliable.

Destructive tests of non-chemical nature almost always make use of the microscope.

1.6.1.2 THICKNESS BY MICRO-SECTIONING.

This is the classical metallurgical laboratory technique in which a piece is removed from the anodized specimen by careful cutting and is mounted in one of the usual mounting mediums so that when polished it provides a cross-section through the anodic coating at right angles to the surface being examined for thickness. Sometimes a thin sheet of unanodized aluminium foil is placed around the specimen before mounting to protect the anodic coating and to achieve contrast between the coating (which always appears a grey colour) and the mounting medium. The coating thickness can then be measured directly through a suitable calibrated eyepiece. This method is specified in B.S. 5411: Part 5.

The method only gives a measure of coating thickness at one

point, to achieve a measure of average coating thickness over an area of a part or a whole part then many sections have to be taken, and the results averaged. Accurate results are only obtained ($\pm 0.8\mu\text{m}$) if mounting has avoided tapering effects. But this test is the referee method for most anodic coating thicknesses.

1.6.2 NON-DESTRUCTIVE THICKNESS TESTS.

With the exception of eddy current measuring devices and direct micrometer measurements other non-destructive tests are very dependent upon the nature of anodized material, particularly as influenced by the alloy, anodizing process and sealing method used.

1.6.2.1 THICKNESS MEASUREMENT WITH AN OPTICAL SPLIT-BEAM MICROSCOPE.

This technique enables the direct measurement of the coating thickness of a transparent film (not applicable to thick hard anodic films) where a beam of light is projected on to the surface of the coating at 45° incidence, part of the light is reflected from the upper surface of the coating, whereas the remainder is reflected from the interface between the film on the metal.

Owing to the optical geometry of the microscope the coating is revealed as a grey band in the eye piece (being effectively the distance between the reflected and refracted beams) and its thickness may be directly measured on a vernier scale. This method is especially useful for the measurement of bright anodized sulphuric acid coatings up to $20\ \mu\text{m}$ thick. With opaque or etched silver coatings the definition of the film is appreciably lost, and with coloured coatings the refracted beam is dispersed rendering measurement impossible.

The method is specified in B.S. 1615: 1972. Appendix D and in I.S.O. 2128.

1.6.2.2 EDDY CURRENT THICKNESS TESTING.

This has become the most widely used non-destructive testing technique in production use, and has the advantage that it can be used on a wide range of components and is not affected by brightness or mattness of the surface, the presence of a dye, etc. It is based on the fact that at a suitably chosen high frequency the film thickness is directly proportional to the capacitance:

$$C = \frac{F \epsilon}{4 \pi d}$$

Where C = capacitance.

ϵ = dielectric constant of the coating.

F = the area under test.

d = the thickness of the insulated film.

Eddy current devices comprise a coil energised with a high frequency alternating current connected to an instrument having a scale calibrated directly in coating thickness. The reaction of the eddy current generated in the material varies strongly with the separation of the coil from that material.

Firstly, the instrument is allowed to 'warm-up' and then zeroed by placing the coil on an unanodized test piece of the same alloy specification in the same form as the anodized test material. The coil is then placed on an anodized material (of the same specification and fabricated form as the anodized test material) of which the coating thickness has been accurately determined by micro-sectioning, in order to calibrate the instrument. (Sometimes plastic foils of known thickness are used).

The coating thickness of the anodized test material is then directly measured. Used properly the thickness of anodic coatings can be measured to 1 or 2 microns.

The following precautions should be taken:

- (a) The alloy surface condition of the reference and test piece should, as far as possible, be identical.
- (b) Special probes must be used for curved surfaces.
- (c) Accurate measurements will not be obtained using plastic foil calibration.
- (d) One measurement is never sufficient, at least five and preferably ten should be averaged.

Guidance on the use of eddy-current instruments is provided by Latter.⁽⁷⁷⁾ The method is specified in B.S. 1615: 1972, Appendix C and in I.S.O. 2360.

1.6.2.3 THICKNESS BY ELECTRICAL BREAKDOWN VOLTAGE OR RESISTANCE.

It had been observed by early investigators that there was an approximately linear relationship between film thickness and electrical breakdown voltage of anodic oxide coatings.⁽⁵⁴⁾ Beyond 15-25 μm however, the relationship becomes increasingly non-linear.

Since the method relies on the breakdown of the coating at a very high applied voltage, a spark occurs at breakdown giving a black mark on the anodized material. Thus, the test is only applicable to coatings on non-significant surfaces. This method is specified in B.S. 1615: 1972, Appendix T and I.S.O. 2376.

The use of resistivity (measuring the voltage required to produce a constant flow across the coating - say 100 microamps) has been suggested as a low-cost thickness tester because electrical resistance is roughly proportional to the film thickness.

The results obtained vary significantly with the sealing process

employed and with the relative humidity. Unless the entire history of the anodized material is known, such electrical procedures are useless as test methods.

Johnson⁽⁷⁸⁾ indicates that the least expensive and most readily performed (on a production basis) of the methods determining coating thickness would be the "growth method". This is based upon the theory that the growth process is inwards toward the metal and the first formed coating is at the outer surface, and the last formed is at the metal-coating interface. Since growth of the coating is inward from the original surface, it would seem that there should be no increase in external dimensions. This is not true, however, since aluminium oxide occupies a greater volume than the metal from which it was formed. This volume growth is fairly consistent over a wide range of alloys, and the dimensional increase produced by conventional anodizing is approximately 30 per cent of the coating thickness, with hard anodizing the increase is approximately 50 per cent.

With this test it is only necessary to accurately determine a suitable gauging dimension on a particular sample part prior to anodizing, and then inspect the same part after coating using a micrometer. This method tended to show a slightly lower thickness than the stripping method and would result in a more conservative measurement of coating thickness. He compared three thickness methods and found the results to agree within 5 to 10 per cent.

1.7 COATING RATIO.

The coulombic efficiency for the formation of porous oxide films on aluminium in sulphuric acid has been determined by many workers. This efficiency can be expressed in terms of coating ratio, which is

given by

$$\frac{\text{Weight of oxide formed}}{\text{Weight of aluminium consumed}}$$

Edwards and Keller⁽⁷⁹⁾ investigated the relationship between the weight of oxide formed and the weight of metallic aluminium lost. This was done by weighing a sheet of aluminium and anodizing it electrolytically for a determined period. The coated specimen was then weighed, the oxide coating dissolved off without attacking the metal, and the bare sheet re-weighed. From these measurements, the weight of aluminium reacting and lost from the sheet and the weight of oxide formed can be calculated. This data can be calculated as an "efficiency ratio" R, which is the ratio of the oxide formed to the weight of aluminium reacting.

If all of the aluminium reacting appeared as oxide, the efficiency ratio would be $(\text{Al}_2\text{O}_3/2\text{Al}) = 1.89$. The data calculated by Edwards and Keller show no values above about 1.46. This was explained by the fact that some of the formed oxide dissolved in the electrolyte. Keller and Edwards did not take into account adsorbed ions such as sulphate from the electrolyte. This would tend to raise the apparent value of the efficiency ratio, while the dissolution of the oxide by chemical attack caused by the electrolyte would lower the efficiency ratio.

Anderson⁽⁸⁰⁾ stated that practical values of the efficiency ratio could be represented by the equation.

$$R = (1 - S) (n \text{ Al} + \text{Al}_2\text{O}_3) / 3\text{Al},$$

where n is the fraction of the diffusing Al^{3+} ions that have not penetrated to the solution; S is the fraction of oxide layer that is dissolved by the acid. It was stated that R can never be greater than 1.59 in this type of film.

Mason and Slunder⁽⁸¹⁾ stated that the "coating ratio" is a measure of the overall anode efficiency with respect to coating formation. No assumptions regarding the possible composition of the coating are required in the calculation of this "coating ratio". A coating ratio lower than 1.89 (theoretical) indicates that alumina has been dissolved by the electrolyte either chemically or electrochemically.

They demonstrated that within certain limits the coating ratio is increased by decreasing the concentration of the electrolyte or the temperature, or by increasing the current density.

In a later paper⁽⁸²⁾ the above mentioned work was extended to include conditions favouring higher coating efficiencies which result in improved physical properties. Low temperatures and high current densities, which permit a shorter time of immersion in the electrolyte, and the addition of substances such as oxalic acid to the electrolyte, favour the formation of such coatings. The paper is mainly an investigation of the competition between the rate of solution of the coatings. Hence, when high-current densities and low temperatures are employed to produce thick oxide coatings, it appears that the rapid formation of solution products of the pores causes a decrease in the rate of solution of the oxide coating, which in turn produces higher coating ratio values.

In the U.S.A. and in Great Britain, the "coating ratio" is sometimes used as a control method for evaluating the efficiency of the anodizing process in production work.

1.8 PRETREATMENT AND STRUCTURE.

In electroplating, the coating is deposited at the cathode

(negative electrode) and is conductive. In anodizing the coating is produced at the anode (positive electrode) and is non-conductive. The anodic coatings grows by conversion of the surface of the aluminium to oxide and is not a deposited coating, as with electroplated coatings.

The structure and appearance of anodic oxide coatings vary considerably with the basis metal composition. Streaky coatings may be due to structural deformation in cold working, while the dendritic structure of some castings may be reproduced on the anodic oxide coating.

Surface preparation also affects the appearance and quality of a hard anodic coating. Csokán⁽⁸³⁾ showed that while untreated aluminium produces uniform but slightly rough coatings, mechanical polishing before anodizing gives a fine grained, smooth and more attractive film. Electropolishing may give rise to a non-uniform structure showing glassy oxidation zones with fine lines between the primary nuclei of the anodic coating, explained by Csokán as due to the thin oxide film left on the surface by electropolishing.

Kape⁽⁵⁵⁾ showed that chemical polishing and electropolishing caused the hard anodic coating to be very glossy, and the metal assumed an almost enamelled appearance. Etching, was satisfactory, provided it was not overdone, as a heavily etched surface was prone to "burn" in the initial stages of the anodic treatment. A buffed surface gave a finish similar to that produced by chemical polishing or electropolishing.

1.9 THE EFFECT OF ALLOY COMPOSITION ON HARD ANODIZING.

Because of the many and varied applications for anodic films on aluminium and the desire for improved quality, a thorough understanding is required of the behaviour of the elements and intermetallic compounds during anodizing. Alloying elements and intermetallic compounds of the basis metal influence the anodic oxidation process

and the physical-chemical properties of the hard anodic films in a variety of ways. The elements exist in the alloy and subsequently in the hard anodic film finely divided, either in the elemental state or as intermetallic compounds. (Silicon may be observed as massive elemental particles.) The concentration of these elements in the hard anodic film depends on their solubility in the electrolyte as the electrochemical reaction proceeds.

Surface finish, maximum film thickness, hardness and wear resistance and the colour of the hard anodic film and solubility in its electrolyte are all influenced by these elements.

The production of anodizing quality aluminium involves the control of the intermetallic particle size and distribution, it is important to avoid gross particles and to prevent the clustering of particles.

A number of the commercial hard anodizing processes were developed as a result of the difficulty encountered during the anodizing of certain alloys. It is not possible to hard anodize aluminium alloys containing over 3 per cent copper or 7.5 per cent silicon using the d.c. Martin Hardcoat process⁽⁸⁴⁾ or Alumilite process⁽⁸⁵⁾. The result being that the Hardas⁽⁸⁶⁾ and Sanford⁽⁸⁷⁾ processes and others were developed to deal with such "difficult" alloys. These processes were all developed by industry and most of the published work was carried out on examining the effects of fixed anodizing schedules on the properties of films formed on a wide range of industrial alloys.

A number of investigators have worked on the behaviour of intermetallics when conventional anodizing is carried out on the aluminium alloys, and it may be justified to relate the effects obtained to those that would be obtained when hard anodizing of the

alloys is carried out.

Keller et al^(88,89) grouped the alloying elements into three classifications: those that form solid solutions and have little effect on the anodic film; those that form intermetallic compounds which are either not appreciably dissolved or oxidized by the anodic oxidation, or are readily dissolved or oxidized by the treatment.

Spooner⁽⁹⁰⁾ by determining the chemical composition of anodic films formed in sulphuric acid on commercial aluminium alloys tried to establish which alloying elements were inert, or partially or totally dissolved. Wood et al⁽⁹¹⁾ were the first to report the use of electron probe microanalysis to determine the chemical composition across anodic films. Wood and Brock⁽⁹²⁾ later substantiated the original work and extended it to the examination of the anodic behaviour in sulphuric acid of a few small constituents, illustrating the behaviour with back scattered electrons. Cote et al⁽⁹³⁾ carried out investigations into four aluminium alloys using the electron probe microanalyser and classified the compounds according to their reactivity during anodizing.

Thompson⁽⁹⁴⁾ states that alloys with greater than 0.5 per cent copper impart to their hard anodic films an olive green colour, particularly apparent when wet.

Copper imparts low electrical resistivity to the film whilst in the process of oxide formation, which under ideal conditions encourages the formation of thick hard films. Surface finish deteriorates depending on grain size and direction and the heat treated state of the alloy. Alloys containing a high proportion of manganese are coloured medium grey to black depending upon thickness. The heat treated state of these alloys is critical.

Zinc alloying additions encourage the formation of thick moderately hard films, though the film to base metal bond is brittle and chips easily, particularly above 5 per cent zinc. Films are clear or light grey in colour depending on thickness.

Magnesium alloying additions encourage the formation of thick films and electrical resistivity is low during film formation. Certain alloys suffer from brittle film to parent metal bond when hard anodized in a 10 per cent volume electrolyte. Films are clear or light grey depending on thickness.

Silicon is a constituent of numerous casting alloys and its influence is modified by the presence of other alloy additions, the casting technique and heat treatment.

All silicon containing alloys anodize medium to dark grey in colour, hardness, wear resistance and maximum film thickness varying with alloy, casting technique, heat treatment and electrolyte strength. Surface finish is highly sensitive, particularly to modified and unmodified structure.

Hence, where one or more alloying elements dominate, their influence is not predictable and the behaviour of that alloy has to be determined by direct experimentation.

1.10 HARD ANODIZING* - COMMERCIAL PROCESSES.

Hard anodizing - deep anodizing, double anodizing, hard coating - has been practised for many years and it is doubtful who first recognized, and when, that a cooled solution of sulphuric acid, when used as an electrolyte, produced anodic coatings on aluminium of high surface hardness.

In 1904, F. Fischer⁽⁹⁵⁾ produced coatings up to 300 μm thick in 24 per cent H_2SO_4 electrolyte by anodizing aluminium tubes while they were cooled internally. Later patents of German origin⁽⁹⁶⁾ claimed processes for producing friction resisting or anti-frictional surfaces, while Aluminium Colour Inc., patented a low-temperature glycerine - sulphuric bath in 1923,⁽⁹⁷⁾ just after Gower and Windsor Bowen's "Soft and Hard Film" patent⁽⁹⁸⁾ of 1932. These early patents, were however, not commercially exploited to any great extent and indeed, did not cover the combination of essentials which are necessary for a good hard anodizing process. The technique used by the majority of the hard anodizing processes involving the use of low temperatures, high current densities and high formation voltages, in dilute electrolytes which have the combined effect of reducing both the rate of dissolution of the anodic oxide film (alumina) and also the time required to form a film of given thickness.

The hard anodizing process came into its own during the Second World War, when the aircraft industry demanded the light weight of aluminium, coupled with rigid corrosion resistance requirements.

*Except where otherwise stated, reference is made to hard anodizing as carried out in H_2SO_4 - H_2O solutions.

The first work carried out in the production of thick hard anodic coatings for engineering applications with oxalic acid was described by Schenk⁽⁹⁹⁾ and with sulphuric acid by Tomashov⁽⁵²⁾ and Smith.⁽¹⁰⁰⁾

Tomashov's⁽⁵²⁾ was one of the first publications to discuss in depth the production, properties and utility of hard coats. He showed that by cooling the sulphuric acid electrolyte (20 per cent vol.) to between 1 - 3°C and using 2 to 5 A/dm² and thus slowing down the rate of dissolution of the oxide, coatings of up to 250 μm could be obtained with excellent wear resistance and heat insulation. During four hours of treatment he built up oxide coatings of 200 μm thickness using a gradual rise in voltage from 23 to 120 volts as the oxide thickness increased.

In the case of aluminium alloys, lower voltages were required. The porosity was also found to vary with the alloy composition, greater porosity being found in highly alloyed aluminium.

In later work on this process,⁽¹⁰¹⁾ it was found that these coatings, as distinct from thinner coatings, were only partially hydrated, and both hydration and porosity were more pronounced at the surface, as shown by a decrease in the microhardness in the top layers. Film growth in 10 - 30 per cent (vol) sulphuric acid at 0.5°C and 2 - 4 A/dm² was limited by sparking and the thickness at which this occurred increased with acid concentration.

A number of commercial hard anodizing processes have been developed since the Second World War using direct or superimposed a.c. on d.c. Some of these processes are referred to in Table 1.6⁽³⁶⁾ below. With reference to this table it can be seen that apart from one or two exceptions, most of the hard anodizing processes use a sulphuric

Table 1.6(36) COMMERCIAL PROCESSES FOR HARD ANODIZING.

ELECTROLYTE	TEMP °C	CURRENT DENSITY (A/dm ²)	STARTING & FINAL VOLTAGE (volts)	PROCESS TIME (min)	THICKNESS (µm)	NAME OF PROCESS WITH REFERENCE.
15% H ₂ SO ₄	+14 - +4.4	2.0 - 2.1	26 - 120	90	50	Aluminium Co. of America (85)
15% H ₃ BO ₃ +4% Na citrate	+60 - +70	0.4 - 0.6	100 - 300	240	200	Finsterwalder (102) (Isolations GmbH)
10% H ₂ SO ₄	+10	250 W/dm ²	15-25 - 80	60	100 - 130	Hiduran Process (103) (High Duty Alloys Ltd.)
15% H ₂ SO ₄	-1 - +4.5	2.0 - 2.5	25-30 - 40-60	60 120 240	25 - 35 75 - 80 150	Martin Hard Coat Process (84) (Aluminium Co. of America)
10% H ₂ SO ₄ +H ₂ C ₂ O ₄ · 2H ₂ O	+8 - +10		25 - 60	60	25 - 30	Alumilite Process 225, 725 (85)
10-15% H ₂ SO ₄	0 - +4	5.0	a.c. 10-12 - 60-70 with 20-24 - 120-140 d.c. superimposed	60	50 - 60	Alumilite Process 226, 726 (104) (Aluminium Co. of America)
6 - 8% H ₂ C ₂ O ₄ · 2H ₂ O			WITH ALLOY			Hardas Process (86) (Hard Aluminium Surfaces Ltd.)
6 - 7% H ₂ SO ₄ +3-6% organic addn	+4.5 - +18 +4.5 - -18	1.3 - 2.0	10 - 150	40	65	Sanford Process (87) (Sanford Process Corp.)
10-20% H ₂ SO ₄	-6 - +10		30 - 280	160	115 - 150	Tomashov-Balobsheski Process (105)
10-15% H ₂ SO ₄	+8	4.0	20-25 - 60	60	55 - 80	Alcoa Process (106)
5.5% HCOOH +8% H ₂ C ₂ O ₄ · 2H ₂ O	+15 - +25	3.0 - 6.0	45 - 90		100 - 250	Lelong-Segond-Herenguel Process (107)
20% H ₂ SO ₄	1 - 3	2.5	23 - 120	240	200	KEIN Process (52)

acid electrolyte at slightly lower concentrations than the conventional anodizing process* Localized overheating is counteracted by vigorous stirring of the electrolyte, while to minimize dissolution of the anodic oxide, the temperature is kept below 5°C. The Martin Hard Coat (M.H.C.) process developed by Burrows⁽¹⁰⁸⁾ of the Glen L Martin Co., and later acquired by the Aluminium Co. of America was probably the first real claim for a hard anodizing patent which covered the production of hard, abrasion resistant coatings produced in 5 to 70 per cent sulphuric acid, at around 0°C, agitated uniformly throughout the anodizing cycle. This process is particularly suitable for the production of thick coatings.

Unfortunately, the patent was not particularly well phrased and implied that solid carbon dioxide had to be used for cooling, and that carbon dioxide had to be bubbled through the electrolyte during the course of the anodic process. The method of agitation was also not defined. As a result, quite a number of patentees issued their versions of basically the same process, taking into account the basic factors required for good hard anodizing technique. These being:

- (i) Efficient flow of electrolyte over the work, to remove heat formed as fast as it builds up, during anodizing.
- (ii) Low-temperature operation, by external cooling systems.
- (iii) Use of sulphuric acid, with or without organic additives.

*In this thesis "Conventional sulphuric anodizing" refers to conditions of: 15 - 25 per cent (wt) H₂SO₄, 21 - 30°C, 1.0 - 1.5 A/dm² current density at 13 - 20 volts and coating thicknesses up to about 30 μm.

An in depth study of the M.H.C process was carried out by Gillig.(109)

Where thinner films are required it had been found possible to work at slightly higher temperatures, and this has been made use of in a range of alternative processes of the Aluminium Co. of America designated Alumilite 225 and 226 for wrought alloys and Alumilite 725 and 726 for cast alloys.(85,104)

A limitation associated with the d.c. process is a tendency to "burning" unless the anode is provided with efficient agitation and electrical contact. (A brief discussion of "burning" is given in Appendix IV).

According to Jenny,(110) alloys containing over 3 per cent copper or 7.5 per cent silicon are difficult or impossible to treat by d.c. processes.

1.10.1 USE OF DILUTE SULPHURIC ACID ELECTROLYTES.

Most of the work on the use of dilute sulphuric acid electrolytes to form hard anodic coatings was carried out in Hungary by Csokán.(35,36,37) The electrolytes used contained 0.5 to 2.0 per cent sulphuric acid. Under these conditions, 150 - 200 μm coatings can be built up in one hour at 20 - 80 volts and at temperatures of between -5°C to 5°C with higher hardness values. e.g. 450 - 520 Kg/mm^2 (35) and lower porosities, e.g. 2 - 4 per cent, than in concentrated acid. (The porosity is normally 14 - 20 per cent).

In these dilute solutions evidence is given that not only the structure of the main coatings but also the formation of the barrier layer is different than in more concentrated acid.(36) These coatings have barrier films the thickness of which goes through a maximum of approximately 38 nm at a voltage of 40 -50 volts. Analysis of the coatings shows that they contain approximately 25 per cent anhydrous

aluminium sulphate as well as boehmite.

Csokán and Hollo⁽¹¹¹⁾ produced coatings from 100 - 250 μm thick in 0.1M sulphuric acid at a temperature of -1 to $+1^\circ\text{C}$ and at 45 - 60 volts the hardness of which was as high as 600 - 620 VPN. They found that below 30 volts true hard films do not form and that above 70 - 75 volts local overheating occurs, so an intermediate working range must be observed when anodizing in dilute sulphuric acid.

Csokán found that groups of pores nucleated at distinctly separate sites on the electrode surface^(35,36) which developed into irregular, distorted, pore cellular structures with a fibrous nature which could be observed as blocks of oxide growing randomly on the electrode surface. These blocks, which differ in size, shape and orientation, increase in thickness and spread laterally, presumably due to pore formation and growth at their peripheries, with increasing anodizing time. At the same time newer blocks of oxide form between the growing larger areas and eventually all merge to give a continuous thick hard anodic film which appears, in section, to have a prismatic structure. The preferential anodization of certain sites leading to these oxide blocks appeared to be related to subgrain structures of the substrate.⁽³⁶⁾ This nucleation and growth process was observed continuously during hard anodizing using optical microscopy and cine film techniques.⁽³⁷⁾

Plant practice in Hungary⁽¹¹²⁾ is to work from -1 to $+1^\circ\text{C}$ at 50 - 65 volts and a current density varying from 4 to 20 A/dm^2 .

Although such electrolytes do give hard coatings, throwing power difficulties in recesses and blind holes would be expected under practical conditions.⁽¹¹³⁾ Another disadvantage of the very dilute sulphuric acid bath is that the electrolyte may freeze on the cooling

coils at low temperature, and this must be prevented by the use of adequate circulation of electrolyte.

1.10.2 CURRENT SUPPLY.

The choice and control of the current supplied to the work is very important in the anodizing process. One of the simplest operating techniques is constant current anodizing. One of the practical drawbacks to constant current (or constant current density) hard anodizing is that over the anodizing time, the total wattage input continues to rise. This means that the rectifier required must be able to cope with a peak load rather than a much lower average demand load, and that the heating of the film increases significantly with time.

Instead of using continuous control an alternative method suggested in the Sanford Process⁽⁸⁷⁾ is to allow the current to fall by up to a fixed percentage of the original before raising the controlling voltage. This process probably makes the widest use of addition agents. It was developed principally to cope with difficult aluminium alloys (the initial starting point voltage of the process depends upon the nature of the aluminium surface) and is described as a sulphuric acid bath containing small additions of peat extract, nonyl alcohol, polyethylene glycol and methyl alcohol. This solution is used at -10°C and a $50\ \mu\text{m}$ coating is claimed to be obtained at 1.0 to 2.0 A/dm², the voltage being raised in stages from 15 to 60 volts.

The Hiduran process⁽¹⁰³⁾ uses constant wattage d.c. power, in place of the constant current density source usually employed for hard anodizing. The electrical supply is controlled by an integrator which measures voltage and amperage and controls the supply to keep

them constant. Constant wattage enables the rate of heat extraction to be kept constant throughout the process, decreasing the liability of burning at edges and corners. However, burning may occur in the critical initial first 10 minutes of anodizing before the anodizing conditions have become stabilized.

The experiments of Kape⁽⁵⁵⁾ were carried out to clarify the influence of the anodizing variables. Most of the experimental work was carried out in 10 per cent (vol) sulphuric acid at 10°C, using constant wattage. He proved that this method was capable of giving good results in the hard anodizing of various aluminium alloys.

Blumenfeld and Schurig⁽¹¹⁴⁾ studied hard anodic coatings of 25 - 100 μm thickness as applied to 6061-T6 aluminium alloy using constant wattage d.c. power as used by Kape.⁽⁵⁵⁾ The effects of temperature, wattage and treatment time on the rate of build-up of the anodic coating was discussed with their relationship to abrasion resistance and dielectric breakdown voltage. A comparison was made between the properties of hard anodic coatings obtained from hard coatings applied with the use of constant wattage to those obtained from the M.H.C. and Alumilite 226 processes. The authors concluded that a considerable time saving could be obtained if constant wattage was used, and from data, obtained the optimum operating conditions for constant wattage hard anodizing of 6061 - T6 aluminium alloy was a wattage density of 240 W/dm^2 and a temperature of between 5 to 10°C.

Most hard anodizing carried out in the U.K. employs direct current. However, a number of processes employing other forms of current have been developed and introduced industrially. The more important processes will be discussed below but the other processes will be

mentioned in the Extended Bibliography.

The development of hard anodizing processes using superimposed a.c. on d.c. was influenced by Jenny's work⁽¹¹⁰⁾ with oxalic acid as the electrolyte. A d.c. voltage of 60 volts was used with superimposed a.c. to give current densities from 1.0 to 3.0 A/dm² in up to 6 per cent oxalic acid held at 20°C. The maximum film thickness obtained increased with acid concentration but at high current densities the relative growth rate decreased as the acid concentration increased. Jenny's work also showed that the abrasion resistance of the coatings was greater for conventional anodizing when produced by combined currents.

[The use of a.c. is made possible by a rectifying action, as a result of which only the anode directed half-waves bring about the formation of the oxide layer.]

Campbell⁽⁶³⁾ used the same superimposed a.c. conditions as Jenny but lowered the bath temperature to 4°C. It was found that as the a.c. component was increased the hardness of the film increased, this effect being particularly marked in the outer layer of the coating. It was also noted that even with the use of an a.c. component there was still a tendency for the anode to "burn", but the minimum critical voltage needed to prevent this was governed by the d.c. limits. The value of the a.c. component being primarily to raise the permissible current density, thereby increasing the growth rate of the film for the same d.c. voltage. i.e., if the d.c. voltage is limited below the critical burning voltage and the current density increased by the superimposition of a.c., both the relative rate of dissolution of the oxide film and the tendency to "burning" are greatly reduced.

A commercial process using this technique (Hardas Process⁽⁸⁶⁾)

was developed by Campbell. It was originally operated in an oxalic acid electrolyte but soon developed into a sulphuric-oxalic acid mixture and subsequently became almost exclusively a dilute sulphuric acid process operated between 6 - 10 per cent (vol). There are no addition agents. In practice, the hard anodizing process is controlled by the treatment time and the current density, the electrolyte concentration and the temperature being constant. The current density is adjusted to the particular alloy composition and should be maintained at a constant level by raising the voltage as the film thickness increases. The magnitude of the a.c. component requirement varies with the alloy composition. i.e., permits the hard anodizing of high copper containing alloys.

In high current density anodizing processes operated with a.c. or with a.c. superimposed on d.c. the smell of hydrogen sulphide is frequently detected, probably due to the cathodic reduction of sulphuric acid at the high local temperatures developed⁽¹¹⁵⁾ the oxide film is also tinted yellow. A patent⁽¹¹⁶⁾ claiming to eliminate the cathodic reduction of the H_2SO_4 (to form H_2S gas) in favour of electrolysis of H_2O to yield hydrogen as been published. A more recent description of the process has been given by Eyre and Gabe⁽¹¹⁷⁾ who investigated the parameters of a.c. anodizing in sulphuric acid. i.e., concentration of acid (5 - 15 per cent), temperature (19 - 25°C) and additive concentration (10 - 30 g/l).

To summarize, the advantages claimed for these processes over direct current hard anodizing are:

- (1) The ability to hard anodize difficult to process alloys, such as high copper alloys of aluminium, which normally are sensitive to burning.

(ii) Higher rates of current input, hence faster film build-up and greater productivity.

and (iii) The ability to achieve thicker coatings (up to 250 μm or more) on specific alloys.

An explanation that has been offered to account for these advantages is that there is an anode cooling effect between current peaks which helps to avoid burning.

Defence Specification 151⁽⁶⁴⁾ gives general guide lines on how hard anodizing may be carried out, leaving the electrolyte to be used up to the anodizer. It specifies that hard anodizing can be carried out in any suitable electrolyte. e.g. a 10 per cent solution by volume of sulphuric acid in water. The chloride content of the electrolyte should not exceed 0.20g NaCl per litre. It is necessary to maintain a low temperature at the surface of the work and this may be achieved by providing rapid flow of the cooled electrolyte over all surfaces undergoing treatment. The electrolyte is usually maintained at a temperature between -5 and $+5^{\circ}\text{C}$. The cathode should consist of lead, carbon or suitable conducting material which is substantially insoluble in the electrolyte. Good electrical contact to the cathode must be ensured. Auxiliary cathodes may be operated with direct current or with a combination of alternating and direct currents. The current density in a typical sulphuric acid electrolyte may vary from 2.7 to 43.0 A/dm^2 depending on the process employed and the alloy being treated: likewise the final voltage may vary from about 40 to 120 volts, depending largely on the thickness of coating required and alloy. Particular attention should be given to maintaining the

required degree of agitation. The temperature of the electrolyte must be within 2°C. i.e., +2°C of the nominal value.

The generality of the specification allowing any suitable electrolyte to be used in hard anodizing enables a large number of "Jobbers" to offer hard anodizing. While most of them employ sulphuric acid with d.c. at low temperature, others have introduced their own variations (basically to overcome patent law) using mixed acids or different electrolytes some of which operate at higher temperatures and frequently the conditions will be adjusted to suit the particular alloy being processed.

1.10.3 THE USE OF MIXED ACID ELECTROLYTES.

These electrolytes usually enable the anodizer to operate the process at higher temperatures, thus giving a saving on the cost of refrigeration. Wernick and Pinner⁽¹¹⁸⁾ give examples of these mixed acid electrolytes, the majority of which are based on the sulphuric acid electrolyte (the H₂SO₄ increases the conductivity of the electrolyte and hence reduces the operating voltage) with the addition of other acids added to reduce the aggressiveness of the sulphuric acid to enable harder and more compact films to be obtained.

Special types of mixed acid electrolytes are used in Integral Colour anodizing processes, in which the colour is produced during the anodizing process itself. They are sometimes referred to as "self-colour anodizing" or "hard colour anodizing" processes. They are all used at high voltages (up to 100 volts or more) and, as a result the hardness and abrasion resistance are higher than that of films produced in a sulphuric acid electrolyte, hence, the name "hardcolour". They were developed industrially in North America and were a response to

the demand for highly durable colour anodizing finishes for monumental buildings.

The earliest processes used were the oxalic acid anodizing processes developed in Japan.⁽⁶⁾ The first industrial integral colour anodizing process was the "Kal color" process of Kaiser Aluminium, which was introduced in the late 1950's.^(119,120) Since then numerous processes have been developed and patented and are adequately described by Wernick and Pinner.⁽¹²¹⁾

There is an important difference between hard anodizing and integral colour anodizing, which is that integral colour anodizing depends on close control of the acid anion and dissolved aluminium, both of these can be raised considerably with no detriment to the hardness of the coating, although the colour will tend to become lighter. Hence, the control of the electrolyte for colouring is more critical than for hard anodizing.

The properties of many organic electrolytes have been demonstrated by Kape.⁽¹²²⁾

He suggested that organic acid apart from other effects, is acting as a high conductivity carrier for a dilute sulphuric acid electrolyte. Similar effects were noted when the author was working with conventional electrolytes in solution with organic solvents.⁽¹²³⁾

Thompson⁽⁹⁴⁾ states that the benefits to be derived from the additions made to certain commercial processes are doubtful, and at best marginal, and their control can be rendered difficult by chemical instability and the need for complex analysis. (The use of microprocessors may remove this difficulty in the future.) The author also gives a table showing the comparison of sulphuric acid and organic acid electrolytes for anodizing aluminium. See Table 1.7 below.

Table 1.7(94) Comparison of sulphuric acid and organic acid electrolytes for anodizing aluminium.

	SULPHURIC ACID ELECTROLYTE	ORGANIC ACID ELECTROLYTE
Cost of chemicals.	Inexpensive.	Expensive, high state of purity required.
Make-up.	Tap water.	Deminerallized water.
Chemical stability.	High degree of stability.	Generally some decomposition occurs.
Contamination of electrolyte.	Not greatly affected.	Sensitive to halides.
Chemical analysis.	Straight forward.	More complex.
Typical abrasion value. (Jet Test method).	Hard anodic value 20% volume, HE 9 35 g/ μm HE 15 2.5 g/ μm Sulphuric acid conventional film. (architectural) 2.0g/ μm	HE9 type alloys 4.5 g/ μm
Solubility of anodic film in electrolyte.	Varies with electrolyte strength.	Low at all concentrations.
Operating temperature.	0°C + 5°C	Ambient temperature.

CHAPTER TWO

2. EXPERIMENTAL PROCEDURE AND TECHNIQUES.

2.1 INTRODUCTION: This chapter describes the preparation of the samples, the materials and equipment used, the anodizing conditions and post-anodizing treatment of specimens, and details of all the experimental techniques used to assess the specimens.

2.2 MATERIALS USED.

A number of aluminium alloys were used in the investigations carried out. The majority of work, however, was carried out on super purity aluminium (99.98 wt per cent) and commercial purity aluminium (99.5 wt per cent) of anodizing quality, both in the form of bright rolled, annealed sheet, 0.9 mm thick, with the following compositions (wt per cent) as given in Table 2.1.

Table 2.1 Composition of Super and Commercial purity aluminium.

ELEMENT	SUPER PURITY (wt per cent)	COMMERCIAL PURITY (wt per cent)
Al	>99.9800	>99.500
Mg	0.0005	0.060
Cu	0.0020	0.015
Si	0.0050	0.150
Fe	0.0060	0.190
Mn	0.0015	- - - -
Ti	- - - - -	0.025

The other alloys used were H30, two Al-Mg-Si alloys (I and II) 2002, 6009, 6010, HS30/3, SIDAL, BB2, BB3, 2117 HP, 2117 CP, 2117A, 2036, 5782 and 609. (See Appendix I for compositions.)

But as stated above, most work was carried out on the super and commercial purity aluminium, basically because these alloys were readily available.

2.3 SPECIMEN SIZE.

Specimen size varied with respect to what current density was required. The most common size being 50 mm long by 15 mm wide.

2.4 CHEMICAL SOLUTIONS.

AnalaR grade reagents were used throughout, except where otherwise stated.

2.4.1 ANODIZING SOLUTIONS.

Various percentage by volume sulphuric acid-deionised water solutions were used.

2.5 SPECIMEN PREPARATION.

Specimens were guillotined to the appropriate shape and size, degreased with acetone, dried in air and stored in a desiccator containing anhydrous silica gel until required.

2.6 PRETREATMENTS.

A standard sequence was employed before and after anodizing. The sequence was as follows:

- (i) Obtain the surface required on the aluminium alloy. i.e., As rolled, sand blasted, mechanically abraded or polished, chemically etched, chemically polished, electropolished, etc.,
- (ii) Dip in acetone - degreases the specimen surface.

- (iii) Calculate the surface area required to give the current density required. A profile meter was not available to enable the true surface area to be calculated, so obviously for the different surface treatments it was not possible to know exactly the true value for the surface area because the surface profile is very different for say a sand-blasted surface and an electropolished surface. The calculated value of current density would therefore be slightly higher than the true current density value. [A worked example of how the current density was calculated is given in Appendix II.]
- (iv) The remaining surface was protected by PVC adhesive insulating tape or stop - off lacquer. [See 2.7.]
- (v) Dip in acetone - decreases the specimen surface.
- (vi) Water rinse - deionised water.
- (vii) ANODIZE specimen.
- (viii) Water rinse specimens under running water for at least three minutes to remove traces of anodizing solution from the specimen surface.
- (ix) Dry specimen between absorbant paper towel.
- (x) Specimen stored in desiccator until required.

A number of surface preparations were investigated to observe the effects they had on the appearance and quality of the hard anodic oxide coating. These preparations are briefly described below.

2.6.1 "AS RECEIVED".

Bright rolled, annealed aluminium sheet of anodizing quality. Obtained by passing aluminium sheet through highly polished rolls and

annealed at the aluminium fabricators factory - The British Aluminium Company who kindly donated all of the super purity and commercial purity aluminium used throughout the investigation. This preparation was only obtained on super purity and commercial purity aluminium.

2.6.2 SAND BLASTED.

Obtained by placing the specimen under a nozzle, through which a jet of compressed air and fine abrasive particles are expelled at high velocities which blast into the surface of the aluminium, giving a highly deformed surface with a uniform matt appearance.

2.6.3 MECHANICALLY ABRADED AND POLISHED.

Only with respect to the Al-Mg-Si (I and II) and H30 alloys. The specimens was abraded on a rotating abrasive paper disc, using water as a lubricant and the minimum applied pressure, so as to avoid bevelling of the surface. Initial grinding employed a grade P100 disc to remove any deformed areas. Subsequent grindings employed grade P180, P240, P400, P600 and P1200 discs, altering the direction of scratches for each change of paper. A final polish was carried out on rotating wheels imbedded with 6 μm and 1 μm diamond paste particles with white spirit used as a lubricant.

2.6.4 CHEMICAL ETCHING.

Alkaline treatment given. Specimens were etched using a 10 per cent (wt) sodium hydroxide solution, [100g of sodium hydroxide dissolved in 1,000 cm^3 of deionised water] at a temperature of $60 \pm 1^\circ\text{C}$ for two minutes, removed, immediately desmuted in 50/50 per cent (vol) HNO_3 - H_2O solution, and washed in distilled water and dried.

2.6.5 CHEMICAL POLISHING.

Super purity aluminium chemically polished in 78 per cent (vol) H_3PO_4 - 16 per cent (vol) H_2SO_4 - 6 per cent (vol) HNO_3 - 0.5 per cent (wt) $CuSO_4$ solution at $98^\circ C$ for 90 seconds, removed, immediately desmuted in 50/50 per cent (vol) HNO_3 - H_2O mixture, washed in distilled water and dried.

2.6.6 ELECTROPOLISHING.

Carried out on super purity and commercial purity aluminium, using the Battelle type solution⁽¹²⁴⁾ which consisted of 95 per cent (vol) H_3PO_4 - 5 per cent (vol) H_2SO_4 and 12.5 g/l CrO_3 at $82 \pm 2^\circ C$ at a current density of approximately 10 A/dm².

Whilst carrying out electropolishing, surface defects known as ICING DEFECTS were observed under certain conditions. These defects were studied in an attempt to understand how they came about. Operational conditions of the electropolishing process were investigated, i.e., solution composition, variable voltage/constant current, constant voltage/variable current, bath temperature, agitation, and no agitation.⁽¹²⁵⁾ More detail of the findings of this work will be given in the following chapters.

2.6.7 HEAT TREATMENT.

Heat treatment of the cast alloys Al-Mg-Si I and II was carried out in a furnace thermostatically controlled at a temperature of $540^\circ C$. Twelve specimens; two I, two II, four "As rolled" super purity aluminium, and four "As rolled" commercial purity aluminium, were kept at a temperature of $540^\circ C$ for two hours. After two hours one I, II, two super purity and two commercial purity specimens were water

quenched, while the remaining specimens were allowed to cool to room temperature. (Aging was not considered). The I and II alloys were subsequently mechanically polished and anodized. Whilst the super purity and commercial purity alloys were anodized directly, with no polishing or etching treatment after heat treatment.

The effect of scoring the surface of the specimen was also investigated.

2.7 ANODIZING - EXPERIMENTAL SET-UP.

Anodizing was carried out in a 10 per cent (vol) sulphuric acid (AnalaR grade sp.gr. 1.84) - 90 per cent (vol) deionised water solution - 500 cm³ volume, [Except where otherwise stated.] contained in a one litre capacity glass beaker. The beaker was contained in a PVC tank 46 cm long by 30 cm wide and 17 cm high, which was lagged externally by 2 cm of sheet foamed polystyrene. Cooling was effected by the circulation of a refrigerant, 60 per cent (vol) water/40 per cent (vol) anti-freeze (methanol and ethylene glycol) from an external "Grant" flow heater pump (Type FH15) thermostatically controlled with an operational range between -10 to 80°C, capable of maintaining the refrigerant to $\pm 0.1^{\circ}\text{C}$. The surface of the refrigerant was covered with polythene chroffle balls to minimise fluid and temperature losses.

The agitation⁽¹²⁶⁾ of the electrolyte was effected by using nitrogen passed through a porous ceramic tube placed horizontally under the specimen to be anodized, giving vertical circulation of aerated electrolyte.

[Air agitation is an important factor in anodizing, since it alters the temperature at the areas where the anodic films is being formed and so influences the characteristics of the anodic coating.



The agitation produces uniform bath temperature and also uniform bath composition. Practically all of the electrical energy used during anodizing is converted to heat energy. This heat is dissipated by cooling the electrolyte and by using air agitation or mechanical stirrers and reciprocating anodes. Insufficient agitation, which leads to higher electrolyte temperatures, can cause soft coatings or dissolution of the coating and basis metal often termed as "burning". Hence, agitation is important in controlling the film thickness obtained, in that it affects the degree of re-dissolution of the anodic oxide coating during anodizing.]

Electrical connections to the anodizing bath were established via a lead cathode sheet (-ve electrode) and the aluminium specimen (+ve electrode) to be anodized using "crocodile" clips (insulated by PVC tape) with leads running to a rectifier. (A Farnell, stabilised Power Supply. Type H60V/25A.) Modified to give a constant current output of 0.5 Amps.

Anodizing was effected by immersing the specimen "live" to the required depth in the electrolyte, (The remaining surface of the specimen being protected by either PVC insulating tape or "Fortolac" stop-off lacquer. The PVC tape was preferred for protecting the super and commercial purity aluminium because of their shape, i.e., sheet. Whilst because of size and shape, i.e., Al-Mg-Si alloys circular and H30 alloy was quite small, the stop-off lacquer was favoured for these alloys.) for the required length of time (using a stop watch) or until the voltage reached the maximum capacity (60 volts) of the rectifier. The temperature of the electrolyte was monitored throughout the immersion period. Most of the anodizing was carried out at constant current density.

The current densities used were considerably higher than usually used in industry. (Thompson⁽⁹⁴⁾ stated that commercial hard anodizing was carried out at current densities in the order of 4.6 to 23.2 A/dm² in 10 per cent sulphuric acid at temperatures of 0°C \pm 5°C.) The main reason for the use of high current densities being that the time of immersion of the specimen in the electrolyte would be reduced, effectively minimising the dissolution of the anodically formed oxide by the solvent action of the sulphuric acid, thereby producing the densest possible hard coating.

A schematic representation of the laboratory set-up of the apparatus used for the anodizing of the aluminium alloys is shown in Fig. 2.1.

2.8 SCANNING ELECTRON MICROSCOPY. (S.E.M.)

A Cambridge S150 type stereoscan electron microscope fitted with a "Kevex" energy dispersive x-ray microanalyser was extensively used to examine the surface topography of the anodized specimens.

The S.E.M. is basically a device in which the surface of the specimen is scanned by an electron beam which becomes scattered. A television picture of the scattered beam is presented on a screen. A high depth of field is achieved and scanning electron microscopy enables direct examination of the surface at magnifications up to x30,000.

The "Kevex" facility allows energy dispersive analysis of x-rays. It uses a solid state x-ray detector with sufficient resolution to allow an energy/intensity spectrum to be obtained. It directly sorts out the x-rays in relation to their energy and from the peaks obtained it is possible to identify elements present on the surface and just below (a few microns) the surface of the specimen by the x-ray energy (KeV) value obtained.

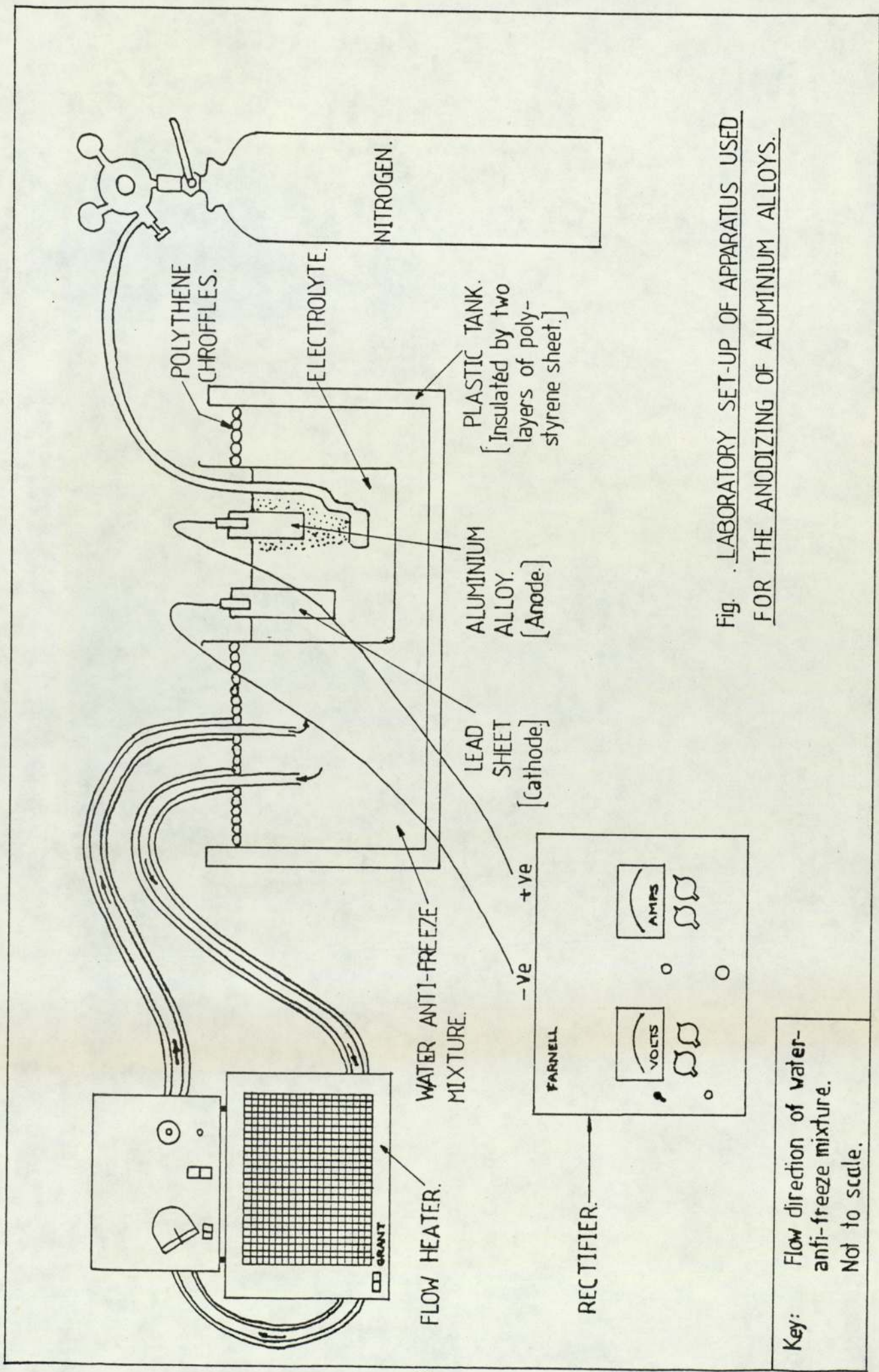


Fig. . LABORATORY SET-UP OF APPARATUS USED FOR THE ANODIZING OF ALUMINIUM ALLOYS.

Key: Flow direction of water-anti-freeze mixture. Not to scale.

Thus, direct examination of the surface and the capacity for accurate quantitative analysis of any surface features observed can be carried out by using the instruments above.

Specimens used for examination were cut into manageable sizes and mounted on an aluminium S.E.M. stub. Because the anodic coating produced by anodizing is an oxide, it is electrically insulating in nature. Therefore, to view the topography of the specimen the surface must be made electrically conducting, so that an electron image can be formed. This was achieved by vacuum carbon coating or gold/palladium coating the surface to make it electrically conductive. Gold/palladium coating allows a sharper image to be produced, but unfortunately does not allow the use of the "Kevex" facility. The reason being that these elements would mask any other elements of lower atomic number present. Therefore, all of the coatings were carbon coated, allowing the "Kevex" facility to be used if needed.

The S.E.M. was used to view many surfaces during the investigation of hard anodizing. Types of surface examined are indicated below:

- All pretreated surfaces before anodizing.
- Anodized surfaces.
- Chemically stripped surfaces.
- Cross sections of anodic oxide coatings.

Electron emission from specimens is greatest when the surface is at 45° to the electron beam, i.e., 45° tilt angle. However, the surface profile of the anodized specimens appeared to be so very different at differing tilt angles to the electron beam that it was decided to take photographs of the topography of the specimen at an angle of 10° to the electron beam (80° tilt angle) and 70° to the electron beam (20° tilt angle) as well as the 45° tilt angle to the

electron beam. Using this technique⁽¹²⁷⁾ it was possible to obtain highly magnified views of the specimens surface, viewing at a low glancing angle of 10° and a near perpendicular view of the surface. Therefore, care must be taken to remember the viewing angle when interpreting the photoelectron-micrographs obtained.

2.9 OPTICAL MICROSCOPY.

Normal illumination was used to study surface features on hard anodic films. Sectional views of these films were also obtained. Optical microscopy was also used to measure the thickness of films by the use of a vernier scale eyepiece fitted to the microhardness instrument.

2.10 POTENTIAL-TIME INVESTIGATIONS.

Potential - Time curves were obtained for a number of alloys whilst anodizing by connecting a "Servoscribe 700" potentiometric recorder to the appropriate terminals. i.e., anode (specimen) to the positive terminal and cathode (lead sheet) to the negative terminal. By selecting a suitable rate at which the recording paper passed the recording pen (vertical movement only) on immersion of specimen the rate of change of the cell potential was plotted against time of immersion during the course of anodizing.

[Previous workers⁽²⁷⁾ on anodizing aluminium, measured the contributions of the potential drop between the electrodes and the cathodic overpotential to the cell voltage and found the value to be 0.5V and so could be neglected. This effect was also neglected in the present work.]

All of the potential - time curves were obtained from specimens

anodized in 10 per cent (vol) H_2SO_4 , with the temperature, current density and pretreatment being variables.

Curves were obtained for the following:

- (i) Alloy I and II abraded to P180 and mechanically polished to diamond paste $1\ \mu m$ condition. Anodizing at a temperature of $- 8 \pm 2^\circ C$ at the same current density.
- (ii) Super and commercial purity aluminium in "As rolled" condition. Anodizing at a temperature of $- 8 \pm 2^\circ C$ at different current densities.
- (iii) H30 alloy abraded to P180 and mechanically polished to diamond paste $1\ \mu m$ condition. Anodized at a temperature of $- 8 \pm 2^\circ C$ at different current densities.
- (iv) Super and commercial purity aluminium in "As rolled" condition. Anodized at a temperature of $+ 6 \pm 2^\circ C$ with different current densities.
- (v) H30 alloy abraded to P180 and mechanically polished to diamond paste $1\ \mu m$ condition. Anodized at a temperature of $+ 6 \pm 2^\circ C$ with different current densities.
- (vi) Super and commercial purity aluminium in "As rolled" condition. Anodized at a temperature of $+ 17 \pm 2^\circ C$ with different current densities.
- (vii) BB2, 2117CP, 2117HP, 5182, 609 and 2002 alloys both "As rolled" and etched condition. Anodized at a temperature of $-5^\circ C$ with different current densities.

2.11 MICROHARDNESS TESTING.

Anodized specimens were cut (because of the coatings brittleness when flexed a "Junior" hacksaw was used) and mounted in cross-section in conductive bakelite.

The "micro" was then mechanically polished as described in 2.5.3 earlier. The tests were carried out on coatings using a Miniload Leitz Wetzlar instrument. The coating was indented with the test diamond for 30 seconds with a known load which produced a diamond shaped indentation, the mean value of the two diagonals produced was calculated and by using the formula below or referring to tables, the hardness number VPN (Vickers Pyramid Number) was obtained.

The VPN's were obtained for the bulk aluminium and profile hardness readings across the anodic coating. A minimum of three readings were taken and an average of these was taken to give the value of VPN given in the results.

Vickers formula

$$Hv = \frac{1854.4 \times P}{(d \times 0.168)^2}$$

where Hv = Vickers hardness Kg/mm²
P = measuring force in grammes
d = length of diagonal in μ m's
(1 μ m = 0.001mm)

Hardness measurements made close to the film/substrate interface or the film/mountant interface resulted in distorted indentations which gave misleading results.

The thickness of the coating was also measured at the same time as hardness using the vernier scale on the microhardness instrument.

2.12 DETERMINATION OF THICKNESS BY CHEMICAL STRIPPING.(128)

The stripping solution consisted of:

Phosphoric acid (d 1.75) 3.5 per cent (v/v)

Chromic acid (AnalaR) 2.0 per cent (w/v)

Deionised water - used gently boiling.

The active agent in the solution is the phosphoric acid and the chromic acid prevents attack of the aluminium base.

Procedure:

- (i) Weigh the clean and dried anodized specimen (to five decimal places) of known surface area.
- (ii) Immerse specimen in stripping solution until constant weight is attained. (Specimens were immersed for well over 20 minutes.)
- (iii) Specimen removed, washed in running water and dried and reweighed.

The loss in mass [(i) - (iii)] is taken as the mass of the anodic coating and the following calculation was carried out to establish the average thickness.

$$T = \frac{1000 M}{a \rho}$$

where T is the thickness of the coating (μm)

M is the mass of the coating (mg)

a is the surface area of the anodic oxide (in mm^2)

ρ is the density of the coating (in g/cm^2), taken as 2.5.

The above mentioned stripping solution was also used on the "micro" cross-sections and S.E.M. photoelectron micrographs of the hard anodic coating were obtained.

2.13 COATING RATIO.

The coulombic efficiency for the formation of porous oxide films on aluminium in sulphuric acid can be expressed in terms of a coating ratio which is given by $\frac{\text{weight of oxide formed}}{\text{weight of aluminium consumed}}$ and was determined for certain aluminium alloys with variable conditions.

The aluminium specimen to be used was carefully weighed just prior to oxide formation; let this weight be W_1 . Anodizing was then carried out for the required time under controlled, known conditions, and the specimen was reweighed; weight W_2 . The specimen with its oxide film was immersed in a solvent that dissolved only the oxide film. (See 2.11.)

Following oxide removal, the specimen was then reweighed; weight W_3 . The coating ratio was then calculated from the weighings.

Thus,

$$\text{Coating ratio} = \frac{W_2 - W_3}{W_1 - W_3}.$$

2.14 ELECTROLYTIC DETACHMENT OF ANODIC OXIDE FILM. (129)

Procedure: The air dried anodized specimen was immersed in a perchloric acid (70 per cent) - methanol (abs) solution with a composition of 1:5 parts by volume held at 21°C. The specimen was made anodic by the sudden application of voltage (60 volts) until the coating detaches itself and falls to the bottom of the beaker. The cathode was an aluminium sheet bent to fit around the specimen. The detached film was carefully removed from the solution and washed and dried. The detached glass-like film was examined with the S.E.M.

CHAPTER THREE.

3. RESULTS.

3.1 ANODIZING OF THE ALUMINIUM ALLOYS.

Except where otherwise stated, all anodizing was carried out in a one litre glass beaker containing 500 cm³ of 10 per cent v/v AnalaR grade sulphuric acid (sp.gr. 1.84) - 90 per cent v/v deionized water solution.

Initial experiments were conducted on a series of specimens which had been subjected to different pretreatments as explained in Section 2.5. Representative results from the experiments carried out have been selected to avoid unnecessary duplication.

Anodizing was carried out at a constant current. The current density values were obtained by dividing the current by the measured surface area of the samples exposed to the electrolyte.

The cell voltage between the anode and cathode was measured continuously during anodizing and the values obtained are given in the following tables. The temperature of the electrolyte was noted throughout anodizing and only after long anodizing times (greater than 30 minutes) did the temperature rise slightly. All specimens were examined visually and certain specimens were viewed both optically and by Scanning Electron Microscopy.

3.1.1 PRETREATMENTS.

Table 3.1. Experiment 3.1.

ALLOY & PRETREATMENT:	Super purity aluminium (S.P.Al.) "As rolled"	
TEMP. OF BATH:	Initial -8°C	Final -6°C
VOLTAGE BETWEEN ANODE & CATHODE:	Initial 26 V	Final 42 V
ANODIZING TIME:	110 minutes	
CURRENT DENSITY:	5.1 A/dm ²	
OBSERVATIONS:	Gradual increase in voltage with increasing anodizing time. "Crazing" over surface and gold colouration obtained, surface smooth to the touch, topography examined with S.E.M. (See Fig. 3.1) and metallographic cross section gave measured thickness of anodic coating to be 275 μm. The microhardness value at base metal/anodic Coating was 572 VPN decreasing to 424 VPN at anodic coating/mountant interface. Microhardness value of base metal was 27 VPN.	

Table 3.2. Experiment 3.2. S.P.Al. "As rolled", c.d. 23.8 A/dm², electrolyte temperature -8°C.

ANODIZING TIME (secs)	VOLTAGE BETWEEN ANODE & CATHODE		OBSERVATIONS
	INITIAL VOLTAGE	FINAL VOLTAGE	
15	34	30	Surface appearance dulled slightly. Topography examined with S.E.M. (See Fig. 3.2).
30	34	30	Apparent dissolution on one side of the specimen. See Figs. 3.3(i) and (ii).
60	34	30	Light and dark areas on the surface. See Fig. 3.4
300	34	30	"Crazing" over surface. See Figs. 3.5(i) and (ii).

Table 3.3. Experiment 3.3. S.P.Al "As rolled", c.d. 39.7 A/dm², electrolyte temperature -8°C.

ANODIZING TIME (secs)	VOLTAGE BETWEEN ANODE & CATHODE		OBSERVATIONS
	I.V.	F.V.	
1	36	32	No visible difference to surface. See Figs. 3.6(i) and (ii).
5	36	32	No visible difference to surface. See Fig. 3.7.
15	36	32	Slight dullness to surface appearance. See Fig. 3.8.

Table 3.4. Experiment 3.4. C.P.Al "As rolled", c.d. 6.6 A/dm², electrolyte temperature -8°C .

ANODIZING TIME (secs)	VOLTAGE BETWEEN ANODE & CATHODE		OBSERVATIONS
	I.V.	F.V.	
5	34	30	No visible difference to surface. See Figs. 3.9 (i) and (ii).
15	34	30	No visible difference to surface. See Figs. 3.10 (i) and (ii).

Whilst anodizing C.P.Al "As rolled" in electrolyte at -8°C with a c.d. of 60 A/dm² (I.V. 28V. - EV. 40V) for 52 seconds, spherical defects appeared on the surface. See Figs. 3.11(i) and (ii).

Table 3.5. Experiment 3.5. S.P.Al "Sand blasted" (See Fig. 3.12),
c.d. 5.4 A/dm², electrolyte temperature
-8°C.

ANODIZING TIME (min)	VOLTAGE BETWEEN ANODE & CATHODE		OBSERVATIONS
	I.V.	F.V.	
41	27	53	Light grey colouration with "powdery" appearance. Coating thickness 60-75 m with a hardness of 664 - 500 VPN. See Fig. 3.13.)

Table 3.6. Experiment 3.6. C.P.Al "As rolled", c.d. 33.0 A/dm²,
electrolyte temperature -8°C.

ANODIZING TIME (min)	VOLTAGE BETWEEN ANODE & CATHODE		OBSERVATIONS
	I.V.	F.V.	
8	30	60	Dark grey colouration, crazing over entire surface. (See Figs. 3.14(i) and (ii)).

Table 3.7. Experiment 3.7. 5% H₂SO₄ at -6°C and c.d. 22.1 A/dm².
At such a low temp. there was a slight problem with
solution forming ice. Overcome by increasing agitation.

ALLOY & PRETREATMENT	ANODIZING TIME (min)	VOLTAGE BETWEEN ANODE & CATHODE		OBSERVATIONS
		I.V.	F.V.	
I, P180 Abraded	15	26	60	Abraded pattern prominent on surface. See Fig. 3.15.
I, 1 μm polish	12	24	60	"Dendritic" pattern over entire surface. See Figs. 3.16(i) and (ii).
II, P180 Abraded	18	26	60	Abraded pattern. See Fig. 3.17.
II, P180 Abraded	23	26	60	No agitation, powdery appearance "Burning". See Fig. 3.18.
II, 1 μm polish	14	25	60	Dendritic pattern on surface. See Figs. 3.19(i) and (ii).

Table 3.8. Experiment 3.8. c.d. 33 A/dm², electrolyte temperature -8°C.

ALLOY & PRETREATMENT	ANODIZING TIME (min)	VOLTAGE BETWEEN ANODE & CATHODE		OBSERVATIONS
		I.V.	F.V.	
H30, P180 abraded	2½	29	60	Light grey colouration. See Fig. 3.20.
H30, 1 μm polish	2	28	60	Light grey colouration. See Figs. 3.21(i) and (ii).

Table 3.9. Experiment 3.9. Scored surface, electrolyte temperature -8°C .

ALLOY & PRETREATMENT	ANODIZING TIME (min)	VOLTAGE BETWEEN ANODE & CATHODE		OBSERVATIONS
		I.V.	F.V.	
I, $1\ \mu\text{m}$ polish	6	25	60	Dendritic pattern. c.d. $11\ \text{A}/\text{dm}^2$. See Fig. 3.22.
II, $1\ \mu\text{m}$ polish	$7\frac{1}{2}$	26	60	Dendritic pattern. c.d. $11\ \text{A}/\text{dm}^2$. See Fig. 3.23.
C.P.Al "As rolled"	$16\frac{1}{2}$	26	40	Crazing over surface and gold colouration. Thickness of coating $100\ \mu\text{m}$ and at score line $50\ \mu\text{m}$, hardness of 540 VPN. c.d. $6.6\ \text{A}/\text{dm}^2$. See Fig. 3.24.

3.1.2 ETCHING.

Table 3.10. Experiment 3.10. S.P.Al etched in 10% NaOH at 60°C for 2 mins. (See Fig. 3.25.) Anodized at 35.7 A/dm² in 10% H₂SO₄ at -8°C.

ANODIZING TIME (secs)	VOLTAGE BETWEEN ANODE & CATHODE		OBSERVATIONS
	I.V.	F.V.	
15	32	33	Slight milk colouration See Figs. 3.26(i) and (ii).
30	32	29	Slight milk colouration See Figs. 3.27(i) and (ii).
120	32	47	Grey colouration. See Figs. 3.28(i) and (ii).
480	32	60	No agitation. Crazing over surface "blotchy" appearance. See Fig 3.29.

Table 3.11. Experiment 3.11. S.P.Al etched in 10% NaOH at 60°C for 2 mins and anodized at 11.0 A/dm² in 10% H₂SO₄ at -8°C (-6°C on removal).

ANODIZING TIME (min)	VOLTAGE BETWEEN ANODE & CATHODE		OBSERVATIONS
	I.V.	F.V.	
57	32	56	Both anodization and dissolution of the surface appeared to had taken place. See Figs. 3.30(i),(ii) and (iii).

Table 3.12. Experiment 3.12. All of the alloys shown in Appendix I were etched in 10% NaOH at 60°C for 2 mins and anodized at various current densities in a 10% H₂SO₄ solution at -8°C. Six of these alloys experimental details are given below.

ALLOY TYPE	ANODIZING TIME (min)	VOLTAGE BETWEEN ANODE & CATHODE		CURRENT DENSITY (A/dm ²)	OBSERVATIONS
		I.V.	F.V.		
BB3	17	23	60	10.4	Cellular cracked pattern whilst wet, gold colouration also. Dark grey colouration when dry. See Fig. 3.31.
5182	17½	22	60	9.0	Gold colouration when wet, dark grey when dry. See Fig. 3.32.
2117CP	15	22	60	10.4	Yellow colouration when wet and dry. See Fig. 3.33.
2117HP	18½	22	60	9.0	Yellow colouration when wet grey when dry. See Fig 3.34.
2002	17	25	60	10.9	Yellow colouration when wet straw colouration when dry. See Fig. 3.35.
609	14½	25	60	10.4	Gold colouration wet dark grey when dry. See Fig. 3.36.

3.1.3 CHEMICAL POLISHING.

Table 3.13. Experiment 3.13. S.P.Al, chemically polished (See Fig. 3.37) in 78% H₃PO₄ - 16% H₂SO₄ - 6% HNO₃ -0.5% CuSO₄ @ 98°C for 90 secs and anodized at various current densities in 10% H₂SO₄ at -8°C.

ANODIZING TIME (min)	VOLTAGE BETWEEN ANODE & CATHODE		CURRENT DENSITY (A/dm ²)	OBSERVATIONS
	I.V.	F.V.		
1	26	24	41.6	Matt appearance, loss of reflectivity.
2	26	38	41.6	Loss of reflectivity - slight gold tint.
4½	26	60	41.6	Gold colouration. Crazing over surface and pitting. See Fig. 3.38.
1	25	25	18.9	Orange peel effect.
13	25	60	18.9	Gold colouration. Crazing over surface and pitting.
1	25	25	10.5	Matt appearance - loss of reflectivity.
36	25	60	10.5	Deep gold colouration. Crazing over surface and pitting.

3.1.4 ELECTROPOLISHING.

The electropolishing of S.P.Al in a solution which consisted of a mixture of 95% (v/v) H_3PO_4 , 5% (v/v) H_2SO_4 , 12.5 g/l CrO_3 at $82 \pm 2^\circ C$ at a constant current density of $10.0 A/dm^2$ was carried out. A most interesting defect was observed under certain conditions - called ICING. (See Figs. 3.39(i) and (ii).) Specimens were electropolished for different times to study the nucleation and growth of these icing defects. See below.

Table 3.14. Experiment 3.14.

TIME OF ELECTROPOLISHING (sec)	VOLTAGE REACHED (V)	OBSERVATIONS
10	2	Etched surface. See fig 3.40.
60	48	Reflectivity begins to increase, with gassing and icing defects present. See Figs. 3.41(i), (ii) and (iii).
120	52	Gas streaks and icing defects present. See Fig. 3.42
300	60	High reflectivity at top of vertically suspended specimen. Icing defects at bottom. See Fig. 3.39(ii).

Some specimens on which icing defects had been formed were subsequently hard anodized. See Figs 3.43(i) and (ii), which shows the typical surface appearance of a specimen that had been electropolished for 120 secs under the same conditions as mentioned above and anodized in 10% H₂SO₄ at -8°C for 18 minutes at a current density of 10 A/dm². The applied voltage was 25 volts at the start of anodizing and rose to 40 volts at the end. The anodizing gave rise to a gold colouration and crazing. The icing defects did not appear to be anodized and were specular in appearance.

By changing the conditions of the electropolishing bath the icing defects could be avoided and a typical highly reflective electropolished surface is shown in Fig. 3.44 and the resulting anodized surface in Fig. 3.45. This surface was obtained by anodizing in 10% H₂SO₄ at -6°C for 37 minutes at a current density of 8.9 A/dm², resulting in a gold colouration and crazing.

3.1.5 HEAT TREATMENT.

Table 3.15. Experiment 3.15. S.P.Al heat treated and air cooled, c.d. 5.5 A/dm², electrolyte temperature -8°C.

ANODIZING TIME (min)	VOLTAGE BETWEEN ANODE & CATHODE		OBSERVATIONS
	I.V.	F.V.	
27	31	40	Dark grey colouration. Glass-like appearance, smooth to the touch, crazing of surface. See Fig. 3.46.

Table 3.16. Experiment 3.16. S.P.Al heat treated and water quenched, c.d. 5.3 A/dm², electrolyte temperature -8°C.

ANODIZING TIME (min)	VOLTAGE BETWEEN ANODE & CATHODE		OBSERVATIONS
	I.V.	F.V.	
34	29	40	Grey-silver colouration Glass-like appearance, smooth to the touch. See Fig. 3.47.

Table 3.17. Experiment 3.17. C.P.Al heat treated and air cooled, c.d. 7.1 A/dm², electrolyte temperature -8°C.

ANODIZING TIME (min)	VOLTAGE BETWEEN ANODE & CATHODE		OBSERVATIONS
	I.V.	F.V.	
17	32	40	Grey-silver colouration, smooth to the touch. Crazing of surface. See Fig. 3.48.

Table 3.18. Experiment 3.18. C.P.Al heat treated and water quenched, c.d. 6.9 A/dm², electrolyte temperature -8°C.

ANODIZING TIME (min)	VOLTAGE BETWEEN ANODE & CATHODE		OBSERVATIONS
	I.V.	F.V.	
22	28	40	Dark grey colouration. Glass-like appearance smooth to the touch. See Fig 3.49.

Table 3.19. Experiment 3.19. Alloy I, heat treated and air cooled and mechanically polished to $1\ \mu\text{m}$, c.d. $22\ \text{A}/\text{dm}^2$, electrolyte temperature -8°C .

ANODIZING TIME (min)	VOLTAGE BETWEEN ANODE & CATHODE		OBSERVATIONS
	I.V.	F.V.	
11	23	60	Dendritic appearance plus porosity. See Fig. 3.50.

Table 3.20. Experiment 3.20. Alloy I, heat treated and water quenched and mechanically polished to $1\ \mu\text{m}$, c.d. $22\ \text{A}/\text{dm}^2$, electrolyte temperature -8°C .

ANODIZING TIME (min)	VOLTAGE BETWEEN ANODE & CATHODE		OBSERVATIONS
	I.V.	F.V.	
12	23	60	Dendritic appearance plus porosity. See Fig. 3.51.

Table 3.21. Experiment 3.21. Alloy II, heat treated and air cooled and mechanically polished to $1\ \mu\text{m}$, c.d. $22\ \text{A}/\text{dm}^2$, electrolyte temperature -8°C .

ANODIZING TIME (min)	VOLTAGE BETWEEN ANODE & CATHODE		OBSERVATIONS
	I.V.	F.V.	
12	24	60	Dendritic appearance plus porosity. See Fig. 3.52.

Table 3.22. Experiment 3.22. Alloy II, heat treated and water quenched and mechanically polished to $1\ \mu\text{m}$, c.d. $22\ \text{A}/\text{dm}^2$, electrolyte temperature -8°C .

ANODIZING TIME (min)	VOLTAGE BETWEEN ANODE & CATHODE		OBSERVATIONS
	I.V.	F.V.	
10	24	60	Grey colouration, dendritic appearance plus porosity. See Fig. 3.53.

3.2 POTENTIAL vs TIME.

Anodizing was carried out in a 10% (v/v) sulphuric acid electrolyte.

Table 3.23. Experiment 3.23. Temperature of electrolyte -8°C .

ALLOY	PRETREATMENT	ANODIZING TIME (min)	CURRENT DENSITY (A/dm^2)	SEE FIGURE
I	P180 Abraded	13.0	22.0	3.55(A)
I	$1\ \mu\text{m}$ polish	7.5	22.0	3.55(B)
II	P180 Abraded	11.0	22.0	3.55(C)
II	$1\ \mu\text{m}$ polish	6.0	22.0	3.55(D)

Table 3.24. Experiment 3.24. Temperature of electrolyte -8°C.

ALLOY	PRETREATMENT	ANODIZING TIME (min)	CURRENT DENSITY (A/dm ²)	SEE FIGURE
S.P.Al	As rolled	5	55.5	3.56(A)
S.P.Al	As rolled	16	22.2	3.56(B)
S.P.Al	As rolled	30	13.8	3.56(C)

Table 3.25. Experiment 3.25. Temperature of electrolyte -8°C.

ALLOY	PRETREATMENT	ANODIZING TIME (min)	CURRENT DENSITY (A/dm ²)	SEE FIGURE
H30	1 μ m polish	1	59.5	3.57(A)
H30	1 μ m polish	3	19.5	3.57(B)
H30	P180 Abraded	1½	59.5	3.57(C)
H30	P180 Abraded	5	15.4	3.57(D)

Table 3.26. Experiment 3.26.

ALLOY	PRETREATMENT	TEMP. (+2°C)	ANODIZING TIME (min)	CURRENT DENSITY (A/dm ²)	SEE FIGURE
S.P.Al	As rolled	6	5	38.4	3.58(A)
C.P.Al	As rolled	6	3½	41.6	3.58(B)
H30	1 μm polish	6	5	17.5	3.58(C)
C.P.Al	As rolled	17	9	37.0	3.58(D)

Table 3.27. Experiment 3.27.

ALLOY	PRETREATMENT	TEMP. (+2°C)	ANODIZING TIME (min)	CURRENT DENSITY (A/dm ²)	SEE FIGURE
S.P.Al	As rolled	6	35	12.4	3.59(A)
C.P.Al	As rolled	6	27	13.3	3.59(B)
C.P.Al	As rolled	17	70	13.3	3.59(C)

See Fig. 3.54 showing powdery coating.

Table 3.28. Experiment 3.28. Temperature of electrolyte -5°C .
Etched specimens etched in 10% NaOH
solution at $60 \pm 2^{\circ}\text{C}$ for 1 minute.

ALLOY	PRETREATMENT	ANODIZING TIME (min)	CURRENT DENSITY (A/dm ²)	SEE FIGURE
BB2	As rolled	11	15.2	3.60(A)
BB2	As rolled	22	8.8	3.60(B)
BB2	Etched	11	15.2	3.60(C)
BB2	Etched	22	8.8	3.60(D)
5182	As rolled	7	16.4	3.61(A)
5182	As rolled	14	9.0	3.61(B)
5182	Etched	8	15.6	3.61(C)
5182	Etched	16	8.5	3.61(D)
2117CP	As rolled	7½	15.9	3.62(A)
2117CP	As rolled	15	8.7	3.62(B)
2117CP	Etched	7½	15.9	3.62(C)
2117CP	Etched	15	8.7	3.62(D)
2117HP	As rolled	8	14.9	3.63(A)
2117HP	As rolled	16	8.1	3.63(B)
2117HP	Etched	9	14.2	3.63(C)
2117HP	Etched	18	7.7	3.63(D)
2002	As rolled	8	15.9	3.64(A)
2002	As rolled	16	8.3	3.64(B)
2002	Etched	9	15.9	3.64(C)
2002	Etched	19	8.3	3.64(D)
609	As rolled	8½	16.7	3.65(A)
609	As rolled	13	9.6	3.65(B)
609	Etched	7½	17.0	3.65(C)
609	Etched	14	9.4	3.65(D)

3.3 MICROHARDNESS.

A 50g load was applied to the test diamond for 30 seconds and the VPN on cross-section of oxide coating was obtained. A load of 50g was chosen because loads less than this resulted in difficulty with actually viewing the diamond impression. Kape⁽⁵⁵⁾ stated that the value of hardness varied with the load used; indicating that for loads of 20g or below the hardness figure was dependent on the load applied, but for loads of 50g and above the hardness was independent of the load applied.

Table 3.29. Vickers hardness values of coatings on various alloys, hard anodized in 10% H₂SO₄ at -8°C for various current densities.

SPECIMEN	COATING THICKNESS μm's (vernier scale measurement)	DISTANCE FROM METAL/METAL OXIDE INTERFACE μm's	HARDNESS NUMBER (VPN)	
			BASIS METAL	OXIDE
Exp. 3.5 S.P.Al "Sand blasted".	74	-	27	-
		18	-	644
		33	-	601
		58	-	584
Exp. 3.11 S.P.Al "NaOH etch".	130	-	26.8	-
		25	-	641
		50	-	617
		75	-	593
		90	-	564
115	-	516		
Exp. 3.7 Alloy I, 1 μm polish.	79	-	62	-
		18	-	514
		36	-	498
		60	-	420

Table 3.29 continued.

SPECIMEN	COATING THICKNESS μm 's (vernier scale measurement)	DISTANCE FROM METAL/METAL OXIDE INTERFACE μm 's	HARDNESS NUMBER (VPN)	
			BASIS METAL	OXIDE
Exp. 3.28 2117HP "As received"	53	-	84	-
		13	-	612
		25	-	583
		43	-	517
Exp. 3.28 2002 "As received" (8.3 A/dm ²)	60	-	67	-
		14	-	603
		34	-	568
		56	-	512
Exp. 3.38 No.1 C.P.Al "As rolled" 5 mins @ 7.2 A/dm ²	17	-	28	-
No.1 C.P.Al "As rolled" 5 mins @ 10.1 A/dm ²	45	-	-	-
		15	-	539
		35	-	468
No.1 C.P.Al "As rolled" 5 mins @ 19.5 A/dm ²	82	15	-	673
		49	-	522
		71	-	452
No.2				
C.P.Al "As rolled" No.2 5 mins at 26.6 A/dm ²	93	15	-	465
		60	-	581
		82	-	723
No.2 5 mins @ 14.0 A/dm ²	75	15	-	573
		60	-	448
No.2 10 mins @ 7.2 A/dm ²	50	15	-	466
		40	-	452

See Fig. 3.66. Shows typical hardness indentation profile across the anodic oxide film.

3.4 THICKNESS.

The thickness was determined by the chemical stripping technique. C.P.Al "As rolled" was anodized in 10% H₂SO₄ at -8°C (See Table 3.30); 15% H₂SO₄ at -8°C (See Table 3.31); 20% H₂SO₄ at -8°C (See Table 3.32) at different current densities, i.e., high, medium and low relative to each other.

This was also carried out in 5.4% H₂SO₄ (See Table 3.33); 16.6% H₂SO₄ (See Table 3.34) and 27.6% H₂SO₄ (See Table 3.35) at 0°C.

Also in 10% H₂SO₄ at ∞ 21°C (See Table 3.36).

Table 3.30. Experiment 3.29. C.P.Al. "As rolled", anodized at three current densities in 10% (vol.) H₂SO₄ at -8°C. [Thickness-Time graph plotted in Fig 3.67.]

ANODIZING TIME (min)	VOLTAGE BETWEEN ANODE & CATHODE		CURRENT DENSITY (A/dm ²)	OXIDE THICKNESS (μm)
	I.V.	F.V.		
3.0	24	27	19.2	17.2
5.0	24	29	19.2	33.0
7.5	24	34	19.2	51.5
10.0	24	38	19.2	68.8
15.0	24	56 - 58	19.2	108.9
3.0	24	25	10.7	9.6
7.5	24	27	10.7	25.6
15.0	24	31	10.7	54.6
30.0	24	40 - 42	10.7	120.3
47.0	24	60	10.7	184.5
15.0	24	28	5.8	29.2
30.0	24	31	5.8	56.6
60.0	24	37	5.8	121.8

Table 3.31. Experiment 3.30. C.P.Al "As rolled", anodized at three current densities in 10% (vol.) H₂SO₄ at -8°C. [Thickness - Time graph plotted in Fig. 3.67.]

ANODIZING TIME (min)	VOLTAGE BETWEEN ANODE & CATHODE		CURRENT DENSITY (A/dm ²)	OXIDE THICKNESS (μm)
	I.V.	F.V.		
2.0	24	27	22.2	16.6
3.0	24	28	22.2	26.4
5.0	24	33	22.2	41.4
7.5	24	42 - 44	22.2	63.0
10.5	24	60	22.2	94.4
3.0	23	24	11.5	11.6
7.5	23	27	11.5	30.0
15.0	23	32	11.5	61.7
22.0	23	54 - 56	11.5	94.4
30.0	23	58 - 60	11.5	128.7
15.0	24	28	6.3	32.5
30.0	24	32	6.4	67.0
60.0	24	56	6.3	139.6

Table 3.32. Experiment 3.31. C.P.Al "As rolled", anodized at three current densities in 20% (vol.) H₂SO₄ at -8°C. [Thickness-Time graph plotted in Fig. 3.69.]

ANODIZING TIME (min)	VOLTAGE BETWEEN ANODE & CATHODE		CURRENT DENSITY (A/dm ²)	OXIDE THICKNESS (μm)
	I.V.	F.V.		
2.0	24	27	19.2	15.8
3.0	24	29	19.2	21.5
5.0	24	31	19.2	35.8
7.5	24	42 - 44	19.2	54.3
11.0	24	60	19.2	81.7
3.0	22	23	10.4	10.8
7.5	22	27	10.4	26.4
15.0	22	33	10.4	55.0
20.0	22	38	10.4	74.4
29.0	22	60	10.4	108.4
15.0	24	29	5.8	46.2
30.0	24	33	5.8	60.9
60.0	24	52 - 54	5.8	126.0

Table 3.33. Experiment 3.32. C.P.AL "As rolled", anodized at three current densities in 5.4% (vol.) H₂SO₄ at 0°C. [Thickness-Time graph plotted in Fig 3.70.]

ANODIZING TIME (min)	VOLTAGE BETWEEN ANODE & CATHODE		CURRENT DENSITY (A/dm ²)	OXIDE THICKNESS (μm)
	I.V.	F.V.		
1	24	26	29.6	10.0
2	24	28	29.6	20.4
5	24	40	29.6	55.3
8.5	24	58 - 60	29.6	88.8
2	24	25	15.4	10.7
10	25	32	15.4	54.3
15	24	38	15.4	78.4
24	25	60	15.4	138.6
2	25	25	8.5	6.3
15	25	30	8.5	43.4
30	25	39	8.5	85.0
61	25	60	8.5	185.0

Table 3.34. Experiment 3.33. C.P.Al "As rolled", anodized at three current densities in 16.6% (vol.) H₂SO₄ at -0°C. [Thickness-Time graph plotted in Fig. 3.71.]

ANODIZING TIME (min)	VOLTAGE BETWEEN ANODE & CATHODE		CURRENT DENSITY (A/dm ²)	OXIDE THICKNESS (μm)
	I.V.	F.V.		
½	22	23	29.9	4.9
1	22	26	29.6	10.8
2	22	28	29.6	26.4
5½	24	60	29.6	65.2
2	22	25	15.4	13.1
5	23	29	15.4	27.6
10	23	39	15.4	55.3
15	24	60	15.4	93.4
2	23	23	8.5	5.9
7	23	26	8.5	20.0
15	23	32	8.5	44.0
43	23	60	8.5	129.7

Table 3.35. Experiment 3.34. C.P.Al "As rolled", anodized at three current densities in 27.6% (vol.) H₂SO₄ at -0°C. [Thickness-Time graph plotted in Fig. 3.72.]

ANODIZING TIME (min)	VOLTAGE BETWEEN ANODE & CATHODE		CURRENT DENSITY (A/dm ²)	OXIDE THICKNESS (μm)
	I.V.	F.V.		
½	23	27	29.6	7.3
1	23	32	29.6	13.0
2	23	39	29.6	22.1
3½	23	60	29.6	42.1
1	23	25	15.6	5.8
2	23	29	15.4	11.5
5	23	40	15.4	28.9
9½	23	60	15.4	56.6
2	28	27	8.5	6.1
4	28	24	8.5	12.1
10	28	34	8.5	29.9
23½	26	60	8.5	70.3

Table 3.36. Experiment 3.35. C.P.Al "As rolled", anodized at three current densities in 10% (vol.) H₂SO₄ at ~21°C. [Thickness-Time graph plotted in Fig. 3.73.]

ANODIZING TIME (min)	VOLTAGE BETWEEN ANODE & CATHODE		CURRENT DENSITY (A/dm ²)	OXIDE THICKNESS (μm)
	I.V.	F.V.		
3.0	21	23	25.6	23.0
5.0	21	25	25.6	46.0
7.5	21	26	25.6	59.4
12.0	21	46 - 48	25.6	94.0
14.5	21	60	25.6	115.0
3.0	22	22	12.8	10.5
7.5	21	22	12.8	28.7
15.0	21	25	12.8	57.4
30.0	21	27	9.8	80.0
60.0	21	38	8.2	130.2
15.0	21	20	6.4	27.0
30.0	19	21	6.3	57.8
60.0	20	29	6.4	110.2

3.5 COATING RATIO.

Coating ratios of a number of C.P.Al "As rolled" specimens, anodized at two current densities (24.0 and 8.5 A/dm²) and three different temperatures (-8.0, 5.0 and 20°C) were obtained for various anodizing times. See Table 3.37 below.

Figures 3.74(i) and (ii) show the appearance of post anodized specimens before stripping off the anodic oxide coating.

Coating ratios of the alloys BB2, 5182, 2117CP, 2117HP, 2002 and 609 were also obtained, both for the "As received" and "Etched" condition. See Table 3.38 below.

Table 3.37. Experiment 3.36. C.P.Al "As rolled" 10% H₂SO₄ electrolyte.

ANODIZING TIME (min)	VOLTAGE BETWEEN ANODE & CATHODE		TEMP. °C	CURRENT DENSITY (A/dm ²)	THICKNESS OF OXIDE μm	COATING RATIO
	I.V.	F.V.				
2	26	30	-8	24.0	18.9	1.78
3½	26	38	-8	24.0	33.3	1.93
4	26	42	-8	24.0	38.1	1.93
5	26	45	-8	24.0	48.4	2.00
6½	26	60	-8	24.0	66.4	1.99
2	26	26	-8	8.5	6.6	1.73
7	26	31	-8	8.5	22.1	1.79
15	26	34	-8	8.5	48.2	1.87
25	26	46	-8	8.5	84.2	1.96
30	26	50	-8	8.5	102.5	1.99
2	24	28	5	24.0	18.3	1.64
3½	24	33	5	24.0	31.6	1.71
5	24	38	5	24.0	45.9	1.81
7	24	44	5	24.0	65.1	1.90
9½	24	60	5	24.0	91.7	1.97
2	24	24	5	8.5	6.4	1.58
7	24	25	5	8.5	21.1	1.73
75	24	28	5	8.5	45.4	1.75
25	24	35	5	8.5	75.4	1.77
30	24	40	5	8.5	95.0	1.86
2	22	23	20	24.0	17.5	1.60
5	22	30	20	24.0	45.2	1.67
7	22	34	20	24.0	60.3	1.73
9	22	42	20	24.0	77.9	1.76
11½	22	60	20	24.0	100.0	1.79
2	22	21	20	8.5	5.9	1.54
7	22	22	20	8.5	20.1	1.61
15	22	23	20	8.5	45.8	1.62
25	22	26	20	8.5	62.1	1.63
30	22	32	20	8.5	85.6	1.65

- General observations concerning the above experiment were,
- (i) an increase in temperature meant the initial base voltage required, dropped by approximately two volts per 13-15°C increase.
 - (ii) increased time of anodizing gave an increase in weight of oxide formed.
 - (iii) decrease in temperature gave an increase in weight of oxide formed.
 - (iv) from (i) and (iii) it can be concluded that for the current densities used in this experiment that by decreasing the temperature and increasing the immersion time, gave an increase in oxide thickness. (Indicating that the limiting film thickness had not been reached.)
 - (v) At 20°C the oxide coatings formed were grey in colouration and for the 24.0 A/dm² specimens crazing was observed after 5 minutes anodizing and after 9 minutes for the 8.5 A/dm² specimens. At 5°C and -8°C the oxide coatings formed were gold in colouration and crazing was observed slightly earlier than for the 20°C specimens.

Fig. 3.74(i) shows how the appearance of the specimens change with increasing process time and decrease in temperature for specimens anodized at 24.0 A/dm². Fig. 3.74(ii) shows the appearance of specimens anodized at 8.5 A/dm².

Graphs of coating ratio plotted against time are given in Figs. 3.75 and 3.76.

Table 3.38. Experiment 3.37. Anodizing carried out in 10% H₂SO₄ at -5°C.

Key: * Signifies an etched surface.

ALLOY	ANODIZING TIME (min)	CURRENT DENSITY A/dm ²	THICKNESS OF OXIDE	COATING RATIO (μm)
BB2	11	5.2	65	2.02
BB2	22	8.8	73	1.92
BB2*	11	15.2	66	2.00
BB2*	22	8.8	73	1.91
5182	7	16.4	47	2.06
5182	14	9.0	47	1.89
5182*	8	15.6	51	1.98
5182*	16	8.5	52	1.90
2117CP	7½	15.9	44	1.95
2117CP	15	8.7	47	1.90
2117CP*	7½	15.9	47	2.00
2117CP*	15	8.7	47	1.86
2117HP	8	14.9	44	1.85
2117HP	16	8.1	47	1.67
2117HP*	9	14.2	51	1.92
2117HP*	18	7.7	50	1.83
2002	8	15.9	50	2.06
2002	16	8.3	48	1.84
2002*	9	15.9	54	2.02
2002*	19	8.3	59	1.86
609	8	16.7	54	2.00
609	14	9.6	47	1.92
609*	7½	17.0	50	1.97
609*	14	9.4	49	1.90

3.6 ELECTROLYTIC DETACHMENT OF ANODIC OXIDE FILM.

This technique, developed by Spooner, was found to be very successful in detaching large pieces of oxide. Unfortunately due to lack of time the full potential of this technique could not be investigated. However, anodic oxide films formed on all of the alloys considered in this work were successfully detached.

When the specimen was made the anode and then immersed and the voltage applied, a vigorous reaction occurred and the oxide film dropped into the solution. On removal from the solution the oxide film was rinsed in running water and then carefully dried in air. Coatings were detached from S.P.Al and C.P.Al which were colourless to gold in colouration and transparent. Examination with the S.E.M. showed very little. Coatings detached from BB3 and 2117CP for example showed interesting features of the metal - metal/oxide interface (oxide side examined with the S.E.M.). See Figs. 3.77 (i),(ii) and (iii) and Figs. 3.78(i),(ii) and (iii). These detached oxide films were opaque and tinted grey, yellow and gold in colouration.

Anodizing of S.P.Al in oxalic acid gave the characteristic yellow colouration. On trying to detach this film however small pieces of oxide film fell into the solution, while undercutting of the bulk oxide occurred. This allowed a knife to be placed between the basis metal and the oxide making it possible to lever the oxide film off the specimen.

Spooner states that the mechanism of the detachment of the oxide films by this technique is not clear, but he believes that it is due to sudden evolution of large amounts of oxygen. The accompanying pronounced local electrical heating effect is also a factor. The average current density is 100 Amps or more per dm^2 , while the actual

value in the pores is greater. Gas evolution occurs probably at the base of the pores adjacent to the barrier film. This contributes to the penetration of the barrier film, which permits electrolyte flow to the metal substrate which becomes polished. The film ruptures laterally, either before or after penetration, at the metal-barrier layer interface or close to it and detaches itself and falls into the solution.

3.7 MISCELLANEOUS EXPERIMENTS.

The variation of current density on the same specimen was carried out on C.P.Al "As rolled". The specimen was masked to the required area and anodized in 10% H₂SO₄, removed and washed and dried and then re-masked and anodized again. This was carried out for low current densities to high current densities and from high current densities to low current densities. See Table 3.39 below. After anodizing the specimens were cut and metallographically mounted and cross-sections produced. These were mechanically polished and then placed in the phospho-chromic acid stripping solution for 20 minutes. The resulting structure was then observed with the S.E.M. See Figs. 3.79 and 3.80(i) and (ii) .

Table 3.39. Experiment 3.38. Temperature of electrolyte 0°C.

	ANODIZING TIME (min)	VOLTAGE BETWEEN ANODE & CATHODE		CURRENT DENSITY (A/dm ²)
		I.V	F.V	
No.1 See Fig. 3.79.	5	24	25	7.2
	5	25	29	10.1
	5	33	45	19.5
No.2 See Figs. 3.80(i) and(ii).	5	28	45	26.6
	5	26	37	14.0
	10	25	33	7.2

A number of other anodized specimens were cut and metallographically mounted and polished to produce cross-sections of the oxide coating. These were also treated in the $H_3PO_4 - CrO_3$ boiling mixture and the resulting structures viewed with the S.E.M. A number of interesting features were observed and some examples of what was obtained are given in Figs. 3.81(i) and (ii), 3.82(i) and (ii), 3.83(i) and (ii), 3.84 and 3.85(i),(ii) and (iii).

When determining the thickness of anodic oxide film by the chemical stripping method, the specimens left after the oxide was removed obviously left the interface where the oxide was growing. It was therefore considered pertinent to examine this surface. As a control, aluminium without anodic treatment was placed into the oxide stripping solution for 30 minutes and on removal and examination showed that very little attack of the aluminium had occurred. Specimens examined were taken from Experiments 3.29, 3.30, 3.31 and 3.13 (No. 4). See Figs. 3.86(i) and (ii), 3.87 (i) to (xi), 3.88 (i),(ii) and (iii), and 3.89(i) to (ix).

Also C.P.Al "As rolled" anodized in 10% H_2SO_4 at $-8^\circ C$ and 11.5 A/dm^2 (Initial voltage 26V, final voltage 40V) anodized for $27\frac{1}{2}$ mins, crazing over surface and gold colouration and 52 A/dm^2 at $-8^\circ C$ (Initial voltage 26 V, final voltage 60 V) immersed for $3\frac{1}{2}$ minutes crazing over surface and silver colouration. See Figs. 3.90 and 3.91.

C.P.Al etched in NaOH and then anodized in 27.6% H_2SO_4 at $0^\circ C$ for 2 minutes at three current densities - 29.6, 15.4 and 8.2 A/dm^2 . See Figs. 3.92(i) and (ii), 3.93(i) and (ii) 3.94(i) and (ii).

3.8 FIGURES FROM EXPERIMENTAL WORK.

- * All specimens were anodized in 10% H_2SO_4 (vol) at $-8^\circ C$ unless otherwise stated differently.
T.a. - Tilt angle of specimen to electron gun in the Scanning Electron Microscope.

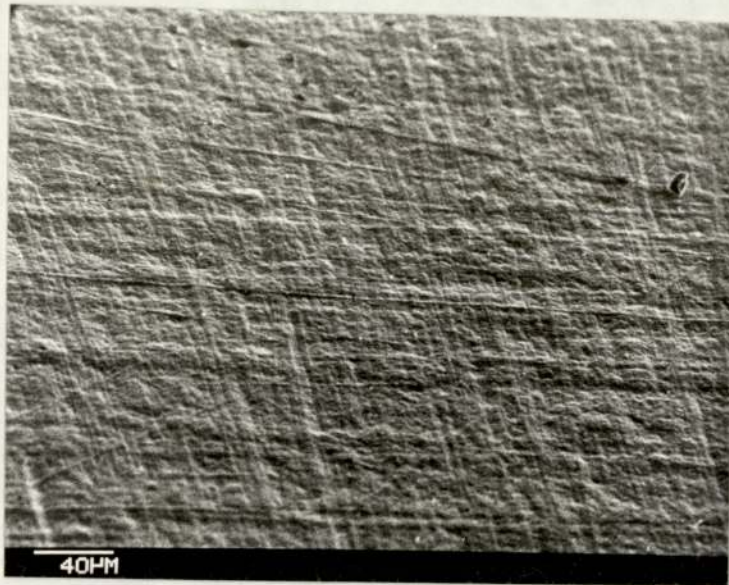


Fig. 3.1 Typical surface topography of S.P. Al in the "As rolled" condition after hard anodizing for 110 minutes at $5.1 A/dm^2$. T.a. 70° (See note above*).

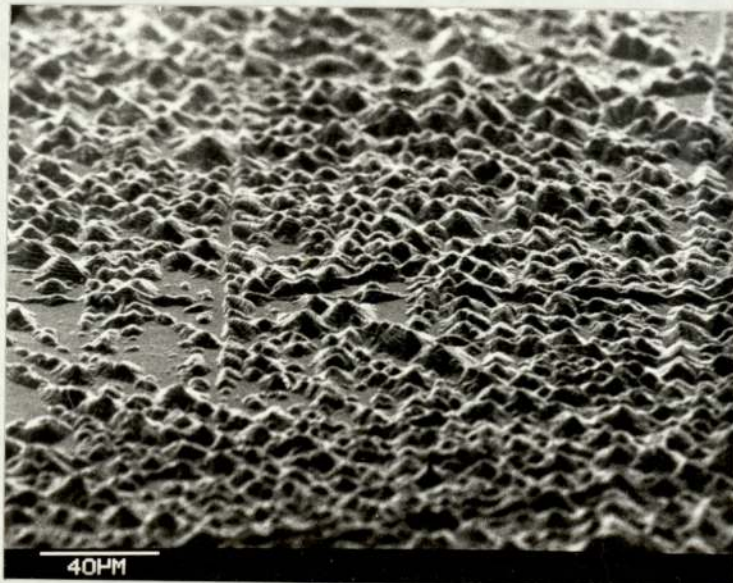


Fig. 3.2 S.P. Al "As rolled", after 15 secs anodizing at $23.8 A/dm^2$, showing hillock shaped features. T.a. 70°

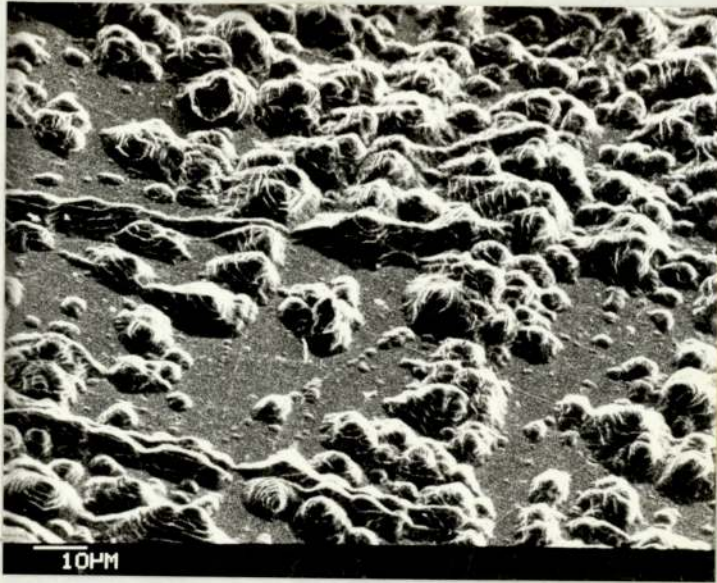


Fig. 3.3(i) S.P.A1 "As rolled", after 30 secs anodizing at 23.8 A/dm². T.a.70°



Fig. 3.3(ii) As Fig. 3.3(i), showing greater detail. T.a.70°

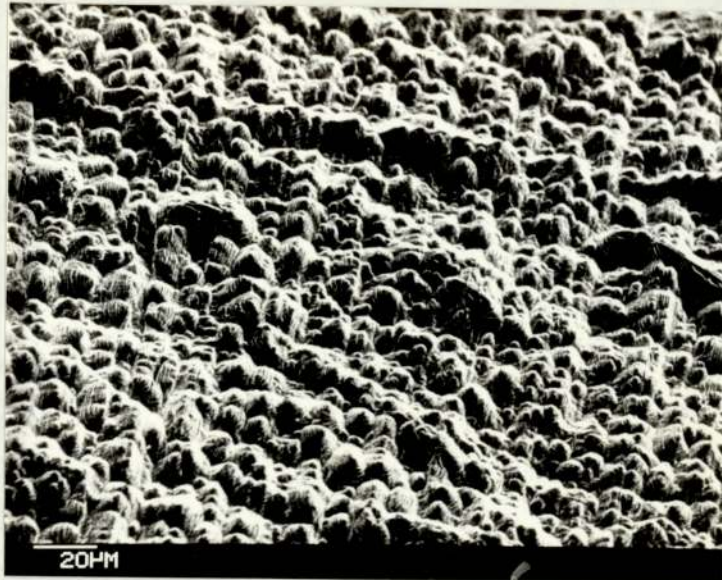


Fig. 3.4 S.P. Al "As rolled", after 60 secs anodizing at 23.8 A/dm^2 . T.a. 45°



Fig. 3.5(i) S.P. Al. "As rolled", after 300 secs anodizing at 23.8 A/dm^2 . T.a. 70°



Fig. 3.5(ii) As Fig. 3.5(i), showing greater detail of the concentric ring cracks formed due to growth of the alumina. T.a.70^o



Fig. 3.6(i) S.P.Al "As rolled", after 1 sec anodizing at 39.7 A/dm². T.a.70^o

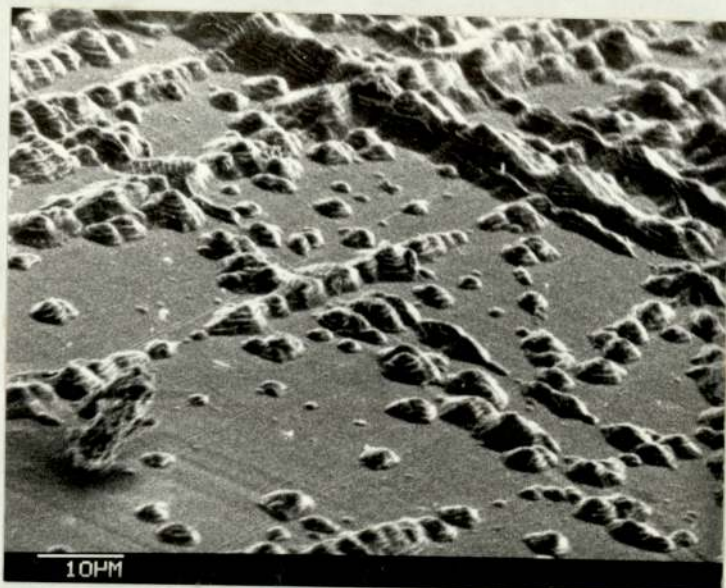


Fig. 3.6(ii) As Fig. 3.6(i), showing greater detail of hillock shaped features. T.a.70°

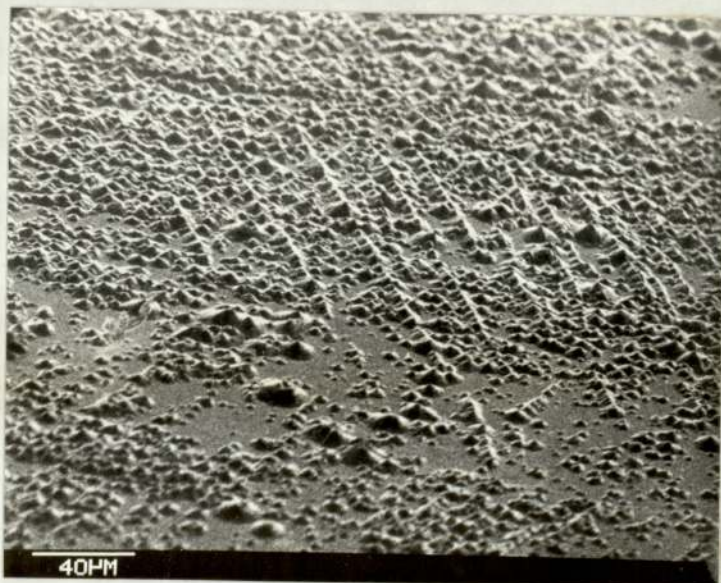


Fig. 3.7 S.P.Al "As rolled", after 5 secs anodizing at 39.7 A/dm². T.a.70°

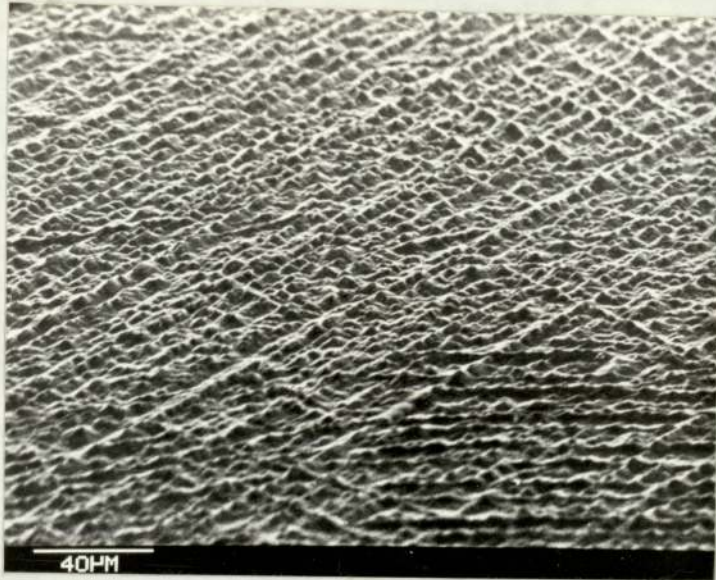


Fig. 3.8 S.P. Al. "As rolled", after 15 secs anodizing at 39.7 A/dm^2 . T.a. 70°



Fig. 3.9(i) C.P. Al. "As rolled", after 5 secs anodizing at 6.6 A/dm^2 . T.a. 70°

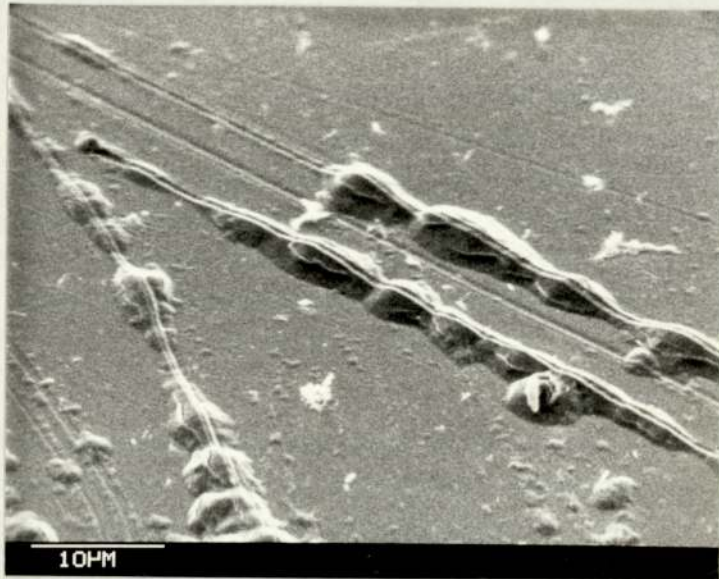


Fig. 3.9(ii) As Fig. 3.9(i), showing greater detail.
T.a. 70°

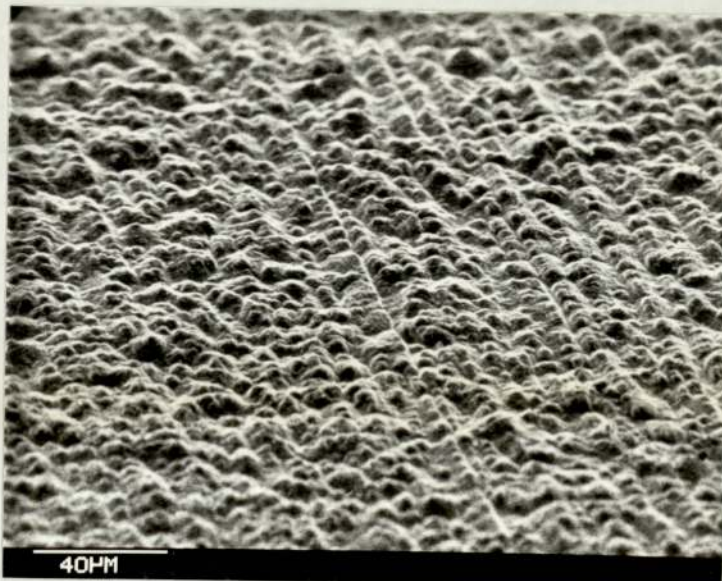


Fig. 3.10(i) C.P.Al, "As rolled", after 15 secs
anodizing at 6.6 A/dm^2 . T.a. 70°



Fig. 3.10(ii) As Fig. 3.10(i), showing greater detail.
T.a. 70°

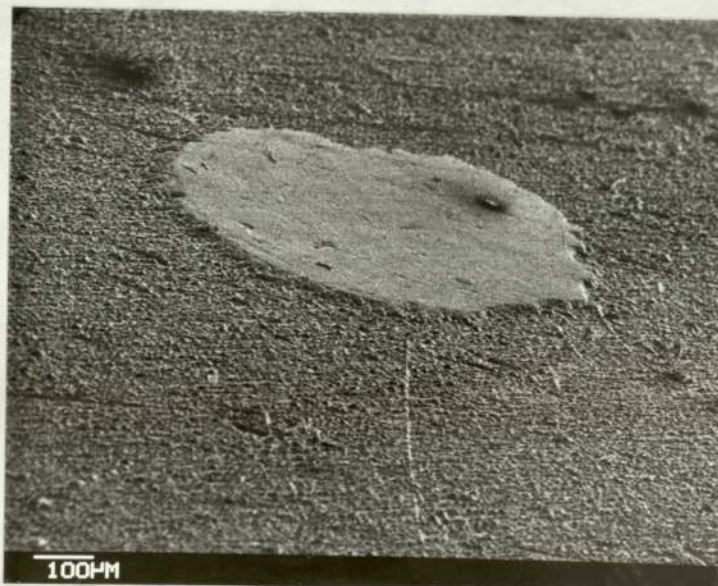


Fig. 3.11(i) C.P.Al "As rolled", after 52 secs
anodizing at 60 A/dm^2 . Shows circular
defect. T.a. 70°

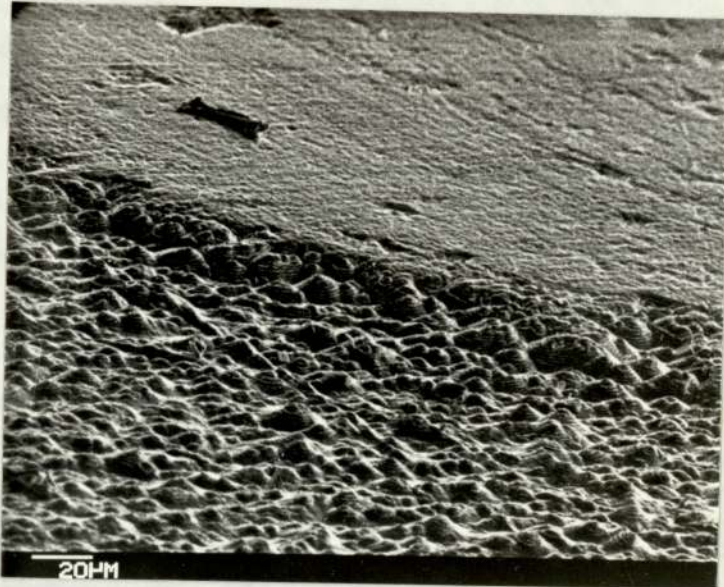


Fig. 3.11(ii) As Fig. 3.11(i), showing greater detail of the defect surface. T.a. 70°



Fig. 3.12 S.P.Al surface after being sand blasted. T.a. 70°

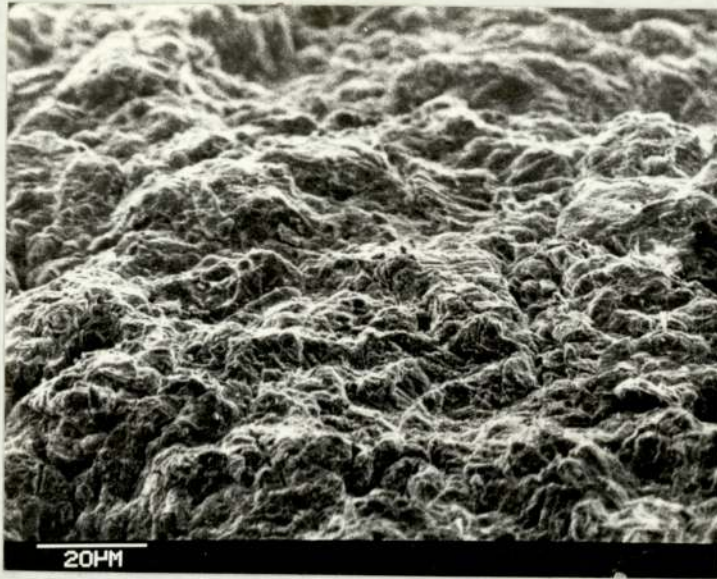


Fig. 3.13 As Fig. 3.12, after 41 minutes anodizing at 5.4 A/dm². T.a. 70°.



Fig. 3.14(i) C.P.Al "As rolled", after 8 minutes anodizing at 33 A/dm². Shows how at high glancing angles the hillock shaped features resemble "rosettes". T.a. 10°.



Fig. 3.14(ii) As Fig. 3.14(i) at a low glancing angle of T.a. 70°



Fig. 3.15 Alloy I, P180 abraded, after 15 minutes anodizing in 5% H_2SO_4 at $22.1 A/dm^2$. T.a. 45°

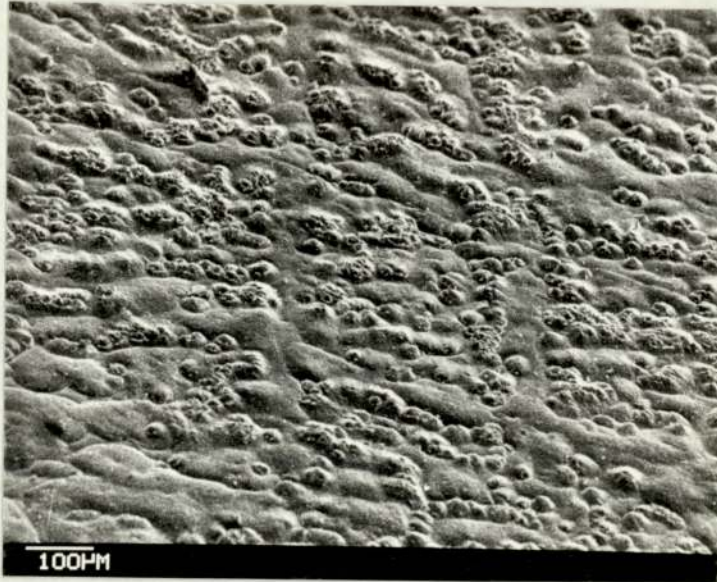


Fig. 3.16(i) Alloy I, 1 μm polish, after 12 minutes anodizing in 5% H₂SO₄ at 22.1 A/dm². T.a. 70°



Fig. 3.16(ii) As Fig. 3.16(i), showing more detail. T.a. 70°



Fig. 3.17 Alloy II, P180 abraded, after 18 minutes anodizing in 5% H_2SO_4 at $22.1 A/dm^2$. T.a. 70°



Fig. 3.18 Alloy II, P180 abraded, after 23 minutes anodizing in 5% H_2SO_4 at $22.1 A/dm^2$. No agitation, shows "burning". T.a. 45°



Fig. 3.19(i) Alloy II, 1 μm polish, after 14 minutes anodizing in 5% H₂SO₄ at 22.1 A/dm². T.a. 45°



Fig. 3.19(ii) As Fig. 3.19(i), showing oxide growth at grain boundaries. T.a. 45°

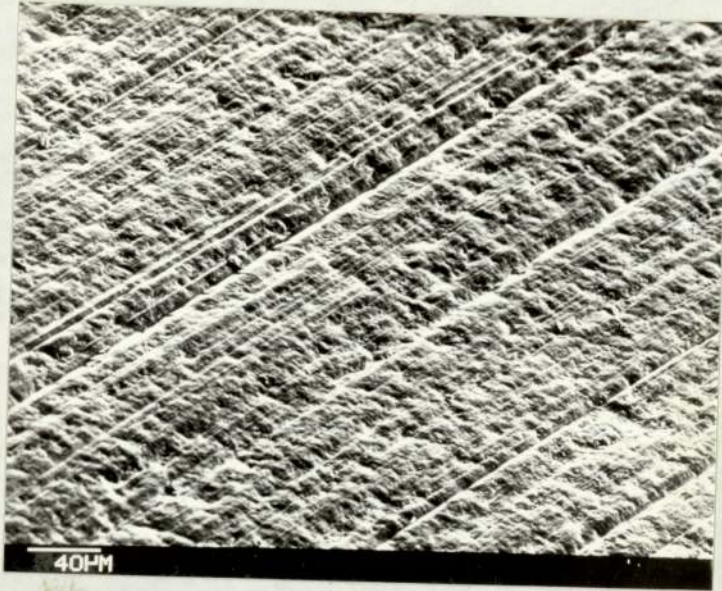


Fig. 3.20 H30 alloy, P180 abraded, after 2½ minutes anodizing at 33 A/dm². T.a. 45°



Fig. 3.21(i) H30 alloy, 1 μm polish, after 2 minutes anodizing at 33 A/dm². T.a. 70°

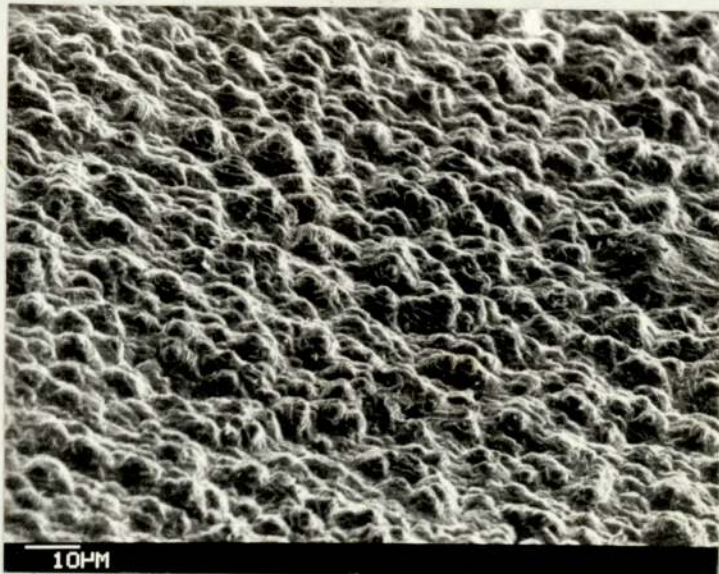


Fig. 3.21(ii) As Fig. 3.21(i), giving greater detail of surface produced. T.a. 70°

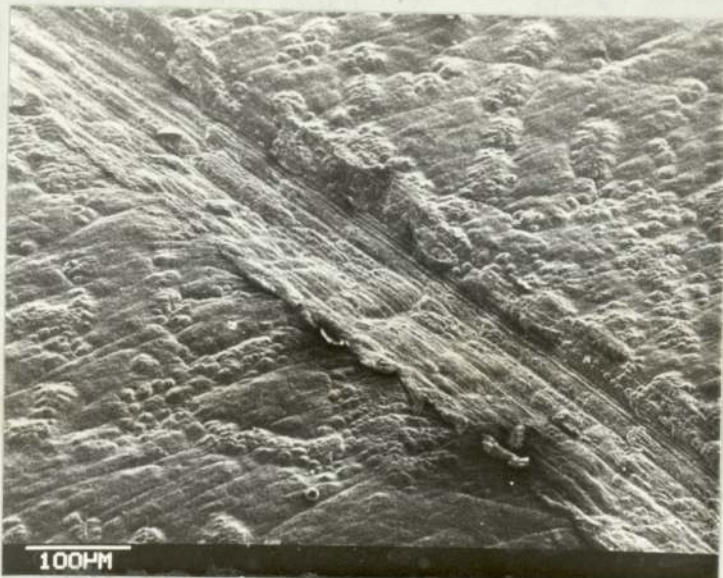


Fig. 3.22 Alloy I, $1\mu\text{m}$ polish, scored, after 6 minutes anodizing at 11 A/dm^2 . T.a. 70°



Fig. 3.23 Alloy II, 1 μ m polish, scored, after 7½ minutes anodizing at 11 A/dm². T.a. 70°

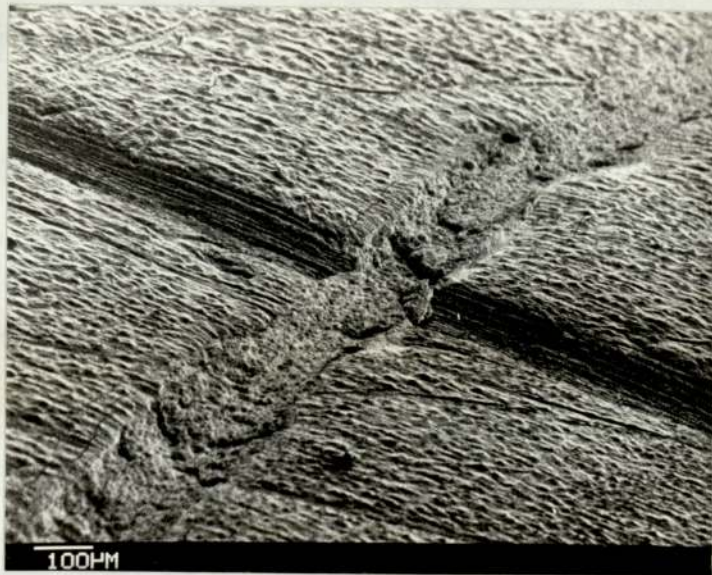


Fig. 3.24 C.P.Al "As rolled", scored, after 16½ minutes anodizing at 16.6 A/dm². T.a. 70°

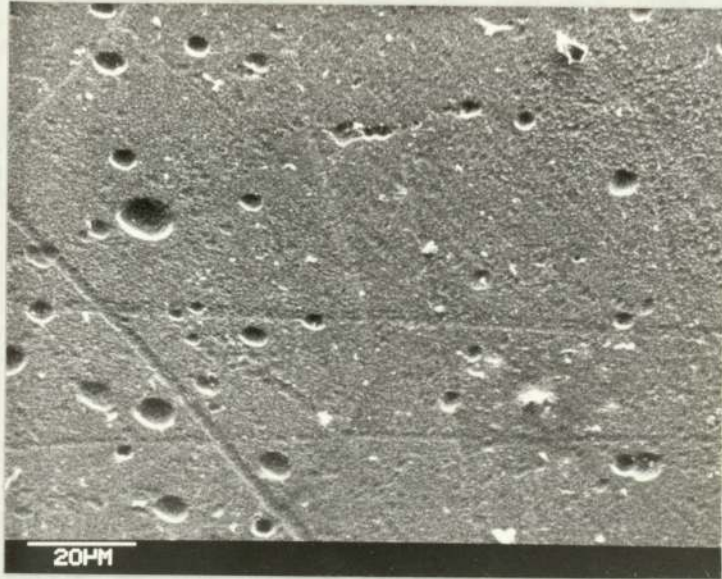


Fig. 3.25 S.P. Al etched in 10% NaOH at 60°C for 2 minutes, showing scratch lines and etch pits. T.a. 45°

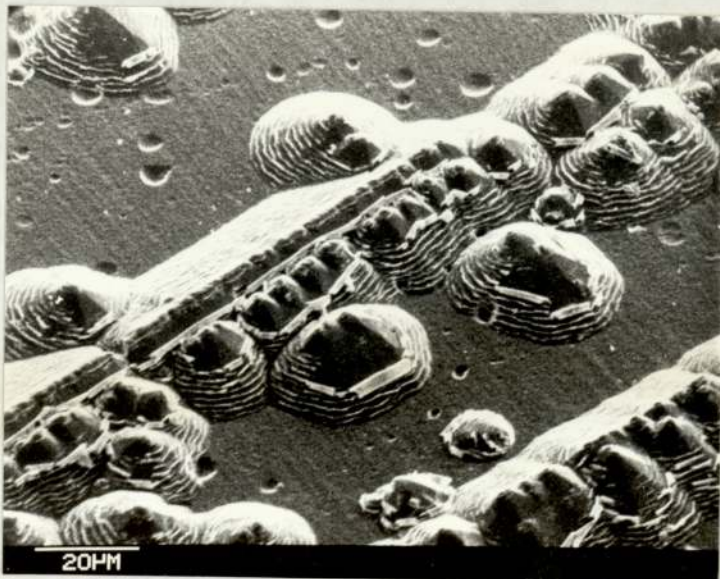


Fig. 3.26(i) As Fig. 3.25, after 30 secs anodizing at 35.7 A/dm². T.a. 45°



Fig. 3.26(ii) As Fig. 3.26(i), but unscratched region.
T.a. 45°

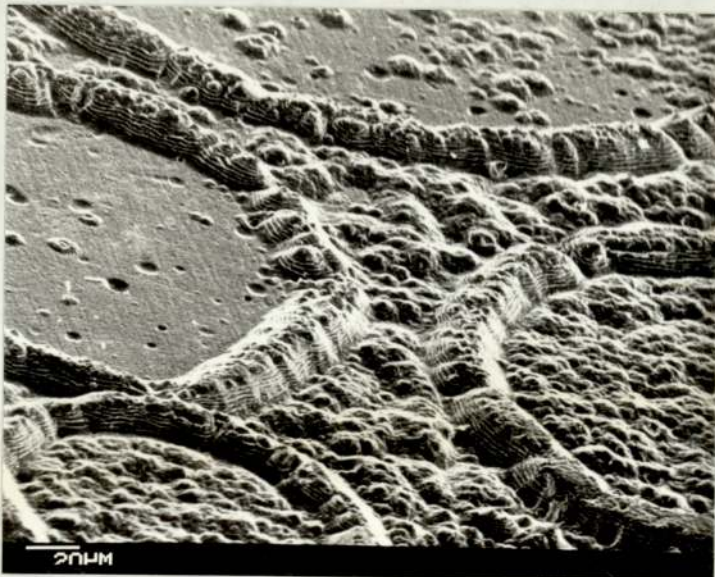


Fig. 3.27(i) As Fig. 3.25, after 30 secs anodizing
at 35.7 A/dm^2 . Showing defect rings.
T.a. 70°



Fig. 3.27(ii) As Fig. 3.27(i) at a different position on the surface at a high glancing view. T.a. 10°



Fig. 3.28(i) As Fig. 3.25, after 120 secs anodizing at 35.7 A/dm^2 . Shows spalling and curling of outer layer of oxide. T.a. 10° .

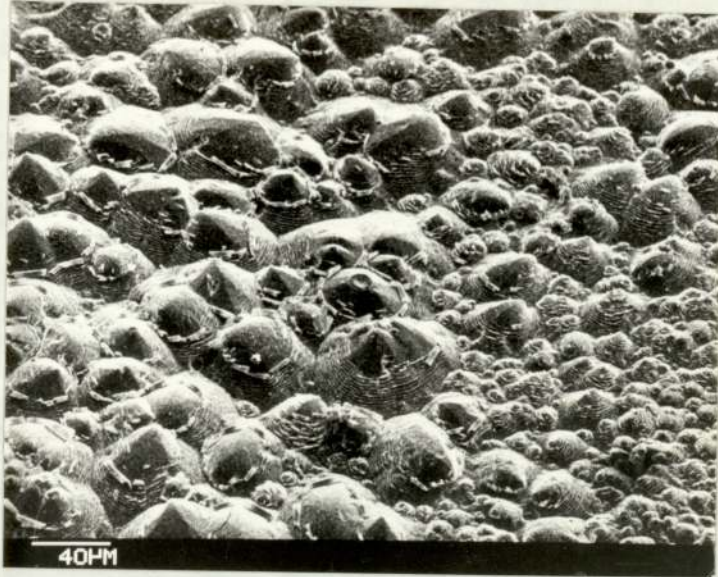


Fig. 3.28(ii) As Fig. 3.28(i) at lower glancing angle. T.a. 45° .

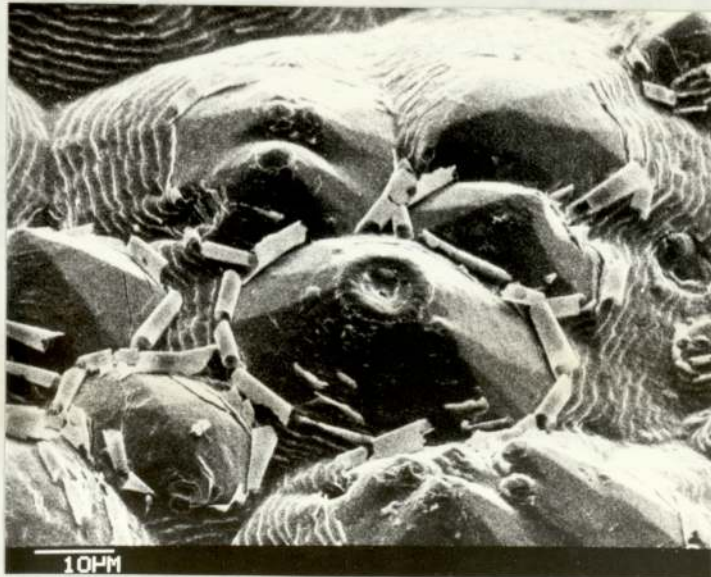


Fig. 3.28(iii) As Fig. 3.28(ii), showing greater detail of spalling and curling of outer layer of oxide. T.a. 45°

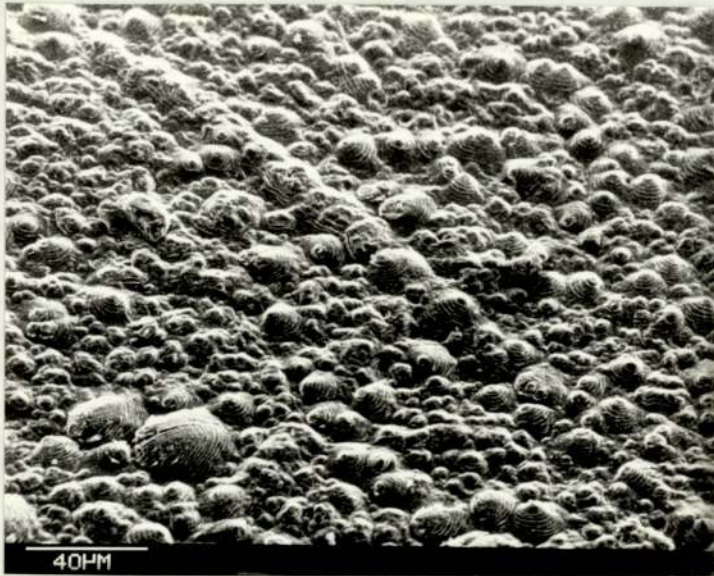


Fig. 3.29 As Fig. 3.25, after 480 secs anodizing
at 35.7 A/dm^2 . T.a. 45°



Fig. 3.30(i) As Fig. 3.25, after 57 minutes anodizing
at 11 A/dm^2 . T.a. 45°

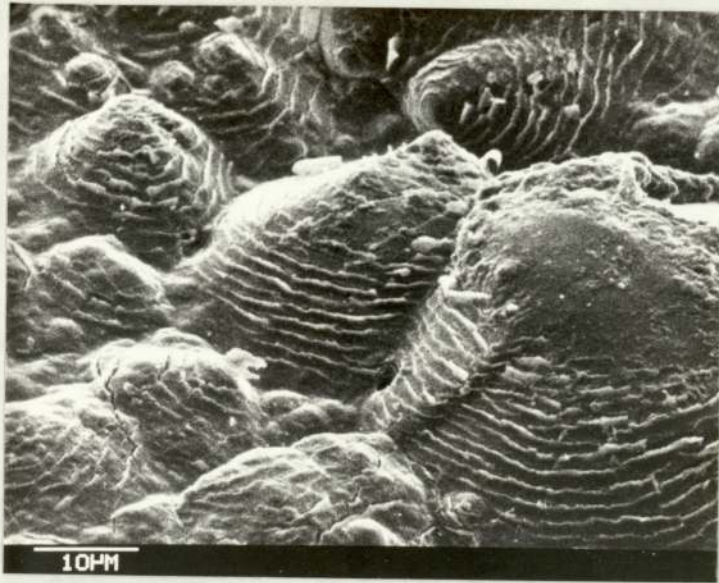


Fig. 3.30(ii) As Fig. 3.30(i), showing greater detail. T.a. 45°



Fig. 3.30(iii) As Fig. 3.30(ii), showing greater detail. T.a. 45°



Fig. 3.31 Alloy BB3 etched in 10% NaOH at 60°C for 2 minutes, after 17 minutes anodizing at 10.4 A/dm². T.a. 45°



Fig. 3.32 Alloy 5182 (etched), after 17½ minutes anodizing at 9 A/dm². T.a. 45°



Fig. 3.33 Alloy 2117CP (etched), after 15 minutes anodizing at 10.4 A/dm². T.a. 45°



Fig. 3.34 Alloy 2117HP (etched), after 18½ minutes anodizing at 9 A/dm². T.a. 45°

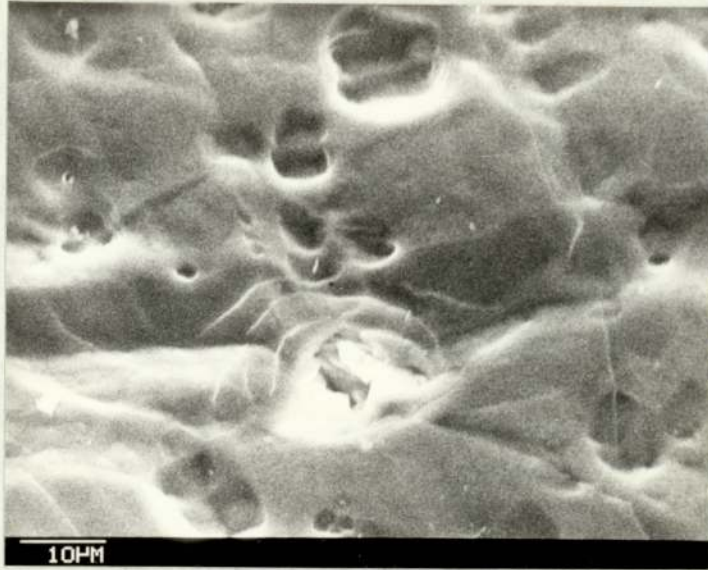


Fig. 3.35 Alloy 2002 (etched), after 17 minutes anodizing at 10.9 A/dm². T.a. 45°



Fig. 3.36 Alloy 609 (etched), after 14½ minutes anodizing at 10.4 A/dm². T.a. 45°



Fig. 3.37 S.P. Al chemically polished in 78% H_3PO_4 - 16% H_2SO_4 - 6% HNO_3 - 0.5% CuSO_4 at 98°C for 90 secs. T.a. 45°



Fig. 3.38 As Fig. 3.37, after $4\frac{1}{2}$ minutes anodizing at 41.6 A/dm^2 . T.a. 45°

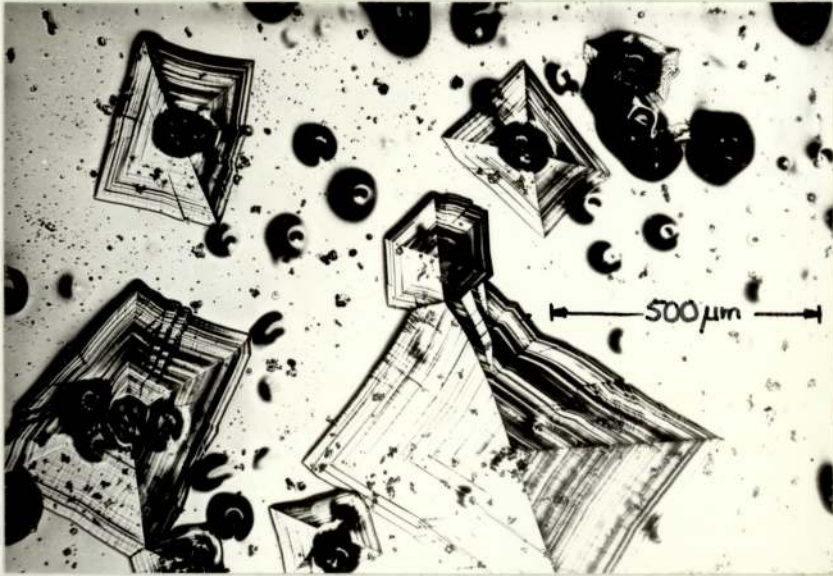


Fig. 3.39(i) Optical photomicrograph of pyramid shaped icing defects - gassing defects also visible.

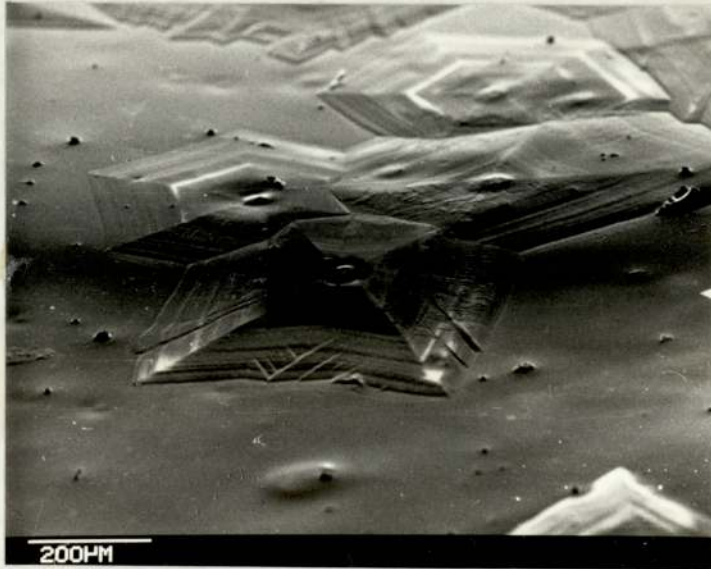


Fig. 3.39(ii) Typical icing defects showing strations and central blip. T.a, 70°

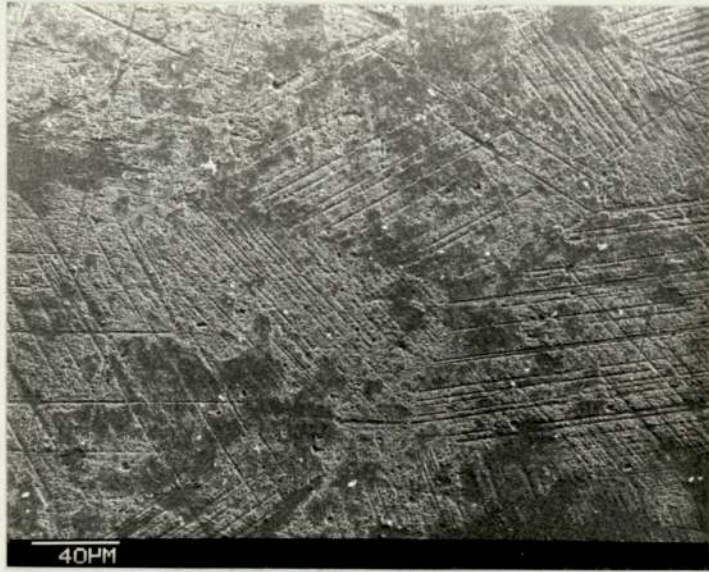


Fig. 3.40 S.P.Al etched surface showing scratch lines and etch pits. T.a. 45°

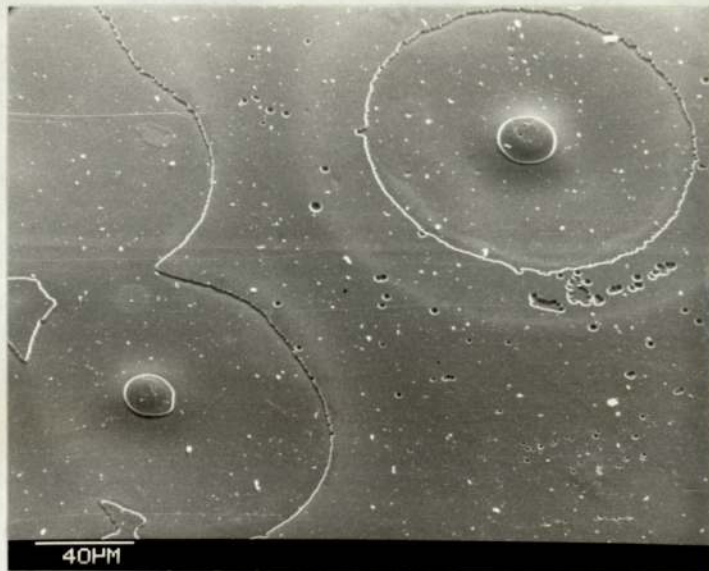


Fig. 3.41(i) S.P.Al electropolished for 60 secs, showing gassing defects and radial spread dissolving the air-formed oxide film. T.a. 45°

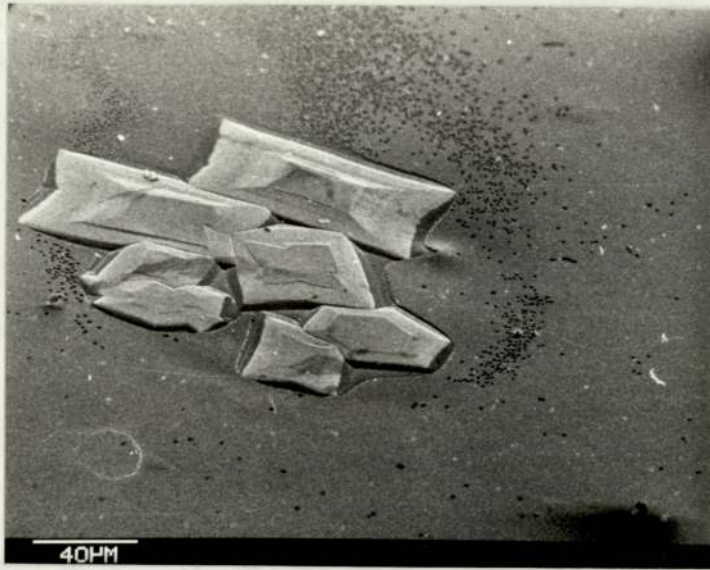


Fig. 3.41(ii) As Fig. 3.41(i), showing icing defects formed at high current density regions. T.a. 70°

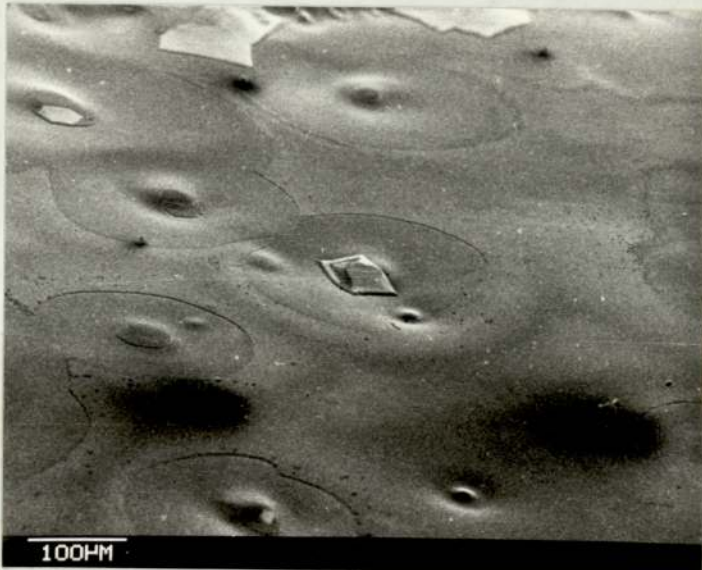


Fig. 3.41(iii) As Fig. 3.41(i), showing the association of icing defects with gassing defects. T.a.70°



Fig. 3.42 Icing defect around a gassing defect after 120 seconds electropolishing. T.a.80°



Fig. 3.43(i) Surface topography after electropolishing and then hard anodized. Shows depressions at sites of prior icing defects. T.a.45°



Fig. 3.43(ii) As Fig. 3.43(i), showing greater detail of the depressions at the sites of prior icing defects. T.a. 70°



Fig. 3.44 S.P.Al electropolished for 90 secs at 10 A/dm^2 , showing a few gassing defects. T.a. 70°



Fig. 3.45 As Fig. 3.44, after anodizing for 37 minutes at 10 A/dm^2 . Showing the replication of the gassing defects and the characteristic nodular oxide growth. T.a. 70°

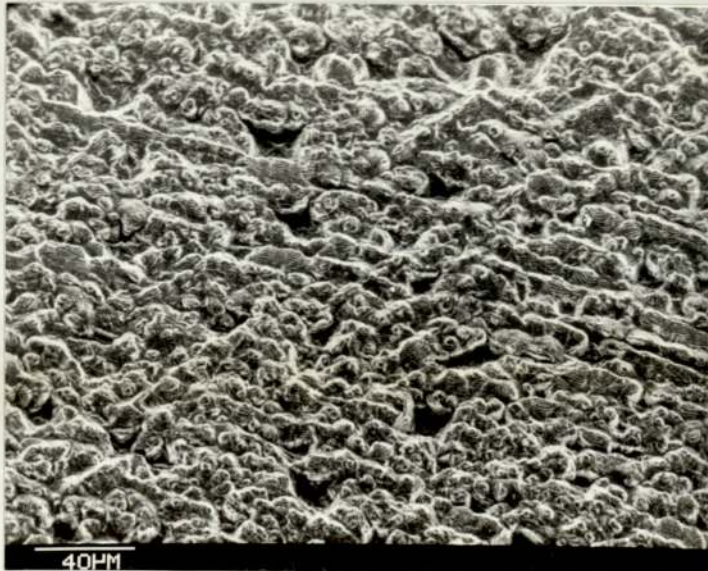


Fig. 3.46 S.P.Al heat treated and air cooled, after 27 minutes anodizing at 5.5 A/dm^2 . T.a. 45°

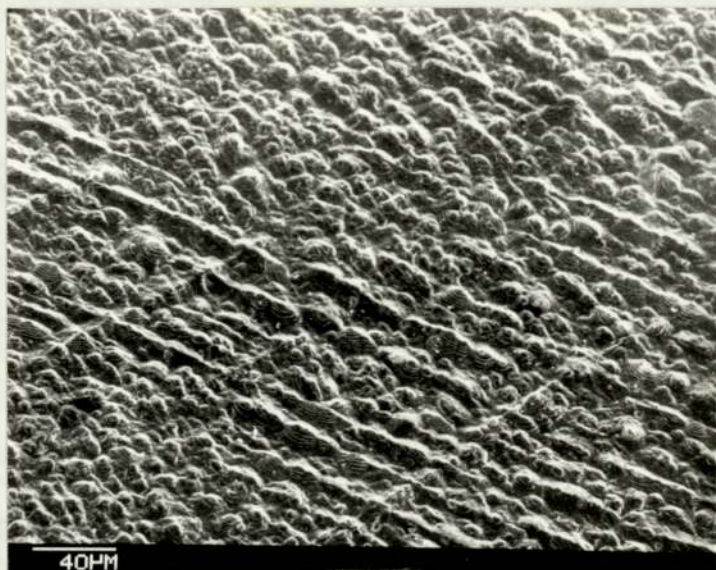


Fig. 3.47 S.P.Al, heat treated and water quenched,
after 34 minutes anodizing at 5.3 A/dm^2 .
T.a. 45°

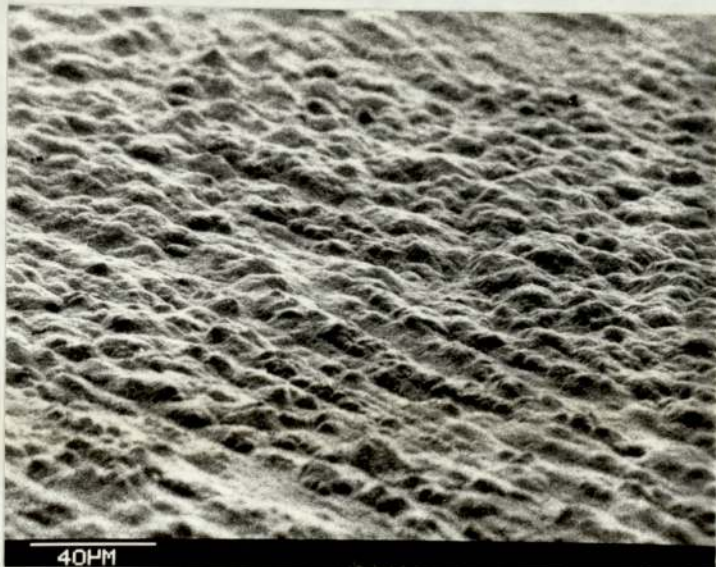


Fig. 3.48 C.P.Al, heat treated and air cooled, after
22 minutes anodizing at 7.1 A/dm^2 . T.a. 70°



Fig. 3.49 C.P. Al, heat treated and water quenched, after 17 minutes anodizing at 6.9 A/dm^2 . T.a. 45°

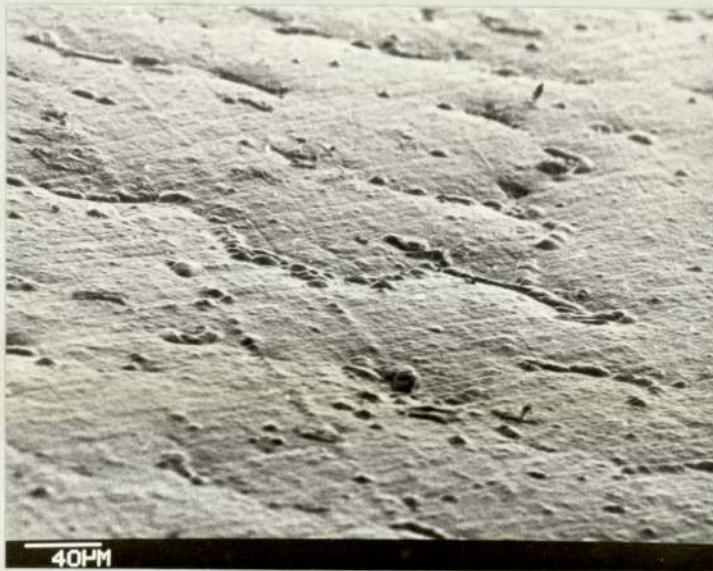


Fig. 3.50 Alloy I, heat treated and air cooled and mechanically polished to $1 \mu\text{m}$, after 11 minutes anodizing at 22 A/dm^2 . T.a. 70°



Fig. 3.51 Alloy I, heat treated and water quenched and mechanically polished to $1\mu\text{m}$, after 12 minutes anodizing at 22 A/dm^2 . T.a. 70°

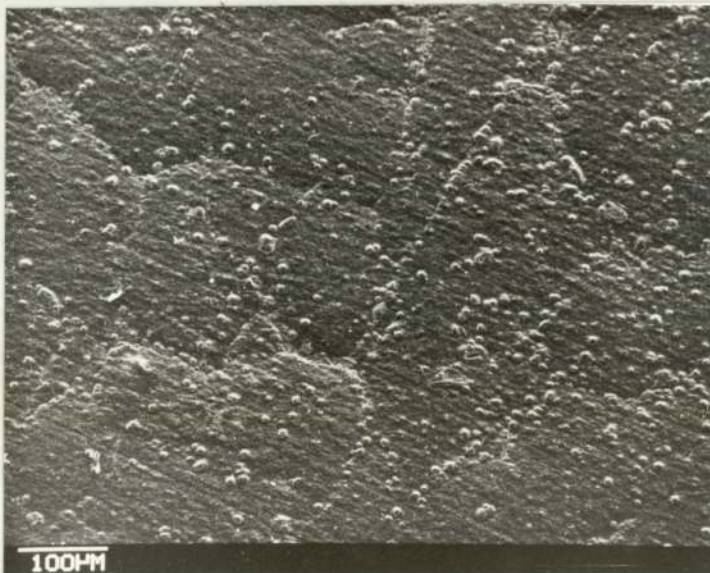


Fig. 3.52 Alloy II, heat treated and air cooled and mechanically polished to $1\mu\text{m}$, after 12 minutes anodizing at 22 A/dm^2 . T.a. 10°

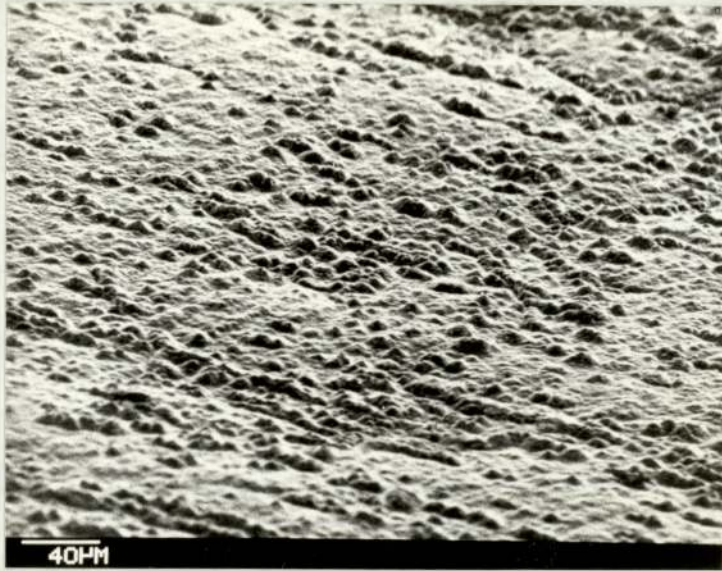


Fig. 3.53 Alloy II, heat treated and water quenched and mechanically polished to $1\mu\text{m}$, after 10 minutes anodizing at 22 A/dm^2 . T.a. 70°

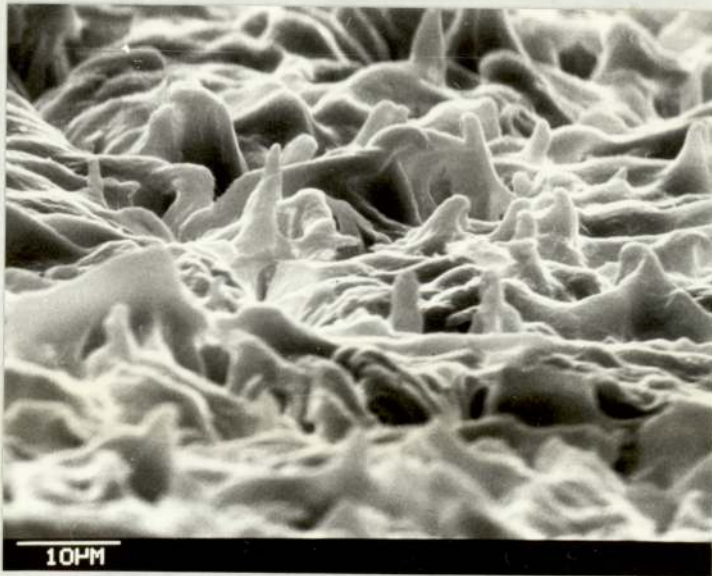


Fig. 3.54 C.P.Al "As rolled", after 70 minutes anodizing at 13.3 A/dm^2 in $10\% \text{H}_2\text{SO}_4$ at 17°C . Shows a powdery coating. T.a. 70°

Fig. 3.55 Potential vs Time Curves for Anodized Specimens from Experiment 3.23.

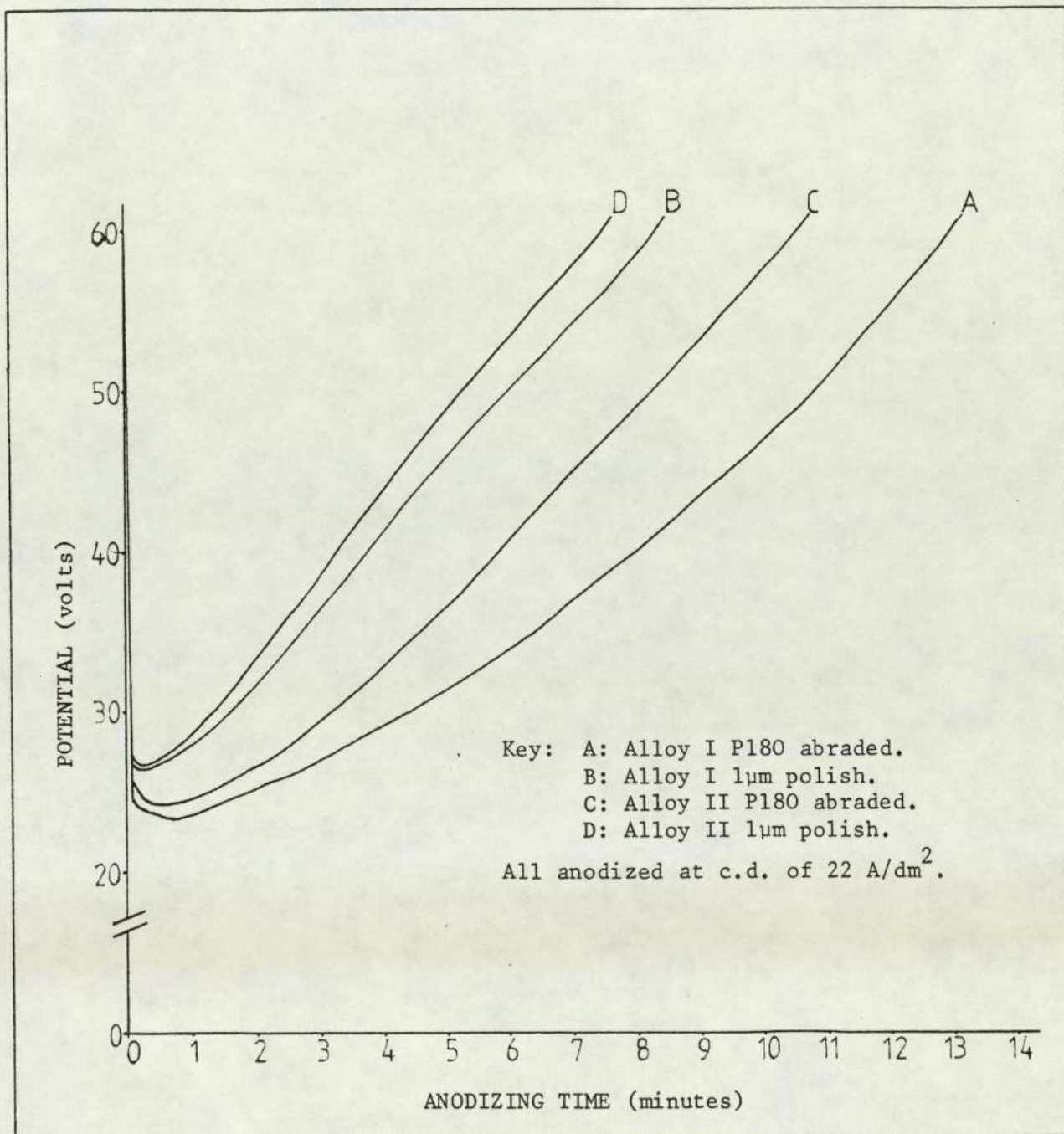


Fig. 3.56 Potential vs Time Curves for Anodized Specimens from Experiment 3.24.

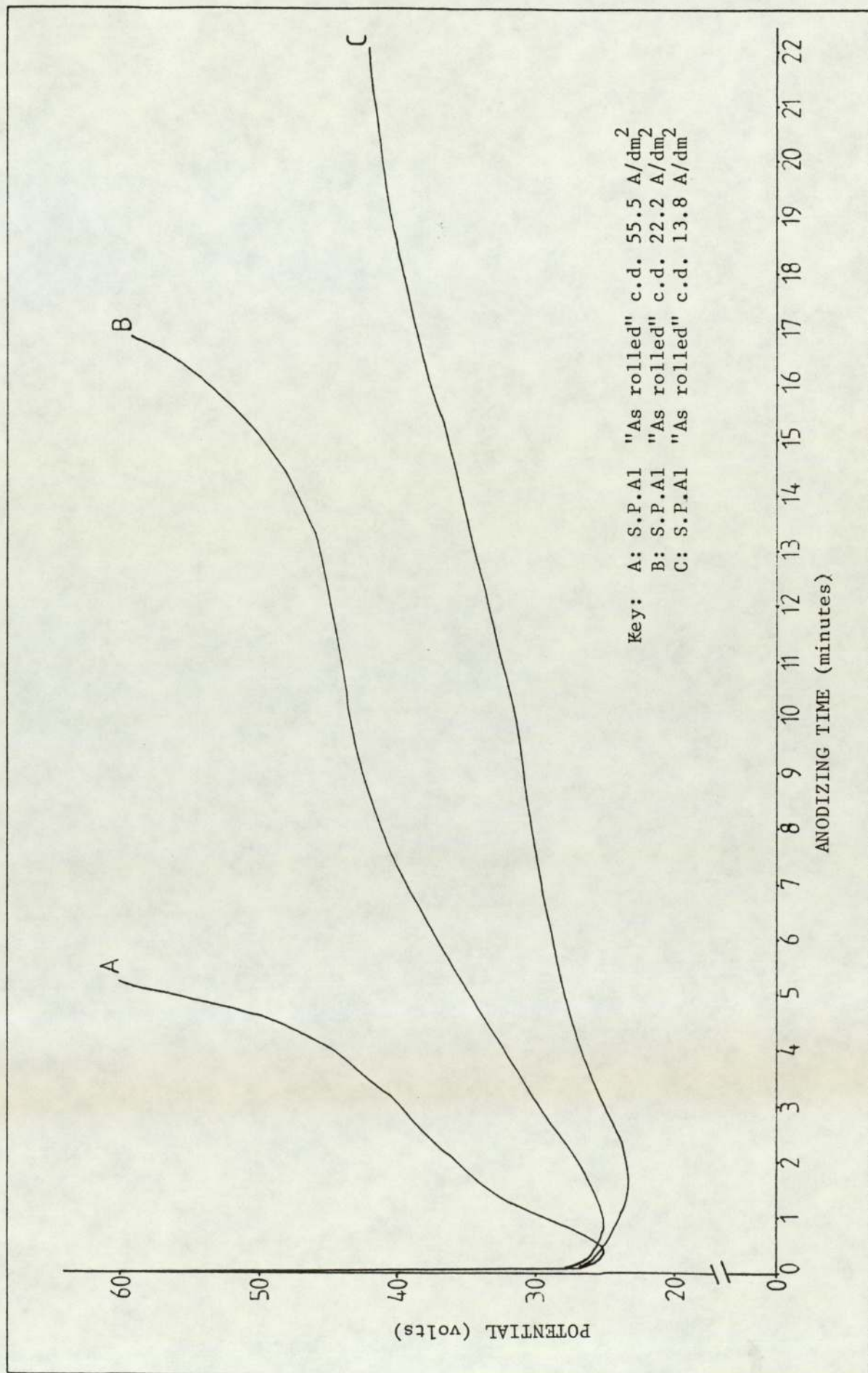


Fig. 3.57 Potential vs Time Curves for Anodized Specimens from Experiment 3.25.

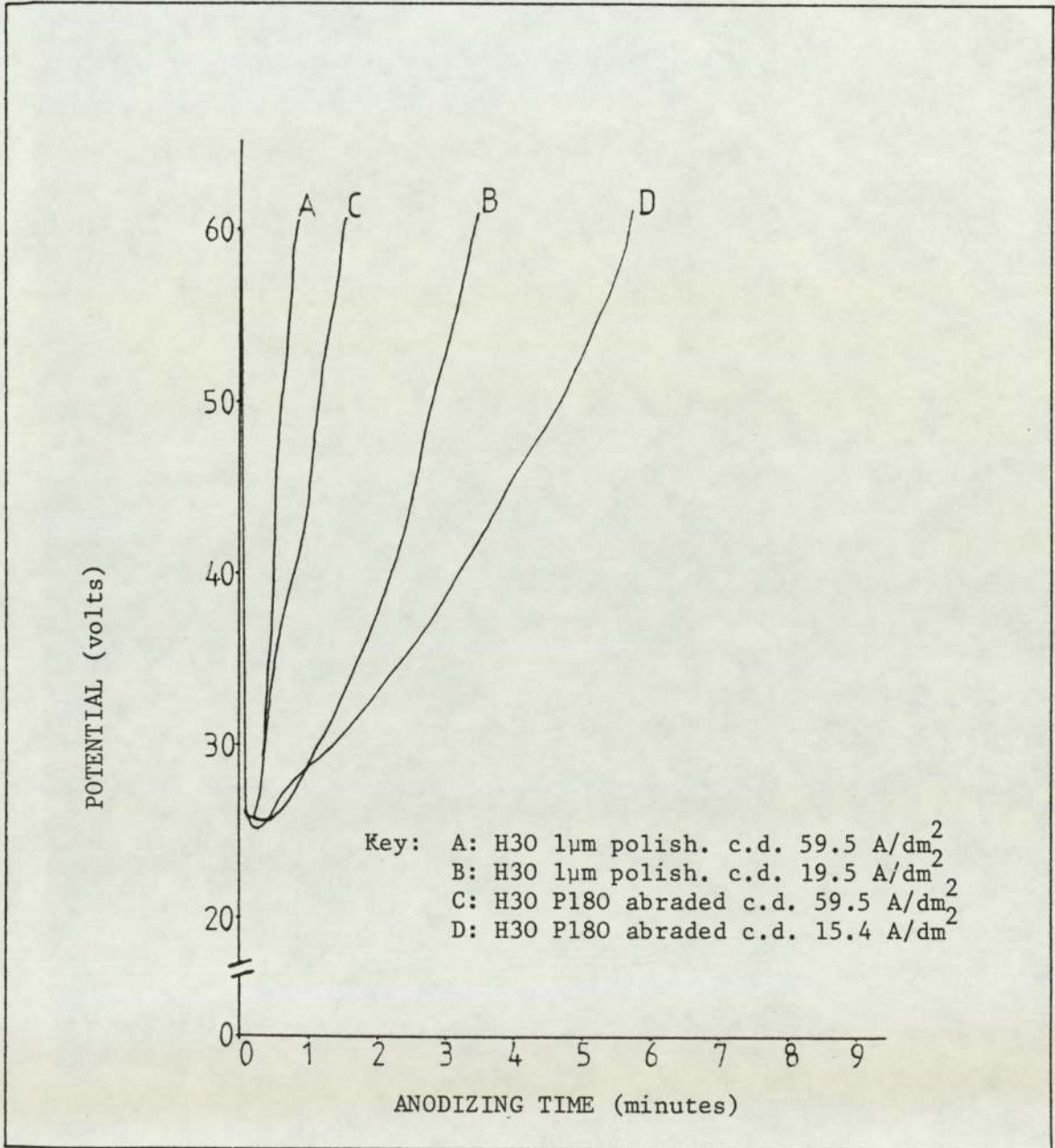


Fig. 3.58 Potential vs Time Curves for Anodized Specimens
from Experiment 3.26.

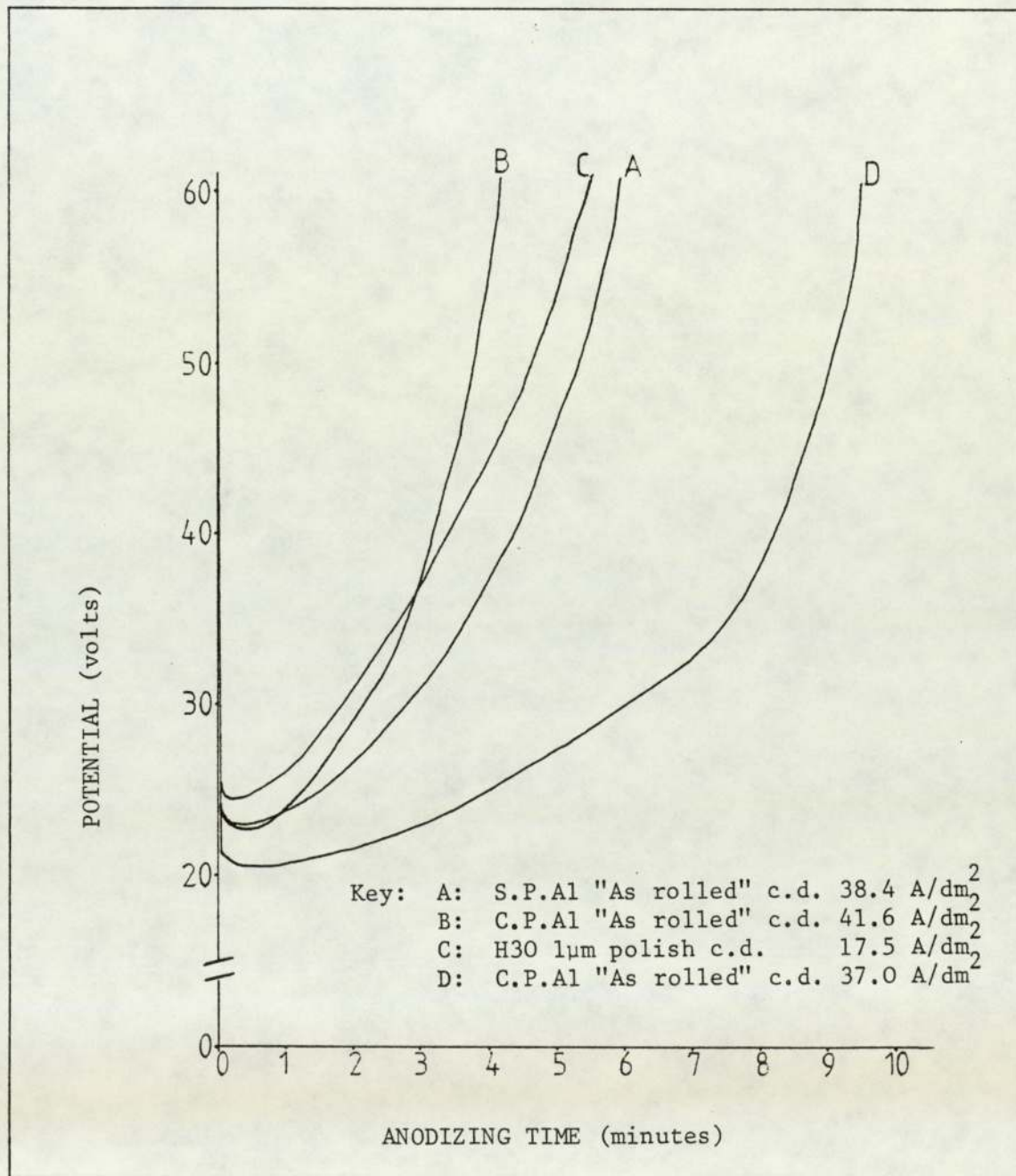
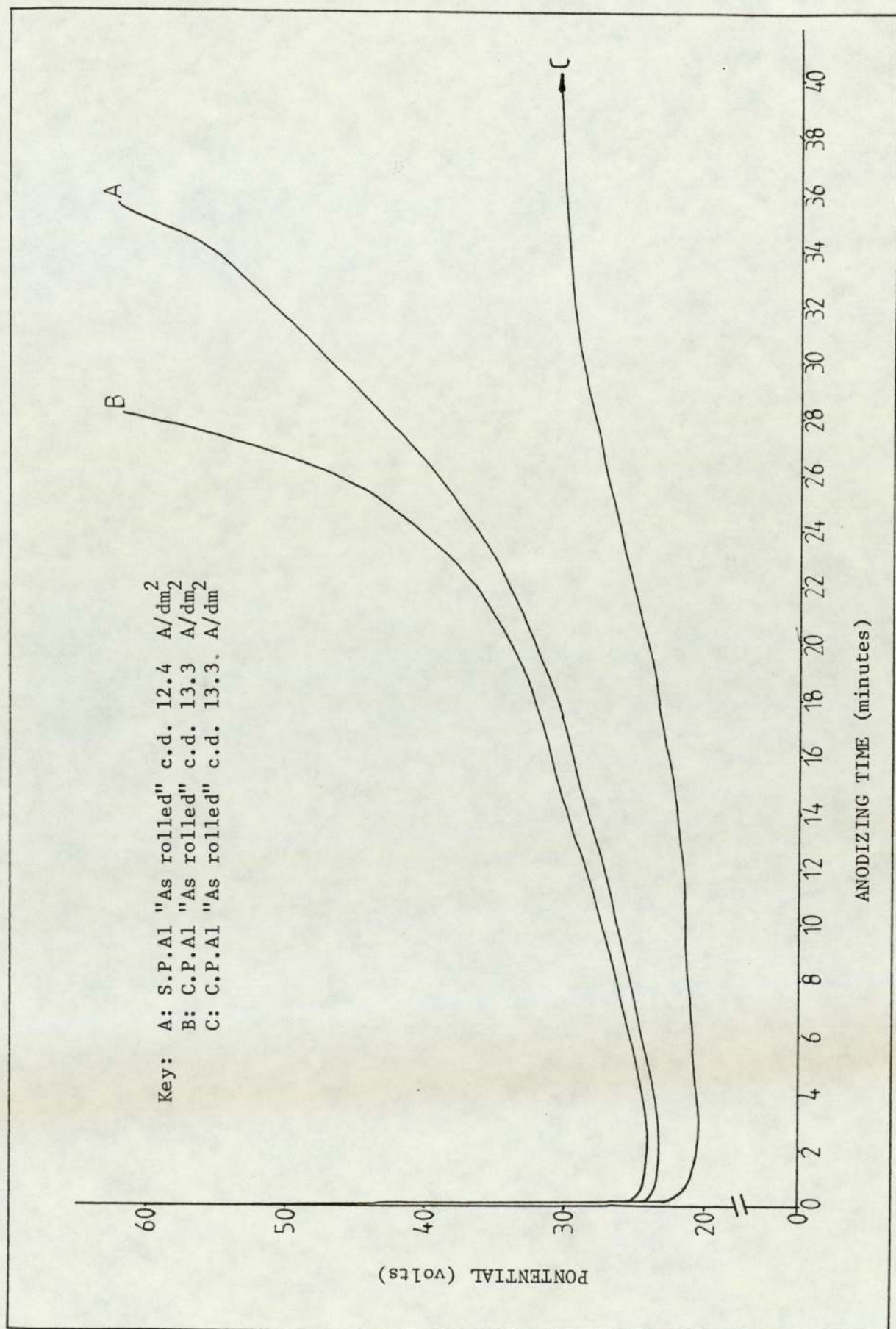


Fig. 3.59 Potential vs Time Curves for Anodized Specimens from Experiment 3.27.



Note: For Fig. 3.60 to 3.65
* Signifies specimen etched.

Fig. 3.60 Potential vs Time Curves for Anodized Specimens from Experiment 3.28.

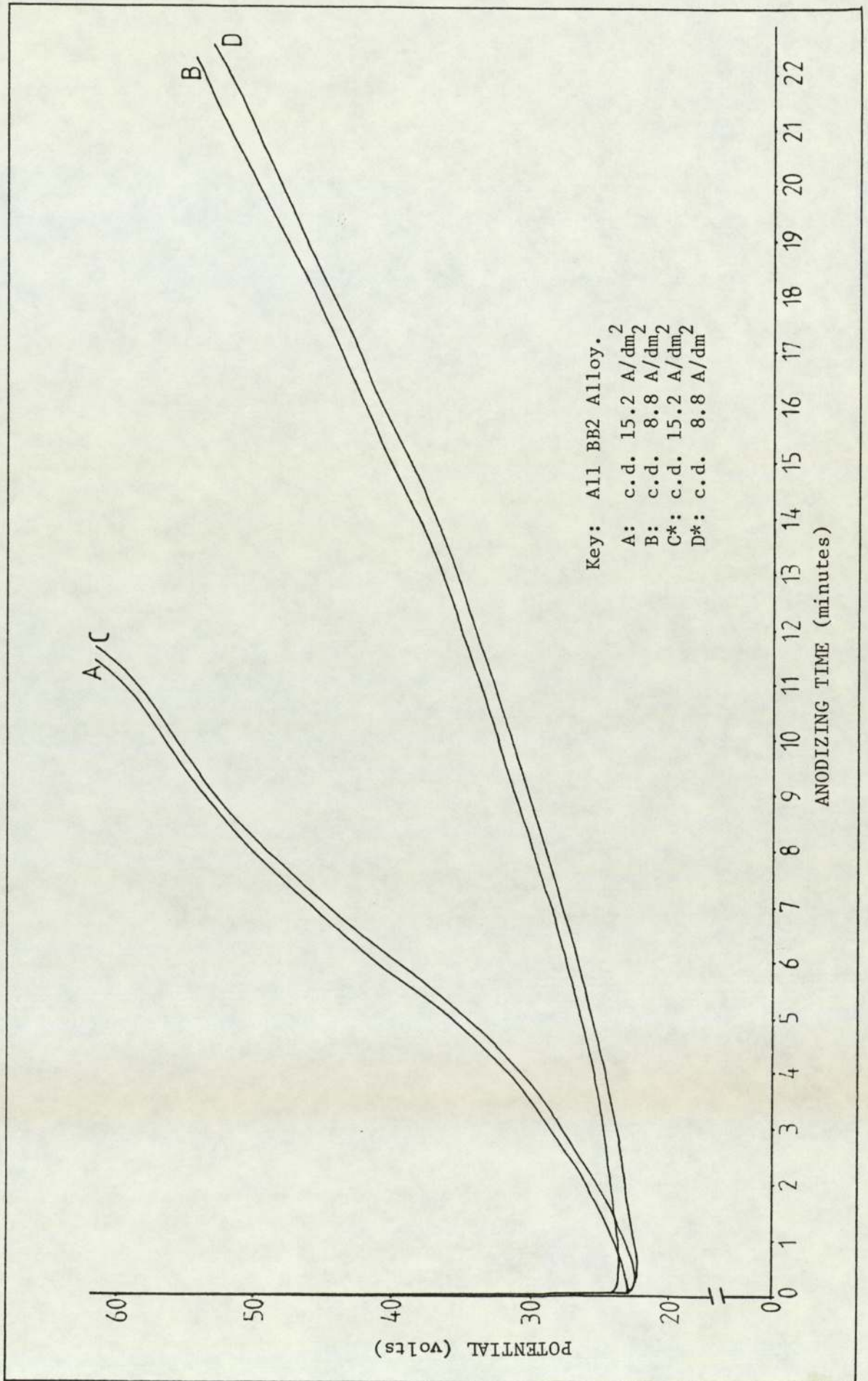


Fig. 3.61 Potential vs Time Curves for Anodized Specimens from Experiment 3.28.

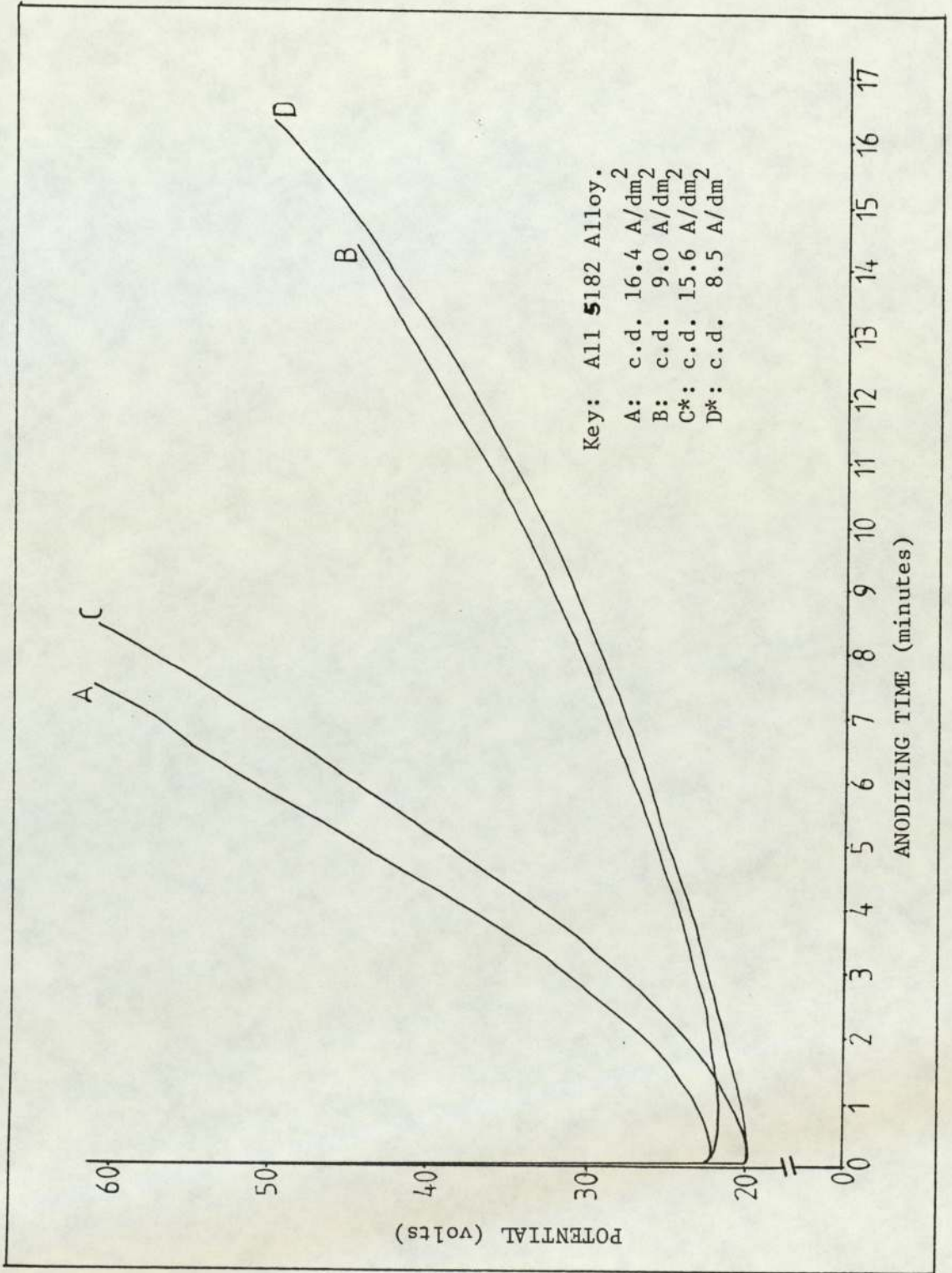


Fig. 3.62 Potential vs Time Curves for Anodized Specimens from Experiment 3.28.

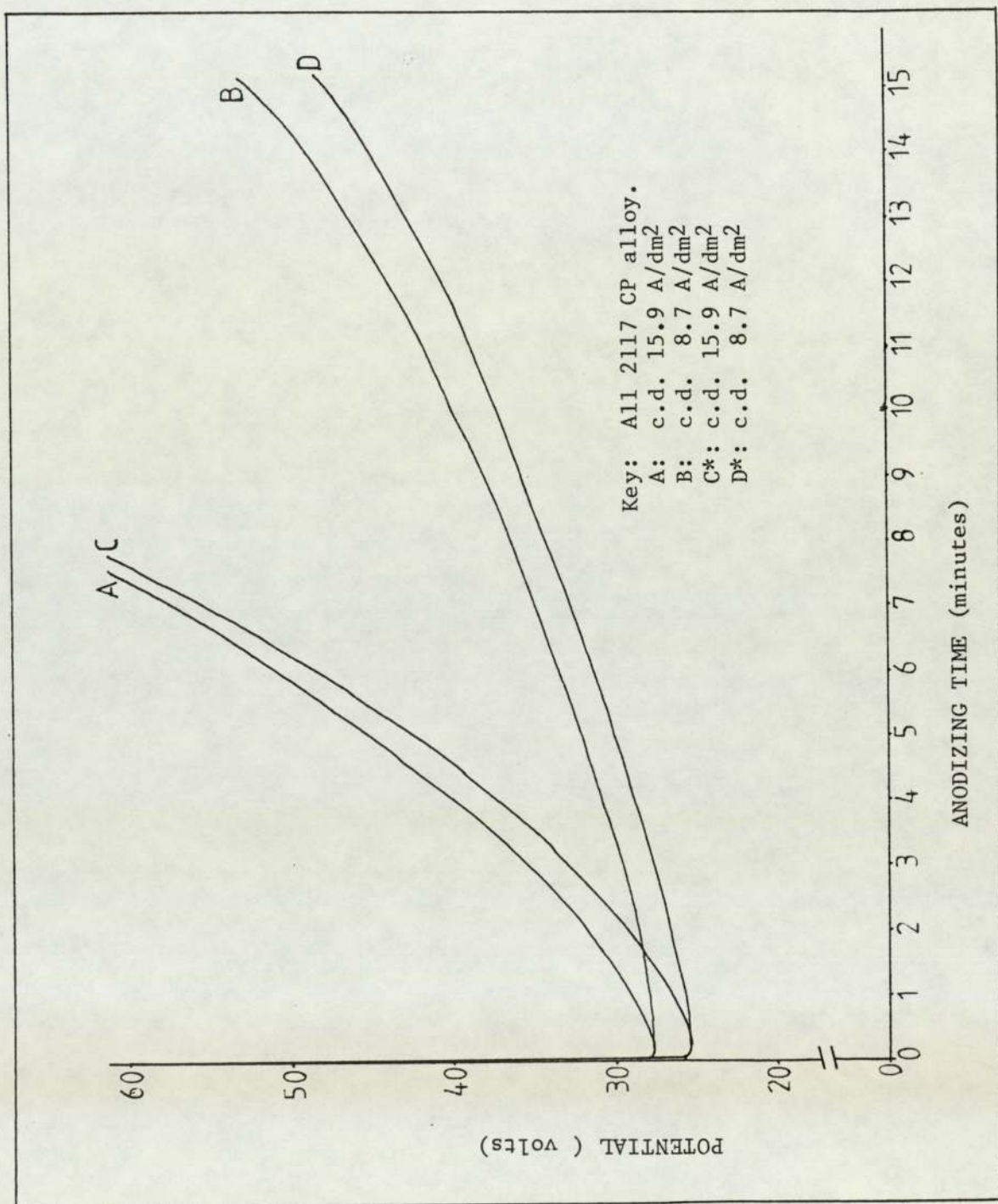


Fig. 3.63 Potential vs Time Curves for Anodized Specimens from Experiment 3.28.

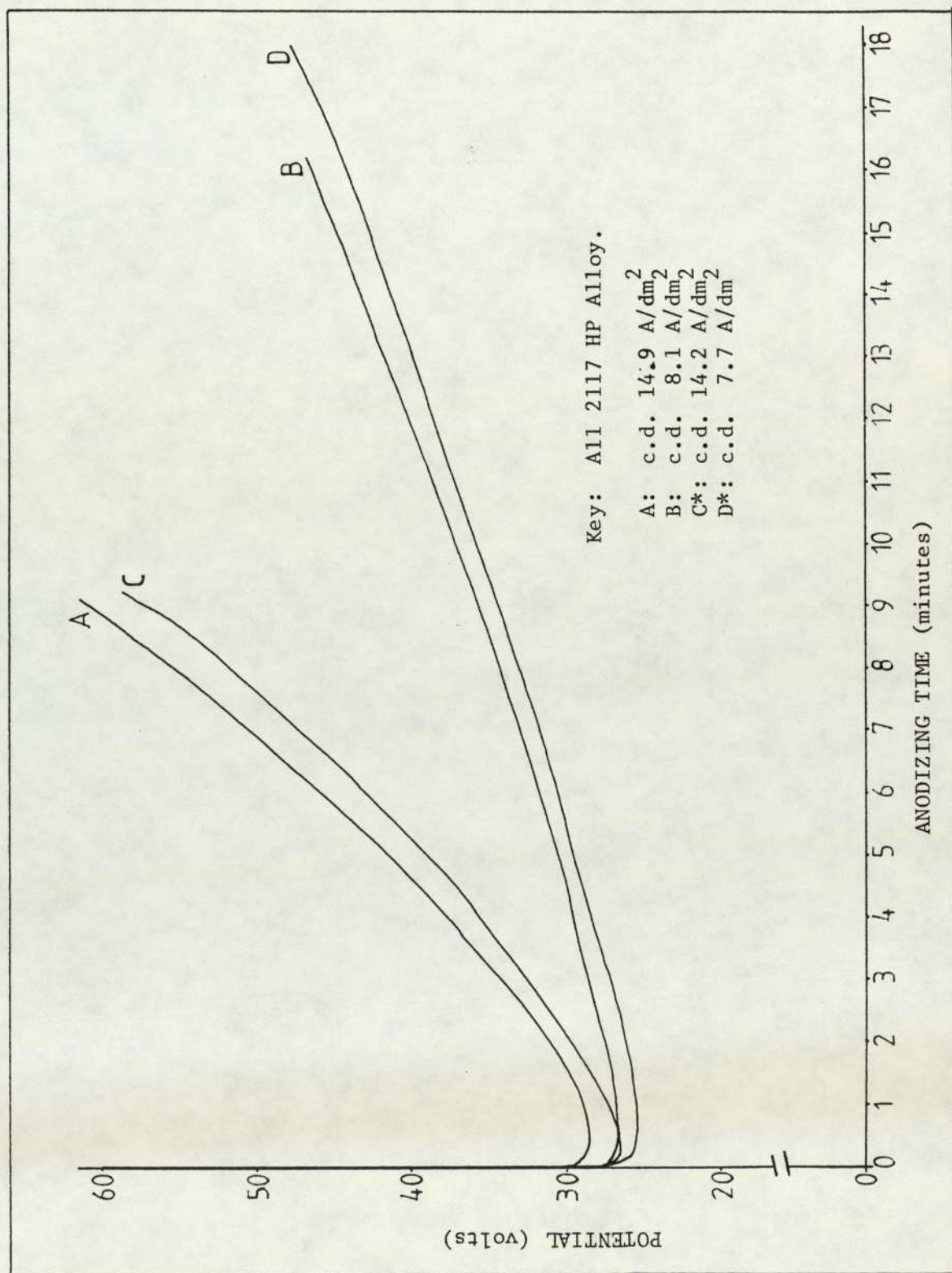


Fig. 3.64 Potential vs Time Curves for Anodized Specimens from Experiment 3.28.

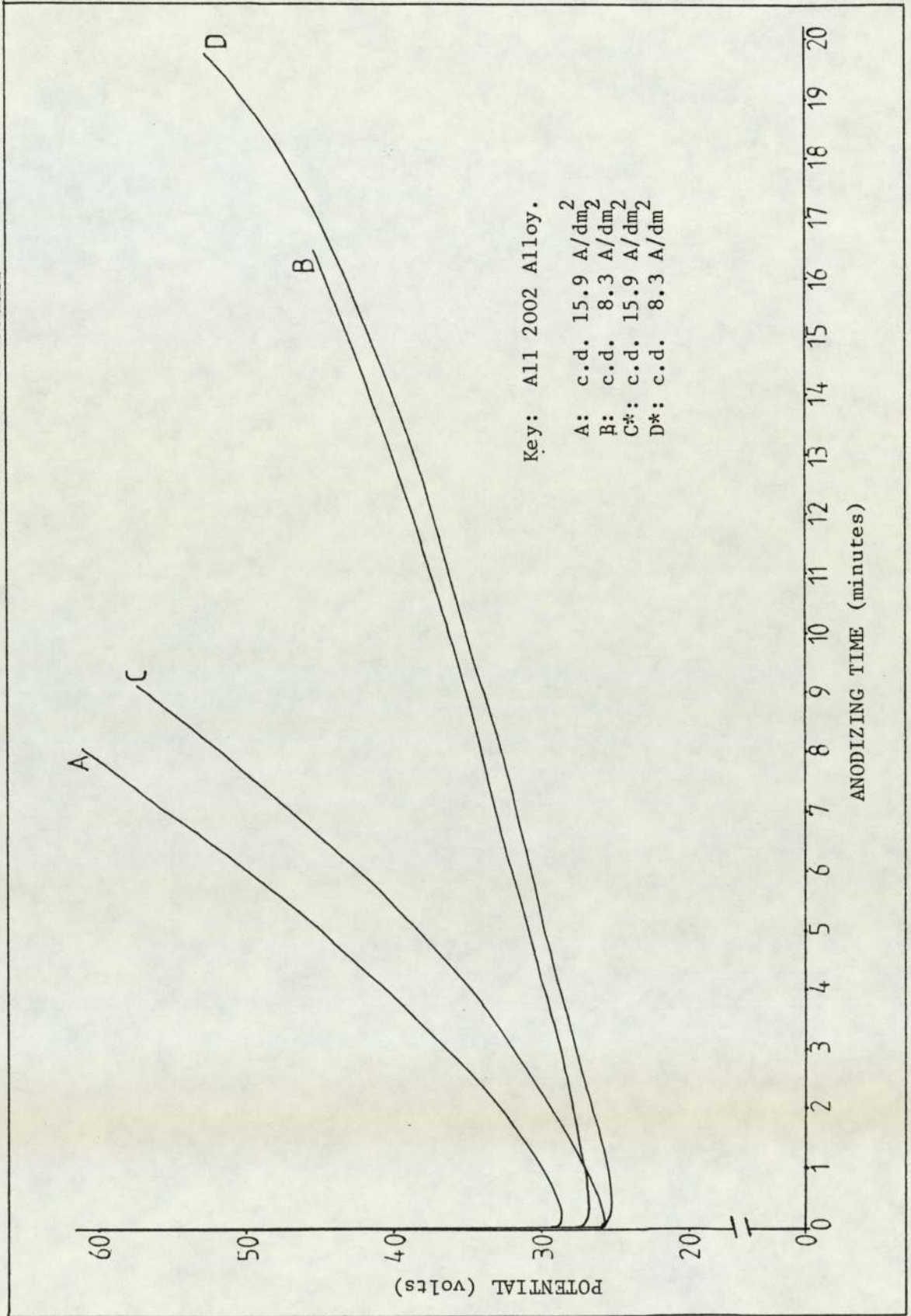
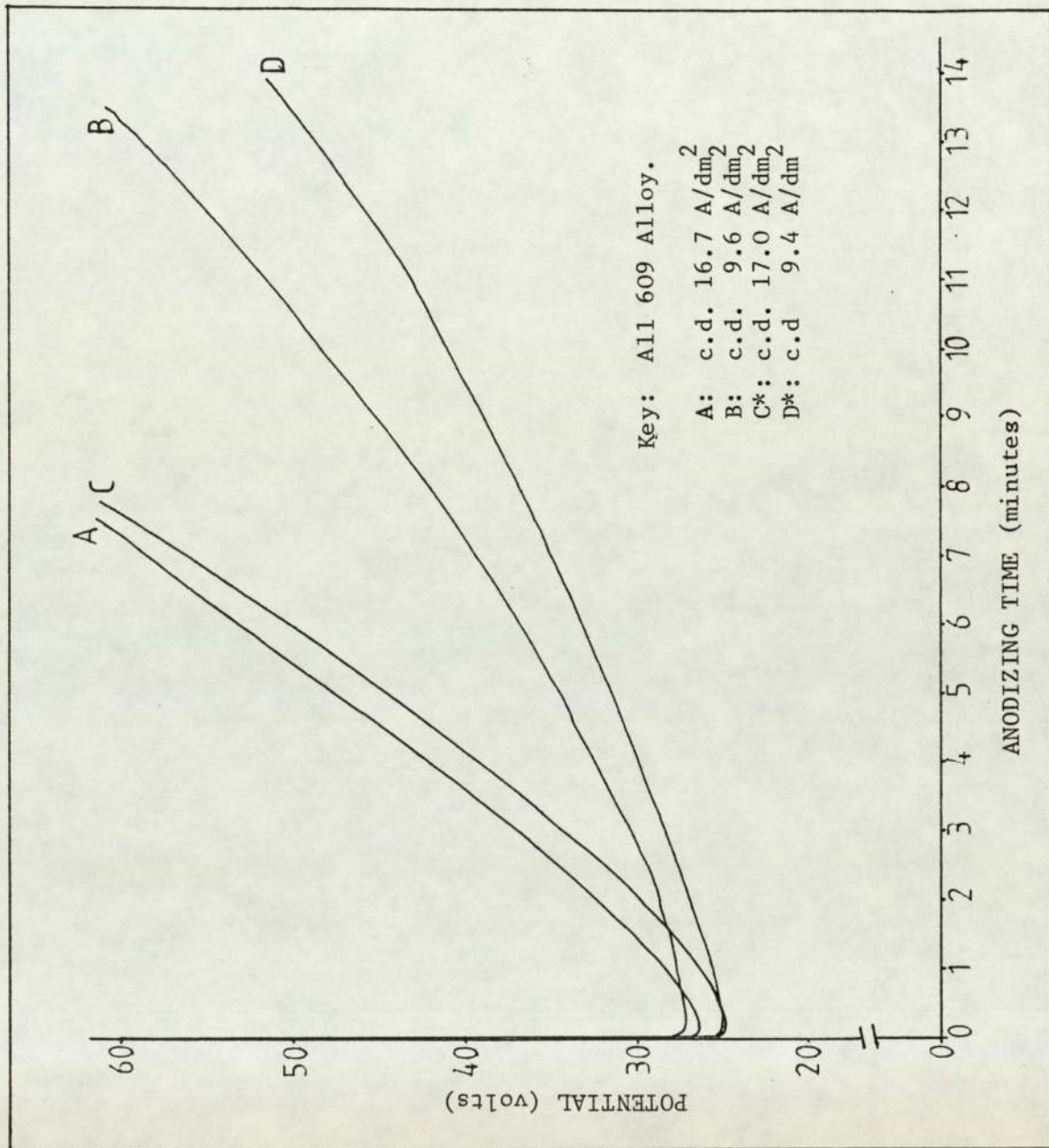


Fig. 3.65 Potential vs Time Curves for Anodized Specimens from Experiment 3.28.



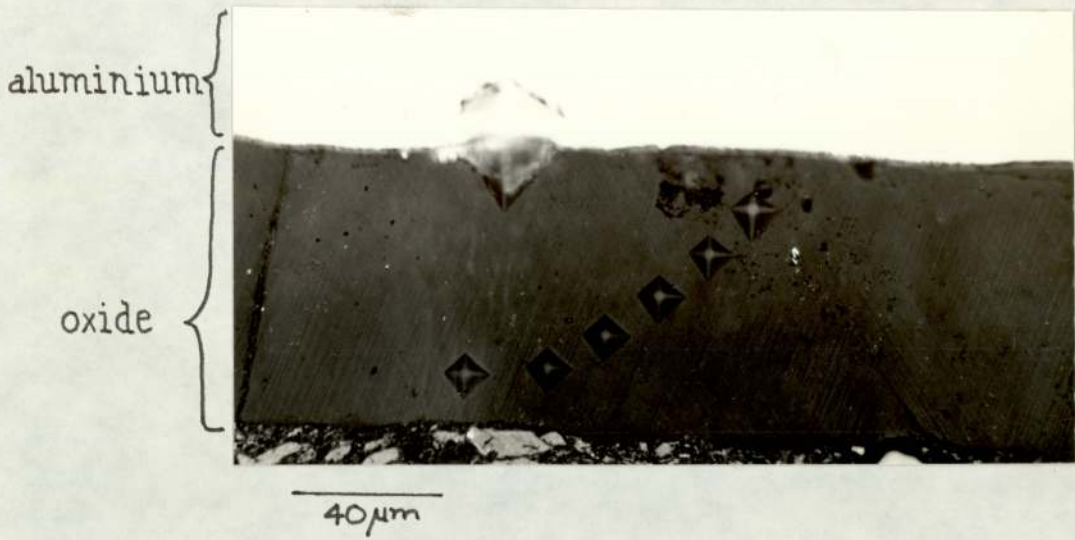


Fig. 3.66 Microhardness indentation ladder across oxide.

Fig. 3.67 Plot of Thickness against Time for data from Experiment 3.29.

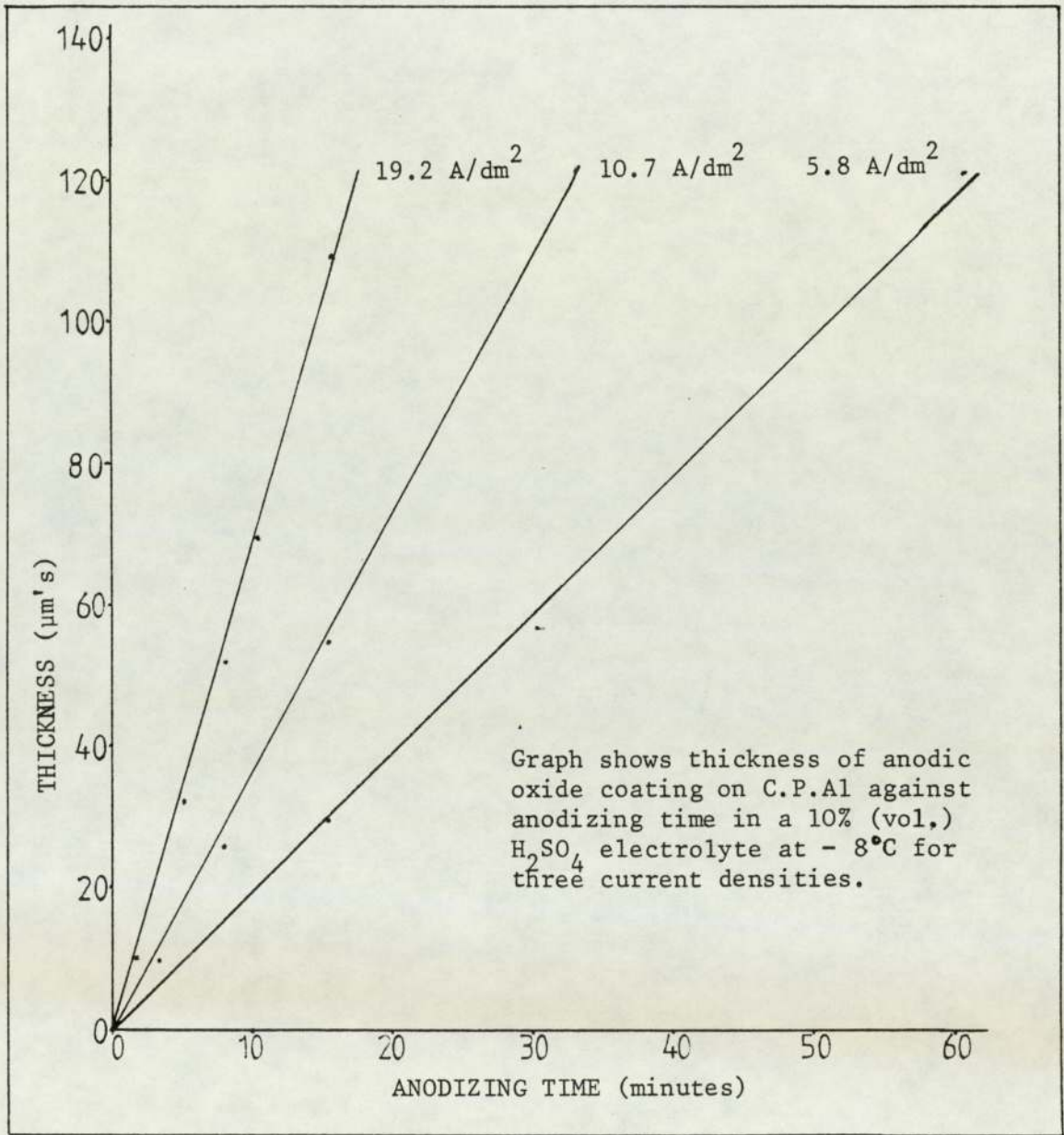


Fig. 3.68 Plot of Thickness against Time for data from Experiment 3.30.

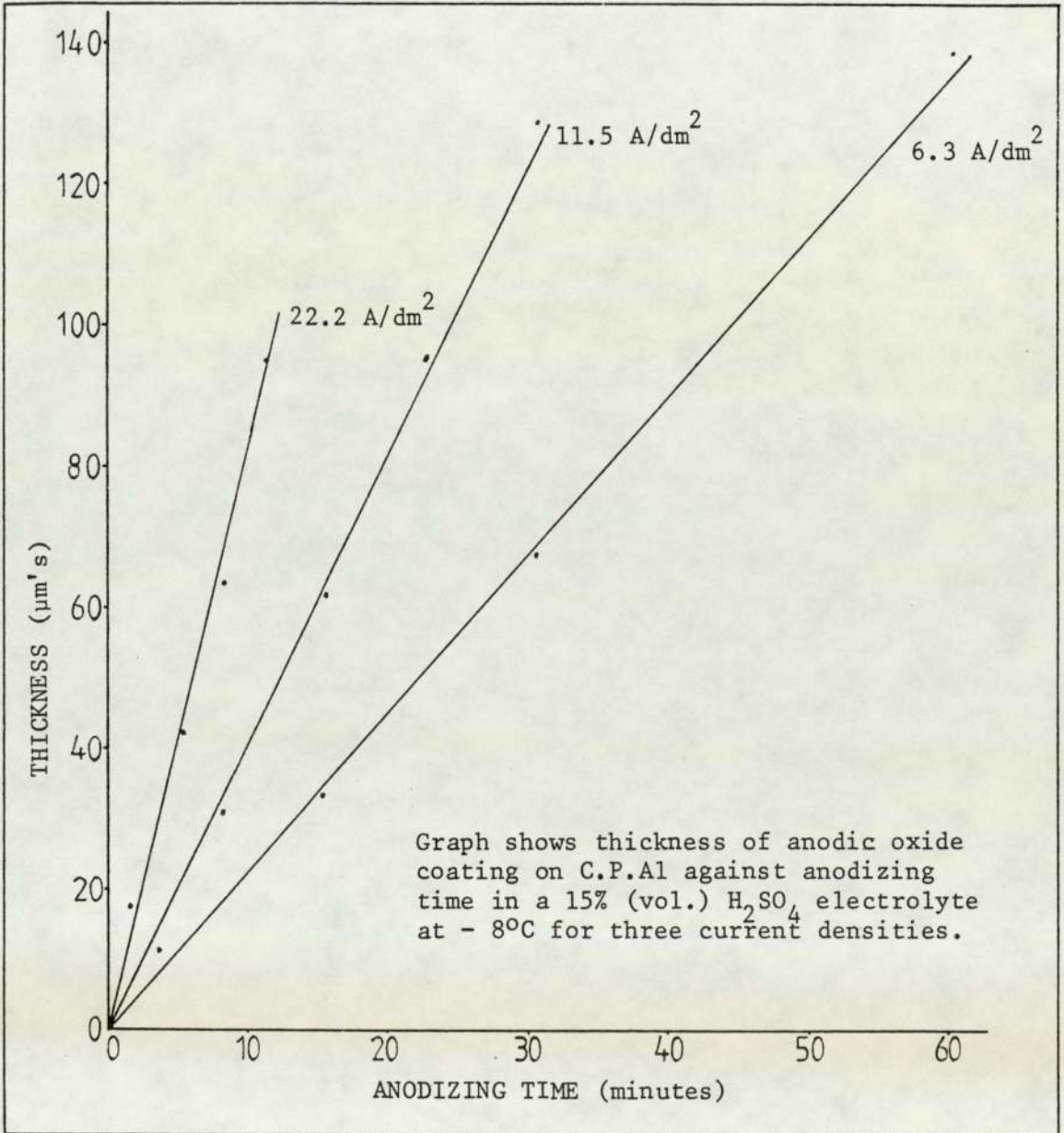


Fig. 3.69 Plot of Thickness against Time for data from Experiment 3.31.

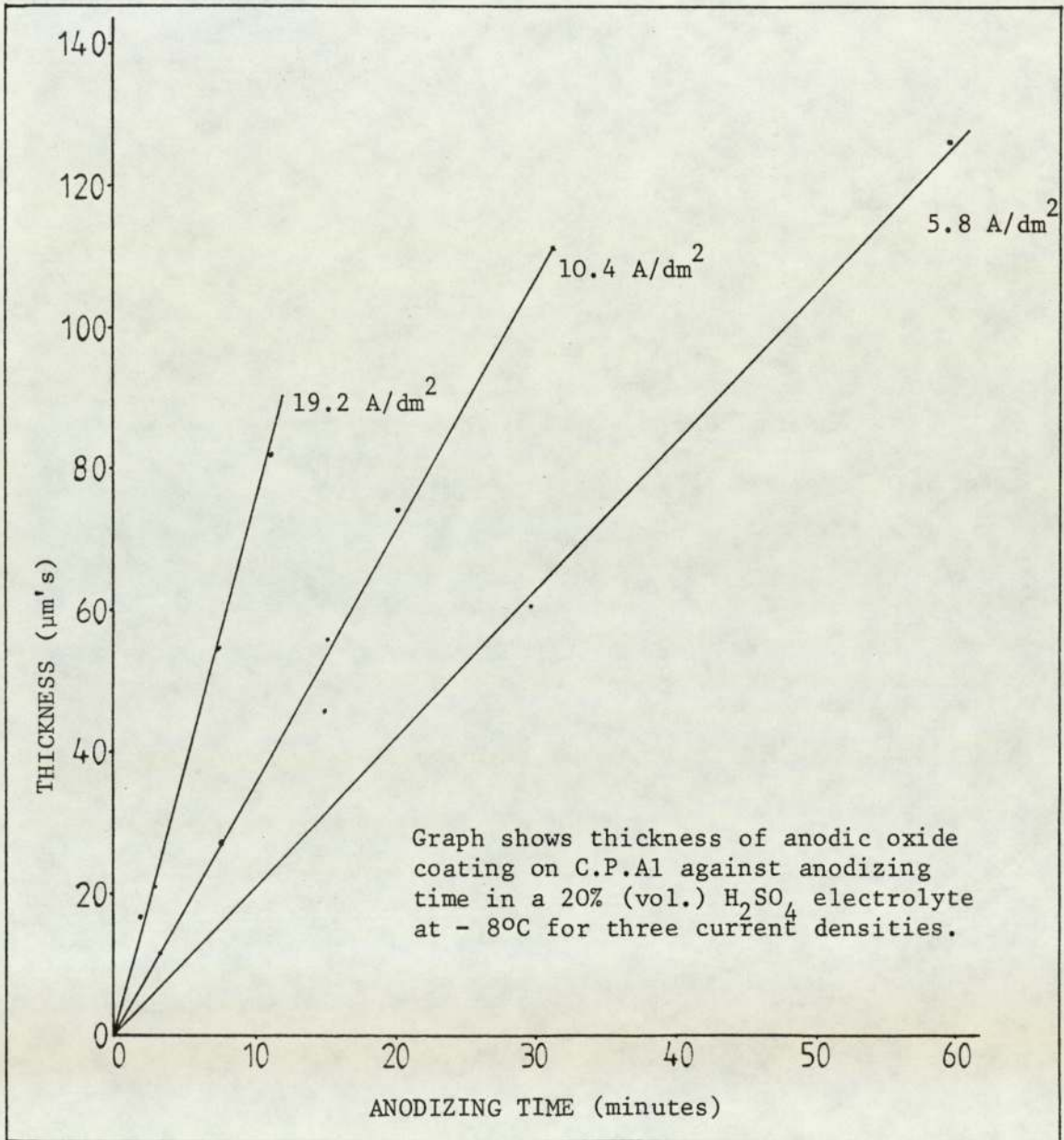


Fig. 3.70 Plot of Thickness against Time for data from Experiment 3.32.

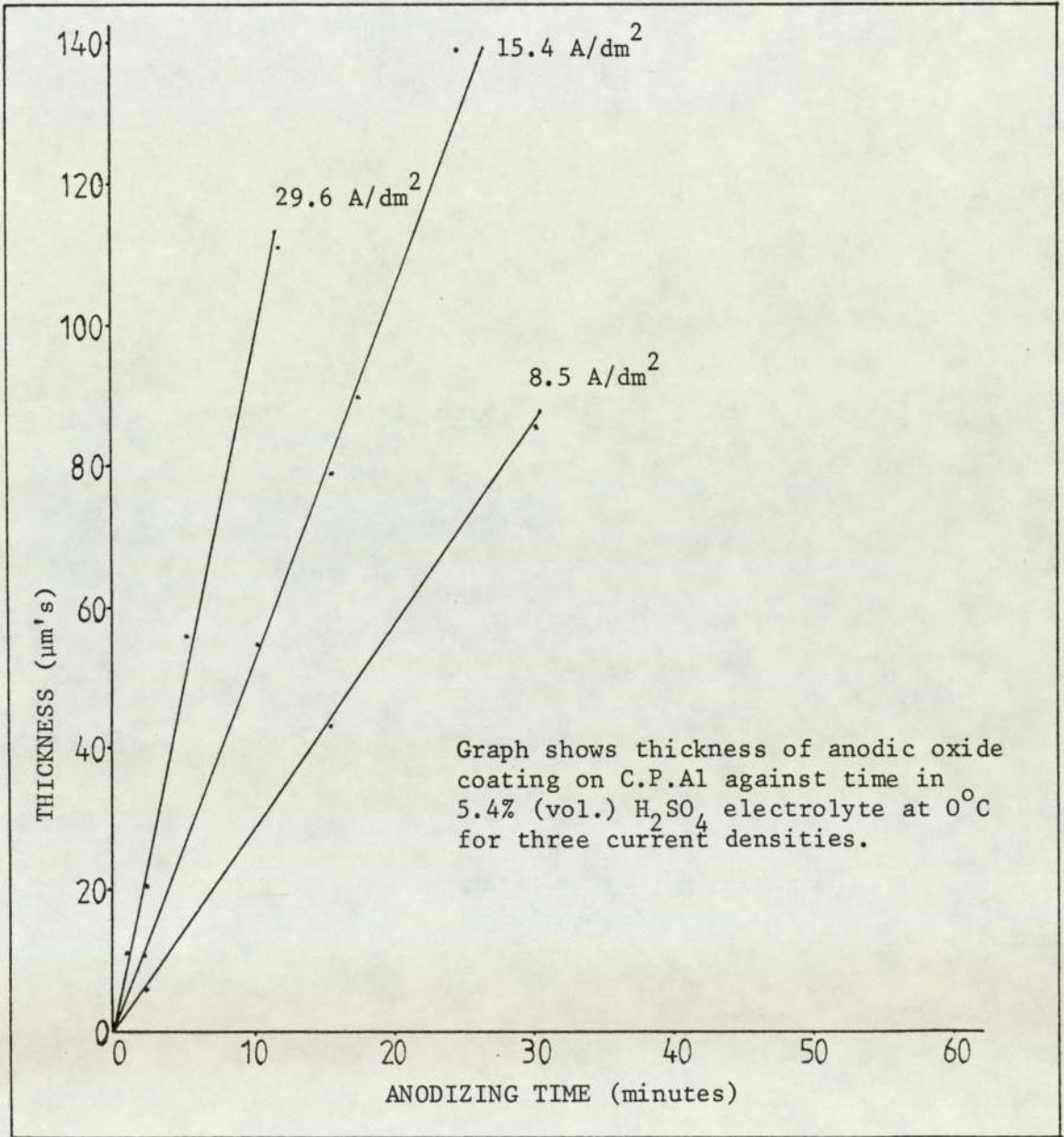


Fig. 3.71 Plot of Thickness of against Time for data from Experiment 3.33.

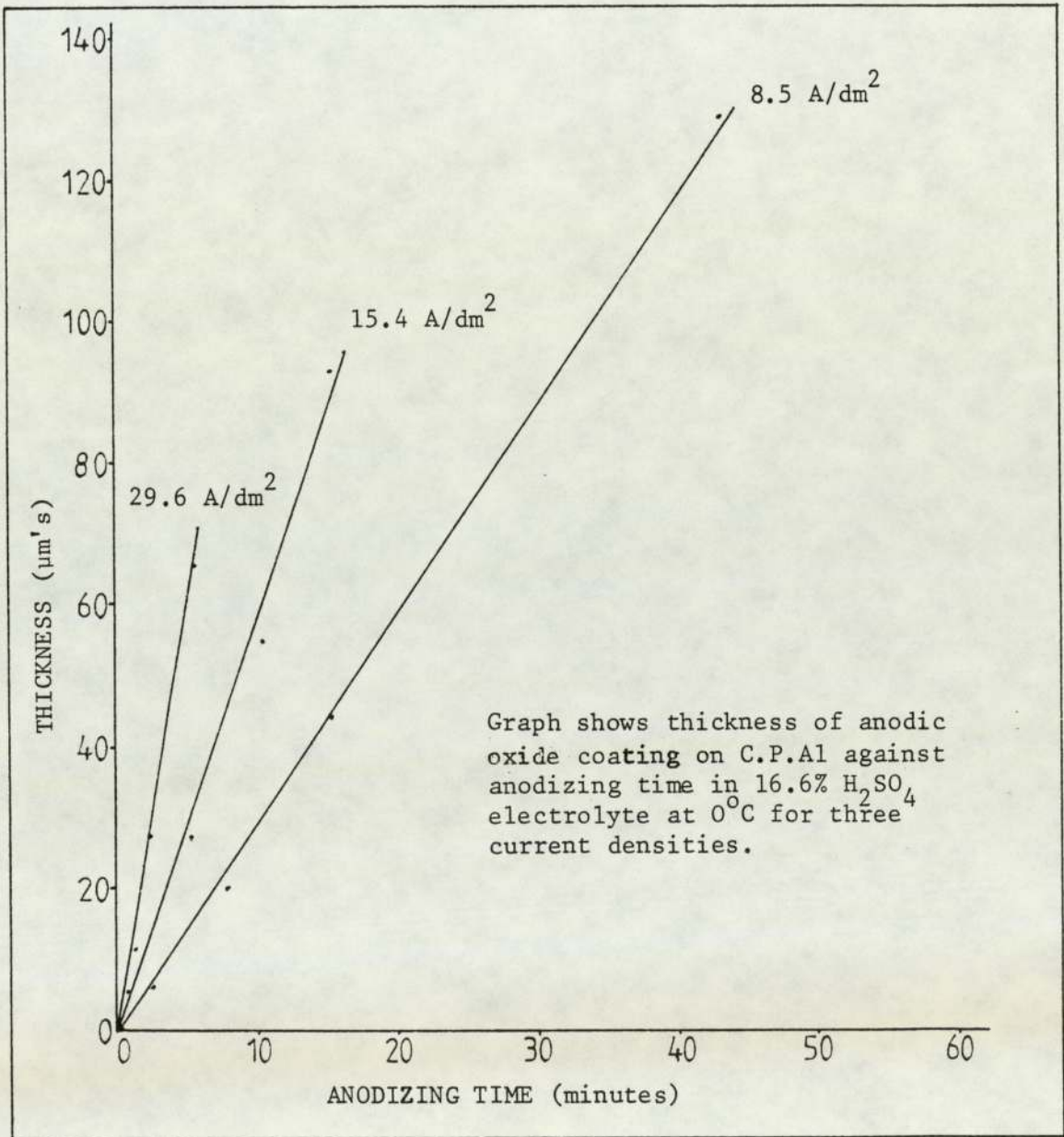


Fig. 3.72 Plot of Thickness against Time for data from Experiment 3.34.

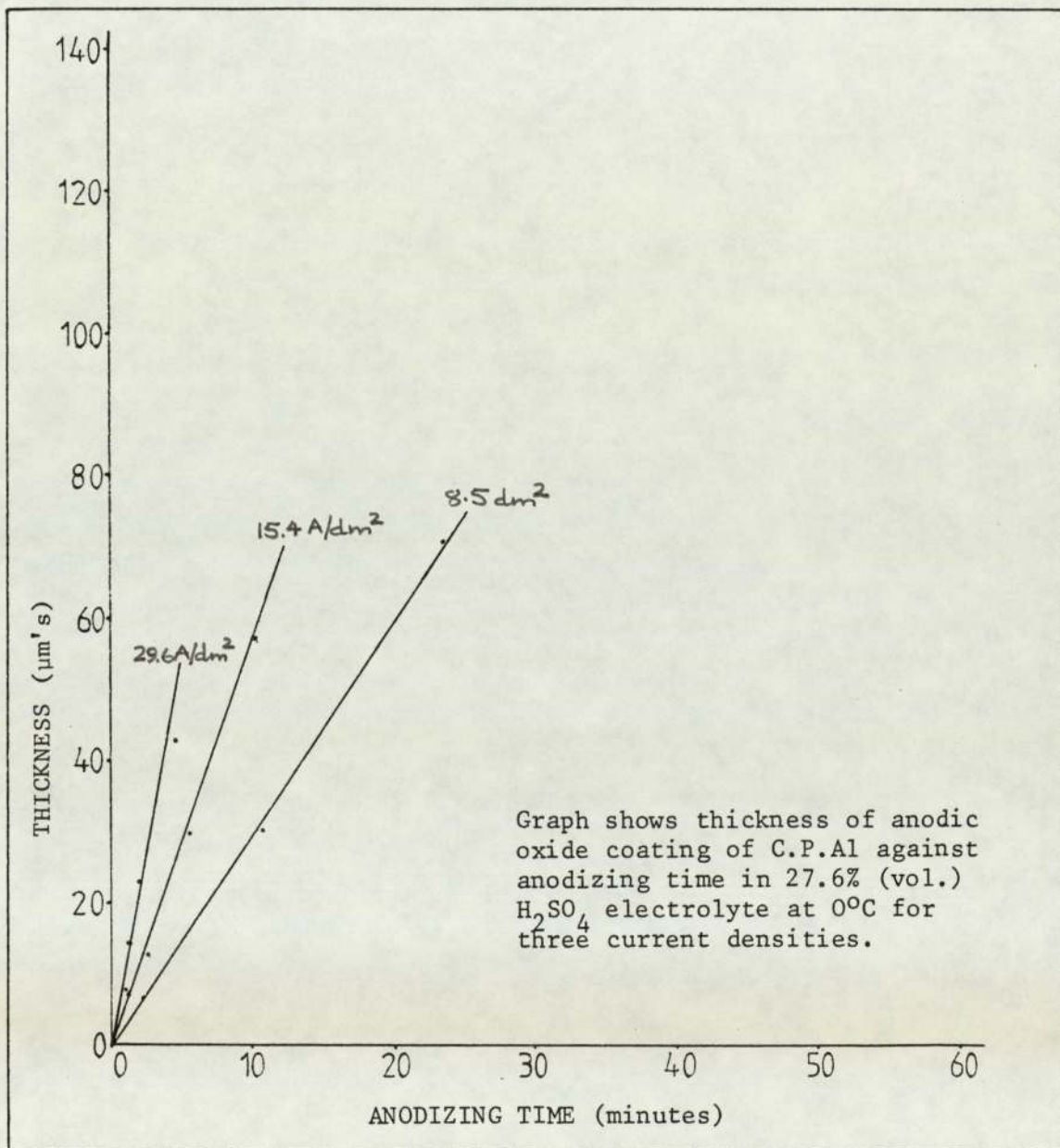


Fig. 3.73 Plot of Thickness against Time for data from Experiment 3.35.

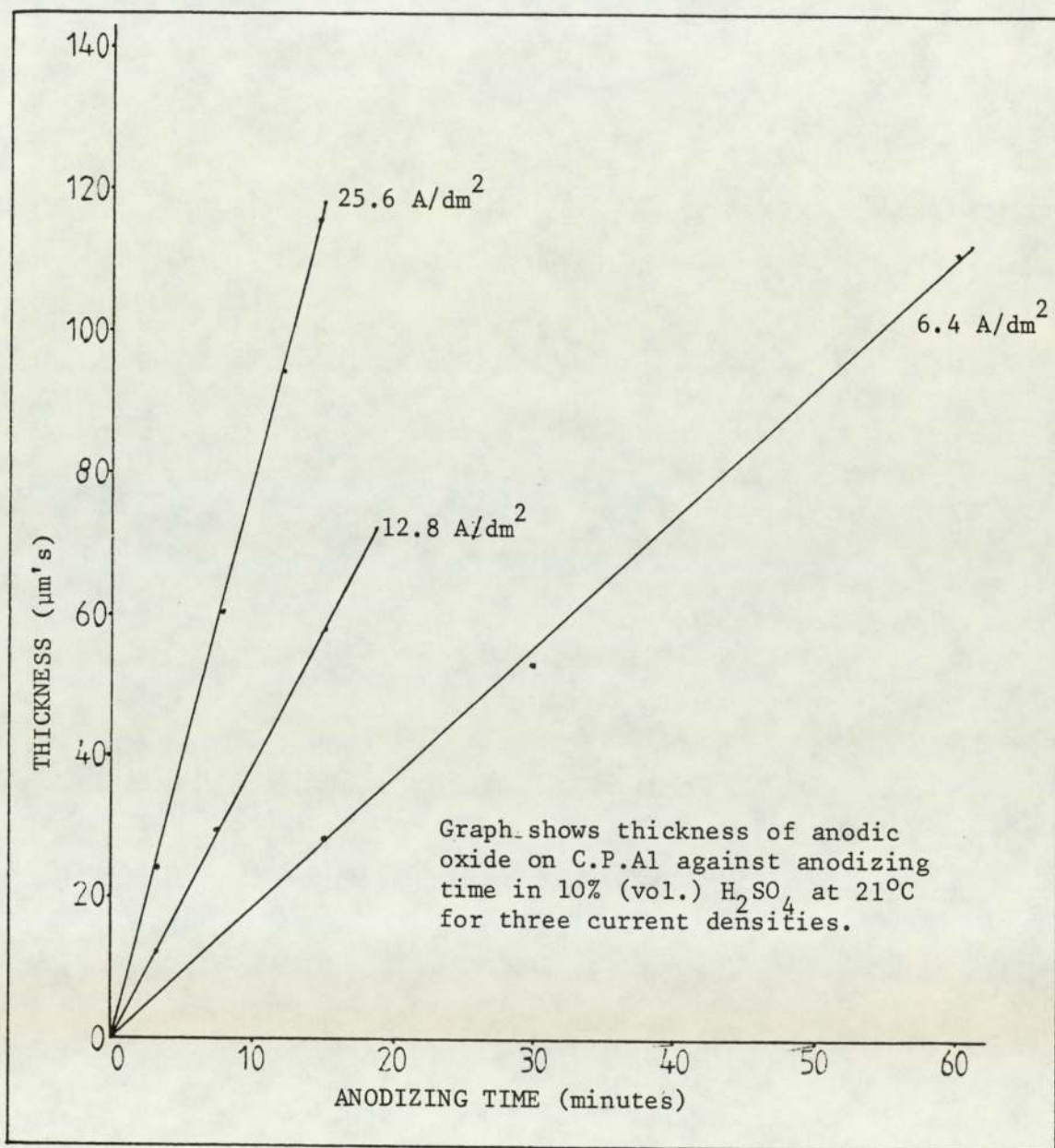


Fig. 3.74(i). Effect of temperature and immersion time on surface appearance when anodizing carried out at 24.0 A/dm².

SPECIMEN No.	TEMP °C	CURRENT DENSITY	ANODIZING TIME
1	-8	24.0 A/dm ²	2
2	-8	"	3½
3	-8	"	4
4	-8	"	5
5	-8	"	6½
6	5	"	2
7	5	"	3½
8	5	"	5
9	5	"	7
10	5	"	9½
11	20	"	2
12	20	"	5
13	20	"	7
14	20	"	9
15	20	"	11½

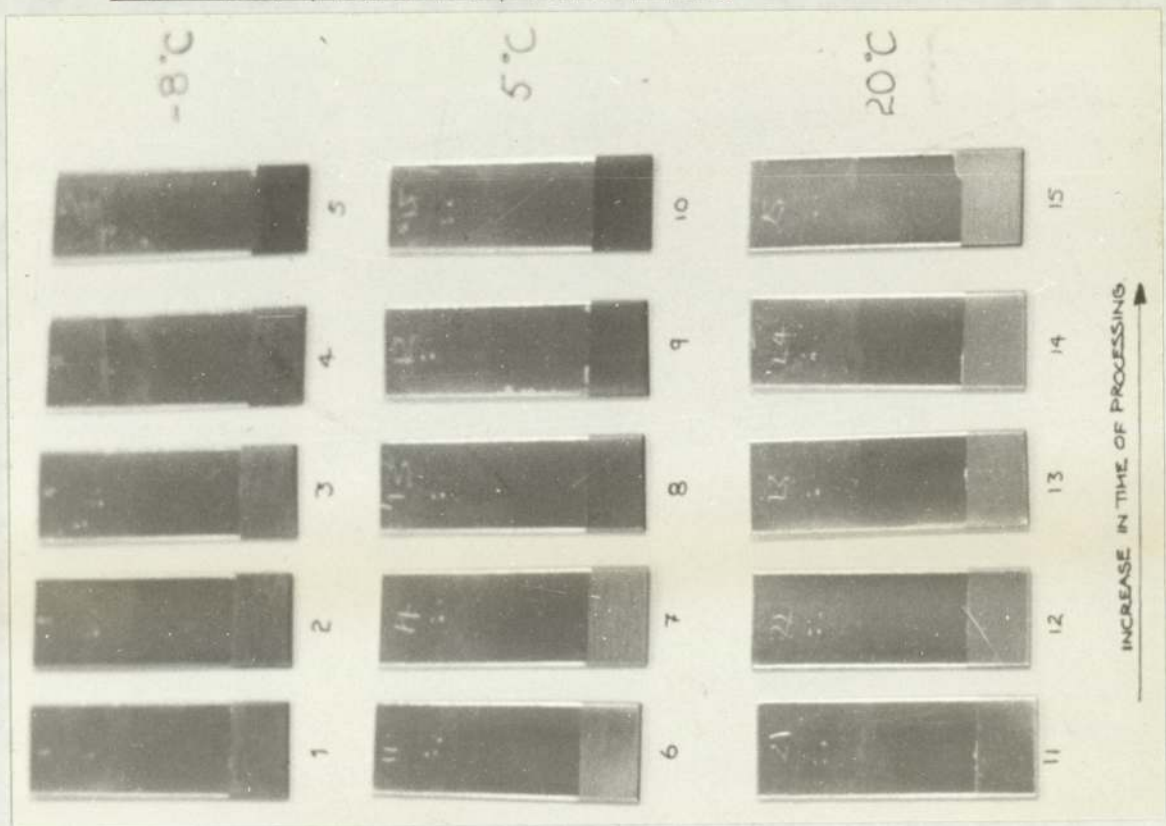


Fig. 3.74(ii). Effect of temperature and immersion time on surface appearance when anodizing carried out at 8.5 A/dm^2 .

SPECIMEN No.	TEMP °C	CURRENT DENSITY	ANODIZING TIME
1	-8	8.5 A/dm^2	2
2	-8	"	7
3	-8	"	15
4	-8	"	25
5	-8	"	30
6	5	"	2
7	5	"	7
8	5	"	15
9	5	"	25
10	5	"	30
11	20	"	2
12	20	"	7
13	20	"	15
14	20	"	25
15	20	"	30

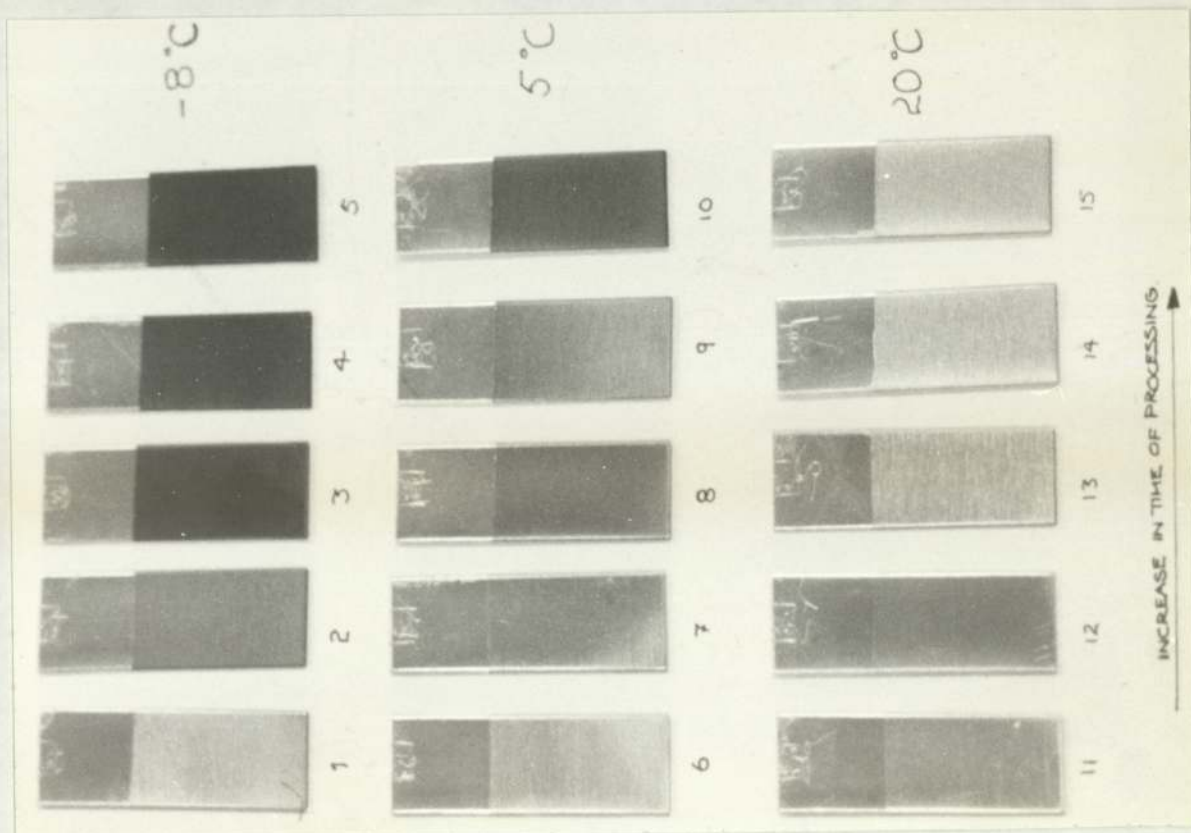


Fig. 3.75 Effect of Temperature and Time of anodizing on coating ratio at a constant current density of 24 A/dm².

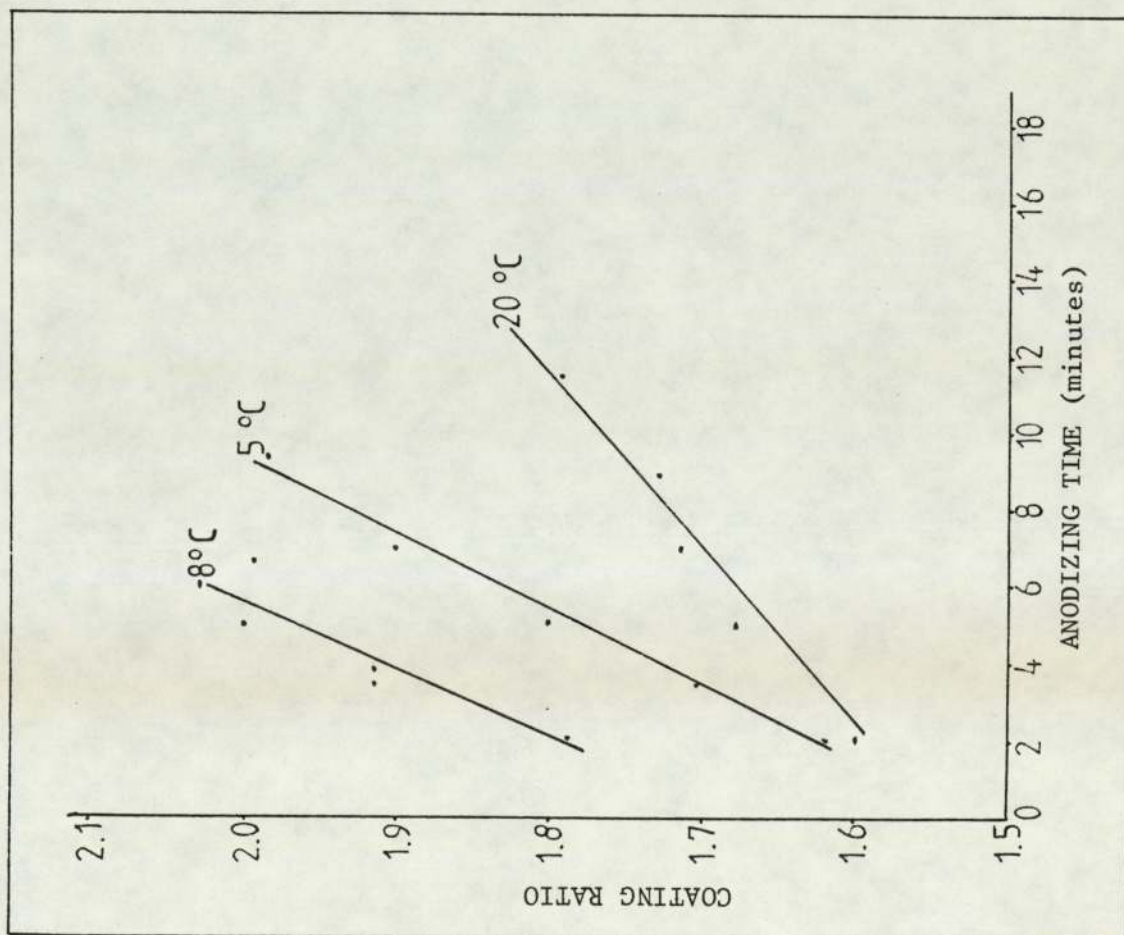


Fig. 3.76 Effect of Temperature and Time of anodizing on coating ratio at a constant i_2 current density of 8.5 A/dm².

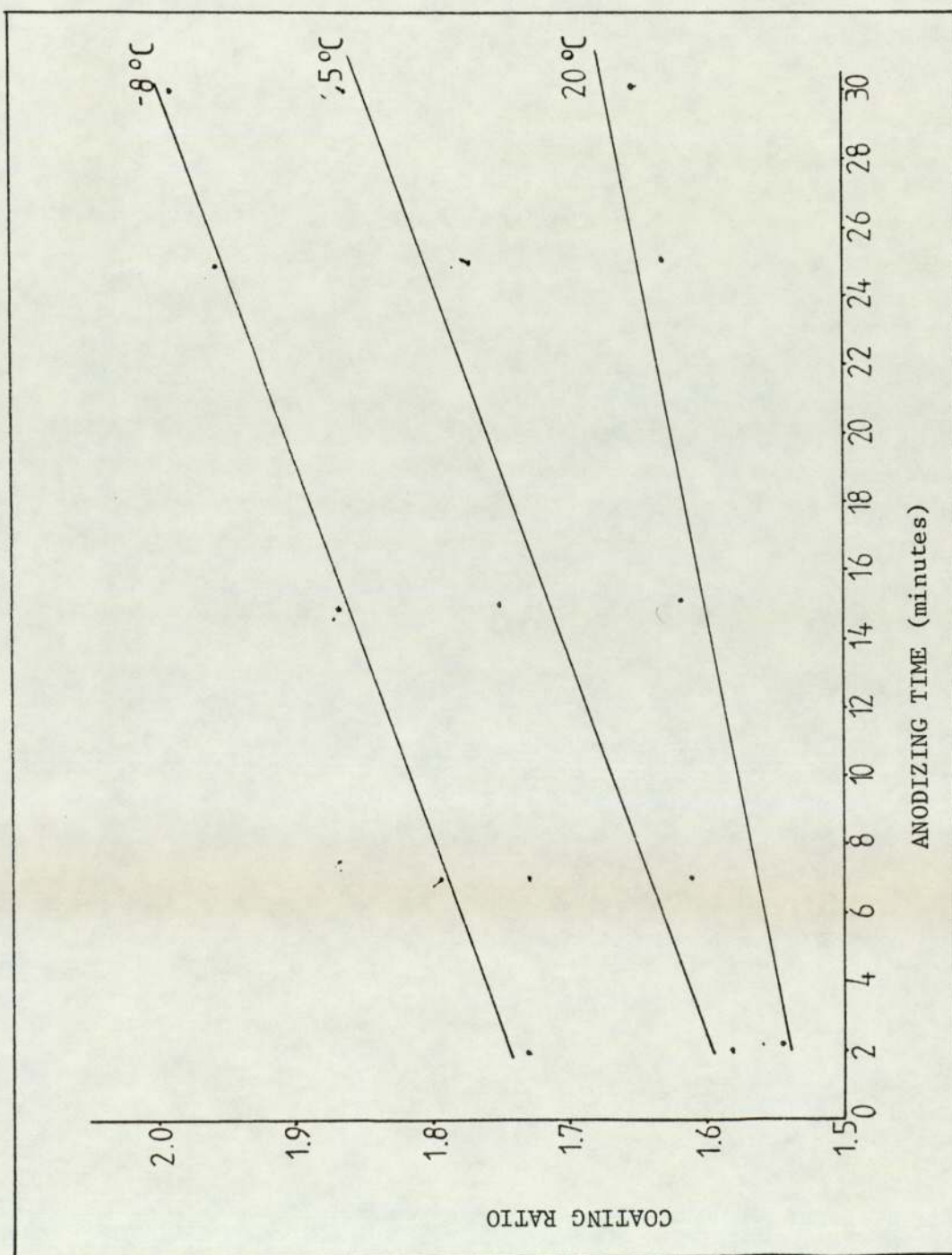




Fig. 3.77(i) Underside of oxide electrolytically detached from alloy BB3. T.a. 45°



Fig. 3.77(ii) As Fig. 3.77(i). T.a. 10°



Fig. 3.77(iii) As Fig, 3.77(i). T.a. 60°



Fig. 3.78(i) Underside of oxide electrolytically detached from alloy 2117CP. T.a. 45°



Fig. 3.78(ii) As Fig. 3.78(i), after showing greater detail. T.a. 45°

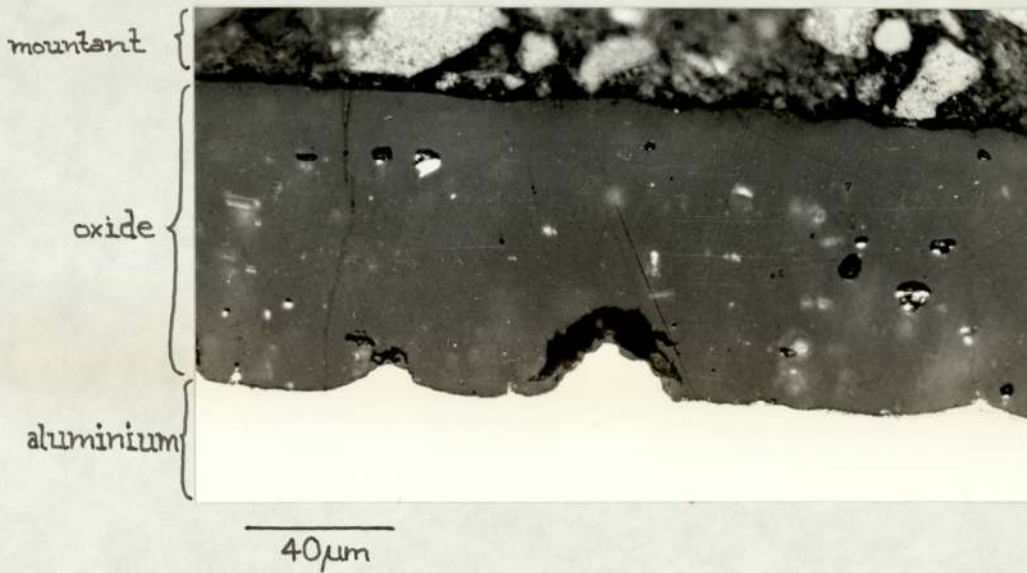


Fig. 3.78(iii) Optical photomicrograph of cross-section showing "conical asperities" of unanodized aluminium.

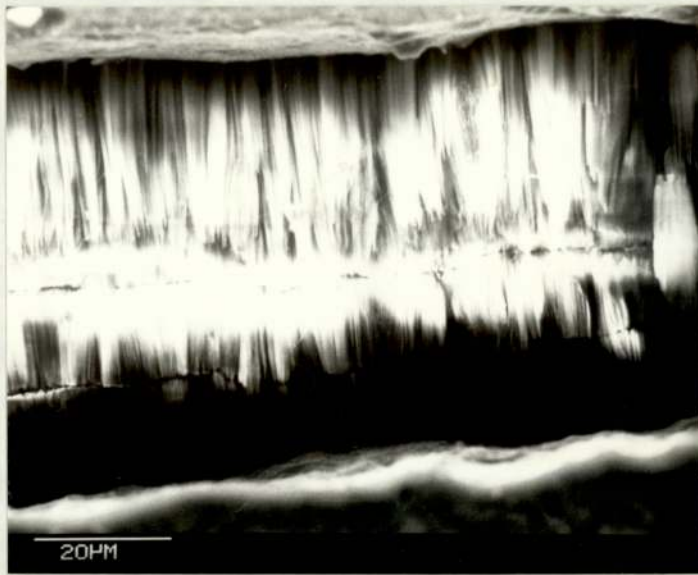


Fig. 3.79 Cross-sectional view of specimen No.1 from Experiment 3.38, showing structure after chemical dissolution of oxide. T.a. 10°

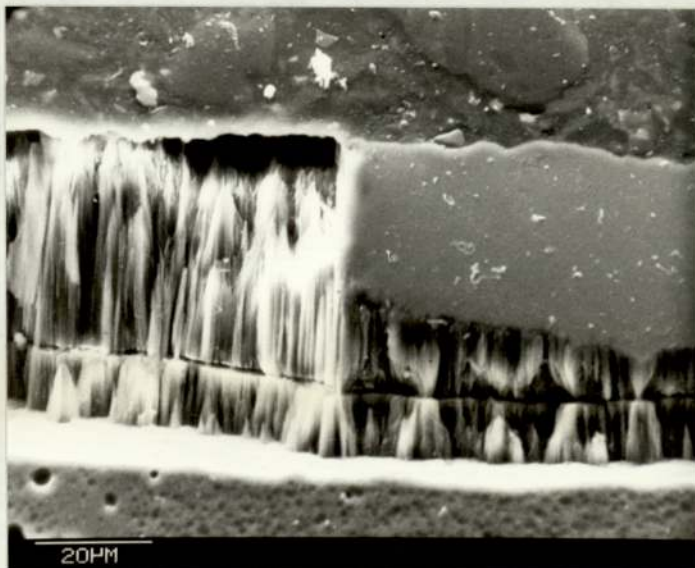


Fig. 3.80(i) Cross-sectional view of Specimen No.2 from Experiment 3.38, showing structure after chemical dissolution of oxide. T.a. 10°

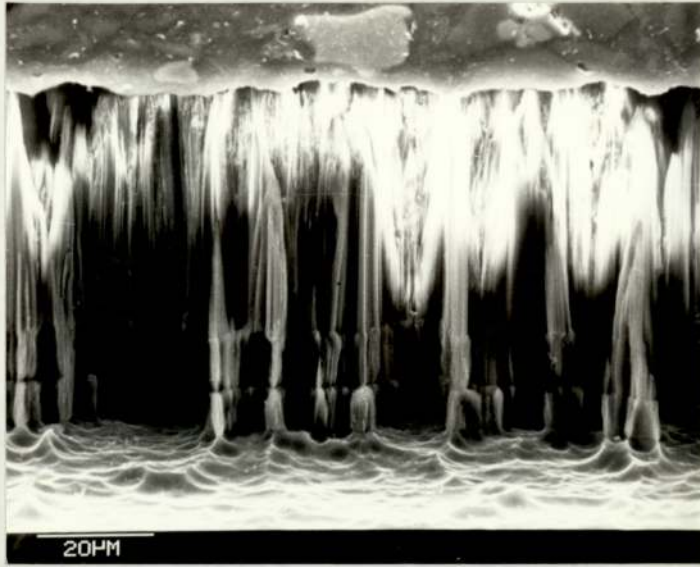


Fig. 3.80(ii) As Fig. 3.80(i). T.a. 10°



Fig. 3.81(i) Cross-sectional view of C.P. Al, chemically polished and anodized for $4\frac{1}{2}$ minutes at 41.6 A/dm^2 , after chemical dissolution of oxide. T.a. 10°



Fig. 3.81(ii) As Fig. 3.81(i), showing greater detail. T.a. 10°



Fig. 3.82(i) Cross-sectional view of C.P. Al, chemically polished and anodized for 13 minutes at 18.9 A/dm^2 , after chemical dissolution of oxide. T.a. 10°

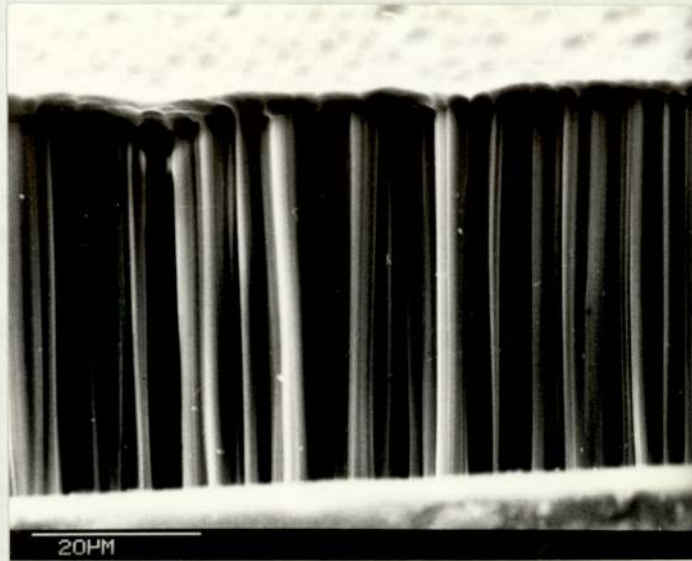


Fig. 3.82(ii) As Fig. 3.82(i). T.a. 10°

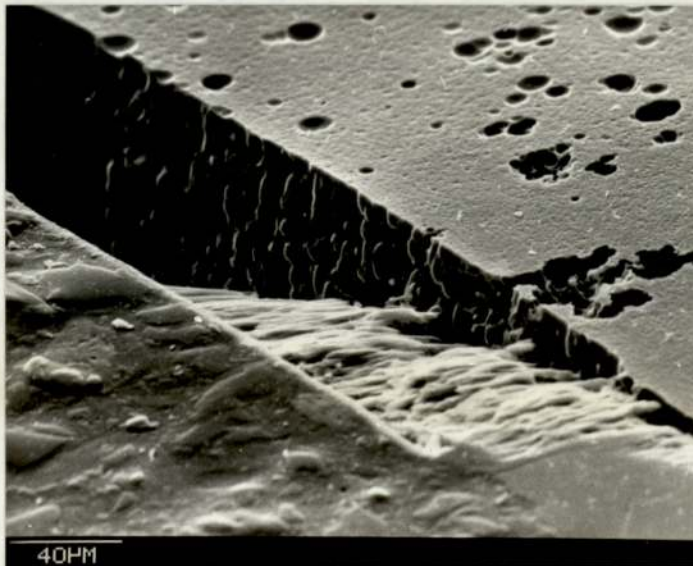


Fig. 3.83(i) As Fig. 3.82(i). Showing "island" growth at basis metal-oxide interface T.a. 55°

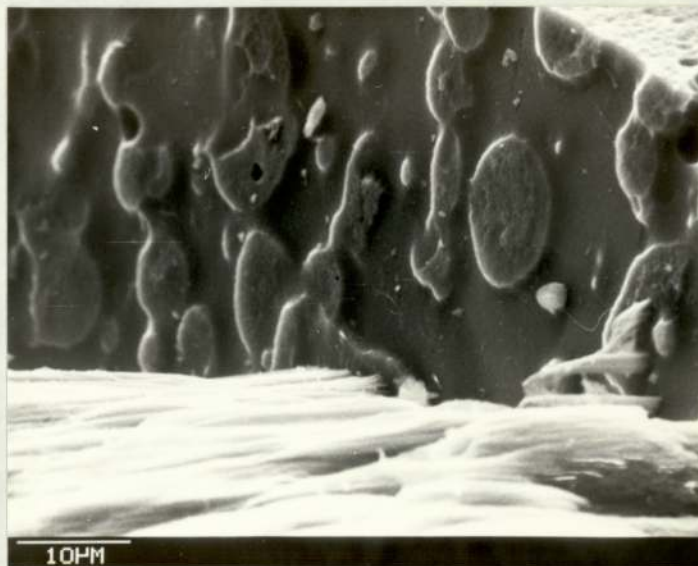


Fig. 3.83(ii) As Fig. 3.83(i), showing more detail.
T.a. 55°



Fig. 3.84 Same pretreatment as 3.81(i) but anodized
for 36 minutes at 10.5 A/dm^2 , after chemical
dissolution of oxide. T.a. 60°

Fig. 3.85(i), (ii) and (iii) are a sequence of electron-
photomicrographs showing "sheet" of oxide . T.a. 60°

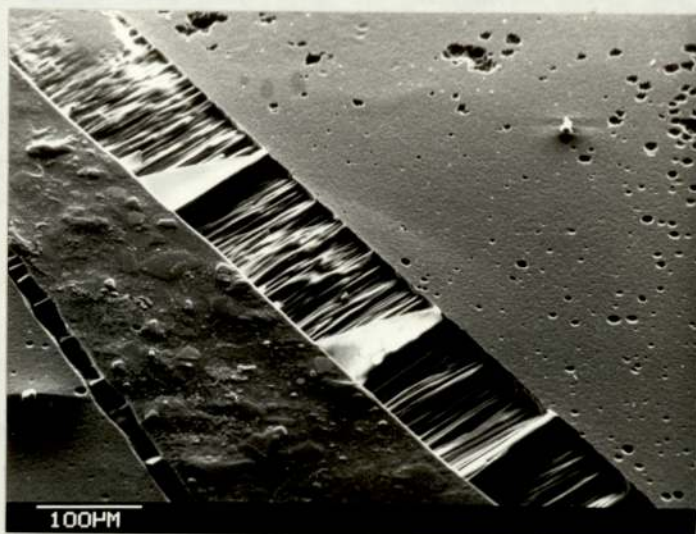


Fig. 3.85(i)

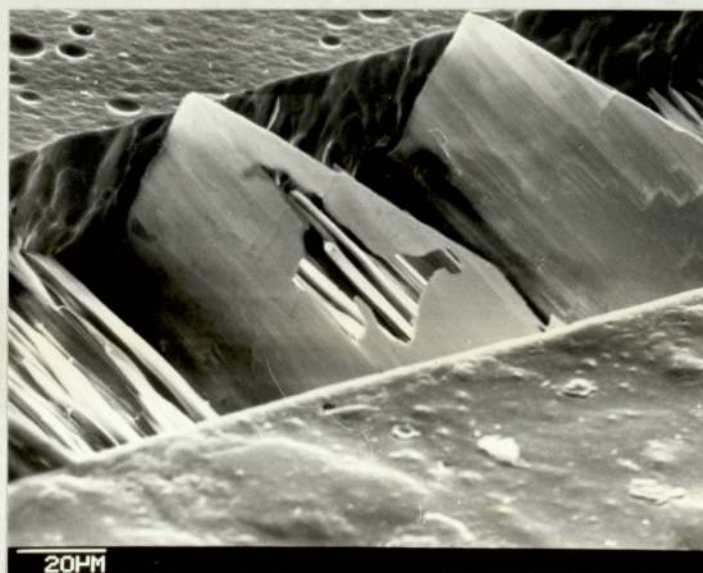


Fig. 3.85(ii)



Fig.3.85(iii)

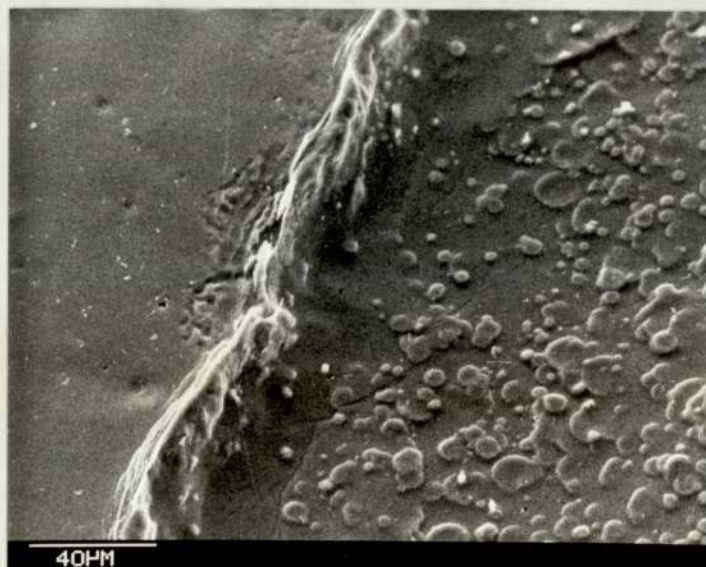


Fig. 3.86(i) Interface of chemically polished C.P. Al with unanodized surface to the left and the oxide chemically removed surface to the right. T.a. 45°

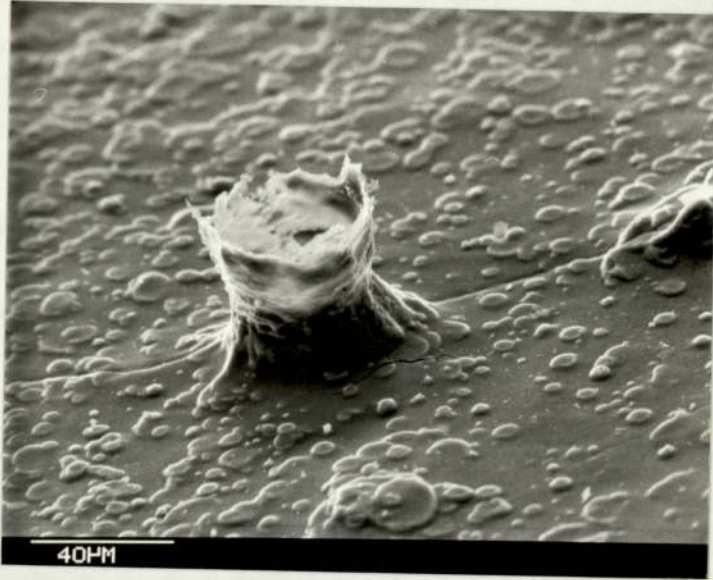


Fig. 3.86(ii) As Fig. 3.86(i), but on basis metal with oxide removed showing another feature - a cylinder of material. T.a. 70°



Fig. 3.86(iii) As Fig. 3.86(ii) showing greater detail. T.a. 70°

Fig. 3.87(i) to (xi). C.P.Al "As rolled", anodized in 10% H₂SO₄ at -8°C and oxide chemically stripped in boiling H₃PO₄-CrO₃ solution. T.a. 45



Fig. 3.87(i) 15 minutes anodizing at 5.8 A/dm²



Fig. 3.87(ii) 30 minutes anodizing at 5.8 A/dm²



Fig. 3.87(iii) 60 minutes anodizing at 5.8 A/dm²



Fig. 3.87(iv) 3 minutes anodizing at 10.7 A/dm²

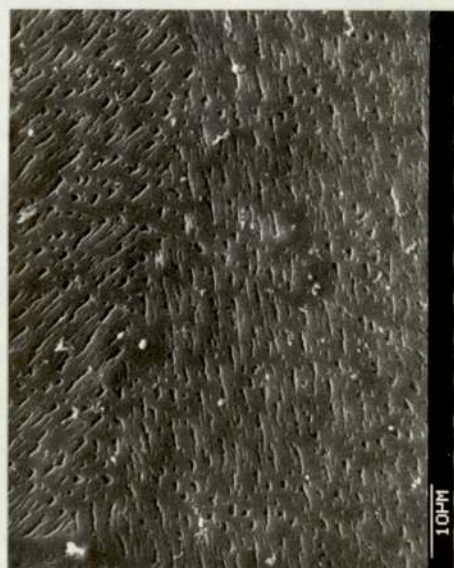


Fig. 3.87(v) 7½ minutes anodizing at 10.7 A/dm²



Fig. 3.87(vi) 30 minutes anodizing at 10.7 A/dm²



Fig. 3.87(vii) 47 minutes anodizing
at 10.7 A/dm²



Fig. 3.87(viii) 3 minutes anodizing
at 19.2 A/dm²

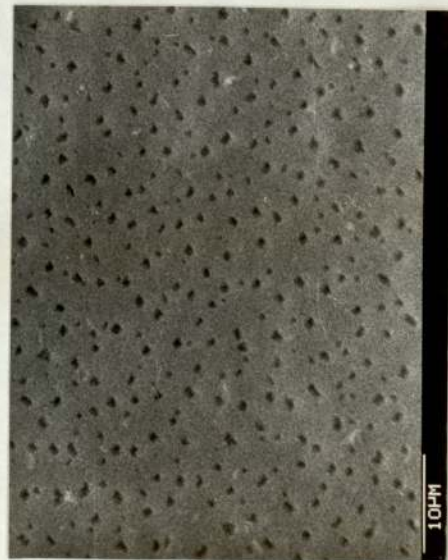


Fig. 3.87(ix) 7½ minutes anodizing
at 19.2 A/dm²



Fig. 3.87(x) 10 minutes anodizing
at 19.2 A/dm²



Fig. 3.87(xi) 15 minutes anodizing
at 19.2 A/dm²

Fig. 3.88(i) to (iii) C.P.Al "As rolled", anodized in 15% H_2SO_4 at $-8^\circ C$ and chemically stripped in boiling $H_3PO_4 - CrO_3$ solution. T.a. 45°

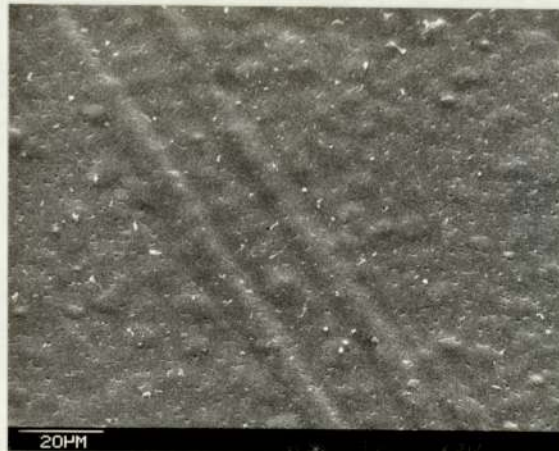


Fig. 3.88(i) 15 minutes anodizing at $6.3 A/dm^2$

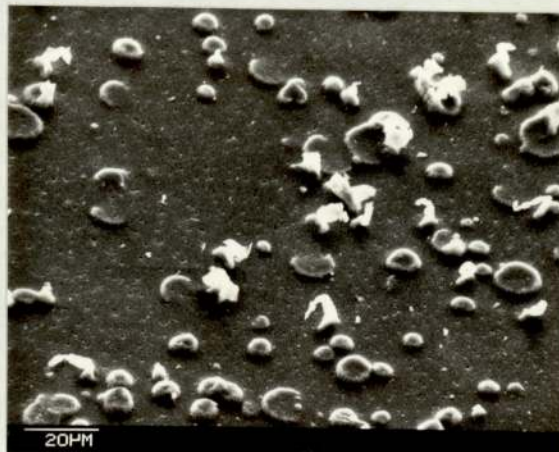


Fig. 3.88(ii) 30 minutes anodizing at $11.5 A/dm^2$

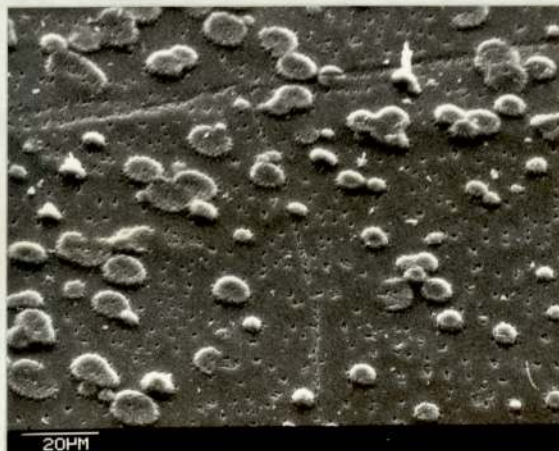


Fig. 3.88(iii) $10\frac{1}{2}$ minutes anodizing at $22.2 A/dm^2$

Figs. 3.89(i) to 3.89(ix). C.P.Al "As rolled" anodized in 20% H₂SO₄ at -8°C and chemically stripped in boiling H₃PO₄ - CrO₃ solution. T.a. 450



Fig. 3.89(i) 15 Minutes anodizing at 5.8 A/dm²

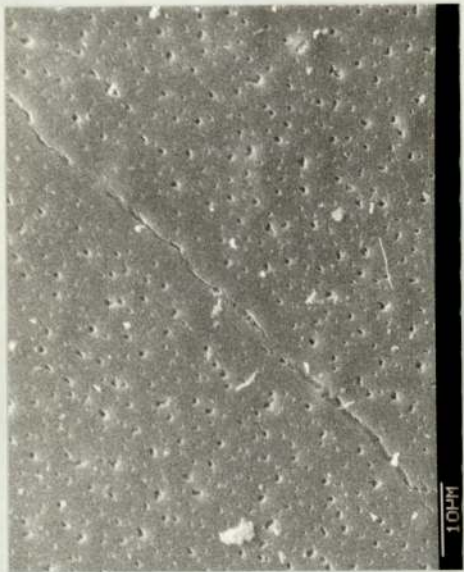


Fig. 3.89(ii) 30 minutes anodizing at 5.8 A/dm²



Fig. 3.89(iii) 60 minutes anodizing at 5.8 A/dm²

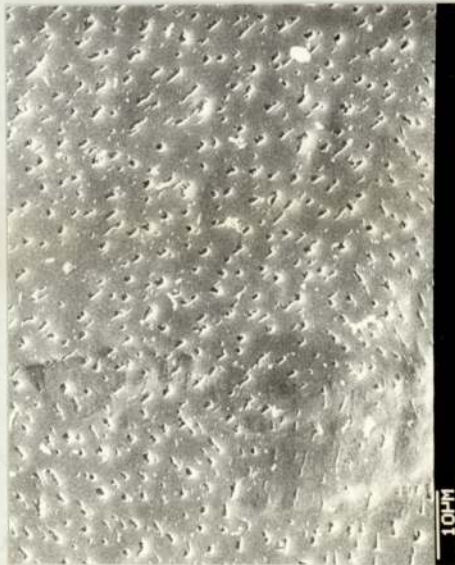


Fig. 3.89(iv) 3 minutes anodizing at 10.4 A/dm²

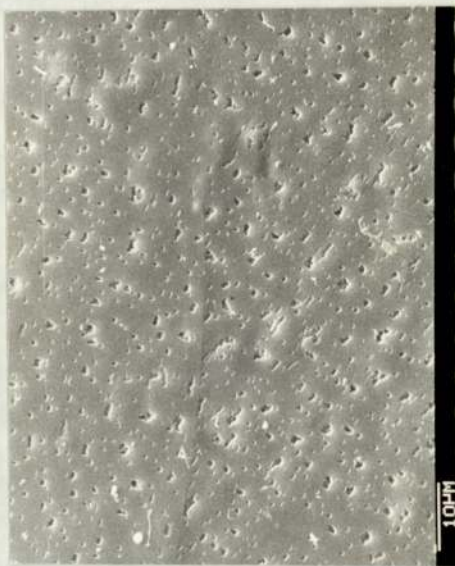


Fig. 3.89(v) 7 1/2 minutes anodizing at 10.4 A/dm²

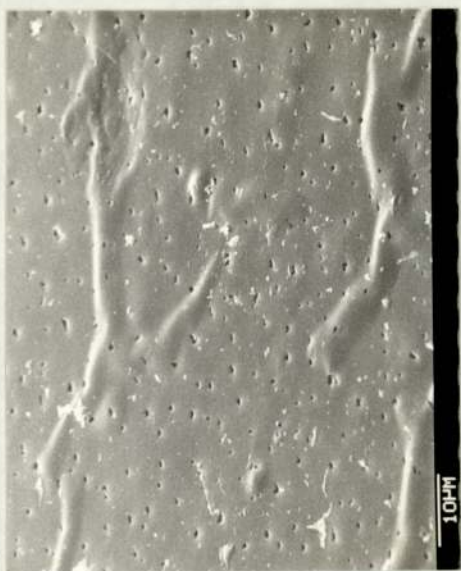


Fig. 3.89(vi) 29 minutes anodizing at 10.4 A/dm²

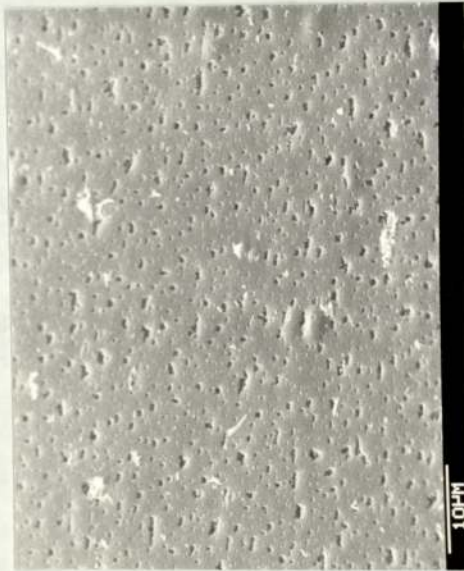


Fig. 3.89(vii) 3 minutes anodizing at 19.2 A/dm²

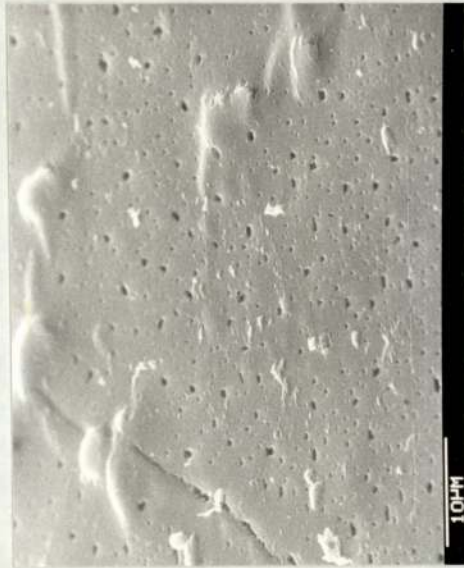


Fig. 3.89(viii) 7½ minutes anodizing at 19.2 A/dm²

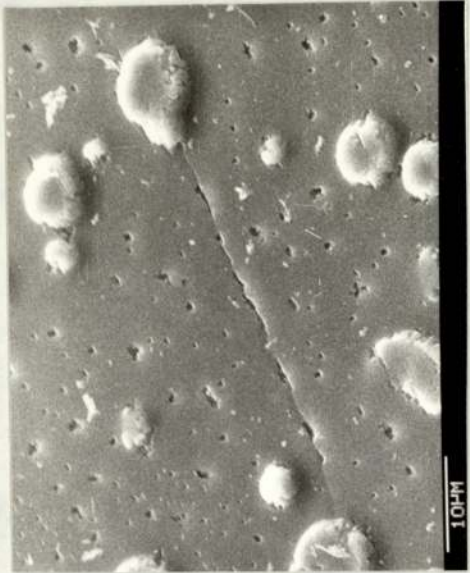


Fig. 3.89(ix) 11 minutes anodizing at 19.2. A/dm²

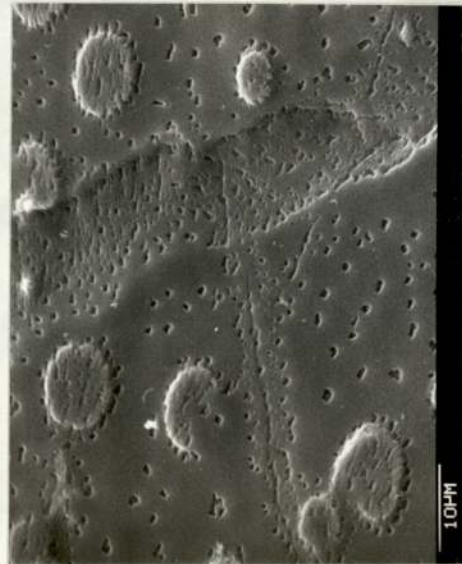


Fig. 3.90 C.P.Al "As rolled", anodized in 10% H₂SO₄ at -8°C for 3 minutes at 52 A/dm² and oxide chemically stripped off. T.a 45°

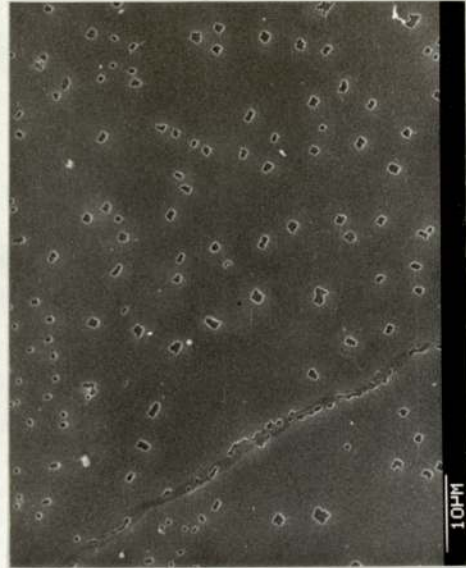


Fig. 3.91 C.P.Al "As rolled", anodized in 10% H₂SO₄ at -8°C for 3 minutes at 11 A/dm² and oxide chemically stripped off. T.a 45°

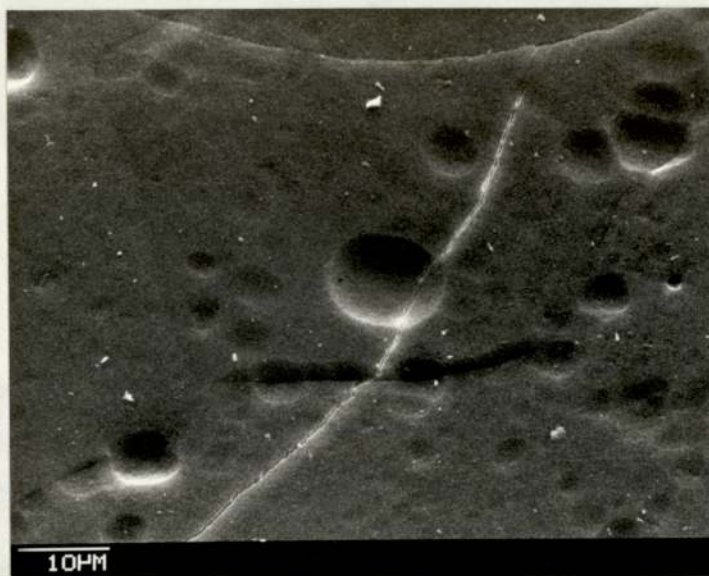


Fig. 3.92(i) C.P. Al etched in 10% NaOH, anodized for 2 minutes at 29.6 A/dm² in 27.6% H₂SO₄ at 0°C. T.a. 45°



Fig. 3.92(ii) As Fig. 3.92(i), with anodic oxide chemically stripped off. T.a. 45°



Fig. 3.93(i) C.P.Al etched in 10% NaOH, anodized for 2 minutes at 15.4 A/dm² in 27.6% H₂SO₄ at 0°C. T.a. 45°



Fig. 3.93(ii) As Fig. 3.93(i), with anodic oxide chemically stripped off. T.a. 45°

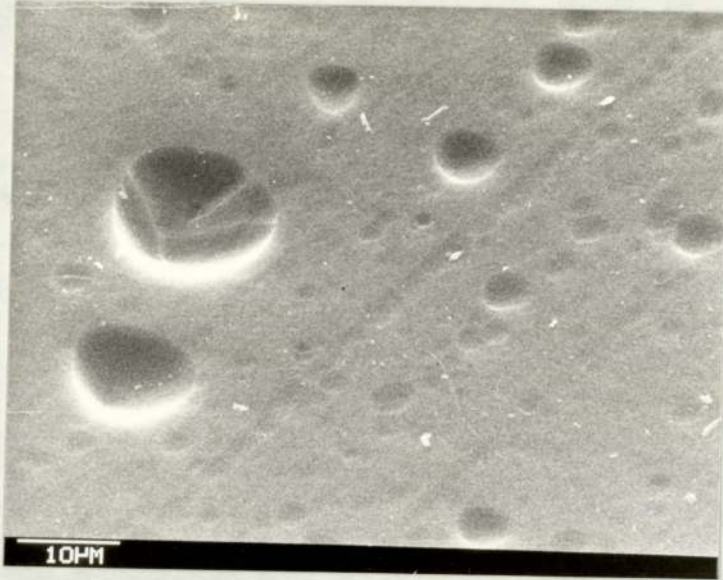


Fig. 3.94(i) C.P. Al etched in 10% NaOH, anodized for 2 minutes at 8.2 A/dm² in 27.6% H₂SO₄ at 0°C. T.a. 45°

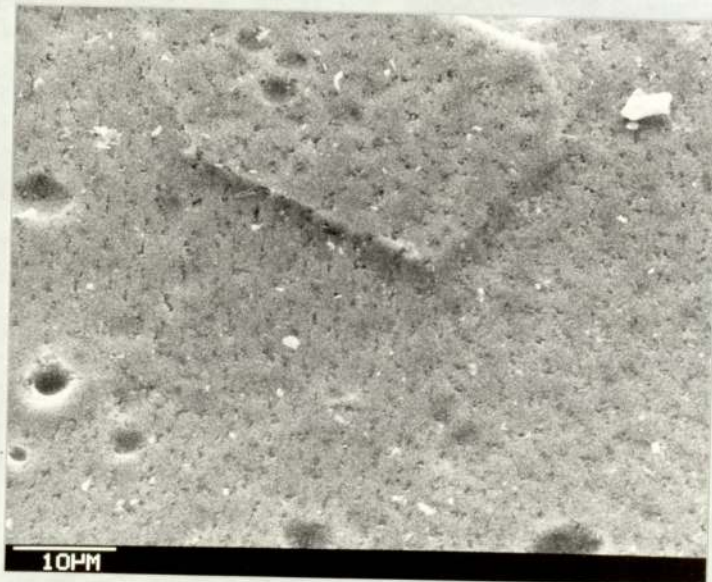


Fig. 3.94(ii) As Fig. 3.94(i), with anodic oxide chemically stripped off. T.a. 45°

CHAPTER FOUR

4. DISCUSSION.

- 4.1 INTRODUCTION. In this chapter the experimental results are discussed in the following sections.
- 4.2 Nucleation and Growth of Hard Anodized Films.
- 4.3 Icing Defects.
- 4.4 Potential - Time.
- 4.5 Microhardness.
- 4.6 Thickness.
- 4.7 Coating Ratio.
- 4.8 Examination of detached oxide film and anodized specimen after anodic oxide film removal.

4.2 NUCLEATION AND GROWTH OF HARD ANODIZED FILMS.

Anodic coatings reproduce the surface upon which they are formed; therefore the surface texture and composition of the aluminium alloy are of great importance. Fig. 3.1. shows the "surface" defects present from rolling the super purity aluminium. The hard anodizing process affected the appearance of the films; The colour, hairline crazing and surface roughness all changed. The colours obtained depended on the base metal composition, current density, voltage, film thickness and electrolyte composition. The crazing* of the oxide film may occur whilst the anodizing process is in progress, but is certainly noticeable when the specimen is removed from the bath and increases as the surface warms up after removal. It most readily occurs when thick anodic films form on a smooth aluminium surface; anything which tends to minimise stresses in the film, such as a heavily etched metal surface or fine particle distribution in the film, reduces the risk of crazing. Surface roughness is generally increased by hard anodizing and if a fairly smooth surface finish is required, then it is customary to hone the oxide to the desired finish.

Fig. 3.2 shows the heterogeneous nucleation and development of hillock - shaped features on the surface of the super purity aluminium. Similar features have been observed optically and electronoptically by Csokán,(35,36,37) Lichenberger-Bajza,(130) Tomashov and Zalivalov(131) and Bailey.(28)

Csokán(35,36,37) has described the development of these thick lens-shaped islands of oxide (rosettes) in very dilute sulphuric acid electrolytes under hard anodizing conditions.

* Term used to describe a fine cracking of the anodic film due to the difference in the thermal expansion coefficient between the oxide film and metal.

He followed the growth of these rosettes by using a cinémicroscopy technique and explained their formation by their originating from primary oxide nuclei at high energy sites, as described by Franck,⁽¹³²⁾ followed by their development into secondary oxidation zones around the nuclei. These zones grow and merge until the entire aluminium surface is covered by anodic oxide.

Bailey⁽²⁸⁾ obtained rosettes when anodizing in sulphuric acid at concentrations lower than 5% at 25°C or at 10% (or lower) at 0°C. He considered that the rosettes developed from embryo current demanding pore colonies, possibly similar to the type envisaged by Renshaw.⁽³³⁾ This was considered to be a feature of the limited throwing power of the anodizing process under low electrolyte conductivity conditions. Under aggressive conditions these areas spread laterally, while in low concentrations of electrolyte the rosettes develop in depth with little lateral spread. i.e., the greater proportion of current is devoted to the development of oxide blocks (rosettes) and the lesser proportion to the oxide film formation of the regions between the blocks. Interference colours on the regions between these blocks showed the current was concentrated in the blocks until the whole surface was covered with rosettes, which merge to give a continuous, although rough coating.

It is also of interest to note that Turner and Lovering⁽¹³³⁾ have also observed such features on aluminium anodized in molten nitrates.

Although the nucleation is heterogeneous in nature there does appear to be a marked preference for the oxide growth to nucleate along rolling defects in the surface of the aluminium. This is further evidence that anodizing nucleates at defects.

In Fig. 3.3(i) the conditions of anodizing were similar to those in Fig. 3.2, but the anodizing time was doubled. It shows the hillock shaped features (previously termed "rosettes" by Csokán) growing laterally and merging into each other. Increasing internal stress in the oxide as it grows has caused layered microcracking of the outer oxide to produce the roughly concentric crack pattern, which appears to be related to the direction of oxide growth.

When viewed at a certain glancing angle, i.e., 10° (See Fig. 3.27(ii)) these rosettes not only appear rose-like but resemble the contour pattern of hills as seen on geographical maps.

Fig. 3.3(ii) shows a magnified view of Fig. 3.3(i). In the bottom right-hand corner of the figure the oxide can be seen to be nucleating and growing along scratch lines.

Defects in the air-formed oxide film are more likely to occur at these scratch lines, so a lower resistance and hence a greater concentration of the applied current would be attracted to these areas. Therefore, it is not surprising that the nucleation and growth of the oxide occurs at such defects in the air-formed oxide.

Fig. 3.4. As anodizing time is increased the hillocks become more densely distributed and the "island" type features that formed initially eventually coalesce and completely cover the whole of the exposed aluminium surface. The rolling direction of the aluminium sheet is still distinguishable, due to the fact that the initial nucleation and growth of these hillocks appeared on rolling lines.

On increasing anodizing time (See fig 3.5(i)) the surface remains very rough. This indicates that once the surface is completely covered by anodic oxide, except for minimal dissolution at the outer surface there is no subsequent change in the surface topography with

further anodizing.

The thickness of the oxide then increases uniformly, forming at the inner metal/metal oxide interface, while the outer surface of the oxide maintains the nodular roughness produced by the initially formed hillocks. The thickness of the oxide is primarily dependent on the current actually passed for a given time under suitable conditions for anodizing.

Fig. 3.5(ii) shows a magnified view of Fig. 3.5(i). Microcracking which is a characteristic of the hillock formation can be seen in more detail, the distance between each crack line being fairly constant. This may indicate that the growth of the oxide proceeds until the stresses are so great that a crack forms to relieve the stress following sequentially by build-up of stress and further cracking.

Increasing the current density increases the rate of nucleation and growth of the hillocks. (See Fig. 3.6(i)). This figure shows quite well the nucleation and growth of the oxide along the line defects present on the aluminium surface. The magnified view in Fig. 3.6(ii) shows the heterogeneous nucleation and growth of the oxide. Increasing the anodizing time increase the proportion of the surface covered by the hillocks, the largest being formed at defects on the aluminium. (See Fig 3.7). At the high current densities used (39.7 A/dm^2) for this particular specimen the time taken for the complete coverage of the aluminium surface with oxide is very short, e.g. 10 secs.

The lines of the hillocks running from the top right of the figure to the bottom left and also the roughness of the film formed are characteristic and typical.

When anodizing commercial purity aluminium in the "As rolled"

condition the characteristic hillock features are formed at relatively low current densities compared with those on super purity aluminium. Fig. 3.9(i) shows this fairly well, whilst Fig. 3.9(ii) shows the growth of the hillocks occurring along scratch lines on the surface of the aluminium. The first indication of the terraced microcracking can also be seen. As with the anodizing of super purity aluminium, increasing the anodizing time gives rise to the merging of the hillocks to form the characteristic rough surface. (See Fig. 3.10(i)). Fig. 3.10(ii) shows the terraced microcracking along scratch lines very clearly.

On a few occasions when the specimen was removed from the anodizing cell and examined visually, circular defects were present on the surface. Because of their shape they were initially considered to have been caused by a bubble or bubbles adhering to the specimen surface and as a consequence the surface beneath the bubble was masked from being anodized with the surface around the bubble being anodized in the normal manner for the hard anodizing conditions being used. However, on electronoptical examination (See Figs 3.11(i) and (ii)) it was seen that the hillocks formed did in fact reach the height of the surface of the defect. If surface masking was occurring then from present understanding of the anodizing process the defect would have been expected to appear lower than the hillocks formed, which obviously did not occur. It would therefore appear that at these surface defects anodizing was in fact taking place, but at a greater rate than that of the formation of the hard anodized hillock features. It is not clear how this came about, but a possible explanation could be that the pre-cleaning procedure left a residue (possibly containing chloride ions) on the aluminium surface. The chloride ions affect

the air-formed oxide making the surface on this area (due to defects) low in electrical resistance. Thus, when anodizing commenced, the oxide formed at these areas in a conventional manner, whilst around the defect areas hard anodizing occurred, to produce the characteristic hillock formation. Another possible explanation may be that the defect is in fact the initial un-anodized air-formed oxide and the surrounding area is anodic oxide that has been chemically dissolved by the electrolyte. However, this is rather unlikely owing to the conditions of the process. i.e., it seems unlikely that after only 52 seconds of immersion the anodic oxide would be attacked in such a uniformly patterned manner giving rise to the hillocks and contour crack patterns observed. If this explanation were true then it would require a complete turn around in what has been observed experimentally in the initial stages of hard anodizing, namely the hillocks growing out of the aluminium surface.

The topography of super purity aluminium after being sand blasted is shown in Fig. 3.12; it shows the characteristically roughened and highly deformed surface. Fig. 3.13 shows the surface after 41 minutes anodizing at a current density of 5.4 A/dm^2 , showing microcracking over the oxide surface and a rounding off of the sharp edges produced by the sand blasting treatment.

As mentioned in Chapter Two sub-section 2.7 the angle at which the specimen surface is viewed within the S.E.M. must be taken into consideration when interpreting the image formed of the surface. Figs. 3.14(i) and (ii) are good examples of such a case in point. Fig 3.14(i) shows the surface of commercial purity aluminium anodized for 8 minutes at 33 A/dm^2 at a high glancing angle, (i.e., 10° from perpendicular) while Fig. 3.14(ii) shows the surface at a low glancing

angle, (i.e., 70° from perpendicular) giving the surface appearance of a mountain range.

Alloy I, P180 abraded and anodized for 15 minutes at 22 A/dm^2 in 5 v/v% H_2SO_4 at -6°C shows the development of hillocks in the direction of the abraded lines. Craze cracks (typically of a mudcrack pattern, on visual inspection, caused by thermal expansion or contraction or by mechanical deformation of the anodized specimen) can also be seen over the surface of the specimen. (See Fig. 3.15).

Fig. 3.16(i) shows the surface of Alloy I, $1 \mu\text{m}$ polished and anodized for 12 minutes at 22 A/dm^2 in 5 v/v % H_2SO_4 at -6°C showing hillock formation at certain points leaving a fairly smooth surface between them. It is this microscopic surface arrangement that gives rise to the dendritic pattern that is observed on visual inspection of the surface. Although it appears that nothing has happened at the smooth regions, by cross-sectioning the specimen it was shown that a fairly substantial thickness of oxide has in fact been formed. Fig. 3.16(ii) is a magnified view of Fig. 3.16(i) showing hillocks in more detail.

Fig. 3.17 shows Alloy II, P180 abraded and anodized for 18 minutes under similar conditions to those used for the above two figures, and also gives a similar topography to that formed on Fig. 3.15.

Fig. 3.18 was anodized as in Fig. 3.17, but the bath electrolyte was not agitated. The appearance of the surface is very different from that obtained with agitation being present. At high current densities, if agitation is not used to dissipate any heat produced during the formation of the oxide (the heat being produced from the resistance to the passage of current plus also the heat of formation of the oxide) then burning (See Appendix IV) of the oxide can occur.

This can be seen with respect to the surface appearance of localized breakdown of the anodic oxide film.

Fig. 3.19(i) shows Alloy II, polished on a $1\ \mu\text{m}$ diamond cloth and anodized for 14 minutes under similar conditions to those used for Fig. 3.15. Once again at lower concentrations of the electrolyte bath the hillocks formed at random positions, but did not totally cover the surface of the alloy. (This could possibly be explained by the poor throwing power which would be expected with the use of such a weak anodizing solution.) The figure also shows microcracking in between the hillocks. Fig. 3.19(ii) shows a different area showing hillocks growing along grain boundaries, microcracking is also present.

Fig. 3.20 shows H30 alloy abraded and anodized for 2 minutes at $33\ \text{A}/\text{dm}^2$ showing the abrasion lines. Fig. 3.21(i) shows H30 alloy polished on a $1\ \mu\text{m}$ diamond cloth and anodized for 2 minutes at $33\ \text{A}/\text{dm}^2$ showing characteristic hillocks. Fig. 3.21(ii) gives a magnified view of the above.

Figs. 3.22 to 3.24 shows the growth of the anodic oxide on scoring. The thickness of the coating at the point of the score line was approximately half that of the unscored area.

The surface of super purity aluminium on etching in a sodium hydroxide solution was characterised by a random distribution of hemispherical etch pits and preferential attack along scratch lines. (See Fig. 3.25). Fig. 3.26(i) shows the etched surface after 15 seconds anodizing at $35.7\ \text{A}/\text{dm}^2$. The nucleation and growth of the anodic oxide film occurred at random points and preferentially along scratch lines where a large number of defects in the air-formed oxide film was more likely. Characteristically shaped hillocks and ridges of anodic oxide were formed. Between the hillocks parts of the

surface can be seen which appear unaltered, growth appears to occur laterally and hillocks can plainly be seen growing into etch pits. Hillocks growing at random points can also be seen in Fig.3.26(ii).

Defects showing circular ridges where hillocks have grown preferentially were obtained on a few occasions. (See Fig. 3.27(i)). These defects may be caused by staining of the surface or more likely, gas bubble adhesion on the surface of the aluminium. It could be envisaged that the gas bubble would adhere to the surface, thus masking the underlying area whilst at the gas bubble/solution interface the current density would be quite high and nucleation and growth at this area would be expected to occur. Hence, explaining the circular ridges that are observed, it is noticed that in the defect at the far left of the figure the surface appears to be unaltered, whilst to the right anodizing has occurred in the defect ring. This could be possibly due to the fact that the oxide bubble detached itself during the anodic treatment thus allowing anodizing to occur whilst the unaltered defect's bubble did not.

Fig. 3.27(ii) shows a different anodized area viewed at a high glancing angle, showing the "rosette" effect given by the terraced layered microcracking as the oxide film grows.

The surface after 2 minutes anodizing is shown in Fig. 2.28(i); it shows oxide layers peeling off the hillocks. (Similar to wood shavings.) The view is from a high glancing angle and the entire surface is covered by anodic oxide. Fig. 2.28(ii) is similar to the above but at a viewing angle of 45 degrees. Fig. 2.28(iii) is a magnified view of the above. It is apparent that internal stress in the oxide has caused spalling of the outer surface layer. Pieces of oxide have cracked, curled and become detached. The direction of the

curl shows the original air-formed oxide at the outer surface has been unable to withstand the expansionary forces of the anodic oxide growing at the metal/metal oxide interface. The pattern of the cracks, which indicate the stress distribution (Hoop stresses) can be clearly seen. The cracks are roughly concentric and are related to the growth of the oxide. These cracks appear to be limited to the outer layer of the oxide which peels away to reveal a smooth surface underneath.

The surface after 8 minutes anodizing (Fig. 3.29) does not appear to have changed. The thickness of the oxide would increase uniformly, while the outer surface of the initially formed oxide maintains its roughness.

The surface obtained after anodizing for 57 minutes at 11.0 A/dm² is shown in Fig. 3.30(i). It shows hillock growth with terraced microcracking of the oxide. Craze cracks are also visible over the surface. Fig. 3.30(ii) is a higher magnification than Fig. 3.30(i) and shows dissolution at smooth surfaces and microcracking. Fig. 3.30(iii) shows the terraced microcracking occurring at approximately 2 μ m intervals as the oxide grew.

Figs. 3.31 to 3.36 are electron photomicrographs of different aluminium alloys with the same pretreatments, i.e., etched and hard anodized under similar conditions. It can be seen that there is very little difference between any of their topographies. The pre-etched randomly distributed hemispherical etch pits are still distinguishable, intermetallic particles can be seen embedded in the oxide and the craze cracks can also be seen. A feature that is conspicuously absent are the hillocks so far seen on all of the alloys anodized. This is not to say of course that they do not appear at all on these

alloys, but only on the particular alloys under study they did not show these hillocks for the particular conditions employed in hard anodizing them. If time had permitted, a more extensive in-depth study of these alloys would have been undertaken.

The surface of the super purity aluminium after chemical polishing is shown in Fig. 3.37, characterised by a fine cellular pattern.

Fig. 3.38 shows the surface obtained on anodizing for $4\frac{1}{2}$ minutes at 41.6 A/dm^2 . The typical hillock features are once again observed with terraced microcracking and crazing around the hillocks.

The appearance or performance in service of anodized alloys is closely connected with the whole metallurgical history of the alloy production, which determines whether the additions or impurities are in homogeneous solid solution, as intermetallic compounds within the grains, or as precipitates at the grain boundaries. The effect of intermetallic compounds in the metal matrix depends on the extent to which they can be taken into solid solution, because up to this point a solution heat treatment may produce a complete dispersion of the second phase, and by rapid cooling (quenching) this uniformity may be sustained without the growth of coarse precipitates.

The heat treatment procedure and subsequent cooling of the super and commercial purity aluminium gave a significantly thicker oxide coating than that of the naturally air-formed oxide. However, for super purity aluminium this appears not to have made a great deal of difference to the surface obtained on forming the anodic oxide. The characteristic hillocks are obtained as they were on "As rolled" surfaces. Figs. 3.46 and 3.47 show hillock growth and terraced microcracking while Figs. 3.48 and 3.49 show that on commercially pure aluminium hillocks are formed but cannot be distinguished clearly.

Alloy I, air-cooled (See Fig. 3.50) shows the formation of hillocks at the grain boundaries, while the same alloy water quenched (See Fig. 3.51) shows a slightly more randomized growth of hillocks. The same comments can be made for Alloy II. (See Figs. 3.52 and 3.53.)

Fig. 3.54 shows the surface of anodized commercial purity aluminium "As rolled" after anodizing for 70 minutes at 13.3 A/dm^2 in 10 v/v% H_2SO_4 at $17 \pm 2^\circ\text{C}$. The surface has been greatly attacked by the electrolyte. Three factors were basically considered to be involved with the surface as shown. These being as follows:

(i) Temperature: This will affect the dissolution rate of the oxide, which is an exponential function of temperature. Dissolution of the film does not proceed in successive parallel layers but occurs at the weak spots, which are at the openings of the pores. Hence, at high temperatures the pore will be wide open and the protective value of the oxide film will be less. In the figure it is seen that the pores have been attacked to such an extent that the thickness of the aluminium oxide cells has been reduced until only thin brittle peaks are left. This defect is well known to anodizers under the name of "powdery" coating. If a finger is passed over the surface the brittle peaks are broken away, the debris remaining in the form of a white powder smudge. Lower temperatures will alleviate this problem, but if high current densities are used a defect called "burning" can occur, which also resembles powdery coatings.

(ii) Current density: The rate of oxidation is proportional to current density. The rate of dissolution should remain unaffected; however, in practice too high a current density increases the dissolution greatly. The majority of the current passes through

the pores. The electrical resistance of the pores is very large. Since the pores act as a resistance, the pores will become heated by the passage of current, and the temperature in the immediate vicinity of the film increases. This may also lead to the formation of a powdery film.

and (iii) Time of treatment: The oxidation and the dissolution are proportional to the time of treatment. Therefore, it is important not to exceed a time for which the length of the pores, i.e., the thickness of the film, will attain a limiting resistance for which the rate of oxidation will be equal to the rate of dissolution.

The formation of hard anodic oxide films in dilute sulphuric acid appears to be a relatively heterogeneous process, involving the preferential development, growth and lateral spreading of thick oxide regions (hillocks) which merge together to form the hard anodic oxide film. The mechanism of the hard anodizing process is the same as conventional anodizing, but is carried out under conditions that give minimum dissolution of the oxide by the electrolyte and minimum pore volume.

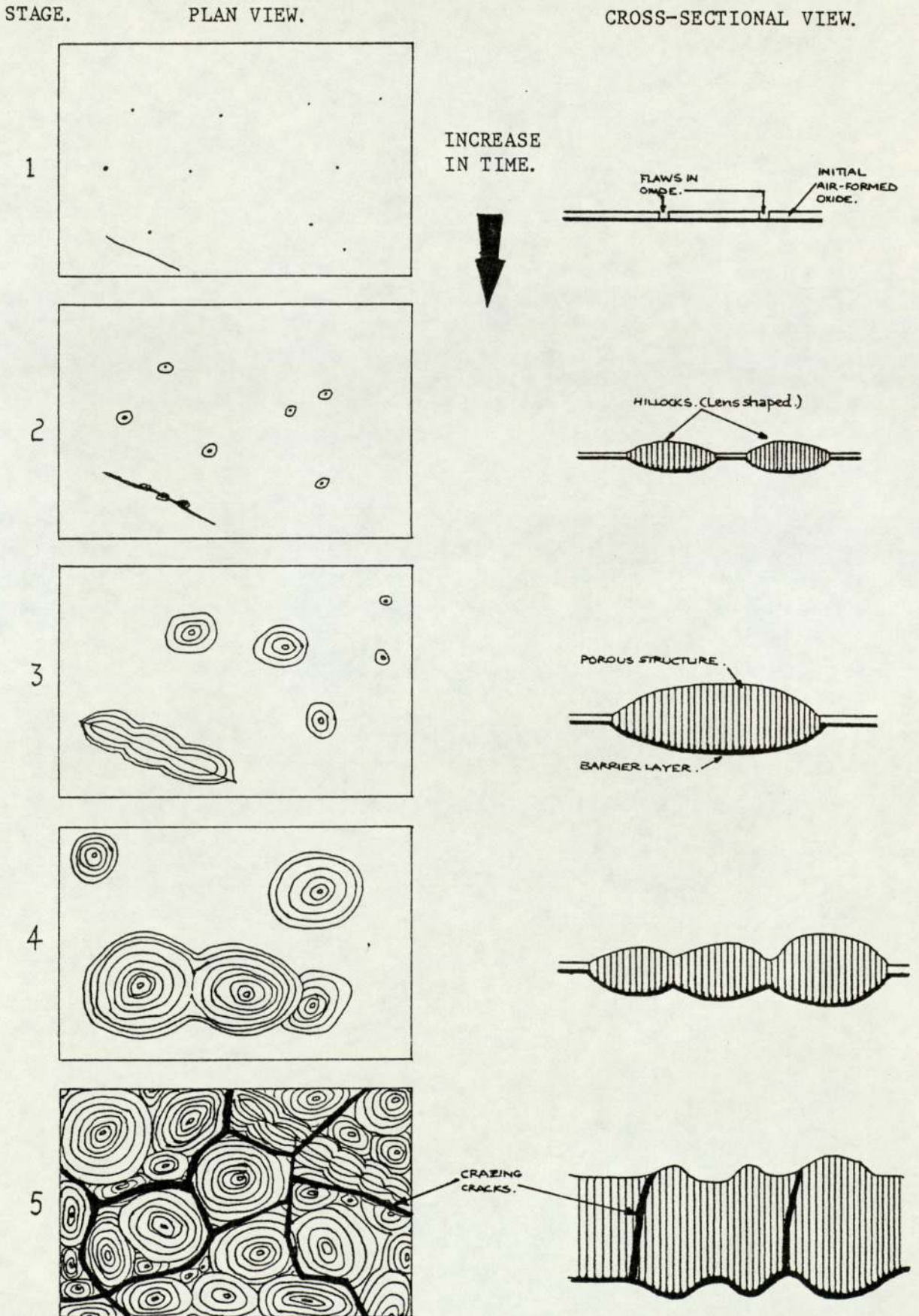
Csokán, (35,36,37) Lichtenberger-Bajza⁽¹³⁰⁾ Tomashov and Zalivalov⁽¹³¹⁾ and Bailey⁽²⁸⁾ all reported the existence of hillock (rosette) shaped features on aluminium that had been hard anodized. Bailey⁽²⁸⁾ considered the rosettes to be the result of the merging of several spreading thicker oxide regions, and could in fact possibly be the tops of "bundles of fibres".

Re-examination of some of Csokán's published photomicrographs (e.g. Fig. 5 on p.8 of Reference (37)) shows rosette rings which it is now realised are growth cracks occurring in the initial air-formed oxide, caused by the expansionary forces (increase in volume)

developed by the anodic formation of the alumina. Crazing of the oxide film is also apparent in Csokán's photomicrographs. The scanning electron photomicrographs (See Figs. 3.3(i), 3.5(ii), 3.26(i) and 3.30(i)), give a visual impression of the microsurface roughness and enables an appreciation of the three dimensional shape of the hillock shaped features. The terraced shape of the surface, which is now evident, must be envisaged when examining the transmission electron photomicrographs published by Csokán (e.g. Figs. 7 and 8 on p.8 of Ref. (37)). Contrast in the electron photomicrographs comes about from the terrace shape of the surface, which was not appreciated at the time; Csokán suggested that the structure was fibrous and referred to the work of Ginsberg and Wefers^(38,39) and Kaden⁽¹³⁷⁾ who had similar photomicrographs which were difficult to interpret and who also suggested the existence of fibre bundles.

Fig. 4.1 below shows a diagrammatic interpretation of the nucleation and growth of the hillock shaped features and their merging to form the thick anodic oxide film.

Fig. 4.1. Diagrammatic representation of nucleation and growth of hard anodic oxide film. (Not to scale.)



The stages inferred are as follows:

- (1) The random flaws in the initial air formed oxide are sites at which it is believed the oxide nucleates and grows.
- (2) The beginning of the growth of the hillock shaped features occurs at random sites and preferentially at the flaws. Thompson, Shimizu and Wood⁽¹³⁹⁾ have found that in the initial stages of anodizing the highly localised processes can occur at flaws which are always present in the air-formed oxide.
- (3) Growth of the alumina proceeds to form the hillocks. We must ask ourselves why the hillocks seem to grow preferentially, for if the hillocks are dense solid alumina then the resistance for such a structure would be very high. Therefore, it would appear that the resistance of the hillocks is lower than the surrounding oxide. This may be explained by the hillocks being porous in structure and will thus allow flow of current and enable growth of the alumina. Also, the barrier layer at the base of the pores must be thinner than the air formed oxide elsewhere; with lower resistance for the passage of current.
- (4) The expansionary forces of oxide formation, initially in the region of the flaw, fracture the oxide surrounding the flaw allowing anodic oxidation to occur progressively in the surrounding region; this gives the characteristic lens - shaped cross section rosette with its rings of spalled outer oxide on the surface. As anodizing spreads to surrounding regions and the hillocks begin to merge there is a fall in the local current density until the entire surface is covered by anodic oxide.
- (5) Except for minimal dissolution at the outer surface there is no subsequent change in the surface topography with further anodizing.

The thickness of the oxide increases uniformly, forming at the inner metal/metal oxide interface, while the outer surface of the oxide maintains the nodular roughness produced by the initially formed hillocks. As the oxide thickens then crazing will be present also.

4.3 ICING DEFECTS.

The electropolishing of aluminium can give a high degree of smoothing to the aluminium surface if the correct operating conditions are used. However, there are various defects that can be experienced with electropolished work. One common defect is the appearance of streaks on the surface due to gas bubbles and inadequate or improper agitation. Flat horizontal faces are liable to give rise to this effect. Another defect, perhaps not as common as gas streaking is known as "Icing". Such defects were formed whilst using electropolishing as a pretreatment before anodizing. They were considered to be such an interesting phenomenon that they were investigated in their own right by the author.

Many workers have published photomicrographs of such defects which are characterised by their pyramidal shape, are randomly orientated and bear no relation to grain size or crystallographic structure of the aluminium upon which they are formed. The defects stood proud of the surrounding electropolished surface where metal removal had taken place. The bases of the defects are rectangular, hexagonal or distortions of these shapes. The pyramid faces are stepped with striations parallel to the bases of the defects.

Fig. 3.39(i) is an optical photomicrograph showing icing defects and Fig. 3.39(ii) is an S.E.M. photomicrograph of icing defects.

In the early stages of electropolishing etching of the super purity aluminium surface actually occurs, (See Fig. 3.40) with preferential attack at scratches on the surface. When the aluminium is immersed live in the electropolishing solution, the applied voltage is low (constant current applied) and the current is concentrated at defects in the air-formed oxide film where there will be a high localized current density. In some places it can be as high enough to evolve oxygen and allow the formation of gassing defects to occur. (See Fig. 3.41(i)). The high current density around the gassing defect gives a high rate of electropolishing locally, forming an annular trough round the central spot where the gas bubble sits. Dissolution of the air-formed oxide proceeds in the low current density regions, radiating outwards and merging until all the air-formed oxide is dissolved. Fig. 3.41(ii) shows the formation of icing defects at high current density regions and Fig. 3.41(iii) shows gassing defects associated with the characteristically pyramid shaped icing defects. Most of the icing defects have a central blip and Fig. 3.42 shows that this particular icing defect has grown around a gassing defect.

Certain specimens on which icing defects had been formed were hard anodized for 18 minutes at 10 A/dm^2 . Figs. 3.43(i) and (ii). Fig. 3.43(i) shows that the anodic oxide film had not formed to the same extent on the icing defects as on the surrounding electropolished regions. The thicker anodic oxide on the electropolished surface leaves the icing defects as depressions in the surface and inverted the stepped striations at the extremities of the icing defects.

The thickness of the porous anodic oxide that forms on the icing defects increases with time. The thickness of the electropolished

film also increased with time, but there is a difference in pore dimensions for each. When icing defects form, the oxide film has the characteristics and pore dimensions of anodized films formed under conditions of low oxide solubility, whereas electropolished oxide has the characteristics and pore dimensions of relatively higher oxide solubility. Hence, when such a surface is transferred from the electropolishing bath at a final applied voltage of 52 volts to a hard anodizing bath for 18 minutes anodizing at 40 volts, the hard anodizing takes place preferentially on the electropolished part of the surface and builds up the thickness of the oxide more than on the icing defects, which already have an anodized oxide present on them. Fig. 3.43(ii) shows greater detail of depressions at sites of prior icing defects.

The surface of super purity aluminium when viewed visually which appeared free of icing defects and gave excellent surface reflectivity was obtained after 90 seconds of electropolishing. Fig. 3.44 shows such a surface with a few randomly distributed gassing defects present.

Fig. 3.45 is the surface as above anodized for 37 minutes at 8.9 A/dm^2 in 10 v/v% H_2SO_4 at -8°C . The surface shows the characteristically shaped hillocks of anodic oxide. (These hillocks form the characteristic roughening of the surface typical of anodized specimens.) Cracking around the hillocks is roughly concentric and is related to the growth of the oxide. At the top of every hillock there appears to be a pit-like depression. This feature may be caused by the effect of dissolution of the oxide by the electrolyte but probably comes about because the central-blip of the gassing defect will have a different oxide thickness from that on the bulk electropolished oxide surface. It would therefore seem that the

thickness of the oxide at this central-blip is greater than that of the bulk electropolished oxide thickness, and so on anodizing, the aluminium oxide surrounding the central-blip will grow preferentially (if Ohm's law is followed) and so the central-blip that stood slightly proud of the surface on electropolishing is, on anodizing, depressed, giving the effect that dissolution has occurred at the apex of each hillock.

From the experimental work carried out the main conclusions are as follows⁽¹²⁵⁾:-

Icing defects are parts of the aluminium surface where electropolishing is prevented by the formation of an anodized oxide film. They occur when the electrolyte composition and polishing conditions are close to the transition from electropolishing to anodizing. The solid crystallising out is likely to be aluminium phosphate in solutions rich in phosphoric acid, but it subsequently dissolves at the outer surface as anodic oxide forms at the aluminium/aluminium oxide interface.

Icing defects are avoided by adjusting the solution composition and operating conditions to those favouring dissolution of aluminium oxide while maintaining the oxidizing power for electropolishing.

4.4 POTENTIAL - TIME.

Evans⁽¹³⁴⁾ has described some important features of potential versus time measurements. The basic shape of the potential - time curves can be explained in terms of solid film formation and dissolution. An oxide film has, in general terms, either higher electronic resistance or higher ionic resistance than the metal, and sometimes both.

(Alumina (Al_2O_3) is known to have a very high electronic resistance.)

Hence, a reduction in circuit resistance is seen as a fall in potential

and an increase in circuit resistance as a rise in potential.

Potential measurements will give an indication of the surface state of the metal. If a metal with a porous film is placed in a liquid, the potential will become more noble (higher) if the film is self-healing, and less noble (lower) if the film is not repaired and corrosion proceeds i.e., if corrosion is developing then the potential will fall with time and if the reaction is stifling itself, it will rise with time. This comes about because a specimen carrying an oxide film interrupted by only small gaps in it will show a higher potential than one carrying an oxide with very many gaps in it. Hence, the movement of potential with time indicates whether the material is becoming passive or is developing corrosion. A shift in potential in a positive (noble) direction indicating passivity and in this case a build-up of oxide.

The aim in anodizing is usually to operate at a particular current density rather than voltage because it is only in this way that the rate of coating formation can be known and controlled. Within normal limits the voltage required to produce a given current density generally decreases with increase in electrolyte concentration and also with an increase in electrolyte temperature. It can therefore be seen that in hard anodizing processes the voltage required to produce a given current density will be higher in value. The increased voltages are needed on reducing the anodizing temperature or lowering the acid concentration, but keeping the current density constant, or on increasing the current density under any particular electrolyte condition. Increasing the anodizing current density without changing the electrolyte strength or temperature involves increasing the anodizing voltage, (This voltage rise is considered to

be due to diffusional difficulties, which limit anion supply to the pore electrolyte, thus reducing the anion incorporation in the barrier layer and decreasing its conductivity.) which decreases the porosity of the anodic oxide coating produced with consequent increase in coating hardness and abrasion resistance. (In fact, at a constant current density and with the voltage varying during oxide film formation, it would be expected that the pore diameter would not be constant throughout the film profile - giving a slight funnel effect and the overall porosity of the anodic film decreasing as it forms.)

One other factor that must be taken into account is that due to the resistivity of the anodic oxide coating, (this will increase the total heat evolved as anodizing proceeds and therefore a capacity for refrigeration of the electrolyte will be required to maintain a constant temperature) the voltage required to maintain a given current density must be increased slowly over the period of anodizing. The adjustment (rate) required and the initial and final voltage are affected by the alloy being anodized. The current required per unit film thickness depends on the effect of the alloying constituents on the conductivity of the coating. The voltage required for anodizing can vary with the condition of the alloy, i.e., whether it is homogeneous or heterogenous. Thus copper alloys in the cast condition anodize at a lower voltage than in the solution heat-treated condition. The difference in behaviour are attributed to the effect of the constituent on the resistance of the coating.

The potential (voltage) - time curves obtained for various alloys under investigation all gave slightly different initial voltages (the reason for this being explained above) and the voltage required to

maintain the selected current density and time of anodizing also varied slightly from specimen to specimen.

Fig. 3.55 shows that when the specimen is immersed "live" at 60 volts into the anodizing bath the potential initially drops (surface active) and within half a minute began to rise (passivity - oxide build-up) steadily until the 60 volts limit of the rectifier was reached and the specimen was removed from the anodizing bath. If Alloy I, P180 abraded is compared with Alloy I, 1 μm polished, the time taken to reach 60 volts is faster for the mechanically polished specimen. Although the current density for each specimen was specified as 22 A/dm², this was the apparent current density (because the true surface area was not obtained) and not the true current density. Therefore, a rough, abraded surface would present more unit surface area to the electrolyte, and the true current density is lower than the apparent. The mechanically polished specimen which was relatively smooth when compared to the mechanically abraded surface would present a surface area close to the measured (apparent) surface current density and would attain a greater oxide growth rate than the mechanically abraded specimen. (This aspect of true and apparent current density will be met throughout the interpretation of the potential - time curves.) The same curves were found for Alloy II, although overall Alloy I (contains a higher percentage of Mg - conducts current easily) anodizes at a greater rate than Alloy II for both of the pretreatments.

Fig. 3.56 shows how by increasing the current density the rate at which voltage needs to be supplied to the anodizing cell during the course of anodizing decreases the film formation time, thus reducing the extent of dissolution of the film formed under the particular

anodizing conditions of the experiment.

Fig. 3.57 shows once again how the surface roughness increases the surface area and hence, lowers the apparent current density and takes longer to form the anodic oxide film. A drop of current density by two thirds increased the anodizing time by a factor of three.

Fig. 3.58. Anodizing at higher temperatures than previously used meant that the conductivity of the bath was higher and the voltage required to maintain the current density lower. The plot of A, B and C at 6°C showed a steep rise in voltage up to 60 volts, whilst for D at 17°C the rise is less steep. By increasing the temperature of the anodizing bath from 6°C to 17°C this trebles the time of anodizing for the commercial purity aluminium.

Fig. 3.59. Anodizing at a lower current density than that applied in Fig. 3.58 for A and B reduced the rise in voltage, whilst raising the temperature gave a nearly linear plot of voltage against time, indicating that the rate of oxide film formation/dissolution was very close to its equilibrium. The commercial purity aluminium anodized at a faster rate than that of the super purity aluminium.

Figs. 3.60 to 3.65 all show basically very similar curves, in that at high current densities the voltage rises steeply, whilst at the low current densities the voltage rises less steeply. The etched anodized specimen follows the same profile as the "As rolled" specimen, but the voltage runs slightly below the "As rolled" profile. (Surface area phenomenon.) The initial voltage is slightly different for each of the alloys, this being dependent upon the constituents present in the alloy.

4.5. MICROHARDNESS.

The pretreatment of the aluminium appeared to have no significant effect on the hardness profile of the oxide film. In the experiments carried out the factors effecting the values of hardness profile were the alloy composition, current density and time of anodizing. The hardest films were produced on high purity aluminium at high current densities and short anodizing times.

The hardness decreased as the film thickness was increased. The hardness of the film varied throughout its depth, the highest values being obtained at the metal-oxide interface (barrier layer) whilst lower values were obtained moving outwards from the interface to the outer surface of the oxide film. The reason for this behaviour can be explained by consideration of the porosity of the film. Even at the low temperatures used in the experiments the solvent action of the electrolyte increases for increased periods of immersion time. This chemical dissolution attack not only occurs in the macropores, whereby the pore mouths are widened by the chemical electrolytic dissolution of the pore wall material, but also by microporosity in which the electrolyte permeates into the pore wall material. Hence, the outer region of the oxide reflects the maximum exposure to the electrolyte and the lowest hardness value.

4.6 THICKNESS OF ANODIC COATINGS.

The thickness of the anodic coating depends on the operating conditions i.e., electrolyte composition, bath temperature, current density, treatment time and composition of alloy. Basically, the increase in film thickness is not linear with treatment time, but a maximum, or limiting; film thickness may be reached when an equilibrium is established between the rate of film growth and the rate of

dissolution of the film in the electrolyte.

However, under the conditions of the experiments carried out, i.e., low acid concentration, low temperature and high current densities the film thickness is apparently linear with respect to the treatment time; for longer treatment times, lower current densities and higher temperatures this would not be the case and the limiting film thickness would be reached.

The film thickness appears to be closely dependent upon the product of current density (number of coulombs supplied) and the treatment time, (which was expected), the concentration and temperature of the electrolyte being constant. The maximum film thickness depends upon the factors mentioned above, and considering alloy composition the thickest coatings were obtained on pure aluminium, whilst the thinnest were obtained with the heat treatable heavy-metal containing alloys.

The growth in dimensions of the specimen was approximately 50 per cent of the coating thickness.

The thickness of the anodic oxide coating may be expressed by the empirical relationship:

$$d = K.A.t$$

where d is the film thickness in microns

A is current density in A/dm²

t is time in minutes

and K is a constant varying between 0.3 - 0.37 according to the anodizing conditions.

4.7 COATING RATIO.

Coating ratio is an analytical concept sometimes employed in determining the effect of alloying constituents in aluminium to evaluate the efficiency of the anodizing process in anodic oxide formation. Anodizing at high current densities under ideal conditions improves the efficiency of the process as expressed by the coating ratio and correspondingly the weight of coating in a given time. Coating ratio will be decreased as metal purity is reduced and as various alloying elements (e.g. Cu) are added; it also decreases with time and can be increased by reducing the bath temperature and acid concentration or by increasing the current density and voltage.

In the experiments carried out, surface preparation of the aluminium was not considered, but other workers⁽⁸¹⁾ stated that the different surface cleaning treatments did not affect the efficiency of the anodic treatment. However, severe etching of the surface might cause a slightly lower coating ratio because of a lower current density per unit of actual area.

The effect of anodizing time at the relatively high current densities caused a progressively steep rise in the coating ratio as can be seen in Figs. 3.75 and 3.76.

Practically it would be expected that higher coating ratios are obtained with thin coatings, rather than thick coatings. Indicating that coatings which remain in contact with the acid electrolyte are gradually dissolved and the greatest coating ratios should therefore be obtained with coatings formed in the shortest time. However, the experiments carried out plainly indicate that the coating ratio was in fact increasing for the time of immersion. An increase in coating ratio with time at low temperature and high current densities is

inevitably associated with a steeply rising voltage.

The rise in coating ratio could possibly be explained by considering that no dissolution of the coating or at most very little took place. Considering the conditions used, this explanation may be feasible but it does seem unlikely. A more likely explanation is that the rapid formation of solution products, i.e., incorporation of electrolyte anion (SO_4^{--}), builds up in the pore channels causing a decrease in the rate of solution of the oxide coatings which in turn produces higher coating ratios. The excess of dissolution products could be thought of as being due to rapid dissolution at the pore base, which cannot be dealt with by the diffusion rate further up the pore channel.

4.8 EXAMINATION OF DETACHED OXIDE FILM AND ANODIZED SPECIMEN AFTER ANODIC FILM REMOVAL.

4.8.1 EXAMINATION OF DETACHED OXIDE FILM.

The oxide film was detached from the anodized specimens as explained earlier and examined electronoptically with the S.E.M. The outer oxide surface, i.e., the first formed oxide, reproduced the pretreated surface texture for all of the alloys anodized. The last formed oxide, i.e., the oxide formed at the metal-oxide interface, produced a different appearance depending upon the alloy anodized. All aluminium alloys, other than super and commercial purity, showed features as seen in Figs. 3.77 to 3.78(ii). These features appeared to be conically shaped voids and microcracking of the oxide was also apparent. These conical features were not observed to any significant extent on the oxide films detached from super and commercial purity aluminium, although microcracking was still apparent.

Metallurgical cross-sectioning of the anodized alloy specimens and optical examination (See Fig. 3.78(iii) for typical view of alloy cross-section.) showed that these features were formed by un-anodized aluminium cones remaining in the oxide whilst the metal-oxide interface recedes away from the apex of such features. Hence, the conically shaped voids observed in the oxide were once filled with aluminium before the oxide was electrolytically detached from the specimen. It is considered that these features come about due to the presence of second phase constituents in the alloys anodized, e.g. MgSi, Al-Fe-Si, FeAl₃, MnAl₆, CuAl₂, Si and others.

Work on the effects of these constituents on the metal-oxide interface was first discussed in detail by Cooke⁽¹³⁵⁾ who postulated a mechanism explaining the formation of these features. He suggested that inert constituents have a higher conductivity than the matrix around them, and therefore cause a concentration of current, which results in the formation of what he called a "conical asperity" beneath them. The growth of such an asperity can be many times the size of the original particle and the extent to which it produces roughening at the metal-oxide interface is strongly dependent on the anodizing voltage used, roughening increasing as voltage rises.

The results obtained in the examination of the detached oxide film appears to confirm what Cooke's mechanism postulated for conventional anodizing.

4.8.2 EXAMINATION OF ANODIZED SPECIMEN AFTER ANODIC FILM REMOVAL.

Cross-sections of the anodizing alloy specimens were polished to 1 μm and placed in a boiling solution of phosphoric -chromic acids, the resulting features obtained were examined with the S.E.M. and typical results obtained are shown in Figs. 3.79 to 3.85.

Fig. 3.79 shows a cross-sectional view of Specimen 1 from Experiment 3.38 after the immersion treatment in the boiling solution of phosphoric - chromic acid. It shows the different thicknesses of oxide formed at the different current densities applied. It can be seen that at every period of change of current density there is a definite demarcation line where growth of oxide restarted. The structure obtained appears to be columnar but could be said to resemble a fibrous structure.

Fig. 3.80(i) shows Specimen 2 from Experiment 3.38 with the same treatment carried out on it as for Fig. 3.79 above. The view is of the specimen at the second stage of anodizing i.e., after being anodized for 5 minutes at 26.6 A/dm^2 and 5 minutes at 14.0 A/dm^2 . It also shows the polished oxide film still unattacked by the chemical stripping solution.

Fig. 3.80(ii). As above but anodized for an additional 10 minutes at 7.2 A/dm^2 , once again showing the three layers of oxide formed for the three different current densities applied.

Fig. 3.81(i). View of oxide appearing to form columns of alumina growing perpendicular to the substrate metal. The surface of the substrate after dissolution of the oxide can be seen to be undulating in nature.

Fig. 3.81(ii). As Fig. 3.81(i) magnified to show the point of contact of the alumina with the substrate metal. Fig. 3.82(i) shows how the solution attacks the anodic oxide film and Fig. 3.82(ii) shows the regular columnar type structure formed as dissolution of the oxide takes place.

At this juncture it may be worthwhile suggesting a possible explanation of how the columnar structure comes about. It must be remembered that the anodic oxide film is being chemically dissolved

and that the way in which the oxide (alumina) dissolves is not necessarily a reversal of the way the porous coating was formed i.e., dissolution of the last formed alumina (that formed at metal-oxide interface) towards the first formed alumina (the oxide further away from metal-oxide interface). This may be made more clear by considering an analogy of the formation and dissolution of a snowflake. Snowflakes will form due to physical changes in the weather, i.e., their formation is dependent upon nuclei (dust or smoke particles), vapour pressure and temperature. When the conditions within the cloud are suitable, water will condense out of the air at a low temperature and freeze to form ice crystals which add on to other crystals and become bigger and heavier, and as they become heavier they start to fall through the cloud gathering up other crystals on the way, to form the characteristically six-sided hexagonally shaped snowflakes. (If conditions are cold enough, the snowflakes will eventually reach the ground.) If a snowflake is observed microscopically and the temperature is slowly raised then it is observed that the snowflake does not dissolve in the way in which it was formed, but appears to dissolve at defects within the structure, (where the atoms will be highly mismatched-high potential energy) until eventually it melts completely to form a water droplet.

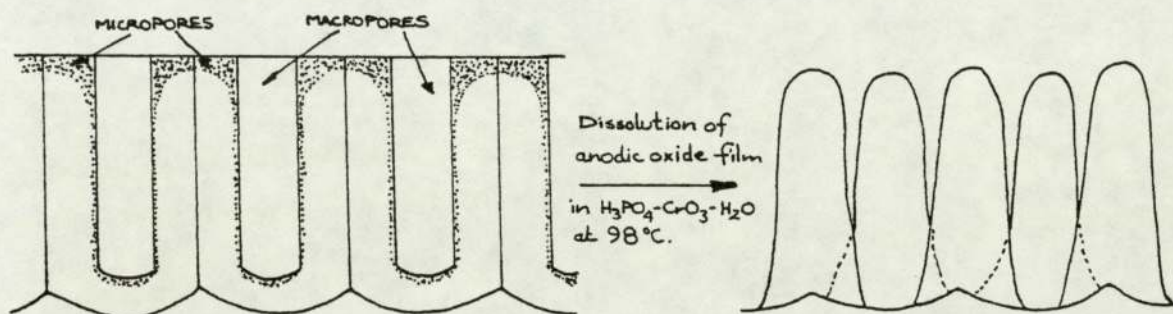
The anodizing process produces the characteristic porous cell structure with the associated microporosity of the macropores.

On consideration of the diagrammatic representation of the structure of the porous anodic oxide film with the microporosity present, (See Fig. 4.2. below) when the polished cross-section is placed into the stripping solution the dissolution will occur preferentially at weak points of the alumina structure, which

will be the micropores, leaving the fairly pure alumina at the cell wall interface standing. Hence, the appearance of columns.

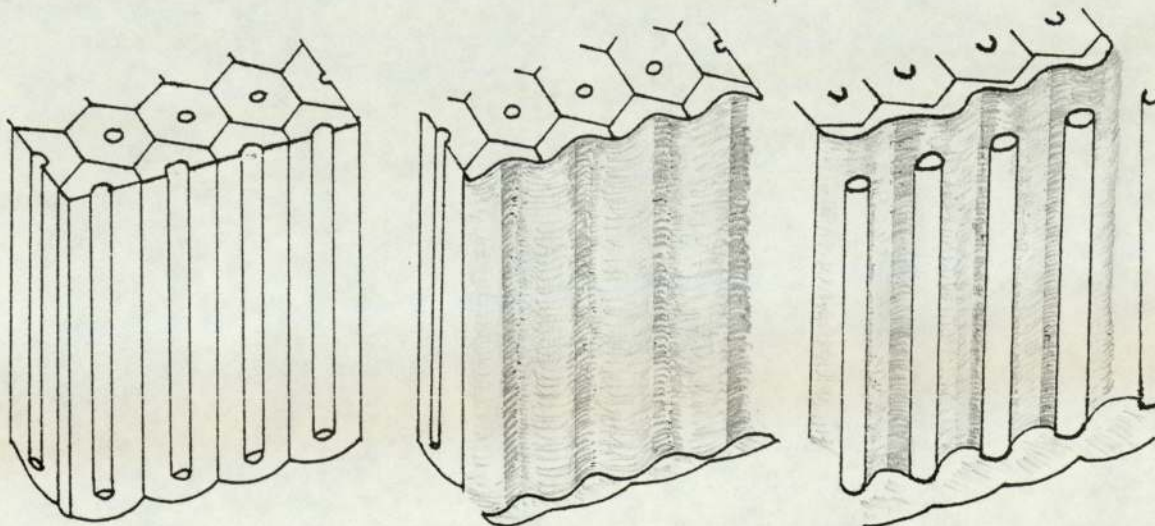
Obviously these columns will eventually be attacked also, but at any particular stage of removal of the specimen from the stripping solution the columns will be observed.

Fig. 4.2. Diagrammatic representation of chemical dissolution of the anodic oxide film. (Not to scale.)



Cross-sectional view of cellular structure of the anodic oxide film showing macro- and micro-porosity.

Columnar type structure.



(a) Structure of oxide before dissolution.

(b) Structure of oxide at intermediate period of dissolution.

(c) Columnar structure.

Fig. 3.83(i) shows when the oxide is dissolved away from the surface of the basis metal it reveals the basis metal surface. With this particular specimen an "island" like formation protruding from the surface of the basis metal is seen. It must be remembered that this surface should ideally resemble the surface after pretreatment, i.e., chemically polished (See Fig. 3.37). Why these "islands" should form is a mystery and cannot be explained at the moment without further investigations being carried out on them. It must be noted, however, that this type of "island" structure only occurs with films formed at fairly high current densities, i.e., greater than 15.0 A/dm^2 , and for anodizing times greater than 10 minutes. It therefore seems highly probable that the "islands" are in some way related to the formation of the hillock type structure mentioned earlier, when aluminium is hard anodized under the conditions used in this investigation.

It may be argued that these "islands" are in fact oxide that has not dissolved; however, I consider that this is not the case because certain specimens when immersed in the stripping solution for well over 30 minutes (which would have completely dissolved any alumina present) and examined, still showed the "island" structure. Also, even if the specimen was re-introduced back into the stripping solution the "island" structure still remained.

Fig. 3.83(ii). As above magnified to show "islands" in greater detail.

Fig. 3.84. The same pretreatment as above but was anodized at a lower current density. The "island" structures are not formed at the lower current densities.

Fig. 3.85(i),(ii) and (iii) shows a feature that was present on

all of the cross-sections of the anodized specimens oxide film after the chemical dissolution treatment. These structures appear to be sheets of oxide apparently unattacked by the solution. It is not certain whether these sheets of oxide are in fact true structural features of the hard anodic oxide or an artifact of the dissolution process itself. This feature obviously requires further investigation. If for example the dissolution of the oxide was carried out in another solution and the sheets were still present then this may indicate that these sheets are in fact a structural feature of the anodic oxide film. If on the other hand these sheets were not present then this may indicate that the sheets of oxide were in fact an artifact of the dissolution mechanism in the phosphoric-chromic acid solution used.

Fig. 3.86(i) shows the interface of a chemically polished surface-un-anodized (left-hand side of figure) and the basis metal surface after oxide removal (right-hand side of figure).

It can be seen that the un-anodized surface has not been attacked to any great extent by the stripping solution, whereas the surface of the metal after oxide removal shows the "island-like" structures over the entire surface.

Fig. 3.86(ii) shows another feature that was observed at a few random points after dissolution of the oxide. It appears to be a cylinder of material that has not been totally dissolved away by the stripping solution. Fig. 3.86(iii) shows a magnified view of Fig. 3.86(ii).

At this point it is important to remember that the surface under examination is the interface at which the anodic oxide was the last to be formed. As a result of oxidation within the pores in the

direction of the basis metal, crater shaped pits are formed in the metal surface under the oxide cells. The relief structure of the basis metal surface, which is revealed by chemically dissolving the oxide, may also be regarded as a characteristic of the oxide film. Each pit in each figure shown, is considered to probably represent bundles of thousands of pores which formed pore channels that grew together.

Figs. 3.87(i) to 3.87(xi) show the pits formed by these pore bundles for increased time of anodizing of "As rolled" commercial purity aluminium for various current densities.

Fig 3.87(i) shows the surface after being anodized for 15 minutes at 5.8 A/dm^2 in 10 v/v% H_2SO_4 at -8°C and then chemical removal of oxide. It indicates that the pore bundles merged together to give intermitant lines of pore bundles. Simple electric field theory shows that if pores are too widely spaced then extra ones will form inbetween and those too close together will merge to form one.

Fig. 3.87(ii) was anodized as above but for 30 minutes and shows that the merging of the pore bundles is less pronounced, indicating that certain pore bundles were ceasing to function. For longer anodizing times, e.g. 60 minutes (See Fig. 3.87(iii)) the pore bundle lines have disappeared to be replaced by point pore bundle formation, which appears as spherical "dots" in the figure. The occurrence of the "dots" is expected. Wood and O'Sullivan⁽¹³⁶⁾ showed that the pore diameter was proportional to the formation voltage and with an increase in voltage the cell size increased and the number of pores decreased accordingly.

Fig. 3.87(iv) anodized for 3 minutes at 10.7 A/dm^2 showing less pronounced elongated pore bundle formation.

Fig. 3.87(v) anodized for $7\frac{1}{2}$ minutes shows a definite grain orientation of the elongated pore bundles. After 30 minutes anodizing at 10.7 A/dm^2 the point pore bundle formation occurs and after anodizing for 47 minutes point pore bundle formation and the "island" formation is present on the surface.

Fig. 3.87(viii) anodized for 3 minutes at 19.2 A/dm^2 , shows less pronounced elongated pore bundle formation than with lower current densities. In fact, point pore bundle formation occurred after only $7\frac{1}{2}$ minutes of anodizing (See Fig. 3.87(ix)). After 10 minutes anodizing the growth of the "island" is taking place and pore bundle growth is particularly prominent at scratch defects. (See Fig. 3.87(x)). After 15 minutes anodizing the distribution density of the point pore bundle growth is less and growth of the "islands" has taken place.

When the concentration of the sulphuric acid was increased from 10 per cent to 15 per cent then the following was observed. In Fig. 3.88(i) the specimen was anodized for 15 minutes at 6.3 A/dm^2 , point pore bundle formation distributed at many points over the surface. Fig. 3.88 (ii) was anodized for 30 minutes at 11.5 A/dm^2 and shows the point pore formation and the formation of "islands". Fig. 3.88(iii) was anodized for $10\frac{1}{2}$ minutes at 22.2 A/dm^2 and shows the point pore bundle formation, particularly along scratch lines and "island" formation.

When the concentration of the sulphuric acid was increased further to 20 per cent sulphuric acid the following was observed. In Fig. 3.89(i) the specimen was anodized for 15 minutes at 5.8 A/dm^2 , point pore bundle formation was observed. Fig. 3.89(ii) was anodized for 30 minutes once again showing the point pore bundle formation. Fig. 3.89(iii) was anodized for 60 minutes and shows large pores

with smaller pores distributed at random within the larger point pore bundles. Fig. 3.89(iv) was anodized for 3 minutes at 10.4 A/dm^2 , showing crystallographic directionality of the point pore bundles. Fig. 3.89(v) anodized for $7\frac{1}{2}$ minutes showing large and small point pore bundle formation. Fig. 3.89(vi) anodized for 29 minutes, showing fewer point pore bundle pits. (Higher formation voltage.) Fig. 3.89(vii) was anodized for 3 minutes at 19.2 A/dm^2 , and shows the point pore bundle formation. After $7\frac{1}{2}$ minutes anodizing (See Fig. 3.89(viii)) large and small point pore bundles present with "islands" showing. After anodizing for 11 minutes the point pore formation was less densely distributed and "island" growth was complete.

Fig. 3.90 was anodized for 3 minutes at 52.0 A/dm^2 in 10 v/v% H_2SO_4 at -8°C and shows the preferential point pore bundle formation along scratches originally present on the metal before the anodic treatment, and around the "island" formations.

Fig. 3.91. As above, but anodized for $27\frac{1}{2}$ minutes at 11.5 A/dm^2 shows point pore bundle formation randomly distributed over the surface with no "island" formations present.

Figs. 2.92(i) to 3.94(ii) are all commercial purity aluminium etched in 10% NaOH for 2 minutes at 60°C and then anodized for 2 minutes at various current densities in a 27.6 v/v% H_2SO_4 solution at 0°C .

Fig 3.92(i) anodized at 29.6 A/dm^2 shows crazing and hemispherical etch pits.

Fig. 3.92(ii) shows the surface after chemical stripping, showing point pore bundle formation.

Fig. 3.93(i) was anodized at 15.2 A/dm^2 giving surface similar to that obtained for Fig. 3.92(i).

Fig. 3.93(ii) shows point pore bundle formation on removal of anodic film.

Fig. 3.94 was anodized at 8.2 A/dm^2 similar to surface obtained for Fig. 3.92(i) and 3.93(i).

Fig. 3.94(ii) as Figs. 3.92(ii) and 3.93(ii).

It was noticed that with the higher concentrated acid and temperature, the point pore bundle formation occurred at a greater density than at the low acid concentrations and temperatures.

CHAPTER FIVE.

5. CONCLUSIONS.

The main achievements of the present work are as follows:-

- (a) The explanation and understanding of nucleation and growth of anodic oxides in Hard Anodizing and Conventional Anodizing.
- (b) The explanation and understanding of icing defects,
- and (c) The relationship between the anodic processes of electro-polishing and anodizing of aluminium.

The following conclusions were drawn.

- 5.1 Nucleation of anodic oxidation of aluminium occurs at defects in the original oxide film.
- 5.2 The mechanism of nucleation and growth is similar for both hard anodizing and conventional anodizing.
- 5.3 The conditions for hard anodizing are those that produce the densest possible oxide.

These are:

- (i) Low temperatures,
- (ii) short processing times,
- (iii) high applied current densities
- and (iv) low acid concentration.

- 5.4 These conditions all minimise dissolution and by doing so, nucleation when hard anodizing, is restricted to defects in the initial air-formed oxide.
- 5.5 The initiation, propagation and growth of the oxide hillocks increases with an increase in current density.
- 5.6 Icing defects are parts of the aluminium surface where electropolishing is prevented by the formation of an anodized oxide film.
- 5.7 Icing defects occur when the electrolyte composition and current density are close to the border line between electropolishing and anodizing.
- 5.8 The solid crystallising out to form icing defects is likely to be aluminium phosphate in solutions rich in phosphoric acid, but it subsequently dissolves at the outer surface as anodic oxide forms at the aluminium/aluminium oxide interface.
- 5.9 Icing defects are avoided by adjusting the solution composition and operating conditions to those favouring dissolution of aluminium oxide while maintaining the oxidizing power for electropolishing.
- 5.10 Potential - Time curves indicate that during anodizing the aluminium becomes passive in nature.
- 5.11 The hardness of hard anodic oxide films (as measured by microindentation) steadily decreases from the metal/metal oxide interface towards the outer surface of the metal oxide.
- 5.12 Thickness of the anodic coating depends on the operating conditions. i.e., electrolyte composition, bath temperature, current density, treatment time and composition of alloy.
- 5.13 The coating ratio increases with time at low temperatures and high current densities.

CHAPTER SIX.

6. FURTHER WORK.

The following are suggestions for further work.

6.1. Present investigations were principally confined to certain types of alloys, i.e., super and commercial purity aluminium. Other alloys will certainly exhibit different properties. Further work on these alloys would provide valuable information on the alloys suitability for hard anodizing.

It would be hoped that a number of techniques would be used in the investigation of the hard anodic oxide films formed. i.e., Ultra-microtomy (of cross-sections) and ion beam thinning to enable information to be obtained both on the alloy before anodic treatment and also on the oxide after anodic treatment. The structure and composition of the hard film can then be studied using the STEM (Scanning Transmission Electron Microscope), and EELS (Electron Energy Loss Spectroscopy) and EPMA (Electron Probe MicroAnalyser).

6.2 Ultra-microtomy of icing defects to discover whether the defect is in fact layered and of a porous oxide nature.

6.3 Influence of intermetallics of alloy on stress and hardness, i.e., solubility and microporosity.

6.4. Investigation into the effect of heat treatment, particularly stress relieving, direction of grain and size and method of basic manufacture, e.g., extrusion, forging and drawing.

6.5 Investigation of mixed acids for hard anodizing. One of the most

effective addition agents for decreasing the solubility of the anodic oxide coating in sulphuric acid is oxalic acid. Investigations into such mixtures would be most valuable in determining whether oxide coatings giving enhanced properties could be obtained.

6.6 Application of different current wave forms. Current interruptions can cause laminations in hard coatings and also effects adhesion. The influence of current surges on the structure and properties has not been studied.

6.7 Influence of impurities in the anodizing electrolyte. (Dissolution studies.) The impurities present will depend on the alloys processed and the age of the bath and the process being used. Examples of impurities present in the electrolyte being, Al, Cu, Fe and Cl ions or salts. (The aluminium build-up occurring as a result of (i) solution of aluminium into the electrolyte and (ii) solution of alumina.) The impurities may cause difficulties if present in appreciable quantities. Chlorides for example can cause localized attack or even perforation of the coating. The use of the atomic absorption spectrophotometer analytical instrument would be envisaged, analysing for elements dissolved in the electrolyte before and after anodizing.

6.8. To substantiate the hypothesis of the "hillock" growth. More in-depth time sequences would be required, using a progressive decrease in the current density applied, and also a progressive increase in electrolyte concentration and temperature. From these sequences, changing one variable at a time, a point should be reached where the "hillock" formation is just detectable at thousands of random points on the specimen.

7. APPENDICES.

APPENDIX 1. CHEMICAL COMPOSITION OF ALUMINIUM ALLOYS USED.

TABLE 7.1. Chemical composition of alloys used.

ALLOY	Si	Fe	Cu	Mn	Mg	Cr	Zn	Ti	V
I	0.6	-	-	-	1.0	-	-	-	-
II	1.0	-	-	-	0.7	-	-	-	-
H30	0.86	0.23	-	-	0.53	0.05	-	-	-
2002	.40	.08	1.8	.02	.52	.07	.02	.03	.01
6009	.79	.25	.31	.26	.51	-	.03	.04	.01
6010	.94	.19	.33	.26	.87	-	.03	.03	.01
HS30/3	.94	.37	.04	.51	.92	.02	.03	.01	.01
SIDAL	.17	.27	.007	.23	1.95	-	.02	.009	.01
BB2	.10	.27	.002	.21	2.0	-	.01	.01	.01
BB3	.18	.40	.03	.38	3.6	.05	.02	.03	-
2117HP	.12	.06	2.0	.03	.38	.01	.02	.03	-
2117CP	.24	.42	2.2	.07	.38	.02	.03	.03	-
2117A	.12	.28	1.88	.16	.18	.01	.02	.01	-
2036	.30	.29	2.10	.28	.32	.02	.06	.03	-
5182	.20	.33	.02	.35	4.78	.01	.02	.035	-
609	1.17	.28	.07	.08	.49	.005	.02	.02	-

APPENDIX II. CALCULATION OF CURRENT DENSITY.

The following is a worked example used for calculating the (apparent) current density of the specimen.

The specimen dimensions were so chosen that, with 0.5 Amps of current flowing, the desired current density could be obtained.

(i) Measure the dimensions of the specimen and calculate the surface area. In this example, let the dimensions of the specimen be 15 mm wide by 20 mm long. Thus, surface area is $15 \times 20 \text{ mm}^2$ which gives a surface areas of 300 mm^2 to be anodized. However, by convention (See Appendix III) the surface area is given in square decimetres, and so this value must be converted from mm^2 to dm^2 .

[i.e ., $100 \text{ mm}^2 \equiv 1 \text{ cm}^2 // 100 \text{ cm}^2 \equiv 1 \text{ dm}^2 //$ Therefore,
 $300 \text{ mm}^2 \equiv 0.03 \text{ dm}^2$]

(ii) The current supplied is known and constant, i.e., 0.5A.

(iii) Current density = $\frac{\text{Current (A)}}{\text{Surface area (dm}^2\text{)}} = \text{A/dm}^2$

(iv) By substituting the values obtained into (iii) then

$$\text{Current density} = \frac{0.5}{0.03} = 16.6 \text{ A/dm}^2$$

Therefore, the (apparent) current density for this worked example is 16.6 A/dm^2 .

APPENDIX III. UNITS.

Current density in this thesis is given in A/dm^2 because of widespread industrial usage and its use in most technical publications. However, SI units are recommended and the following conversion table (See Table 7.2 below) is given to help readers used to SI units.

To convert from A/dm^2 to $A.m^{-2}$ multiply A/dm^2 by a factor of 100 and to convert $A.m^{-2}$ to A/dm^2 divide $A.m^{-2}$ by 100.

Table 7.2 Conversion examples for A/dm^2 to $A.m^{-2}$.

A/dm^2	S.I. units. $A.m^{-2}$
1.0	100
5.1	510
23.8	2380
39.7	3970
60.0	6000

APPENDIX IV. "BURNING" OF ANODIC OXIDE FILM.

A limitation associated with hard anodizing is an effect commonly described as "burning". It is observed mostly with high copper (>5% Cu) containing alloys and in articles that have thin sections and sharp edges.

Many workers in the field of hard anodizing have noted the phenomenon of "burning" of the anodic oxide film and the details from three such workers will be given below.

Basically, one of the main claims of Campbell's Hardas process⁽⁸⁶⁾ is that the highly alloyed materials, used particularly for engineering and aircraft purposes, can be adequately processed, without fear of preferential dissolution of specific parts of such components, i.e., "burning". When burning did occur, Campbell⁽⁶³⁾ observed that it starts from the outer surface and work inwards, thus indicating that adequate agitation is all that is required to stop this effect. Campbell explained the phenomenon in terms of the heat generated by the higher voltage in thick coatings. The coating acts as a thermal barrier which encourages a local build-up of hot acid, producing a soft porous coating with possible damage to the basis metal.

Scott⁽¹³⁸⁾ showed the effect to be an area of soft, powdery, whitish or roughened anodic film, often thinner than that over the remainder of the surface, and frequently observed at the corners of edges of the specimen. In severe cases, the complete dissolution of the film with the resultant electropolishing (leaving a bright smooth cusp) or dissolution of the underlying metal occurred. The defect is associated with a high local current density, with subsequent increase of temperature leading to thermal "runaway", and proceeded by localized

breakdown of the anodic film. It may be prevented by treatment at lower current densities, but little improvement is brought about by increasing the rate of stirring when this is performed by aeration, and further reduction in temperature of the electrolyte even appears to aggravate the effect. Scott anodized thin gauge circular panels (chosen to avoid any complications due to changes in current distribution at sharp corners) and the area of burning was transferred to the plane surface of the panel.

The most effective cure to remove "burning" was to raise the temperature of the electrolyte.

It was thought at first that the "burning" might have been initiated by the limited current -carrying capacity of the thin gauge metal in relation to its surface area, but no consistent differences were apparent between panels of different sizes, which suggested that gauge alone is the significant factor. While the problem seems to be associated with the balance between heat evolution during anodizing (including both the heat of reaction between aluminium and oxygen or hydroxyl ions, as well as the ohmic losses in the adjacent electrolyte, anodic film, metal and jig contacts) and the conduction of heat through the oxide film to the cooled electrolyte, its highly localized nature indicates that an important additional factor is the ability of the metal itself to conduct heat away from any hot spots at the growing points of the film immediately adjacent to the metal/oxide interface and thus maintain a uniform temperature.

Although increasing temperature to stop burning was a well established experimental fact, Scott was unable to put forward any reason why in fact burning should be overcome by increasing electrolyte temperature.

It is the author's opinion that by increasing the temperature of the electrolyte the conditions change from hard to conventional anodizing conditions. When hard anodizing, the growth of the oxide film occurs initially at a few random positions over the aluminium surface, forming hillocks. [i.e., Conformance to ohmic behaviour is presumed to be correct, with the lowest resistance points facilitating the immediate passage of current. As soon as oxide nucleation sites have been established, growth of oxide in these areas takes place. Other sites then eventually become of a lower resistance and oxide nucleation is initiated at those sites.] However, by increasing the temperature the electrolyte is able to form more random nucleation sites owing to the greater dissolution capacity of the electrolyte. Hence, more sites and consequently less current at each point to cause burning, i.e., the process now moves away from the hard anodizing conditions of a few random nucleation sites of high current density toward conventional anodizing conditions of a greater number of nucleation sites of lower current density (constant current density assumed) alleviating the problem of burning occurring.

There is therefore a minimum temperature and maximum current density for hard anodizing any thin gauge article, which is best determined by previous experiment for any given alloy.

Thompson⁽⁹⁴⁾ stated that the processing conditions in hard anodizing were suited to high current densities. (i.e., Normally 3.25 to 16.4 A/dm², though occasionally 31.2 A/dm².) At these high current densities any point weakness, in the form of low electrical resistance, may give passage to a high proportion of the available current and within seconds this point of low resistance will be subject to enormous current densities and the resultant high temperature

will encourage the dissolution of the parent aluminium. Indications of "burning" includes a rise in current and fall in voltage or in a large bath load, oscillating current without the significant falling off which is normal as bath resistance increases.

Parts prone to "burning" were defined as follows:

1. Cases where alloys are mixed or wrongly identified.
2. Components in wrought alloys high in copper usually of thin section.
3. Free machining alloy, particularly where segregation is pronounced, or where thin sections are involved.
4. Wrought alloys high in copper on reprocessing by ac/dc process after chemical stripping.
5. Wrought alloys high in copper when electrolyte strength is below 20 per cent volume in dc process.
6. Aluminium alloys adjacent to foreign metals that have eluded detection.
7. Formation of hot spot where component is inadequately cooled.
8. Where masking medium "lifts" in the later stages of the process.
9. Where a component has been jiggged in such a manner that in the early stages of processing electrical continuity is absent but as power is increased the resistances of the balance of the load exceeds that resistance of the faulty contact; hence current passes, and with the onset of "burning", usually confined to ac/dc process with dynamic processing.

Therefore, the effect of "burning" can be avoided by use of the correct current density/electrolyte composition and temperature relationship, combined with a sound jiggging practice and good movement of the electrolyte across the work load.

8. BIBLIOGRAPHY.

The Surface Treatment and Finishing of Aluminium and its Alloys by
S. Wernick and R. Pinner.

[Hard Anodizing. Chapter 9, pp 563 - 620.]

4th Edition, 1972, Robert Draper Ltd., Teddington. Vol. I and II.

British Standard Specification for Hard anodic oxide coatings on
aluminium for engineering purposes. B.S. 5599: 1978.

Anodizing of aluminium and aluminium alloys.

Defence Specification DEF - 151. March, 1965. Reprinted
December 1977, incorporating amendment No.1.

Metallurgy of Aluminium Alloys by M. Van Lancker.

Chapman and Hall Ltd., 1967.

Anodic Oxide Films by L. Young. Academic Press Inc., London, 1961.

A Guide to Architectural and Industrial Anodizing.

British Anodizing Association.

The Technology of Anodizing by A.W. Brace and P.G. Sheasby,
Techicopy Ltd., 2nd Ed., 1979.

A Guide to Hard Anodizing. Acorn Hardas Technical Brochure.

8.1 EXTENDED BIBLIOGRAPHY.

The vast majority of information given on the hard anodizing process is published by the commercial organizations who develop their particular conditions for their particular processes. As a consequence very little experimental research on the mechanism of hard anodizing or the structure of the hard anodized coating is given in these publications. It was difficult to produce an extensive literature survey without a large amount of duplication concerning the commercial processes. It was therefore decided to produce an extended bibliography, which in no way claims to be an exhaustive collection of publications that could be consulted in the study of hard anodizing. However, it is hoped that it will be of use to any investigator who intends to use the hard anodizing process who requires a quick reference to discover the work that has been carried out on the hard anodizing processes throughout the world from the Martin Hard Coat process through to present day procedures.

J. AIGNER.

On the Problem of Growth Processes of Oxide Coatings on Aluminium Formed in Cold Sulphuric Acid Electrolytes.

Interfinish 8, Basel, Switzerland, 1972, Paper B29. [in FRENCH].

Anodic coatings on aluminium were separated from substrate in the boundary phase and barrier layers was uncovered. Optical microscopy showed well known columnar structure and a laminar structure, the latter being especially prominent in coatings produced at high c.d. and low temp. (Hard anodizing.)

L.I. ASHLEY.

Hardcoat Makes Aluminium Hard as Glass.

Precision Metal Moulding, 1961, 19, (12), 47-48.

Description of the Martin Hard Coat process.

N. BABA, T. MOMOSE and S. TAJIMA.

Anodic Deposition of Sulphur in Oxide Coatings on Aluminium at Low Temperatures.

Metalloberfläche (Munche), 1974, 28, No.2, 44-8.

Anomalous deposition of S during anodizing in H_2SO_4 - ethylene-glycol-water solutions at $-30^\circ C$ is due to reducing action of monovalent Al^+ ions at anode. S is volatilised by heating at $440^\circ C$. S deposited is crystalline orthorhombic and partly S^{2-} . S content of coating depends on bath temp, c.d., water content of electrolyte and H_2SO_4 concn. and is max at 1.5%. Existence of Al^+ ions is demonstrated by rotating disc electrode experiments. S inclusions in anodic coatings are potentially useful in fuel cells or as effluent control electrodes.

D.J. BAK.

Low-Voltage, Hard-Anodizing Process Saves Energy, Cuts Costs.

Des. News, 21 Apr. 1980, 36, (8), 60-61.

By using a max. 20 V d.c. with superimposed a.c., a uniform aluminium oxide coating is formed up to 7 mil thick, having high abrasion resistance on alloy 2024 and 7075. The superimposed a.c. voltage prevents bubble formation and permits the lower d.c. voltage levels, thus giving savings in power and in solution cooling requirements.

J.C BAKALJUK.

Hard Anodizing of Aluminium Alloys.

ATO Archiv f. Technische Ostiliteratur, 1962, Galvanotechnik, 1963, 54, No.7, 371-3.

Hard anodizing in a Russian factory is described. Coatings of 30 μm (1.2 mil) and more are obtained in a bath containing H_2SO_4 (free from HNO_3) 170-200, $\text{Al}_2(\text{SO}_4)_3$ 10-20 g/l at -5 to 0°C, 15-30V initial to 40-120V final voltage, (depends on alloy) at 1.3-2.5 A/dm². Testing is described.

K.H. BAUMANN.

Hard Anodizing of Aluminium Alloys.

Galvano, Ber., 1966, 3, No.2, 83-6.

A Brief review of hard anodizing processes, giving details of solutions and operating conditions with coating properties.

S. BOCACHARD and G. BARNAULT.

Hard Anodizing of Aluminium Alloy Parts.

Rev. Aluminium, June 1970, (386), 631-637. [in FRENCH].

The physical and mechanical properties of anodic films on Al-alloys produced by low-temp. treatment in H_2SO_4 are indicated. These include appearance, density, porosity, roughness, hardness and thermal and electrical properties. Relative merits of 22 cast and wrought alloys of well known types as regards hardness, thermal and electrical insulation and wear resistance of the anodic films are shown. Dimensional aspects of machined pieces, machining of the hard films, dimensional control and partial treatment are discussed.

P.W. BOLMER.

Polarization of Aluminium During Clear-and Hard-Coat Anodizing.

Plat. Surf. Finish., June 1977, 64, (6), 63-68.

Steady state polarization data are reported for the anodic oxidation of aluminium in a variety of electrolytes containing sulphate. Each current-voltage curve has three comparable voltage ranges. The properties of anodic oxides (colour and hardness) correlate with the voltage range in which they are formed. Integrally coloured hardcoats form only in the highest voltage region, above a critical voltage. Clear coatings form at low voltages. In a middle or transition voltage range, coatings take on light colours which are alloy dependent. The current is a maximum at the critical voltage. At higher voltages current decreases with time, and the existence of a steady state is doubtful. The magnitude of the current at the critical voltage and the uniformity of current distribution at higher voltage are affected by sulphuric acid concentration, added anion and its concentration, alloy and temperature. The effects of these anodizing parameters on the colour developed in sulphuric - sulfosalicylic acid electrolytes correlate with their effects on the current voltage curves.

8 references.

C.J.L. BOOKER, J.L. WOOD and A. WALSH.

Thick Oxide Layers on Aluminium

Brit. J. App. Phys., 8, 347, 1957.

Electron micrographs have been obtained of the pore structure in the thick oxide layer formed by anodizing aluminium in sulphuric acid. The pores are shown to be minute tubes of approx' 200 Å dia., running perpendicularly through the oxide and ending almost in contact with the underlying metal. The pore base thickness has been estimated, and the effect of a change in anodizing conditions on the pore base pattern is shown.

L. BOSDORF.

The Hard Anodizing of Aluminium and its Practical Applications.

Alluminio, Oct. 1977, 46, (10), 390-394. [in ITALIAN].

Hard anodizing produces on light alloys extremely hard and thick films, which enable the alloys to withstand wear conditions that in the past required the use of heavy metals. Vickers hardness of 350-570 have been produced on a range of Al alloys by hard anodizing. Hard anodizing also provides high electrical insulation (up to 10,000 V), heat resistance and corrosion resistance much higher than normal anodic films. Several examples of typical applications are given.

L. BOSDORF.

Anodizing Aluminium.

Jahrbuch Oberflächentechnik, 1969, (25), 185-201. [in GERMAN].

Methods for hard anodizing are described and the various Al-Mn, Al-Mg, Al-Mn-Mg, Al-Cu-Mg, Al-Cu-Si-Mn, Al-Zn-Mg, Al-Zn-Mg-Cu, Al-Si and Al-Cu-Ti alloys are listed.

33 references.

A.W. BRACE.

Hard Anodizing of Aluminium and its Alloys.

Electroplating, 1954, 7, (9), 329-334, 376-379.

W.J. CAMPBELL.

Anodic Finishes for Wear Resistance.

J. Metal Finishing, Jan. 1964. v.10, No. 109, 5-15.

Conversion of the surface of Al alloys into Al_2O_3 by various hard anodizing processes. Influence of process parameters on the properties of coating. Limitations of the process and finishing treatment are considered. A wide range of applications for Al alloys result from the resistance to wear and abrasion and other properties of the thick and hard coatings. 8 references.

W.J. CAMPBELL.

How De Havelland Hard Anodize Missile Parts.

Metalworking Prodn., 1961, 105, (5), 59-62.

Al alloy-missile forgings are hard anodized by the Hardas technique at 10-30°C using 30-300 Amp/ft². The Hardas process prescribes rates of flow of electrolyte in relation to the size of the anode and specifies blends of d.c. and a.c. currents which permit the production of hard coatings on alloys containing Si and Cu.

T. CARDIANI.

The Effect of Coating Thickness and Alloy Type and Hard Anodizing.

Aluminio, 1977, 46, No. 10. [in ITALIAN]

Four different alloys were hard anodized by 'S Klerexal' process to 4 thicknesses with 1 series of specimens polished before anodizing. Surface roughness after anodizing was found to be effected only by the nature of the basis metal.

S. CHIN'MIN' F.P. ZALIVALOV and N.D. TOMASHOV.

Influence of Solution Temperature on Properties and Microstructure of Thick Anodic Films.

Zhur. Priklad. Khim., 1963, 36, No.7, 1503-1506.

Examination of films produced at -6,0, +5 and +10°C in 4N H₂SO₄ showed that rise in temp. reduced the wt, thickness and hardness of the films and increased their porosity. Operating conditions other than temp, e.g., method of heat removal (preferably by circulation of the cooled solution) also affect properties of films.

F.L CHURCH.

Mounting Demand for Hard Anodized Aluminium Spurs 40% Expansion.

Modern Metals, 1967, 23, No. 5, 87-8, 90.

Hard anodizing at Universal Metal Finishing, Chicargo Ill., U.S.A. is described.

W.C COCHRAN.

Integral Colour and Hardcoat Anodizing.

Aluminium Finishing Seminar, Paper A7, Aluminium Assoc., 750, Third Ave., New York, N.Y 10017, 1973. pp.16

Four commercial d.c. processes are listed.
17 references.

J. COLLINS.

Design Characteristics of Hard Anodize on Aluminium.

Electrical Manufacturing, Apr. 1959, v.63, 161-163.

Characteristics of the process, electrical and corrosion properties of the film.

D. COSTAIN and E. ELIESCU.

The Hard Anodic Oxidation of the Al Alloy RR. 59.

Cret. Metal. semin., 1961, 3, 534-46.

Also Light Metals Bull., 1962, 24, No. 24, 1127.

Hard anodizing was carried out in oxalic acid, H_2SO_4 and mixed acids of various concentrations and at different temperatures by the constant c.d. and constant wattage methods. The film was studied by microscope and micro-hardness measurement.

W.L. COTTON and R.P. THIERRY

Pitting - A Problem with Hard Anodizing.

14th, Annual Airlines Plating Forum, 1978.

Process developed for producing essentially pit free hard anodized coatings on 7XXX - series Al hydraulic actuators. The process uses a dilute sulphuric oxalic acid solution with a slow current build-up, reduce current density and voltage, and forced solution circulation to minimize localised overheating and void formation in the coating.

18 references.

J. L. COZART.

Hard Anodic Coatings on Aluminium - Physical and Chemical Properties - Evaluation of.

General Dynamics/Fort Worth, Tex. 1 Apr. 59, 21p incl. illus. tables (Rept. No FGT - 2163). (Contracts AF 33 (600) 36200 and AF 33 (657) 7248). Unclassified report. AD-284 360. Div 17 (TISTM/MS) OTS \$2.60.

Hard anodic coatings of approx' 2 mil thickness were applied to bar 7075-T6 and 2024 - T3 Al alloys by the Hardas, Sanford and Alcoa 226 processes. The Alcoa 226 coating was not successfully applied to 2024 - T3 Al due to excessive 'burning' of the material during processing. The hard anodic coating were evaluated by tests to determine their porosity, abrasion resistance, hardness, adhesion and dielectric strength. Tests were also conducted to determine the effect of the coatings on the tensile and fatigue properties of the two Al alloys.

P. CSOKAN.

Hard Aluminium Oxide Coatings by Anodic Oxidation.

Corrosion et Anticorrosion, 1960, 8, No.4, 158-65.

A Hungarian hard anodizing process and plant is described for producing 150-250 μm thick coatings in 1 hour of 450-520 Kg/mm^2 hardness. Parts are degreased in 10% NaOH, (30-90 secs), rinsed, neutralized in 1:1 HNO_3 (30-90 secs), rinsed and H_2SO_4 anodized at low temp. at 40-55V, rinsed in cold and hot water and dried. Photomicrographs of the coating are shown.

P. CSOKAN and G. SINAI.

The Mechanical Properties of Hard Anodized Aluminium Sheet.

Werkstoffe u. Korrosion. 1960, No.4, 224-7.

P. CSOKAN and GY EMOD.

Practical Utilization of Permanent Moulds Made of Aluminium and Coated with Hard Oxide.

Gepesz, 1960, 12, No.12, 489-92; Light Metals Bull. 1962,
24, No.5, 268.

Application of a hard oxide coating 150-300 μm thick on an Al mould instead of a protective coating is described. It cannot be coloured because of its low porosity but does not require sealing. Breakdown voltage, corrosion resistance and thermal behaviour were satisfactory.

P. CSOKAN.

Effect of Surface Structure of Aluminium on Hard Anodic Coatings.

Scheif u. Poliertechnik, 1961, 1, No.1, 26-32.

The effect of surface texture inclusions, contamination and discontinuities of the Al surface in hard anodic coatings is discussed.

P. CSOKAN.

Contribution to Knowledge of the Anodic Oxidation of Aluminium
in Dilute Cold Sulphuric Acid.

Metalloberflache, 1961, 15, No.4, 113-7.

Experiments on anodizing Al in dilute cold H₂SO₄ showed that a different process is involved compared to normal anodizing. 50-250 μm coatings have 450-520 Kg/mm² microhardness, low porosity and good wear resistance and polishability.

P. CSOKAN and G. SINAY.

The Application of Hard Anodized Aluminium Parts in Mechanical
Engineering.

Dechema Monographien, 1962, 45, No. 734-360, 319-28.

Also Rev. Met. Lit., 1964, 21, No. 3, 32.

Hard anodizing of 99.5% pure Al and Al-Mg-Si alloy sheets and investigation of the mechanical properties of the oxide film formed and of its effect on the mechanical properties of the base metal. The following tests were employed: hardness measurements, tensile tests, bending tests and fatigue tests.

P. CSOKAN.

Contribution to the Problem of Chemical and Corrosion Resistance
of Hard Anodizing Aluminium.

Werkst u. Korr., 1963, 14, No.8, 271-7.

Atmospheric exposure - , oxygen chamber -, humidity chamber-, salt spray - and Mylius HCl test on hard anodized coatings produced in the 1% H₂SO₄ bath are reported. The results indicate that the resistance to the atmosphere in urban/industrial, or tropical climates is satisfactory even without after treatment. High humidity and temp. seem to improve corrosion resistance under these conditions. Acid and alkali resistance is more or less unsatisfactory and is the poorer the more heterogeneous the film structure.

K.H. DALE.

Multipurpose Anodizing Electrolyte: A Process for Room Temperature
Hardcoating and Decorative Anodizing.

Plating, Sept. 1972, 59, (9), 843-844.

A multipurpose anodizing electrolyte (for Al alloys) based on additions of 1-2% each of polyhydric alcohol and an α -reactive carboxylic acid in a standard sulphuric bath is discussed. Finishes ranging from thin bright decorative films of $2.5\ \mu\text{m}$ (0.001 in) thickness applied at $1.3\ \text{Amp}/\text{dm}^2$, to a heavy wear resistant engineering films of $125\ \mu\text{m}$ thickness at $3.9\ \text{Amp}/\text{dm}^2$ are possible by only varying c.d. and time. Operating conditions of 21°C and 40 V max. require less refrigeration than other hard coats.

G. ELSSNER.

The Hard Anodizing of Aluminium.

Metall, 1961, 15, (12), 1194-1198.

Details of various processes are given, and applications reviewed.

15 references.

R. FERRI.

The Application of Hard Anodizing to Al-Si Alloy Castings.

Allumino, Jan. 1976, 45, (1), 35-40. [in ITALIAN].

The use of Al -5% Si -0.6% Mg -0.7% Mn alloy castings in place of alloy cast iron for components of flowmeters is described. Good wear, erosion and corrosion resistance were achieved by hard anodizing to produce $40\ \mu\text{m}$ thick oxide film by means of the low temperature H_2SO_4 process. Details are given of the structure and microhardness of the film and its effects on surface finish, micro-geometry, and dimensional variations.

Y. FUKUDA.

High Temperature Hard Anodizing of Aluminium.

J. Metal Finishing Soc., Japan. 1976, 27, No.8, 399-402.

Anodizing characteristics of Al in high temp. solns of tartaric, malic and malonic acids were investigated. Aluminium sheets of 99.99% were anodized in 1 and 3 mol/l soln. of these acids at 40 to 80°C and at 4.67 to 18.7 A/dm². Uniform and integral-coloured films without cracks were formed on Al at relatively high temp. and low c.d. Bath voltage during anodizing in malonic acid bath was 100 V, whereas in tartaric or malic acid bath it was 150V. In malonic acid bath, hard film of Hv 450 to approx' 500Hv were obtained only 60°C, whereas tartaric and malic acid baths hard films of 550Hv to approx' 700Hv were produced even at 60-80°C. Hardness values increased with increasing temp, lower concn and increasing c.d., viz. with increasing bath voltage. Coating ratio increase as temp. was lower and c.d. higher. In tartaric acid bath, recovery of current was observed after sudden drop of anodizing voltage. During recovery, size of cell grew smaller and number of cells increased. Therefore, anodic oxidation in these baths was essentially the same as in H₂SO₄ or oxalic acid anodizing.

J. GLAYMAN.

Hard Anodic Coatings on Aluminium.

Galvano, Mar. 1970, 39, (398), 207-209. [in FRENCH].

The hard anodizing of aluminium in France is briefly reviewed and baths used for process are described.

8 references.

R. R. GREINER.

How to Hardcoat Aluminium.

American Machinist, 1964, 108, No.20, 76-8.

A review dealing with the surface finish, abrasion - resistance, and thickness of hard anodic coating on Aluminium effect of alloy composition on properties and colour, design for hard anodizing and after treatment.

M. HATCH.

Applications of Hard Anodizing at Cessna.
SAE. Paper No. 72 0341, Society of Automotive Engineers, Inc.,
Two Pennsylvania Plaza, New York, N.Y. 10001. 1972, Pp 4.

E. HERRMANN.

Hard Anodizing.

Galvanotechnik, 1960, 51, No.8, 387-92.

Commerical processes are reviewed, including the Finsterwalder
Isolations - M.H.C. -, Hardas - and Sanford processes.

H.E. HORN.

Some Notes on Hard - Coated Aluminium.

Metal Finishing, 1952, 50, (6), 110-112.

Brief general information is given on a new method for
producing a hard surface on Al and some of its alloys. No details
of the process are included. It is suggested that aluminium treated
this way can replace machined steel parts in many cases.

R. IKUTA, S. UEDA and S KOIZUMI.

Effect of Electrical Wave Form on Hard Anodizing of Aluminium.

J. Metal Finishing Soc., Japan, Sept. 1974, 25, (9), 499-504.

[in JAPANESE].

Specimens were anodized at 0°C in 100g/l of H₂SO₄ containing
15g/l C₂H₂O₄, at constant electric quantity of 160 A/min/dm²
changing c.d. and time of pulse current. D.c. (single phase,
fullwave, 3-phase half-wave, and 6-phase half-wave), interrupted
current and superimposed (d.c. and a.c.) currents were compared
with pulse current. Thicker coating is obtained when d.c. wave
form containing high ripple % was applied. When pulsating current
(high output 4 A/dm² 30s. low output 2 A/dm² 7.5 s.) was applied,
hardness of coating was higher than hard anodic oxidation coatings
using d.c. Hardness became higher when ratio of time between
high output and low output was 4:1. Cell size of cross-section
of coatings was independent of current wave forms used. There
was no obvious relation between cell size and hardness.

7 references.

S. ILANGORAN and K.I. VASU.

Hard Anodizing: A Brief Outline.

J. Electrochem. Soc., India, Apr. 1976, 25, (2), 91-95.

The hard anodizing of Al and alloys covering principles of oxide layer growth, alloy selection, preconditioning, formation of the oxide, sealing, and design considerations are reviewed. Some properties of hard anodic coatings and applications are listed.

24 references

G. ITO and S. TSUDA.

Hard Anodizing of Aluminium in Electrolytes of Sulphuric acid - dicarboxylic acids. Studies on Chemical Conversion Treatment of Aluminium and its Alloys.

J. Metal Finishing Soc., Japan, 1966, 17, No.2, 41-5.

In conventional anodizing an abrasion resistance oxide layer is produced only by anodizing at low temps of -10 to 0°C , and require expensive refrigeration plant. By hard anodizing of Al in sulphuric acid - dicarboxylic acids, the efficiency of the formation of oxide film, and hardness and abrasion resistance of the film are improved. Optimum results were obtained with an electrolyte containing 15% (wt) H_2SO_4 with 1 to 5% malonic acid. The film produced at 20°C had almost as high an impact abrasion resistance as that produced with a 15% H_2SO_4 soln at 5°C . The mixed electrolyte could be operated at about 10°C higher than H_2SO_4 alone, without reduction in abrasion resistance being observed.

A. JOGARAO and B. SAMBAMURTHY.

Studies on Hard Anodizing of Aluminium.

Symposium on Electrodeposition and Metal Finishing, Kavaikudi, 1957, 1960, 147-155.

H.A. JOHNSON.

Machanical Properties of Aluminium Hard Anodic Coatings.

Prod. Eng., 1954, 25, (9), 136-141.

H.R. JOHNSON.

Applying Hard Anodic Aluminium Coatings to Various Substrates.

Plating, Aug, 1969, 56, (8), 931.

Novel method of combining hard anodic coating formed from Aluminium with other metal substrate e.g. S/S or Ti. Al substrate is then machined and dissolved away leaving anodic coating bonded to base metal. Provides a surface which has electrical and thermal insulation properties plus good corrosion and wear resistance.

H. KANEMATSU and J. TOGASHI.

Study on the Hard Anodizing for Aluminium and its Alloys.

J. Metal Finishing Soc., Japan, 1961, 12, No.8, 308-13.

Voltage - current curves for anodizing pure Al, 17 S, 52 S and 61 S in H_2SO_4 with d.c. at constant c.d. are divided into three types. When the initial voltage is high but final voltage and the rate of film growth are both low, the voltage vs time curves is parallel to a horizontal axis (time). When both initial and final voltage are high and the forming voltage increases very fast and the rate of film growth is high, the voltage vs time curve is parallel to the vertical line (voltage).

J.M. KAPE.

Architectural and Hard Anodizing.

Metal Finishing J., 1966, 12, (143), 424-428, 436.

Forms of hard anodizing and a number of patented processes are indicated.

15 references.

N.L. KAYE.

Hard Anodizing.

Redondo Beach, C.A. U.S. Pat. 4 152221 (12.9.77).

Continuous spray process for hard anodizing outer peripheral surface of anodisable part by soln. containing surfactant, part of which is transferred at controlled rate through selected spray pattern to form unbroken envelope of electrolyte around periphery, surfactant forming O_2 - containing foam over outer surface, and using anodizing current of short pulses with predetermined RMS value to produce hard, thick, uniform anodic oxide coating.

I. KAZUO, F. AKIO and T. KAZUHIKO.

Hard Anodic Oxide Coating on Al and its alloys and the Effects of Interrupted Current during Anodic Oxidation.

Inst. Phys Chem. Res., 1962, 38, No.6, 635-44.

Also Rev. Mat. Lit., 1964, 21, No.2, 31.

Power requirement for anodizing is reduced by use of Al and alloys are electrolysed in an sulphate soln using interrupted current ratio of 1:1 with a pulse time of $\frac{1}{2}$ - 1 min. Graphs show coating ratio, coating thickness, voltage and time at different pulse rates for the various alloys.

W. KERLE.

Hard Anodizing of Aluminium and its Alloys by the Original Alcoa Process.

Galvanotechnik u. Oberflächenschutz, 1961, 2, No.2, 47-9.

Use of Alcoa hard anodizing process in Switzerland is described. Coating properties are discussed.

C.R. KLEIMANN.

Natural Aluminium Phenomena and Data for Hard Anodizing.

Engineering Bull., 14/62 464, Michigan Dynamics, Inc., Detroit, Mich., U.S.A.; Finish, 1965, 12, No.5, 171.

Design and process details of hard anodizing are presented using various established methods. Coating properties are reviewed.

T. v. d. KLIS.

Hard Anodizing.

Galvanotechniek, 1961, 4, No.11, 238-45.

A literature review of hard anodizing dealing mainly with the M.H.C. and Hardas process.

S. KOIZUMI and S. UEDA.

Characteristics and Structure of Double Anodic Oxidation Coating on Aluminium.

J. Met. Finish. Soc., Japan, July, 1975, 26, (7), 314-319. [In JAPANESE].

Normal anodizing followed by hard anodizing. 10 References.

S. KOIZUMI and S. UEDA.

Effect of the Constituents of Aluminium Alloys on the Formation of Abnormal Layer in Anodic Oxidation Coatings.

J. Metal Finishing Soc., Japan, 1975, 26. No.1, 38-42.

Describes relation between constituents of Al alloys, JIS 1080 -H18, 1100-H24, 5052-H34, 2017-F and 2017-T3 and formation of abnormal layers in anodic oxidation coatings which are obtained by electrolyzing at -5°C for prolonged period in bath of H_2SO_4 containing $\text{H}_2\text{C}_2\text{O}_4$. Concerning high purity Al (1080) abnormal phenomena was noticed neither in V-T curves nor in coating structure observed by optical microscope. However, abnormal layers of 40 and 10-20 μm were found with 1100 and 5052 alloys respectively. Layer is likely to be observed more often with high strength alloy (2017 - F, etc) containing more ppt. of CuAl than 2017 - T3 alloy. 'Island' structure were found by S.E.M. on surface of anodic oxidation coatings of 1100, 2017 - F and 2017 - T3 alloys having abnormal layers. Excess O_2 in anodizing reaction during prolonged electrolysis where current is locally concentrated makes coatings thick but partially leaves surface growths. Cell size of anodic oxidation coating of pure Al and Al alloys is linearly proportional to bath voltage regardless of thickness of coatings. Thickness of barrier layer was also proportional to anodizing time, if electrolysis was conducted at constant c.d. and insulation of barrier layers is high enough. As to 1100, 2017 - F and 2017 - T3 having abnormal layers rise of leakage current was recognised at low voltage after break down of insulation of barrier layer.

S. KOIZUMI and S. UEDA.

Effect of Initial Current Density and Specimen Shape on the Abnormal Layer Growth in Hard Anodizing of Aluminium.

J. Metal Finishing Soc., Japan, 1974, 25, No.8, 453-7.

Describes effect of control of initial c.d., and thickness and area of specimens, on formation of abnormal layers. Al specimens (JIS 1100 - H24) were anodized for prolonged periods in H_2SO_4 containing $H_2C_2O_4$ at $-5^\circ C$. S.E.M. shows that normal layer consists of regular cell structure, while abnormal layer consists of crooked and uneven cell structures. Cause of formation of abnormal layer is supposed to be process of breakdown of coatings. Wear test shows that thicker abnormal layers gives inferior effect on wear resistance. Suitable control of initial c.d. is effective precaution for abnormal layer at thin specimens of 1.0 mm than thick ones of 2.0 mm and more. Rate of coating growth is greater at specimens of small area (100 mm x 25 mm) than ones of large area (100 mm x 100 mm), therefore abnormal layer is easily formed on specimens of small area for prolonged electrolysis.

S. KOIZUMI, R. IKUTA and S. UEDA.

Effect of Electrical Wave Form on Hard Anodized Coatings on Aluminium.

J. Metal Finishing Soc., Japan, Jan. 1972, 24, (1), 26-34. [in JAPANESE].

Studies of effects of application of 3 kinds of d.c. (single phase full wave, 3 phase half wave and 6 phase half-wave) and 5 other kinds of currents (interrupted, pulse, PR, periodic alternate (d.c or a.c) and superimposed d.c. on a.c. current on hard anodic oxidation coatings on Al. Specimens were anodized at $0^\circ C$ for 45 mins., in 100g/l of H_2SO_4 containing 15g/l of $C_2H_2O_4$. Colour of coating anodized by d.c. was dark, but became light when a negative current was applied. Adhesion of coating was extremely poor when PR current or periodic alternate d.c. or a.c. current was applied. Bath voltage was high than using other currents when single phase full-wave or 3 phase half-wave direct current was applied, and cell size of coatings was larger. Except for superimposed (d.c. or a.c) current, it was observed by S.E.M. that cell size became larger when a current including a.c. was applied. Thickness of coating was larger and hardness higher when using d.c. than other currents. Coating ratio was high with d.c., but lower when negative current was applied. Coating ratio was higher when density was higher, i.e., density of each coating indicated almost same tendency as coating ratio. Results of measurements of S intensity of coating by x-ray microanalyser revealed that quantity of S in coating was less than that using d.c. when superimposed (d.c. and a.c) current was applied, although more H_2S gas was evolved near specimens.

16 references.

A.V. KRUSENSTJERN.

Hard Oxide Coating and Their Technical Application.

Mitt. Forschungsgesell, Blechverarb., 1966, 17, NO.6/7, 103-7.

The formation, composition and properties of hard anodized coatings on Aluminium are discussed. Types of hard anodizing processes, self - coloured coatings and applications are dealt with.

V. LAKSHMINARASIMHAN, K.R. NARASIMHAN and B.A. SHENOI.

Hard Anodizing Aluminium and its Alloys.

Metal Finishing, 1967, 65, No.3, 60-2, 66.

The use of mixtures of malonic and oxalic acid was investigated for hard anodizing of aluminium and the influence of addition agents was determined on hardness and abrasion resistance as well as on the bath life using four different alloys. 7 references.

Z. LASZELUSKA.

Parameters in Hard Anodizing.

Metal Finishing, Oct. 1969, 67, (10), 48-54.

Al alloys 2024, 5052, 6061 and 7075 anodized in well agitated 20 wt% H_2SO_4 at $-8^\circ C$ to $-4^\circ C$. c.d's were 2.5 and $5.0 A/dm^2$ processing times 30-120 mins. Results show that temp. has little effect on film thickness and breakdown voltage, provided agitation gives effective heat dissipation. Film hardness and abrasion resistance are temp. independent. However, while thickness and breakdown voltage generally increase with process time, its effect on hardness and abrasion resistance is generally smaller and more variable.

7 references.

P. LELONG, R. SEGOND and J. HERENGUEL.

Hard Anodizing.

Pinturas y Acabados Ind., 1961, 3 No.15, 19-27.

A review of factors influencing hard anodizing. Film formation is illustrated and operating conditions discussed.

Also Anodic Oxidation Process Providing Very Thick Films of Alumina.

Revue de Aluminium. Jan. 1960, v. 37, 67-65.

A process which uses ambient or higher temperatures for electrolysis, and electrolytes weaker than sulphuric acid, consisting of mixtures of organic acids and acid salts, produces hard, uniform films up to 300 microns thick on Al alloys. 18 references.

R. LeMASTER.

Hard Coating of Aluminium.

Modern Castings, 1963, 44, (5), 613-614.

Also Trans. Amer. Found. Soc., 1963, 71, 613-614.

A new anodizing process gives an oxide coating 10 times thickness than obtained previously on aluminium. The coating is stated to be extremely hard and to be suitable for use in aluminium pattern equipment.

M. LERNER.

On Seasonal Fluctuations of Abrasion - Resistance Results for Hard Anodized Aluminium.

Plat. Surf. Finish., Dec. 1979, 66, (12), 40-43.

Seasonal fluctuations occur if abrasion-resistance testing (using Taber Abraser Test) of hard anodized aluminium is performed without humidity control. Although results of abrasion tests normally do not exceed limits specified by present standards, such fluctuations are undesirable and should be eliminated if abrasion becomes a discriminative feature when samples anodized in a different manner are compared.

E. LICHTENBERGER - BAJZA.

Some Recent Observations Concerning Certain Properties of Hard Anodic Oxide Layers.

A Fémipari Kutató In tezet Kozlemenyei, 1960, 4, 297-305. [in HUNGARIAN].

It was shown that oxidation starts at crystal boundaries and that the number and distribution of initial oxide nuclei depends on micro-structure and composition of the metal.

E. LICHTENBERGER - BAJZA, A. DORMONY and P. CSOKAN.

Investigations of the Structure and Other Properties of Hard Aluminium Oxide Coatings Produced on Aluminium by Anodic Oxidation.

Werkstoffe u. Korrosion, 1960, 11, No.11, 701-7.

The onset of hard anodizing in H_2SO_4 solution was investigated and barrier film, porous coating thicknesses and structure reported.

S. LONGO.

The Rapid 'Thermat' Process for Anodizing Aluminium.

Trattamenti e Finitura, 1964, 4, No.6, 223-4.

A review of anodizing solutions used for obtaining thick coatings which require refrigeration is followed by a classification of anodizing electrolytes which make it possible to form thick coatings at ambient temperatures. There are (a) benzene mono- and di- sulphonic acid, (b) 1-p-sulphophenyl - 5 - pyrazolone carboxylic acid, and phenyl hydrazine - p - sulphonic acid, (c) naphthalene di- and tri-sulphonic acid, (d) a reaction product of nonyl phenyl alcohol with an ethylene oxide derivative of propylene in the presence of carboxylic acids, (e) condensation products of phenolformaldehyde with formic, acetic, citric, tartaric or boric acid. The solns. are used at 5-25% conc. pH 2-4 and with a dissociation constant 1.8×10^{-5} to 6.5×10^{-2} at 12-20v, 1.5 - 15 A/dm², 20 - 80°C. One electrolyte referred to in detail is prepared from 150-231 g/l H₂SO₄ with the additive 'Thermath-R' of groups (d) and (e) (above). No details are given of nature or supply of this compound.

I. MACHLIN and N.J. WHITNEY.

Anodizing Aluminium Alloys: Evaluation of Thick (Hard) Coatings.

Metal Finishing, 1961, 59, No.2, 55-7.

Abrasion resistance, breakdown voltage, indentation resistance and salt spray tests are reported on hard anodic coating on a number of alloys. Corrosion resistance depended on continuity rather than thickness of the coating.

N.A. MARCHENKO, A.N. MUTROKHOVA and V.D DOROSHEV.

Rapid Process for Hard Anodizing Aluminium.

Zhur. Priklad. Khim., 1966, 39, No.7, 1471-5.

A solution containing 170-180 g/l H₂SO₄ is used at 15-20°C with vigorous stirring and cooling and is characterized by the use of a high initial c.d. of 15-18 A/dm² at a potential ensuring spontaneous falling off of the power consumption as anodizing proceeds. Oxide films obtained are equal to those obtained by known methods and have been successfully used on pistons of i.c. engines.

N.A. MARCHENKO, S.Kh. LIPKO and L.D. LEVCHENKO.

Solving the Problem of Optimizing the Anodizing Process by the Design of Experiments Technique.

R. Zh. Korr. i Zashch. ot Korr., 1974, 5K 327. [in RUSSIAN].

Effect of combination of factors in accelerated anodizing on rate of formation of anodic film and its compn., i.e., microhardness, surface finish, wear investigated. Independent variables were: initial anodic c.d., A/dm²; anodizing time, min.; concn. of sulphate electrolyte, g/l; electrolyte temp., °C. Effect of those factors on coating thickness in μm and microhardness in Kg/mm² was studied. Mathematical treatment of results aimed at obtaining coatings of thickness 120-130 μm on D16 alloy of hardness 230-270 Kg/mm² led to following recommended conditions, initial c.d. 12 A/dm²; anodizing time 80 min, H₂SO₄ concn. 230g/l; and electrolyte temp. 6°C.

N.A. MARCHENKO, L.D. LEVCHENKO, S.Kh. LIPKO, YU. C. MARCHENKO and A.I. GLADKII.

Selection of Conditions for Deep Anodizing of Aluminium Alloys.

Zashchita Metallov, 1975, 11, No.4, 509-11. [in RUSSIAN].

Work published since 1969 involving design of experiments technique using anodic c.d. time of anodic treatment, concn of soln., and soln. temp. as variables is discussed briefly, and plot is reproduced showing coating thickness as function of hardness. It is shown that previously accepted max. thickness of anodic oxide having satisfactory micro-hardness (280 Kg/mm²) i.e., 50-60 μm, could be at least doubled.

N. MARINKOV.

Hard Anodizing of the Aluminium Alloy Type Al-Cu-Si-Mn.

Galvanotechnik, 15 Feb. 1973, 64, (2), 95-98. [in GERMAN].

The Al-Cu-Si-Mn alloy (containing Cu < 0.5, Mn < 1.0, ∞ 0.8 Mg and Si < 1.2%) can be hard anodized, despite its high Cu content, in a solⁿ containing H₂SO₄ 300-400 g/l, oxalic acid 25 g/l and H₃BO₃ 20 g/l operating at 15°C. Coating 30-35 μm thick can be produced in 90 mins at a c.d. of 1.5 A/dm². Hard anodizing coatings (> 400 Hv) were obtained at the lower H₂SO₄ concentration.

R. MERZ.

The Hard Anodizing of Aluminium and Alloys.
Aluminium Suisse, 1960, 10, (1), 21-6.

Describes the Alcoa process of producing hard coatings on Al. 50 μ m coating with a breakdown voltage of 2,000 - 2,500 V and a corrosion - resistance 4 times that of the normal H₂SO₄ film is obtained. An anodizing plant in Switzerland is illustrated.

A. MOREA, C. BERNARD and A CAMPO.

Surfaces (Paris) (E.N.S.A.M., Dept. Materiaux).
Abrasion Tests on Hard Anodic Oxide Coatings II.

(M.F.A. March/April p.70).

Graphical interpretation of hardness and abrasion test results on hard anodized aluminium is discussed. Relationship between hardness and wear resistance is considered.

M. MOREAU, C. BERNARD and A. CAMPO.

Characterisation of Hard Anodic Oxide Coatings on Aluminium Alloys.

Surfaces (Paris), 1974, 13, No.89, 45-52, 57-63.

Microhardness tests on perpendicular, parallel and oblique sections on Al alloys after hard anodizing have shown linear law of hardness increasing with proximity to substrate. Microhardness tests using 25g load were found to be about 5% higher than tests at 50g load. Hardness values are lowest for plane perpendicular to surface, higher in inclined plane and highest in plane parallel to surface.

J.H. MORSE.

Job Shop Hard Anodizing - Duralectra Comments.

Prod. Finish., April 1974, 38, (7), 76-78.

K. NAKAMURA.

Electrical Properties of Anodic Oxide Films on Aluminium.

J. Metal Finishing Soc., Japan, 1973, 24, No.5, 268-71.

Thick anodic films were formed in 15% wt. H_2SO_4 bath and electrical properties were investigated to clarify effects of electrical and structural imperfections such as impurities, vacancies, and micro-pores. Adsorption currents having long relaxation times were observed, which suggested presence of many traps in films, confirmed by measuring detrapping currents by light irradiation during discharging process. I - V characteristics of films were expressed by $I = KV^n$ ($n = 2$), which indicates that electrical conduction mechanism of films is controlled by only one kind of carrier current limited by space charge in case of shallow trap states. Photo - quenched currents as well as the photo - induced currents were also formed by measuring photo-electric effects of films.

K. OKUBO.

Hardness and Wear Resistance of Semi-Hard Anodic Coating on Aluminium and its Alloys.

J. Metal Finishing Soc., Japan, 1964, 15, No.1, 8-14.

Composition of electrolyte and electrical conditions are determined by composition of the Aluminium. Consideration of electrical conditions of H_2SO_4 and H_2SO_4 - oxalic acid baths for Aluminium and its alloy are reported. Hardness and wear resistance increase with decreasing temp. and concentration, and with increasing d.c., but 17 S alloy indicates a lower value at lower temp. and higher c.d. Addⁿ of oxalic acid to H_2SO_4 baths improve mechanical properties on higher temp. electrolysis though not a lower temp. There seemed to be no close relationship between hardness and wear resistance, but the higher the scratch hardness, the higher the wear resistance.

K. OKUBO.

Studies on Anodizing of Aluminium and its Alloys. II Coatings of Hard Anodizing Aluminium from mixed bath of H_2SO_4 - oxalic - citric - acids.

J. Metal Finishing Soc., Japan. Nov. 1968, 19, (11), 445-450.
[in JAPANESE, with ENGLISH summary].

The hardness increases towards the inner part of cross sections through thick coatings, but slightly decreases near the boundary layer of substrate metal.

11 References.

F. O'NEILL.

Hardcoating: Dark Horse of the Metal Finishing Industry.

Plating, Oct, 1970, 57, (10), 976-980.

Hard anodizing of Aluminium in baths run at lower acidity, higher c.d. and lower temp. than conventional baths produces a coating with a surface hardness comparable to that of case-hardened steel, thereby eliminating galling and greatly improving corrosion resistance and insulating properties. Recommendations are given for altering the hard anodic cycle to produce particular combinations of the above properties. The importance of the optimum alloy composition is emphasized.

A.E. OSTERMANN and K. WELKER.

Surface Treatments for Aluminium. Dusseldorf, Germany, 8-9 Mar. 1978, Aluminium - Zentrale, Dusseldorf, 1978. [in GERMAN].

Some examples of the uses of hard anodized Aluminium components. Aluminium alloys suitable for hard anodizing are listed. Either H_2SO_4 or mixed acid anodizing is suitable. Hard anodizing is not sealed unless unusual corrosion resistance is required. Thicknesses of 40 to 100 μm are usual with 150 μm the practical limit for most alloys and baths. Thickness variations range from +5% for low alloy Al to +20% for alloys with high Cu or Si content.

As-cast surfaces require blasting or etching prior to anodizing. The thermal properties of hard anodic coatings delay the development of cracks in diesel pistons.

8 references.

A.E. OSTERMANN and K. WELKER.

Production and Uses of Hard Oxide Films on Aluminium Structural Components.

Aluminium, June 1978, 54, (6), 396-40. [in GERMAN].

The suitability of Aluminium wrought and cast alloys for hard anodizing is reviewed and the properties of hard oxide films and the parameters influencing them are discussed. The quality of film is determined by material and surface condition. Hard oxide films on Aluminium structural elements improve the performance of these parts in many ways: increased wear resistance, corrosion resistance, heat resistance, resistance to cracking etc. Use in engine building is cited. 8 references.

G.H. POLL.

Faster Hard Anodizing.

J. Prod. Finish., Mar. 1972, 36, (6), 84-87, 89.

Hard anodizing rates for Aluminium are increased by using a threecircuit pulsed current rectifier in a shop producing parts for missiles and jet engines, computer components, hydraulic cylinders etc. The process also makes it possible to anodize the 2024 Al alloys uniformly.

L.R. RAKOWSKI.

Pulsepower Kicks the Dwell Out for Hardcoat Anodizing.

Mod. Met., Aug. 1971, 27, (7), 96, 98.

An improved power supply which delivers a surged power output has eliminated dwell time in hardcoat anodizing. The power supply also needs less refrigeration than a conventional power rectifier, minimizes burning of parts and does away with need for special tanks to process hard to handle alloys. Requires large racks (high c.d.) problem.

T.L.RAMA CHAR

Recent Developments in Hard Anodizing.

[Proc. Internat, Conf.,] Protection Against Corrosion by Metal Finishing, Basle, 1966, 1967, 216-220.

Developments in the electrochemical process of hard anodizing of Al and alloys during 1961-1965 are reviewed. The theory of anodizing and the oxide structure are considered and commercial processes for hard anodizing are tabulated and described.

47 references.

T.L. RAMA CHAR.

New Developments in Hard Anodizing.

Oberfläche - Surface, 1968, 9, No.2, 25-8.

A review of processes and applications.

K.J.ROBINSON and B.W.MOTT.

Surface Hardening of Aluminium.

Product. Eng., 1947, 18, (7), 133-34.

A.RÖMER and G.SARETZ.

Hard Anodizing with Different Types of Current.

Metalloberfläche, 1963, 17, (10), 309-10.

The anodizing of Al-Cu-Mg alloy with mixed a.c./d.c. is described and the hardness and growth rate compared with that for d.c. alone.

Hard Anodizing in d.c. H₂SO₄ process.

As above p. 363-366.

The effect of conc., temp., time, voltage variation and c.d. on growth rate and microhardness of the anodized layer on a high strength Al alloy is described.

J. ROUBINEK and R. KORINEK.

Hard Anodic Oxidation of Aluminium Alloys.

Strojivnstri, Dec. 1959, v.9, 909-913.

Hard oxidation of engine pistons in an electrolyte containing H₂SO₄ at 0°C., and an anodic current density of 4-5 A/dm². Voltage and current density are regulated automatically. Thickness of the oxide layer formed as a function of time. 5 references.

M.F. RUPP and J.H DEDRICK.

How Much Does Hardcoat Anodize Strengthen Aluminium?

Prod. Finish., (Cincinnati). May 1971, 35, (8), 66-68, 70.

Mechanical tests used to evaluate effect of hard coat anodic films on the bending, buckling and compression strengthen characteristics of Aluminium. Results showed that the anodic coatings increased the strength-to-weight ratio, the stiffness and the resistance to deformation.

F. SACCHI.

Applications of Hard Anodizing in Italy.

Trattamenti e Finitura, 1962, 2, No.6, 225-31.

Hard anodizing applications, alloy and process details are reviewed.

W. SCHWAN.

The Hardness of Anodic Coatings on Aluminium.

Indust. Diamond Rev., 1946, 6, (63), 51.

A.O. SCHWEIZ.

Hard Anodizing of Aluminium Alloys.

Aluminium Rundschau, Nov, 1969, 19, (8), 305-326.
[in FRENCH and GERMAN].

Test results are presented, and thickness, composition and hardness data for ranges of commercial coatings on Al-Mg. Al-Cu and Al-Zn alloys tabulated.

7 references.

G.N. SHOKHPNA and G.M. KRAVETS.

Composition and Structure of Thick Anodic Aluminium Oxide Films on Conditions of Formation.

Zashchita Metallov, 1973, 9, No.4, 458-60. [in RUSSIAN].

Results of investigating composition and structure of oxide films deposited on high purity Aluminium from oxalic electrolyte as function of anodizing conditions, i.e., electrolyte concn. and temp., are given. Electron microscope investigation showed that internal, thick anodic film touching metal has cellular structure. Oxide films have porous external surface, pores being irregularly arranged, often at cell boundaries and at surface defects.

G. SINAY and P. CSOKAN.

Mechanical Properties of hard Anodizing Aluminium Sheet.

Blech, 1962, 9, No.12, 650-3.

The physical and mechanical properties of hard oxide coatings on Al alloys produced by the dilute H_2SO_4 process have been determined and compared with uncoated material.

L.F. SPENCER.

Anodizing of Aluminium Alloys - Hardcoating.

Metal Finish., Nov., 1968, 66, (11), 58-63, 68.

Describes process for producing a thick, dense anodic finish on Aluminium.

11 references.

N.S. SPIVAK.

Development of a Fixture and a Procedure for Hard Anodizing the Surfaces of a Long Aluminium Tube with a Deep Blind-Hole.

Springfield Armory, Mass. Technical rept. 4 Oct. 1965. 22p. Rpt. No. sa-TR 18-1095. Proj. AF - D7 - 3 - 20037 - 01 -07- M6. AD -624, 993. Fld. 11/3. CF STI HC \$1.00. MF \$0.50. Unclass.

A rack was designed and a method developed for the hard-anodizing of exterior interior diameters of a long tube. The development of the procedure was complicated by the necessity of hard-anodizing the interior diameter of an extremely deep-blind-hole. The design of the fixture is discussed and the method is outlined.

M. STALZER.

Developments in Hard Anodizing.

Metalloberfläche, 1962, 16, No.1, 11-4.

After a classification of hard anodizing the author describes experiments carried out on the effect of rate of circulation and anodizing at low pressures. The latter permits the use of high c.d.'s i.e., up to $200 A/dm^2$ for short times. 16 references.

A.W. SWEET.

Practical Aspects of Aluminium Hardcoating.

Plating, 1957, 44, (11), 1191 - 1196.

Characteristics of harcoats indicated and processing details given.

N.D. TOMASHOV, F.P. ZALIVALOV and N.N. IGNATOV.

Properties of Thick Anodic Coatings on Commercial Aluminium Alloys.

Sbornik Korr. Met. i. Splavor, Metallurgizolat, 1963,
212- 21; (ref. Zhur. Khim., 1963, No.20, 20K66).

Thickness, hardness, wear resistance, breakdown voltage and porosity of thick coatings produced by hard anodizing on various commercial wrought and cast Aluminium alloys were studied.

N.D. TOMASHOV and F.P. ZALIVALOV.

Aspects of Thick Anodic Films on Aluminium and its Alloys.

Sbornik: 'Anodnaya Zashchita Metallov', 1964, 183-203;
Ref. Zhur. Khim., 1964, No. 23, 23L270.

The growth, structure and wear resistance of thick anodic films are reviewed. The effect upon them of alloy composition is discussed.

R. TOMONO.

Hard Anodizing

Metal Finishing Society of Japan Journal.

Dec. 1959, v.9, 460-465. [JAPANESE]

Alumilite and Hardas processes (temp. of electrolyte solution, current and voltage); pre-and after treatment, wear resistance, thickness and hardness.

J.E. TRANKLA.

Developments in Hard Anodizing of Aluminium.

Light Metals, 1958, 21, (244), 218-219.

Hardas Process applies on efficient coating on all aluminium alloys regardless of configuration of parts, with assured production results.

Characteristics of process:

1. The hardest film yet developed on aluminium.
2. Finest surface finish.
3. Wide range of operation - permitting the application of a hard coat with complete assurance.
4. Consistant build-up giving no lamination.
5. Superior corrosion resistance.

Four important control factors differentiating from conventional anodizing so as to provide a hard-wear-resistant coating on aluminium were;

1. Minimize the attack of the electrolyte on the coating already produced by more rapid development of the coating.
2. The use of higher current density.
3. A lower temperature of electrolyte.
4. The use of improved techniques of agitation.

S. UEDA and M. HASUNUMA.

Wear-Resistance Properties of Hard Anodic Coating (on Aluminium).

Rep. Castings. Research Lab., Wesoda Univ., 1965, (16), 39-42.
[in ENGLISH].

Voltage changes as a function of time are shown to serve as effective guide in considerations of mechanism of coating formation and their properties.

R.V. VANDEN BERG.

Hard Aluminium Finishes Resist-Wear and Abrasion.

Iron Age, 1952, 170, (18), 81-85.

Hard, thicker, and denser anodic surface coatings on Aluminium give considerable better resistance to wear and abrasion. And on Al alloys may well replace heavier metals for many aircraft applications. Other metals such as Cr, Sn, brass and Pb, coated on Al also give good results.

R.V. VANDEN BERG.

Properties of Anodic Hard Coatings on Aluminium.

Machine Design, 1962, 34, No.6, 155-9.

Abrasion, corrosion and electrical resistivity of wrought cast and forged Al alloy parts finished by anodic oxidation. Effect of variations in electrolyte composition on density of coatings noted.

A.D. VILLA.

Characteristic of Hard Anodic Coatings of High Thickness on Aluminium Alloys.

Rivistamenti (Verese), 1972, 1, No.1, 11-2.

Properties of hard anodic coatings on Aluminium are reviewed including hardness, abrasion resistance, thickness and electrical insulation, roughness and fatigue resistance. Suitability of Al alloys and applications are summarised.

A.I. VOL'FSON.

[Formation of] Hard Anodic Oxide Films on Aluminium, with High Electrical Insulating Properties.

Zashchita Metallov, 1967, 3, (4), 485-490. [in RUSSIAN].

Methods of obtaining very hard anodic oxide films with good electro-insulating properties are described and discussed.

12 references.

A. VON KRUSENSTJERN and K.H. YERUND.

Hard Anodic Coatings.

Bander, Bleche, Rohre, 1962, No.4, 169-72.

A review of anodic coating properties and processes.

R. WEINER.

Anodizing and Hard Anodizing.

Galvanotechnik, 1961, 52, No.3, 126-40.

A review dealing with growth and properties of anodic coatings, types of solution, H_2SO_4 , CrO_3 and oxalic acid baths, hard anodizing and testing.

S. WERNICK and R. PINNER.

Surface Treatment and Finishing of Light Metals VIII Hard Anodizing.

Metal Finishing, 1956, 54, (5), 52-55.

Same basic details as obtained from their book.

H.J. WIESNER and H.A. MEERS.

Hard Anodizing of Aircraft Fuel Metering Components.

Proc. Am. Electroplaters. Soc., 1958, 45, 105-17.

Hard anodizing of aircraft fuel metering components is described in a bath containing H_2SO_4 12% oxalic acid 1% (wt) at 48-52°F, 36 A/ft². 10-75 V, for 20 mins using Pb lined equipment and mechanical and/or air agitation and anode rod movement. Thickness determined by chromic-phosphoric acid stripping, a 'growth' method and by the 'Dermatron' electronic thickness tester.

H. WINTERHAGER and R. NISSEN.

Hard Anodizing with Superimposed alternating Current.

(Inst. f. Metallhüttenwesen RWTH, Aachen),
Mitt. Deutsche Forschungsgesellschaft Belchverarb. (Düsseldorf),
1973, 24, No.10 174-82.

Superimposition of a.c. caused reduction in anodizing voltage and temp. rise within coating, making it possible to obtain higher coating thicknesses, especially for Al-Si-12%, Al-Mg-Si-Pb, Al-Mg Si 1% and Al-Zn-Mg-Cu 0.5% alloys as well as lower cooling requirements. A.c. reduces coating thickness at constant c.d. and reduces microhardness. Most important result is considerable increase in abrasion resistance. This effect depends on alloy and was high with Al-Mg-Si 1% and least with Al Mg 3%. There is little effect on coating uniformity. Al-Cu-Mg-Pb could be anodized only with high a.c. component.

M. WRZECIAN.

Hardness of Anodizing Coatings on Aluminium.

Galvano-Organo (Paris), 1973, 42, No. 438, 1080-1.

Review.

M. WRZECIAN.

Hard Anodizing (of Aluminium)

Galvano Organo, Mar. 1976, 45, (463), 199-201. [in FRENCH].

The main processes for hard anodizing and the applications of the coatings are reviewed. Some causes of failures are briefly discussed.

M. WRZECIAN.

The Role of Additives in Hard Anodizing.

Galvano Organo, Dec. 1978, (491), 813-815. [in FRENCH].

The effects of the solution composition and the operating parameters on hard anodized coatings from H₂SO₄ electrolytes are discussed. The influence of addition of oxalic acid, glycollic acid, and glycerine is described.

O. YOSHIMURA, A. SATOMURA, R. AMANO and R. ITO.

Processing Factors in Hard Anodizing.

J. Metal Finishing Soc., Japan, 1960, 11, No.8, 292-7.

The processing factors in hard anodizing, such as temp., c.d., kind of alloy, and two bath composition, were investigated. The best results were obtained on solutions containing (1) H_2SO_4 100g/l and oxalic acid 15g/l, (2) H_2SO_4 380g/l and oxalic acid 10g/l, at -5 to $+10^\circ C$, 2.0 to 4.0 A/dm^2 , d.c., on 61 S, 24 S, AC4A (Silumin) and AC4B alloys. The higher the temperature the lower the c.d. and the lower the bath concentration, the easier and the thicker was the coating forming.

"Burning" and its prevention is discussed.

E.M. ZARETSKIY and T.G PAVOLVSKAYA.

Hard Anodizing of Sintered Aluminium Powder.

Vestnik Mashin., 1963, No.11, 21-2.

Extruded sintered Aluminium powder (SAP) can be anodized in H_2SO_4 (200g/l) at $-5^\circ C$ to $+3^\circ C$ with 2.5 A/dm^2 .

For rolled SAP sheet, 200-350g/l H_2SO_4 should be used at $-5^\circ C$ and with 2.5 A/dm^2 .

New Hard Coating Gains Wear Applications for Aluminium.

Materials and Methods, 1950, 32, (2), 62-64.

M.H.C. finish is a new electrochemical process. Applied "file-hard" coating for Al and Al alloys containing 5% Cu developed by Glenn. L. Martin Co., Thought to be basically a film of Al_2O_3 with thickness from 0.0001 to 0.006 in, the usual value being 0.002 in. The coating has very high wear-resistance properties and possible applications are summarised.

Hard Coating for Aluminium.

Light Metal Age, 1950, 8, (5/6), (5), 35-37.

Also/ As above, M.H.C. but (7/8), 18,20.

Martin Aircraft Company.

Hard Anodic Finishes.

Light Metals, 1957, 20, (230). 156-157 also 167-169.

Hard Oxide Coatings on Aluminium Investigated.

Indust. Finishing (Lond.), 1958, 10, (121), 36-37.

Production of 250 μm - Thick Anodic Coating on Aluminium,

Femipari Kutato Int. Közl., 1959, 3, 219-43, 440, 450, 460.
(Ref. Zhur. Khim., 1960, No.18, 322).

Anodic coatings up to 250 μm thick are obtained in 1 hour in
1- 2.5% H_2SO_4 at 0°C with 40-60V. Tests have confirmed the wear
resistance of such coatings.

U.S. Aircraft Firm Install Hard - Coat Anodizing Plant. Main Use for
Missile Components.

Metal Finishing J., 1960, 6, No.72 486-7.

Description of hard anodizing plant at Douglas Aircraft Co.,
Charlotte, N. Carolina, U.S.A. for missile production.

Also

Douglas Aircraft Installs Large Hard - Coat Anodizing System.
Products Finishing, 1960, 25, No.3, 58-60.

Also

Hard Coat Anodizing.
Iron Age, 1960, 186, No.20, 146-7.

New Hard Anodizing Process for Aluminium.

Plating Management (U.S.A.), 1960, 5, No.3, 13.

Galvano Ref., 1960, 7, No.7, 28.

Hard Anodic Coating for Aluminium.

Materials Design Eng., 1960, 51, No.4, 9.

New Anodizing Technique Cuts Costs.

Ind. Finishing (London), 1961, 13, No.159, 56-57.

Hard anodizing by the Toro Manufacturing Corp., Minneapolis, Min., U.S.A., process is reviewed.

Using c.d. of 500-400 A/ft² to apply on aluminium oxide film of 0.001 in. in 1 min. at 70°F to Aluminium reel. Physical and chemical properties of the coating with attention to colour, electrical resistance and refrigeration requirement.

Hard Anodizing Opens New Markets for Aluminium.

Mod. Metals, June, 1965, v.21, No.5, 66, 68, 70.

Description of the Dura-Kote hard anodizing process to form an oxide film (0.001 to 0.004 in. thick of Rockwell hardness C60) by electrolytic conversion of O₂ liberated from the acid solution in which the Aluminium is immersed. High corrosion resistance, heat resistances, and dielectric strength result, as well as reduction in fatigue strength of up to 25%. Applications cited included the coating of bearing retainers, electronic heat sinks, 355 alloy pistons and 5052-H32 alloy printing rolls.

Anodic Oxidation for Technical Purposes (Hard Anodizing).

Aluminium - Zentrale e.V., 30 Königsallee, Dusseldorf 1. 1969, pp 6 (Pamphlet - GERMAN).

The production of hard, corrosion and wear resistant surface layers by anodic oxidation (Hardas, MHC, Sanford methods) on Aluminium and alloys surface is summarised. Processes, alloy selection (wrought, sand and die cast), layer thickness, cracking, hardness, wear and abrasion resistance and the sealing of anodized surfaces are briefly described.

Hard Anodizing.

Indust. Finishing, Aug. 1970, 22, (266), 25, 27.

A description of a new hard anodizing plant and process is given. The Hardas process enables anodic films to be produced rapidly (0.001 in. in 6 mins) with high hardness value. Components of up to 1 ton wt. and up to 20ft long can be handled.

Hard Anodized Coatings on Aluminium Alloys by the 'Skleroxal ISML' Process.

Alluminio (Milano), 1972, 41, No.1, 32-4.

Description of the "Skleroxal ISML" hard anodizing process. Coating structure is different from that obtained by conventional anodizing. Process is carried out at -8 to +5°C. Thick coating with 450 VPN hardness and 2000 V insulation are produced.

The Hard Anodizing of Aluminium Alloys by the ISML Skelvoxal Process.

Alluminio, 1972, 41, (1), 32-34. [in ITALIAN]

Details are given of a commercial hard anodizing process operated at temp. between -8 and +5°C to give coatings 30 - 300 μm thick. Excellent results are obtained on Al alloys containing Mg, Si, Zn, and Mn provided that Mg and Si are $\leq 5\%$ and Cu is $< 0.5\%$. Good results are obtained on alloys containing Mg and Si 7% and Cu $\leq 2\%$. Test results and typical applications are discussed.

Coating Extends Aluminium Potential.

Iron Age, 1972, 210, No,13, 54.

Description of 'C-H' process for hard anodizing for Al alloys (Universal Metal Finishing Co., Chicago, Ill., U.S.A., Div of C.A. Roberts Co., Melrose Park, Ill.).

A Scanning Electron Microscope Study of Corner Defect in Hard Anodized Aluminium.

Plating, 1976, 63, No.12, 37-9.

To confirm previous claims that secondary anodic layer between hard coat anodic layer and Aluminium would seal cracks and provide additional coverages at sharp corners, author developed technique for S.E.M. examination of aluminium/anodic Aluminium oxide film adjacent surfaces.

Hard Anodizing of Scopes Keeps Sportsmen Happy.

Plating and Surface Finishing, 1978, 65, No.12, 10,12.

Describes hard anodizing of precision scopes for rifles at Colorado Anodizers, 777, Untailla St., Denver, Col., U.S.A.

The "Durkalu' Hard Anodizing Conference.

Galvano-Organo (Paris), 1978, 47, No.491, 811-2.

Description of hard anodizing process for depositing 100 μ m coating in less than half time of conventional process.

Hard Anodizing Comes of Age.

Product Finishing (London), 1978, 31, No.10, 18-9.

Review of booklet issued by British Anodizing Association on anodizing process and design requirements 'A Guide to Architectural and Industrial Anodizing'.

9. REFERENCES.

1. F. Buff, *Liebig's Ann*, 1857, 102 269.
2. W.R. Mott, *Electrochem. Ind.*, 1904, 2, 466.
3. R. Hopfelt, *Brit. Pat. No.* 10,456 (1906).
4. P. MacGahon, *Brit. Pat. No.* 23,007, (1908).
5. G.P. Bengough and J. M. Stuart, *Brit. Pat. No.* 223,994 and 223,995, (1923).
6. *Brit. Pat. No.* 226,536 (1924).
7. C.H.R. Gower and S. O'Brien and Partners. *Brit. Pat. No.* 290,901, (1927).
8. J.D. Edwards, *Trans. Electrochem. Soc.*, 1942, 81, 431.
9. G. Hass, *J. Opt. Soc. Amer.*, 1949, 39, 532.
10. A. Charlesby, *Proc. Phys. Soc.*, 1942, B66, 317.
11. J.W. Diggle, T. C. Downie and C. W. Goulding, *Chem. Rev.*, 1969, 69, 365.
12. P.F. Schmidt and W. Michel, *J. Electrochem. Soc.*, 1957, 104, 230.
13. M.S. Hunter and P. E. Fowle, *J. Electrochem. Soc.*, 1954, 101, 481.
14. M.S. Hunter and P. E. Fowle, *J. Electrochem. Soc.*, 1954, 101, 514.
15. F. Keller, M. S. Hunter and D. L. Robinson, *J. Electrochem. Soc.*, 1953, 100, 411.
16. N.F. Mott, *Trans. Farady Soc.*, 1947, 43, 429.
17. N. Cabrera and N. F. Mott, *Rept. Prog. Phys.*, 1948-49, 12, 163.
18. E.J. W. Verwey, *Physica*, 1935, 2, 1059.
19. J.F. Dewald, *Acta Met.*, 1954, 2, 340.
20. J.F. Dewald, *J. Electrochem. Soc.*, 1955, 102, 1.
21. T.P. Hoar and N. F. Mott, *J. Phys. Chem. Solids*, 1959, 2, 97.
22. S. Setoh and M. Miyata, *Sci. Pap. Inst. Phys. Chem. Res.*, (Tokyo), 1932, 19, 237.
23. C.J.L Booker, J. L. Wood and A. Walsh, *Nature*, 1955, 176, 222.
24. C.J.L Booker, J. L. Wood and A. Walsh, *Brit. J. App. Phy.*, 1957, 8, 347.

25. H. Grubitsch, W. Geymeyer and E. Burik, Aluminium, 1961, 37, 569.
26. M. Paganelli, Alumino, 1958, 27, 3.
27. J.P. O'Sullivan and G.C. Wood, Proc. Roy. Soc. Lon. A., 1970, 317, 511.
28. G. Bailey, Ph.D Thesis, UMIST, 1975.
29. G. Paolini, M. Masaero, F. Sacchi and M. Paganelli, J. Electrochem. Soc., 1965, 112, 32.
30. R.L. Burwell, P.A. Smudski and T.P. May, J. Amer. Chem. Soc., 1947, 69, 1525.
31. R.W. Franklin and D.J. Stirland, J. Electrochem. Soc., 1963, 110, 262.
32. G.C. Wood, J.P.O'Sullivan and B. Vaszko, J. Electrochem Soc., 1968, 115, 618.
33. T.A. Renshaw, J. Electrochem. Soc., 1961, 108, 185.
34. F.P. Zalivalov, M.N. Tyukina and N.D. Tomashov, J. Russ. Phys. Chem. Soc., 1961, 35, 429.
35. P. Csokán, Electroplating and Metal Finishing, 1962, 15, 75.
36. P. Csokán, Trans IMF, 1964, 41, 51.
37. P. Csokán, Trans IMF, 1973, 51, 6.
38. H. Ginsberg and K. Wefers, Metall, 1962, 16, 173.
39. H. Ginsberg and K. Wefers, Metall, 1963, 17, 202.
40. J.F. Murphy and C.E. Michelson, Proc. of Conf. on Anodizing Aluminium, Nottingham, 1962, (Paper 6), p.83, Aluminium Development Association.
41. A.F. Bogoyavlenskii, Anodic Protection of Metals, Paper presented at the First Inter University Conference, Moscow, 1964.
42. T.P. Hoar and J. Yahalom, J. Electrochem. Soc., 1963, 110, 614.
43. A.V. Shreider, J. Appl. Chem., USSR, 1966, 39, 2533.
44. C.E. Alvey, Ph.D Thesis, UMIST, 1975.
45. G.A. Dorsey, J. Electrochem. Soc., 1966, 113, 173.
 ibid , 1968, 115, 1053, 1057.
 ibid , 1969 116, 466.
46. J.P. O'Sullivan, J.P. Hockey and G.C. Wood, Trans Faraday Soc., 1969, 65, 535.
47. J.F. Murphy, Proc. Symp. Anodizing Aluminium, Birmingham 1967, (Paper 1), P.3, Aluminium Federation.

48. S. Wernick, J. Electrodepositors' Tech. Soc., 1934, 9, 153.
49. W Baumann, Z. Phys., 1939, 111, 708.
50. H. Akahori, J. Electronmicroscopy (Japan), 1961, 10, 175.
51. S. Wernick and R. Pinner, "Surface Treatment and Finishing of Aluminium and its Alloys" Draper, Teddington, 4th Ed., 1972, Vol. 1, p.274.
52. N.D. Tomashov, Vestnik Inzhenerov: Tekh., 1946, 59, No.2: Light Metals, 1946, Oct., 429.
53. G .Bailey and G.C. Wood, Trans IMF, 1974, 52, 187.
54. N.D. Pullen, J. Electrodepos. Tech. Soc., 1939, 15, 69.
55. J.M. Kape, 1957, 91, (4), 63-65; (5), 90-92;(6), 109-111; (7), 129-131; (8), 148-150; (9), 171-172; (10), 198-201; (11), 217-219,222; (12), 239-240.
56. E. Hermann, Schweiz. Techn. Z., 1933, 288.
57. W. Schwan, Ind. Diamond. Rev., 1946, 6, 51.
58. H. Fischer, Aluminium, 1937, 19, 358.
59. L.F. Spencer, Metal Finishing, 1968, 66, 58.
60. C.R. Kliemann, Metal Progress, 1965, 88, 63.
61. E.P. Owens, The Iron Age, 1959, 183, Feb. 12, 108.
62. I. Machlin and N.J. Whitney, Metal Finishing, 1961, 59, 55.
63. W.J. Campbell, J. Electrodepositors' Tech. Soc., 1952, 28, 273.
64. Defence Specification DEF-151. March, 1965. Reprinted December 1977. Incorporating amendment No.1.
65. Hard Anodic Oxide Coatings on Aluminium for Engineering Purposes. British Standards Specificatioin BS5599: 1978.
66. W.J. Campbell, Proc. Conf. on Anodizing Aluminium, Nottingham, Aluminium Development Association, 1961, p.137.
67. A.W. Brace, Electroplating and Met. Finishing, 1959, 7, 329, 376.
68. N.D. Pullen, Electroplating and Met. Finishing, 1948, 3, 3.
69. Z. Laszewska, Met. Finishing, 1969, 67, 48.
70. S. Tajima, Product Finishing, 1952, 17, 42.
71. Brit. Pat. No.1,305,842 (1970).
72. A. Oechslin, Schweiz. Alum. Rundschau, 1969, 8, 305.

73. V.E. Lysaght, Metal Progress, 1960, 78, No. 2, 93.
74. C.E. Alvey, G.E Thompson and G.C. Wood, Proc. 10th World Congress on Metal Finishing, Japan, 1980.
75. D.J. George and J.H. Powers, Plating, 1969, 56, 1240.
76. J.M. Kape, Electroplating and Metal Finishing, 1975, 28, No.6, 16.
77. T.D.T. Latter, Finishing Industries, 1977, 1, 13.
78. D.R. Johnson, Plating, 1962, 49, 986, 1079.
79. J.D. Edwards and F. Keller, Trans Electrochem. Soc., 1940, 79, 180.
80. S. Anderson, J. Applied Phys., 1944, 15, 477.
81. R.B. Mason and C.J. Slunder, Ind. Eng. Chem., 1947, 39, 1602 and Metal Finishing, 1948, 46, No.5, 65.
82. R.B. Mason and P.E. Fowle, J. Electrochem. Soc., 1954, 101, 53.
83. P. Csokán, Gépész, 1965, 17, 175.
84. Brit. Pat. No. 701,390 (1953).
85. U.S. Pat. No. 2,692,851 (1950).
86. Brit. Pat. No. 716,554 (1959).
87. Brit. Pat. No. 812,059 (1959).
88. F. Keller and G.W. Wilcox, Metals and Alloys, 1939, 10, 187.
89. F. Keller and G.W. Wilcox, M. Tosterud and C.D. Slunder, Metals and Alloys, 1939, 10, 219.
90. R.C. Spooner, Plating, 1966, 53, 451.
91. G.C. Wood, V.J.J. Marron and B.W. Lambert, Nature, 1963, 199, 239.
92. G.C. Wood, and A.J. Brock, Trans IMF, 1966, 44, 189.
93. J. Cote, E.E. Howlett, M.J. Wheeler and H.J. Lamb, Plating, 1969, 56, 386.
94. D.A. Thompson, Trans IMF, 1976, 54, 97.
95. F. Fischer, Zeitschrift fur Electrochemie, 1904, No. 46, X, 869.
96. Brit. Pat. No. 369,059, (1931).
97. Brit. Pat. No. 403,560 (1933).
98. Brit. Pat. No. 295,390 (1932).
99. M. Schenk, "Werkstoff Aluminium u. sein Anodische oxydation", A. Francke. A.G., Berne, 1948.

100. P. Smith, *Light Metals*, 1946, 8, 515.
101. M.N. Tyukina, N.D. Tomashov and A.V. Byalobcheski, *Trudy Inst. Fiz. Khim. Nauk U.S.S.R.*, 1951, 2; *Issledov Korrozii Metal*, No. 1, 110.
102. Brit. Pat. No. 717,015, (1951).
103. Brit. Pat. No. 727,749, (1953).
104. R.V. Vanden Berg, *Iron Age*, 1952, 170, Oct. 30, 81.
105. N.D. Tomashov and A.V. Balobzheski, *Trudi Inst. Fiz. Chem. Akad. Nauk. U.S.S.R.*, 1951, 2-1, 136; 5-99, 124.

N.D. Tomashov and M.N. Tukina, *Trudi Inst. Fiz. Chem Akad. Nauk, U.S.S.R.*, 1951, 2, 112.
- 106 L. Bosdorf and A. Beyer, *Aluminium*, 1955, 31, 321.
107. P. Lelong, R. Segond and J. Herenguel, *Revue de l' Aluminium*, 1960, 37, 67.
108. C.F. Burrows, *The Iron Age*, 1950, 166, Aug. 24, 73.
109. F.G. Gillig, *Study of Hard Coatings for Aluminium Alloys*, W.A.D.C. Tech. Report. P.B. 111320 (U.S.A), May, 1953, 53.
110. A. Jenny, "Electrolytic Behaviour of Aluminium and other Valve Metals" in "The Anodic Oxidation of Aluminium and its Alloys," English translation by W. Lewis, C. Griffin and Co., London, 1940.
111. P. Csokán and M. Hollo, *M. Werks. u. Korrosion*, 1961, 12, 288.
112. P. Csokán, Thesis for D.Sc. Degree, Hungary; *Hungarian Tech. Abstracts*, 1966, 18, 13.
113. A.W. Brace and P.G. Sheasby, "The Technology of Anodizing Aluminium", Technicopy Ltd, 2nd Ed., 1979.
114. M.A. Blumenfeld and W.F. Schrig, *Plating*, 1960, 47, 1159.
115. Cornell Aeronautical Laboratories Inc. Report reprinted in *Industrial Finishing*, 1958, 10, 36.
116. Brit. Pat. No. 1,439,933 (1976).
117. D. Eyre and D.R. Gabe, *Trans IMF*, 1978, 57, 38.
118. S. Wernick and R. Pinner "Surface Treatment and Finsihing of Aluminium and its Alloys", Draper, Teddington, 4th Ed., Vol 2, p. 577.
119. Brit. Pat. No. 850,576 (1960).
120. Brit. Pat. No. 957,865 (1964).

121. S. Wernick and R. Pinner, "Surface Treatment and Finishing of Aluminium and its Alloys", Draper, Teddington, 4th Ed., Vol. 2 p. 508.
122. J.M. Kape, Trans IMF, 1967, 45, 34.
123. J,M Kape, Plating, 1968, 55, No. 1, 26.
124. C.L. Faust, U.S. Pat. No. 2,550,544 (1951).
125. D.J. Arrowsmith, P.J. Cunningham, J.K. Dennis and E Survila, Trans IMF, 1981, 59, 13.
126. R.C. Spooner, Metal Industry, 1952, 81, 248.
127. A.W. Clifford and D.J. Arrowsmith, Trans IMF, 1979, 57, 89.
128. R.B. Mason, Proc. Amr. Electroplater's Soc., 1941, 79, 139.
129. R.C. Spooner, Nature, 1963, 197, 995.
130. E. Lichtenberger-Bajza, Metall oberflache, 1961, 15, 38.
131. N.D. Tomashov and F.P. Zalivalov, Zhur. Prikl. Khim. 1961, 34, 1799.
132. U.F. Franck. Werkst u. Korrosion, 1963, 14, 367.
133. A.K. Turner and P.G. Lovering, Trans IMF, 1980, 58, 109.
134. U.R. Evans, "The Corrosion and Oxidation of Metal", Arnold, 1961, p.320.
135. W.E. Cooke, Plating, 1962, 49, 1157.
136. G.C. Wood and J.P. O'Sullivan, Electrochimica Acta, 1970, 15, 1865.
137. W. Kaden, Aluminium, 1963, 39, 33.
138. B.A. Scott, Trans IMF, 1965, 43, 1.
139. G.E. Thompson, K. Shimizu and G.C. Wood, Nature, 1980, 286, 471.